Development and Evolution of Shell Sculpture in Gastropods

by

Nicole B. Webster

A thesis submitted in partial fulfillment of the requirements for the degree of

Doctor of Philosophy

in

SYSTEMATICS AND EVOLUTION

Department of Biological Sciences
University of Alberta

Abstract

The shells of molluscs are a beautiful and intriguing tool for studying both the evolution and development of novel morphologies. The mantle secretes a logarithmically spiraled shell through accretionary growth at the apertural margin, not unlike a 3D printer adding material layer by layer. Shell form has been modeled extensively, and the basic mechanics of shell secretion are understood. Shelled molluscs also have an excellent fossil record, which permits historical studies of morphological evolution.

One aspect of shell growth — shell sculpture — has been sorely understudied. This thesis focuses on its evolution and development. Specifically, I examine the evolution and development of the most elaborate form of sculpture, varices — periodic axial shell thickenings, that vary from elaborate wings and spines, to subtle scars. I focus primarily on the gastropod family Muricidae, which exemplifies a diversity of shell sculpture, especially varices and the superficially similar lamellae.

Prior to this work, varices lacked a comprehensive definition, which this thesis provides. I describe all 41 separate evolutionary origins of periodic varices. Overall, varices are more prevalent a) where predation pressure is stronger: in warm, shallow marine waters, b) on high-spired shells and c) in clades with axial ribs. Many origins of varices were clumped phylogenetically, and most arose after the mid-Mesozoic. Although half of all lineages with varices had three or fewer genera, diversification rates in the Tonnoidea correlated positively with the advent of varices.

In many cases, varices are remarkably well aligned between whorls, producing a regular synchronized pattern of sculpture. A physical feedback mechanism, where previous varices guide the placement of future ones was the primary explanation. This hypothesis was

tested in *Ceratostoma foliatum*, which has three aligned alate varices per whorl. By selectively removing or artificially attaching specific varices, I showed that previous shell sculpture was neither necessary nor sufficient to trigger future varix production. Interestingly, new varices grew slightly past their normal position when the physical cue was lacking, and apertural damage caused at least a temporary disruption of synchrony where varices were grown earlier than the normal placement. Overall, some internal regulatory mechanism seems responsible for the synchronization of varices in *C. foliatum*, with some possible fine-tuning by sensing previously grown physical shell cues — varices.

A form of sculpture superficially similar to varices are lamellae — sharp axial, bladelike upliftings. To compare their development to the development of varices, I studied the growth and positioning of lamellae in *Nucella lamellosa*. In contrast to varices, lamellar growth was fast and plastic. Lamellae were produced in one to two weeks, with no evidence of a varix-like growth hiatus. Lamellar spacing increased with increasing shell growth rate, and spacing was irregular, unlike in most varices. Just like varices, previous lamellae need to be removed to permit future shell growth. Removing lamellae experimentally had no effect on the subsequent shell growth rate or lamellar spacing. So, the process of dissolving previous shell sculpture to permit new shell growth does not appear to be rate limiting.

Although the basics of shell secretion are generally understood, little is known about how the mantle changes to produce shell sculpture. Examining the mantle of *Nucella ostrina*, which has both spiral-ribbed and smooth shell forms, showed a relatively straightforward process. Ribs are formed by extending the mantle region responsible for rib formation, thus producing more cells to secrete more shell, and producing a thicker rib than the adjacent inter-rib mantle tissue. This process was examined with multiple techniques: histology,

histochemistry, SEM, TEM, and 3D reconstruction, to understand it from multiple perspectives.

The overall results of this thesis demonstrate the great potential of gastropod shell sculpture as a model to examine developmental patterns and the evolution of novel traits. It has opened a number of avenues for future work. I determined that the mechanisms involved in shell sculpture formation and control may be both more simple and more complicated than previously imagined. Shell secretion is a worthwhile model to examine accretionary growth of hard parts – a mode of skeletal growth common to several animal phyla. It is also a developmental system that differs from most other developmental systems generally studied, which will provide a new perspective on the development and evolution of morphological diversity.

Preface

Chapter 2 has been accepted for publication as:

Webster NB, Vermeij GJ. **In Press**. The varix: Evolution, distribution, and phylogenetic clumping of a repeated gastropod innovation. *Zoological Journal of the Linnean Society*. zlw015.

Both Geerat J. Vermeij (University of California, Davis) and I designed the study, collected and analyzed the data and wrote the manuscript. GJV wrote the introduction and methods, and I wrote the results and discussion and made the figures, all in consultation with each other.

Chapters 3 and 5 will be submitted as coauthored publications with A. Richard Palmer. ARP and I designed the studies. I performed the experiments, ran the analysis, and wrote the manuscript in consultation with ARP.

Chapter 4 has been published as:

Webster NB, Palmer AR. **2016**. Shaving a shell: Effect of manipulated sculpture and feeding on shell growth and sculpture development in *Nucella lamellosa* (Muricidae: Ocenebrinae). *The Biological Bulletin* **230**: 1–14.

ARP and I designed the studies. I performed the experiments, ran the analysis, and wrote the manuscript in consultation with ARP.

Acknowledgments

I could not have done this work on my own, and I am very grateful to all those who helped me along the way.

Thank you to the many gracious funding agencies who put their faith in me, and were interested in my work. I was funded by NSERC (PGSD graduate scholarship), the Conchologists of America Clench/Turner grant, the Raymond Archer Marriott Memorial Fund (Pacific Northwest Shell Club), and the Donald M. Ross Scholarship (BMSC). The University of Alberta has also supported me with the Queen Elizabeth II scholarship, the Dean's Academic Excellence research assistantship, Recruitment scholarship, and the President's Prize of Distinction. The FGSR Graduate student's award, SICB student support, Unitas Malacologia, and the Canadian Society of Zoologists travel award all helped me travel and present my work at conferences, building connections and sharing ideas.

Thank you to my assistants who taught me many things while feeding and photographing snails *ad nauseum*: Jared Sykes, Kelsey Gil, Carissa Keates, and Anna Smith.

Thank you to the Bamfield Marine Sciences Center, and all those people who made Bamfield a home away from home. Thank you especially to Eric for his endless support, and to Beth for teaching me knitting while the snails grew at their pace. Thank you to the Hazel Jones collection (BMSC), the Jim van Es collection (University of Alberta), and the Leslie Atkins collection (University of Alberta) for giving me access to shell diversity to observe, think about, and admire.

Thank you to the Microscopy unit and Arlene: thank you for helping me with so many different aspects of my project with interest and calm willingness.

Thank you to the Pilgrim lab – Dave, Pam, Kendal, Fran, Katie for putting up with my endless questions and lab invasion, even if it didn't pan out in the end. Thank you to the Allison Lab – Ted, Michèle, and Phil for answering my questions and helping me. Thank you to the paleo crew, especially Mike for helping with shell sections and micro CTs.

Thank you Geerat Vermeij for openly sharing your knowledge and enthusiasm, I really enjoyed working with you.

To the Palmer lab – Marjan, Suz, Marjoline, Tetsuto, Javier, Kecia, Tomonari. Thank you for all your support, interest, and guidance, even though we were never in the same place or doing the same thing.

Thank you to my committee, Sally Leys and Lindsey Leighton, for keeping tabs on me, showing me other ways of doing things, and helping me succeed whenever they could.

Thank you to my friends for being there, and forgiving all my absences for my passion. Thank you especially to Amanda Kahn: you let me share my hopes and fears, and read my drafts before they were really ready.

Thank you to my family, for your patience and understanding. Thank you for bending over backwards to help. Especially thank you to my husband, Matthew Wiens. You supported me with all your heart even as you had the same struggles.

Thank you most of all to my supervisor Rich Palmer. Thank you for your endless patience, and driving me to struggle and learn on my own. Thank you for encouraging me to think bigger and be better.

Table of contents

List of figures

Chapter 1 — Introduction

Mollusc shells are an ideal system to examine evolution and development of novel morphologies. The shells are well preserved in the fossil record, providing the basis for deep phylogenetic studies. The beauty and popularity of shells has led to extensive modern and historical shell collections. Furthermore, the accretionary mode of shell growth means that the history of shell secretion during the life of an individual mollusc is recorded in its shell – both growth and damage are preserved. In addition, one great asset of this system is the relative geometrical simplicity of the basic shape: a logarithmic spiral. Shells range from simple to complex with variations in shape, colour, and ornamentation at all taxonomic levels (Abbott and Dance, 1982). Some of this variation is clearly adaptive, such as defensive shell sculpture, while others lack an obvious function, such as many colour patterns (Vermeij, 1995). This variation permits testing of many different evolutionary hypotheses about morphological evolution and the developmental mechanisms underlying such change.

1.1 Shell secretion and morphology

The shell is secreted incrementally from the aperture (growing edge of the shell), with grow beginning at the apex (the larval shell) (Figure 1.1A) by the mantle. The fundamentals of this process are reasonably well understood. The mantle (Figure 1.1B) is a tissue layer that behaves like a flexible hydrostat. It lines the aperture and secretes the different shell layers incrementally (Addadi *et al.*, 2006). Similar to the functioning of a 3D printer, growth is accretionary. Layers are added sequentially at the growing margin of the aperture. The periostracum, a proteinaceous outer layer, is produced in the periostracal groove and the adjacent outer mantle epithelium near the distal margin. The harder calcareous regions of the shell are produced by the more proximal outer mantle epithelium (Furuhashi *et al.*, 2009). This biomineralization can produce two different calcium carbonate polymorphs found in molluscs: aragonite or calcite. Each of these mineral types can be arranged into one of several different crystal microstructures, such as the common prismatic or crossed-lamellar structures, and they can range from the highly regular aragonite tablets to irregular homogenous crystals (Taylor and Reid, 1990; Chateigner *et al.*, 2000). Shell components are secreted into the extrapallial space, which is bounded by the outer mantle epithelium (OME) and the periostracum, although some experiments suggest that this space may not exist

during shell secretion, and that the mantle epithelium directly abuts the shell (Addadi *et al.*, 2006; Marie *et al.*, 2012). Here, a matrix of proteins, glycoproteins, lipids, chitin, and acidic polysaccharides supports and guides the formation of calcium carbonate crystals (Furuhashi *et al.* 2009; Gaume *et al.* 2011; Marin and Luquet 2004). Many details are not yet completely understood, however modern molecular tools are helping to elucidate how this system works (Nudelman, 2015).

Most of our understanding of shell secretion comes from studies of nacreous layer production (Nudelman, 2015). Whether this mechanism applies to other crystal structures is still unclear. In general, β-chitin and silk-like proteins form an inter-crystalline organic matrix, while aspartic acid-rich intra-crystalline proteins guide nucleation and crystal formation by aligning calcium ions in solution (Nudelman, 2015). Although the biomineralization process appears to be deeply conserved across conchiferan molluscs, shell secretomes – all secreted proteins in the shell – also show considerable variability between species, possibly relating to variation in shell architecture (Kocot *et al.*, 2016).

Although many elements of the secretion process are known, few authors mention how a snail controls the shape of its shell or how the mantle is modified to produce shell ornamentation. This represents a major gap in our understanding of shell development.

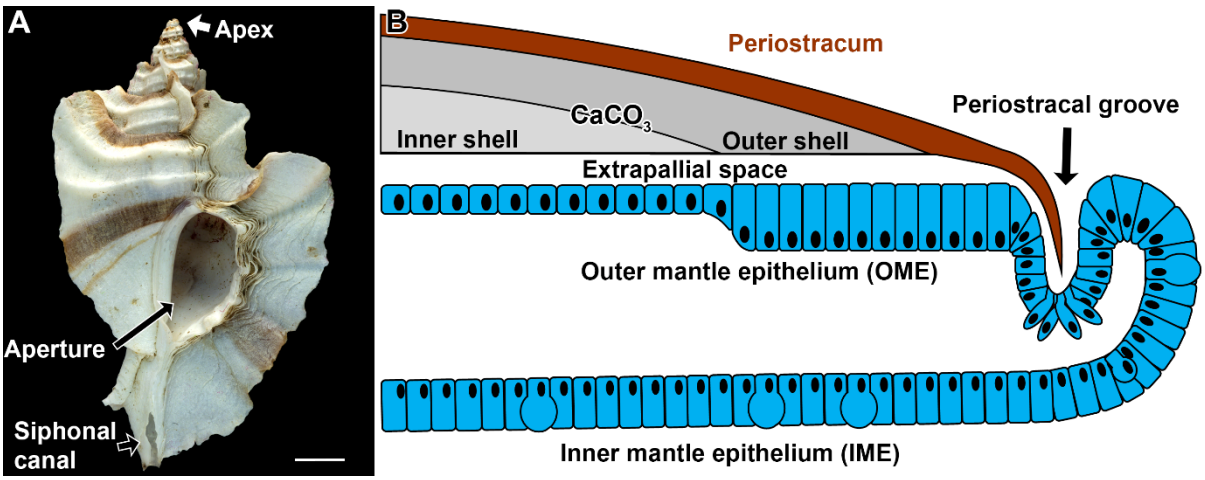

Figure 1.1 General morphology of the gastropod shell (A) and mantle (B). Scale bar = 5 mm.

1.2 Shell modeling

Almost all of our understanding of shell shape and the geometry of shell growth comes from diverse mathematical or computational models (reviewed in Urdy, 2015). These

began as attempts to describe the mathematical shape of helicoid logarithmic spirals and the parameters that affect it (Thompson, 1917), then expanded into examining possible evolutionary constraints related to shell morphospace (Raup, 1966). The types of models, and the questions they could answer, expanded rapidly to accretionary models (Illert, 1987; Okamoto, 1988a; b; Illert, 1989; Ackerly, 1989a; Illert, 1990) and then to growth vector models (Rice, 1998; Hammer and Bucher, 2005; Urdy *et al.*, 2010a; b) that are more biologically relevant, and mimic the 3D printing analogy (Urdy, 2015). Many of these models share interrelated elements that have been analyzed cladistically to better understand how the models themselves have evolved (Stone, 1996).

Despite these many modeling efforts, only a subset of models try to predict the actual *in vivo* mechanism used to grow new shell. Some look at the physical properties of the mantle (Morita, 1991a; b, 1993, 2003; Moulton *et al.*, 2012; Chirat *et al.*, 2013). Others speculate about the underlying signaling mechanisms, whether through lateral inhibition or reaction-diffusion (Meinhardt, 1984, 2009; Hammer and Bucher, 1999), physical feedback systems (Hutchinson, 1989), or neurosecretory models (Saleuddin and Kunigelis, 1984; Ermentrout *et al.*, 1986; Boettiger *et al.*, 2009). Both reaction-diffusion and neurosecretory models fit under the umbrella of lateral activation, local inhibition (LALI) models (Boettiger *et al.*, 2009). Reaction diffusion models are based on Turing patterns where, in its simplest form, two signaling molecules are involved: a fast diffusing activator and slower diffusing inhibitor. In the case of shells, the signaling molecules diffuse along the mantle edge in waves to produce regular and sometimes complex patterns. Spatial instabilities between the diffusing molecules can create patterns that are capable of replicating essentially all shell colour patterns and theoretically most shell sculpture patterns (Meinhardt, 2009). The neurosecretory model of shell pattern formation elaborates on the reaction-diffusion model by adding temporal instabilities by assuming that the snail can sense previous shell patterns through the mantle. This model is based on the neural anatomy of the mantle, assuming that the patterning is derived from nerve and neural secretion signaling (Boettiger *et al.*, 2009)

Sadly, few of these models have been tested. Some studies, especially on ammonites, have taken advantage of 'natural experiments' of abnormal shells, which provide clear examples of how damage can disrupt normal shell growth (Savazzi, 1990; Checa *et al.*, 2002; Savazzi and Sasaki, 2004; Hammer and Bucher, 2005). Only two studies have tested these

models *in vivo*. Checa *et al.* (1998) tested Hutchinson's road-holding hypotheses. Hutchinson (1989) suggested that regular shell coiling is accomplished through physical feedback from previous whorls (turns of the shell), usually in the form of a keel, a ridge on the bottom of each whorl. This keel leads to new shell in the right direction, allowing it to 'hold' to the 'road' left by the shape of previous whorls. When a fake silicone keel was added in *Sphincterichila*, the whorl deviated from the normal growth, following the fake keel instead, as predicted by the road-holding hypothesis (Checa *et al.*, 1998). The opposite experiment was less convincing; when the natural keel was eroded, most snails maintained the normal coiling pattern, rather than deviating towards the apex as predicted. The road-holding hypothesis may therefore account for at least a part of the mechanism that maintains shell coiling (Checa *et al.*, 1998). Some planorbids can correct coiling direction when their center of balance is disrupted (Checa and Jiménez-Jiménez, 1997). In response to a weight glued to one side of the shell, these nearly planispiral shells grew asymmetrically, and changed their axis of coiling to correct for the new center of mass. These species therefore appear to secrete layers of new shell parallel to the substratum regardless of previous shell coiling orientation, at least partially supporting Okamoto's (1988b) hypothesis that the changes in living orientation for heteromorph ammonoids could be determined by the coiling direction. Both of these show experimentally a dynamic program of shell growth, but much remains unknown.

1.3 Shell sculpture

Gastropods exhibit an extraordinary diversity of shell form and shell sculpture. Shell sculpture consists of thickenings or folds on the shell, oriented either perpendicular (spiral sculpture) or parallel (axial sculpture) to the aperture. Many sometimes-overlapping terms apply to different shell-sculpture types, generally based on the shape and size of the sculpture. Ribs are the most common form. They can be axial or spiral, and are generally rounded. Striations are fine spiral lines with low relief, while keels are formed by a single spiral thickening on the bottom of a whorl. Spines are discontinuous protrusions and generally axial, while lamellae and varices are generally medium to high relief axial sculpture (see 1.3.1 *Varices,* and 1.3.2 *Lamellae*, below).

Strong ornamentation is mainly thought to reduce the vulnerability of a snail to shell-breaking predators (Vermeij, 1974, 1978, 1995). Shell ornamentation can a) increase the effective size of the shell (Carter, 1967), b) strengthen it (Vermeij, 1978), c) camouflage it (Seilacher and Gishlick, 2014), c) reduce crack propagation (Danko, 2002), d) distribute crushing forces effectively (Palmer, 1979), e) increase the handling time and work-to-failure of shelled prey (Miller and LaBarbera, 1995), or f) deter soft-mouthed predators with sharp spines and ridges (Palmer, 1979). Other non-defensive functions have also been identified including a) stabilizing the shell in soft substrate (Vermeij, 1995), b) aiding in shell righting (Palmer, 1977; Carefoot and Donovan, 1995), burrowing (Vermeij, 1995), feeding or sensory functions (Spight and Lyons, 1974), c) sexual selection (Schilthuizen, 2003), or possibly even d) aiding in prey capture (Paul, 1981)

1.3.1 Varices

One of the most elaborate forms of shell sculpture is the varix. Varices are formed by periodic thickenings of the shell lip during growth (Carefoot and Donovan, 1995). Varices vary in size from large wing-like flanges to subtle rounded upliftings of the shell; others consist of rows of spines (Figure 3.9). Varices are often defined by their abrupt termination, associated with a suspension of growth, producing a clear break in shell continuity that appears as an axial 'scar' on the shell. Some species produce only a single terminal varix at maturity, creating a heavily reinforced defensive structure (Vermeij and Signor, 1992). Other species produce varices throughout life at regular or irregular intervals, often associated with episodic growth (Savazzi and Sasaki, 2004). In many cases, regularly placed periodic varices produce a strikingly synchronized pattern on the shell, with varices precisely aligned from one whorl to the next, or even between non-adjacent whorls. Synchronization of varices is thought to enhance their primarily defensive function mainly by creating buttressing between whorls as stress relief, and ensuring optimal spacing and placement of defensive features (Savazzi and Sasaki, 2004).

The arrangement of synchronized varices implies a control mechanism to ensure proper spacing and alignment. The most prominent hypothesis to explain this positioning is that a sensory feedback mechanism senses the position of previous sculptural elements, and uses that information to induce the formation of future varices in the correct location accordingly (Elder and Sibatani, 1991; Savazzi and Sasaki, 2004). Previous ornamentation on

the body whorl must be removed to allow continued growth (Vermeij and Signor, 1992; Checa *et al.*, 1998), which provides an obvious cue whereby the mantle detects the position of previous varices and initiates production of a new one in a particular position. This hypothesis easily explains varices that are aligned on adjacent whorls, when the varices are aligned between non-adjacent whorls, as is common where three varices are produced every two whorls (240° apart), this explanation breaks down. Alternate hypotheses include some form of internal regulatory mechanism where soft tissue somehow senses the distance/degrees grown from the last varix produced (Savazzi and Sasaki, 2004) or an endogenous control mechanism (see 1.2 *Shell Modeling* above).

Varices can be considered an evolutionary innovation with diverse forms and multiple functions that have arisen many times independently (Peterson and Müller, 2013). A better understanding of how such sculpture and spacing is controlled developmentally should provide insights about how it has evolved so many times.

1.3.2 Lamellae

Lamellae are superficially similar to varices. This blade-like axial sculpture is thin but tall, and appears to terminate abruptly at its highest point. Subsequent shell growth initiates again from the base of a completed lamella. Lamellae appear to be simpler structures than varices. They are thinner, with less regular spacing, and in general many more occur on a given whorl. A clear distinction between these two forms of shell sculpture is still lacking (G. J. Vermeij, Pers. Comm., Fretter and Graham, 1962; Collins *et al.*, 1996), and little is known about how the growth of lamellae differs from that of varices. One objective of this thesis is to clarify the terminology, to test whether lamellae are associated with a growth hiatus like varices, and to test what may affect lamellar spacing.

1.4 The Muricidae

The Muricidae are a family of neogastropod snails best known for their extraordinary diversity of sometimes highly elaborate shell sculpture (Radwin and D'Attilio, 1976). They are therefore an ideal group to explore the development and evolution of shell sculpture. Muricids are a large family of predatory snails that drill through the shell of their primarily mollusc or barnacle prey (Radwin and D'Attilio, 1976). They demonstrate almost the full

range of gastropod shell sculpture, ranging from simple shell thickenings to complex arrangements of foliaceous blades or spiny varices (Radwin and D'Attilio, 1976).

1.5 Thesis objectives

Much remains to be learned about the evolution and development of shell sculpture. Here I explore two of Sidney Brenner's three questions that interest biologists: 'How did it evolve?' (Chapter 2) and 'How is it built?' (Chapters 3,4,5) (Judson, 1979). These questions are almost entirely unexplored for shell ornamentation in general and varices in particular. The third question, "How does it work?", has been examined in previous studies of the function of shell ornamentation (see 1.3 *Shell sculpture* above).

I approached the question of "How is it built?" from three separate perspectives: an experimental investigation of the growth and control of varix formation (Chapter 3), an analogous study of the growth and control of lamella formation (Chapter 4), and a histological examination of the mantle while growing spiral ribs (Chapter 5). Each chapter focuses on a different muricid species of the subfamily Ocenebrinae: *Ceratostoma foliatum* (Gmelin 1791), *Nucella lamellosa* (Gmelin 1791) and *Nucella ostrina* (Gould, 1852). They all have northeastern Pacific distributions, can be found intertidally, are relatively easy to rear in the lab. They have internal fertilization, and eggs are laid in egg capsules with direct development (Radwin and D'Attilio, 1976). Each has a specific sculpture type of interest.

1.5.1 Evolutionary history of a repeated gastropod innovation: The varix

To better understand the evolutionary history of a particular type of shell sculpture, I looked at the paleontological origins of varices, as well as the modern distributions of varicate gastropods. I compiled a comprehensive survey of all gastropods with varices, both extant and extinct. I counted the total number of independent origins of varices, the degree of variation in form, and created a timeline of when varices arose in different groups. These data were used to look for patterns in timing, circumstance, or predispositions within clades that correlated with the origin of varices (Chapter 2).

1.5.2 How gastropods control synchronized shell sculpture

Here I performed an experimental investigation of the growth and control of synchronized varix formation in *Ceratostoma foliatum*, which is best known for the precise

alignment of three large, foliate varices on every whorl (120° between each varix). This is a prime example of sculpture alignment, which is generally thought to arise via physical feedback from previous shell sculpture that is detected by the mantle during growth (Savazzi and Sasaki, 2004). By experimentally either removing or adding varices to the shells of growing snails, I tested this hypothesis to determine if the presence of varices on the shell was either necessary or sufficient to trigger subsequent secretion of a varix that is aligned to previous varices (Chapter 3).

1.5.3 Effect of manipulated sculpture and feeding on shell growth and sculpture development

Not all shell sculpture appears to be highly regulated. I examined a more variable form of sculpture, axial lamellae, and compared them with the synchrony of varices observed in *C. foliatum. Nucella lamellosa* is more well-known for its prominent shell plasticity. In the presence of predators, snails grow a thick smooth shell with apertural teeth. In their absence, the shell is thinner and usually covered with frilled axial lamellae (Kincaid, 1957; Spight, 1973; A. R. Palmer, 1985; Appleton and Palmer, 1988). Many lamellae with variable thickness and spacing are produced on each whorl. I observed the growth, feeding, and sculpture positioning of control snails and those where I experimentally removed the lamellae (Chapter 4).

1.5.4 How snails grow spiral shell sculpture

To better understand the tissue-level dynamics in the mantle that underlies the production of shell sculpture, I studied sculpture growth in *Nucella ostrina*. *N. ostrina* was of interest because of its shell-sculpture dimorphism; shells are either smooth or spirally ribbed. Genetic crosses have confirmed that this dimorphism is largely controlled by two alleles at a single locus (Palmer 1985). An intraspecific polymorphism with simple genetics removes many confounding factors that might complicate such a comparative study.

Spiral ribs are one of the simplest sculpture forms because regions with or without sculpture are secreted simultaneously by the mantle in rib and inter-rib regions, rather than temporally distinct in the case of axial ornamentation like varices. This allowed me to compare ribbed and smooth snails, as well as the ribbed and inter-ribbed regions of the same snail, to determine how the mantle changes to produce the thickened shell of a rib.

Comparisons were made using histological, 3D reconstruction, histochemical, and ultrastructure techniques.

1.6 Conclusions

My thesis research has advanced the understanding of the evolution and development of shell sculpture using a multidisciplinary approach.

From a malacological perspective, this thesis has delved into unexplored territory. It has expanded our understanding of shell sculpture beyond computer modeling and into the experimental realm. The exploration and analyses performed here addressed several outstanding questions in malacology and shell sculpture: How is it formed? How is that form regulated? When did these forms evolve?

From an evo-devo perspective, the shell forms a unique structure with which to study the development of novel forms. Shell form is highly diverse, yet relatively easy to model. The basic mechanism of shell formation is understood, a single primary tissue is responsible, and shells actively grow throughout life. Many gastropods are easy to rear, with relatively quick developmental times, and are often accessible in egg capsules. All of these characters lend themselves to quantitative and comparative developmental studies.

Gastropods are also an ideal group to explore evolutionary questions. Snails can be used to study both shallow and deep evolutionary divergences. With at least 100,000 living species, and one of the strongest fossil records among animals, some gastropods also record direct evidence of ancient behavior through predatory drilling marks and repaired shell breakage (Leighton, 2002). Recent studies suggest that DNA can even be recovered from the shell itself (Hawk, 2010; Andree and López, 2013; Villanea *et al.*, 2016), so tissue is not required. Considerable work may therefore be done on trait evolution and convergence in gastropods solely with museum specimens.

Chapter 2 — The varix: Evolution, distribution, and phylogenetic clumping of a repeated gastropod innovation[1]

2.1 Introduction

The repeated appearance of similar adaptations has been seen throughout evolution. Leaves, secondary growth leading to woodiness, and winged fruits are all examples of convergent evolution among plants. Snake-shaped vertebrates, crab-shaped crustaceans, bivalved lophotrochozoans, and coloniality are among the hundreds of cases in animals (Conway Morris, 2003; Vermeij, 2006).

Important as these manifestations of convergent and parallel evolution are for understanding the history of adaptation, much remains to be learned about how, when, where, and in which clades the trait or structure in question was acquired and became established. Are there particular times, ecological circumstances, or adaptive predispositions within clades that increase the chance that similar, widely beneficial adaptive traits evolve?

In earlier work on envelopment of the shell by the mantle or foot in gastropods, Vermeij (2005a) suggested that many traits or conditions with multiple independent origins are unevenly distributed among major clades. In some subclades, the trait appears repeatedly, whereas in many others it rarely or never evolved, a pattern of parallel evolution referred to as phylogenetic clumping (Vermeij, 2005a). Although this pattern may be widespread, questions remain about 1) whether phylogenetic clumping is the rule for innovation and 2) the extent to which factors such as adaptive predisposition, time of origin, and geography contribute to it.

Answering such questions requires robust phylogenetic hypotheses about clades that are large enough to include multiple instances of a trait's appearance, as well as a reliable, thoroughly documented fossil record where traits can be recognized in extinct taxa. These sources of data can identify clades and circumstances in which the trait or feature under investigation did not evolve despite the likely benefits of the innovation.

[1] A version of this chapter has been accepted for publication as: **Webster NB, Vermeij GJ**. **In Press**. The varix: Evolution, distribution, and phylogenetic clumping of a repeated gastropod innovation. *Zoological Journal of the Linnean Society*. zlw015.

The convergent structures we consider in this paper are shell sculpture: ontogenetically repeated varices, which are external shell thickenings (ribs, ridges, or flanges) parallel to the outer lip and more prominent than other collabral sculptural elements (Fretter and Graham, 1962; Spight and Lyons, 1974). Varices form part of the passive external armour in many gastropods (Vermeij, 1995). As with many other evolutionary innovations, varices only arose in a few gastropod clades. To assess the conditions under which varices evolved, and the selective agents that favoured their establishment, we documented the number of phylogenetically independent origins and tracked the fates of clades in which varices became established.

Varices take two broad forms that are not mutually exclusive. The first and most common is the terminal varix (Vermeij, 1995). This thickening grows at the apertural margin in a snail with terminal growth, demarcating the end of spiral shell growth and defending the mature aperture. In contrast, many groups have more than one varix on the shell, with periodic thickenings occurring throughout ontogeny, whether the snail has determinate growth or not (Vermeij, 1995). In this paper, we focus on the second form — multiple varices, rather than terminal varices — and will hereafter refer to them simply as varices unless they are specifically identified as terminal varices.

Several questions motivated this research. First, what are the different types and variations of varix structure in gastropods? Second, what are the possible functions of varices? Third, what is the evolutionary history of varices: How many different gastropod taxa bear varices? How are varix-bearing taxa distributed phylogenetically? How do varix-bearing clades differ from other major clades lacking varices? What insights do varices provide regarding the generality of phylogenetic clumping and the repeated appearance of an evolutionary innovation?

2.2 Materials and methods

To characterize varices and to establish their phylogenetic, spatial, and temporal distribution, we conducted a large-scale survey of the taxonomic literature on living and fossil gastropods, supplemented with an examination of all shell-bearing gastropods in the Vermeij collection, as well as the Jim van Es (JVM) and Leslie Atkins (O) collections from the University of Alberta. These were supplemented with online catalogues of shells:

Gastropods.com (Hardy, 2016), Gastropoda Stromboidea (Wieneke *et al.*, 2016), and Digital Murex (Watters, 2016). Using our definition of a varix (see 2.3.1 *Types and variations of varices* below), we consider a gastropod as having varices if at least some individuals of that species bear varices. To limit the scope of this study, we excluded all species bearing a single terminal varix or a single reflected or internally thickened adult outer shell lip. We also excluded cases in which occasional growth pauses were marked by a pronounced but unthickened growth line, as well as species bearing axial lamellae (see 2.3.1 *Types and variations of varices* below).

Savazzi and Sasaki (2004) defined three terms for different types of sculptural alignment, based on their presumed mechanism of alignment. As the underlying mechanism for alignment is unknown, including whether the shell itself provides feedback to maintain patterning, we chose not to follow their definitions. They use the term juxtaposition to mean sculpture that is aligned between whorls without specifying the mechanism, but we prefer the term synchronized for the same effect. Here synchronized sculpture indicates a sculpture pattern where varices are aligned between whorls, regardless of presumed mechanism, rather than sculpture that is aligned due to feedback from other shell features (Savazzi and Sasaki, 2004). We use the term periodic to suggest that a growth pause occurs after varix formation, whereas Savazzi and Sasaki (2004) used the same term to indicate sculpture that is produced at regular intervals due to an endogenous or exogenous timer.

The phylogenetic tree used in this paper was a direct supertree created based on using published expert opinions to merge and expand existing molecular and morphological phylogenies (Nützel, 1998; Colgan *et al.*, 2007; Ponder and Lindberg, 2008; Barco *et al.*, 2010; Oliverio and Modica, 2010; Aktipis and Giribet, 2011; Dayrat *et al.*, 2011; Puillandre *et al.*, 2011; Simone, 2011; Strong *et al.*, 2011; Zou *et al.*, 2011; Takano and Kano, 2014; Galindo *et al.*, 2016), as a comprehensive gastropod phylogeny with sufficient resolution or sufficient varicate taxa is not yet available (Table A1.1). Taxa were included either due to the presence of varices or as large or important avaricate groups to show where varices are absent. We aimed to make conservative estimates of relationships, especially relating to the number of origins of varices or when phylogenies disagreed. Number and timing of varix origins were also informed by the fossil record and information published by experts on the

various clades. No analysis and no conclusions were based on the tree, it was simply a demonstration of the relative relationships between the varicate taxa.

2.3 Results

2.3.1 Types and variations of varices

Here we define a varix as follows: A varix is an axial (or collabral = parallel to the apertural margin) thickening on the shell surface that differs from other axial sculptural elements on the same shell such as individual growth lines, ribs, or lamellae by being thicker, abaxially more elevated, wider, and spatially further apart than smaller elements (Figure 2.1, 2.2). In most cases, therefore, species with varices possess two sizes of axial sculpture. In some cases, the smaller form of sculpture produced along with varices is termed an intervarical rib or node. Unlike lamellae, where growth after the varix is discontinuous, shell deposition generally continues on the apertural side of a varix. Furthermore, many varices appear to be associated with a pause in growth — although this has not been tested in most cases — and usually terminate in an upraised lip, such that further shell growth appears after an axial scar that marks a growth arrest. This characterization of varices is purely descriptive and implies nothing about function or about the mode or timing of formation.

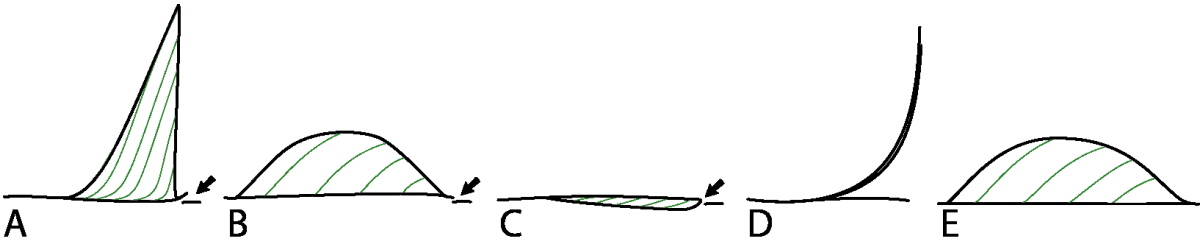

Figure 2.1. Cross-sectional outlines of different axial shell sculpture. A) A thick varix with a triangular shape and an upraised lip, where shell is deposited on both sides of the varix, similar to *Ceratostoma*. B) A rounded varix with upraised lip, similar to *Cerithium*. C) An internal varix with internal thickening and terminal scar, reminiscent of *Eulimidae*. D) A thin lamella (not a varix) with no shell deposition or upraised lip on the apertural side and lacking an intervarical rib, reminiscent of *Trophon*. E) An axial rib (not a varix) without a lip. Green lines indicate theoretical, successive accretionary layers; arrows indicate breaks in shell secretion causing a 'scar' or upraised lip.

In a few cases, such as the ocenebrine muricid genus *Namamurex* (Pliocene of South Africa) and the ellobiid genera *Pythia* and *Ellobium*, varices occur in the absence of coaxial sculpture other than growth lines. We consider these taxa varicate because of the consistent

placement of axial thickenings and their close similarity to varices on related species that also have smaller ribs or lamellae.

Varices vary considerably in form, placement, and number per whorl, and there are other superficially similar sculpture types that we do not consider varices (Figure 2.3). Most true varices are rounded thickenings to varying degrees, but in some groups (especially Muricidae) they can be sharply angled, lamellose, and recurved, often bearing elaborate spines that may branch via the elaboration of spiral sculpture. In a few cases, these varices appear more as internal thickenings of the shell, with external scars denoting their location (i.e. some Eulimidae, Cancellaridae, and *Pythia*) (Figure 2.2D). Varices are usually distributed on both the spire and last whorl of the shell, either scattered (asynchronous varices) or precisely positioned to align between whorls (synchronous varices). We call these multiwhorl varices. Alternatively, varices appear in specific locations relative to a terminal aperture, generally placed dorsally or ventrolaterally on the last whorl. We call these subterminal varices, which are probably functionally analogous to dorsal or lateral knobs, at least in some cases.

In addition to excluding species with a single terminal varix, cases in which the mantle- or foot-covered adult shell develops lateral thickenings (callus) are not included. These are produced by preferentially depositing shell material along the periphery of the ventral side. This condition, which causes the shell to appear dorsoventrally flattened, is widespread in cypraeoideans (Foin, 1989) and marginellids and in the Oligocene to Miocene stromboidean *Orthaulax*. These thickenings differ from varices in that they are secondarily formed once spiral growth of the shell has ceased, rather than being sculptural elements produced at the outer lip during spiral growth.

A special case we also excluded consists of a dorsal or lateral hump or knob in the adult shell, formed approximately at 90° or 120° from the aperture (although the actual angle varies considerably; Sälgeback and Savazzi, 2006). This feature resembles a varix because it is substantially more elevated than other nodes or tubercles and it is confined to the dorsal or lateral side of the adult shell, but it differs from a true varix in being axially short and thus not formed as an elaborated rib or lamella. In most cases, one dorsal knob per shell is present (e.g. many strombids and nassariids), but for a few groups (e.g. Muricidae and Cassidae) a dorsal knob can form at earlier growth stages.

2.3.2 Function

Many functions have been proposed for shell sculpture, most of which centre around defence by reducing the risk of predation in some way (Carter, 1967; Spight and Lyons, 1974; Vermeij, 1974, 1982, 1995; Palmer, 1979; Miller and LaBarbera, 1995; Donovan *et al.*, 1999; Sälgeback and Savazzi, 2006). Varices may aid in defence in a number of ways. First is deterrence – spines and ridges are painful to soft-mouthed predators (Palmer, 1979). Second is obstruction – large structures prevent gape/claw-limited predators from getting a grip on the shell (Vermeij, 1978). These two functions are most effective when the sculpture is large, as in muricid-type varices, or specifically placed, as in synchronized varices or knobs on the last whorl. Third is structural – shell thickenings reinforce the shell and help prevent catastrophic breakage by slowing shell crushing, impeding shell peeling (Vermeij, 1995), preventing crack propagation (Danko, 2002), or increasing the force or work required to break the shell (Miller and LaBarbera, 1995). Defence through structural reinforcement generally applies to all forms of shell sculpture; however, we would expect that the extra thickening of varices is more effective than other types of shell sculpture, although this has not been tested experimentally. Vermeij (1982) observed that all unsuccessful attacks by calappid crabs on varicate gastropods involved a subterminal varix that prevented a peel or other breakage from extending up the spire.

The synchrony of varices between whorls has an added defensive advantage by allowing additional stress relief between whorls (Savazzi and Sasaki, 2004). Synchrony also ensures specific placement of varices relative to the aperture. A varix across from the aperture will specifically obstruct the grip of predators peeling the aperture, and a dorsal varix can help prevent shell crushing by increasing effective diameter. Synchronous shell growth ensures this is always the case (Savazzi and Sasaki, 2004) except for short periods of shell growth interspersed with long pauses.

Varices may have a few other special functions. In some groups, such as the Personidae and Eulimidae, varices are associated with changes in the direction of the shell-coiling axis, although the relationship between these two factors is unclear. Varices may help breakup the outline of the shell, and promote epibiont growth to increase shell camouflage (Carefoot and Donovan, 1995; Vermeij, 1995). Another possible function of varices, specifically tested in the muricid *Ceratostoma foliatum* (Gmelin, 1791), is to aid in

righting the shell after falling (Palmer, 1977; Carefoot and Donovan, 1995; Sälgeback and Savazzi, 2006). The angular distribution of varices may make the shell more likely to land upright. More generally, a dorsal protrusion prevents the shell from landing upside down, thus reducing the righting time, which is also thought to apply to the dorsal knob in strombids, cassids, and other groups (Savazzi, 1991). The curved spiny varices of *Murex pecten* Lightfoot, 1786 may act as a cage that can trap mobile prey (Paul, 1981),although this is not well documented, or they may help prevent the snail from sinking into soft substrate by distributing the weight of the shell over a broader area, which might apply to other soft-sediment dwelling species with broad varices (including the terminal varices of apporhaids) (Seilacher and Gunji, 1993).

Varices may also allow a different form of shell growth; periodic growth via rapid growth spurts, which has several advantages over continuous/constant growth. Periodic growth minimizes the period of vulnerability by allowing the snail to build up resources for another growth spurt while the aperture is defended by a varix. By contrast, continuous growth involves more time spent when either the aperture is relatively weak or the cost of producing a constantly thick shell is relatively high. Other shell structures, including siphonal canals and a crenulated outer lip (for clamping the shell onto rock), can be formed discontinuously in varicate gastropods (Seilacher and Gunji, 1993; Sälgeback and Savazzi, 2006; Vermeij, 2014). With periodic growth, the siphonal canal is functional most of the time, without needing constant remodeling. This is especially true for the upturned siphonal canals of muricids, cerithiids, personids, tonnoids, and some nassariids – all groups with varices. This is less applicable to species with straight siphonal canals that can more easily be grown continuously without constant remodeling.

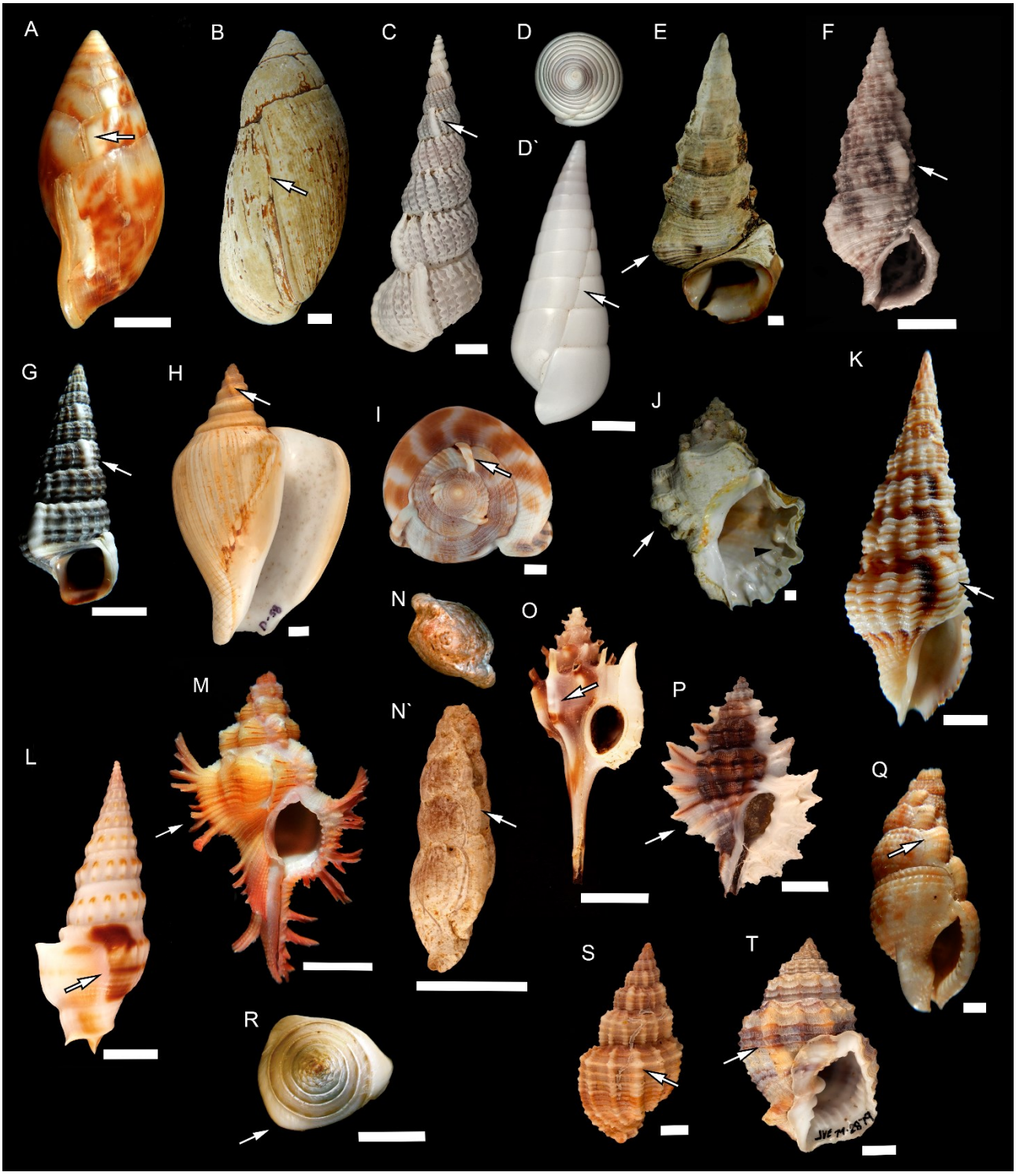
A
B
C
D
D`
E
F
G
H
I
J
K
N
O
M
N`
P
Q
L
R
S
T

Figure 2.2. Examples of varices.A) Ellobiidae: *Pythia scarabaeus* L., 1758, lateral view. B) Ellobiidae: *Ellobium aurisjudae* L., 1758, dorsal view. C) Epitoniidae: *Cirsotrema varicosum* L., 1822, JVM3131, lateral view. D-D') Eulimidae: *Melanella martinii* A. Adams in Sowerby, 1854, JVM1093, apical view (D), lateral view (D'). E) Batillariidae: *Pyrazus ebeninus* Bruguière, 1792, oblique apical view. F) Cerithiidae: *Cerithium eburneum* Bruguière, 1792, JVM1132, apical view. G) Potamididae: *Cerithideopsis californica* Haldeman, 1840, apical view. H) Strombidae: *Laevistrombus canarium* L., 1758, O365D-58., apertural view. I) Cassidae: *Phalium areola* L., 1758, JVM851, apical view. J) Bursidae: *Crossata ventricosa* Broderip, 1833, apertural view, arrowhead: hollow varix. K) Pseudomelatomidae: *Inquisitor* sp., apertural view. L) Drilliidae: *Imaclava pilsbryi* Bartsch, 1950, JVM3053, lateral view. M) Muricinae: *Chicoreus nobilis* Shikama, 1977, apertural view. N) Aspellinae: *Aspella pyramidalis* Broderip, 1833, JVM1488, apical view. N') Dorsal view. O) Typhinae: *Haustellotyphis cumingii* Broderip, 1833, JVM1362, apertural view. P) Ocenebrinae: *Eupleura nitida* Broderip, 1833, JVM1504, apertural view. Q) Colubrariidae: *Colubraria tortuosis* Reeve, 1844, apertural view. R) Columbellidae: *Strombina fusinoidea* Dall, 1916, JVM1634, apical view. S) Photinae: *Phos senticosus* L., 1758, JVM1676, dorsal view. T) Cancellariidae: *Bivetiella cancellata* Linnaeus, 1767, JVM2879, apertural view. Scale bars = 5 mm; arrows indicate one (not all visible) varix. JVM and O represent the University of Alberta collection specimen numbers, specimens without collection numbers come from the Vermeij collection.

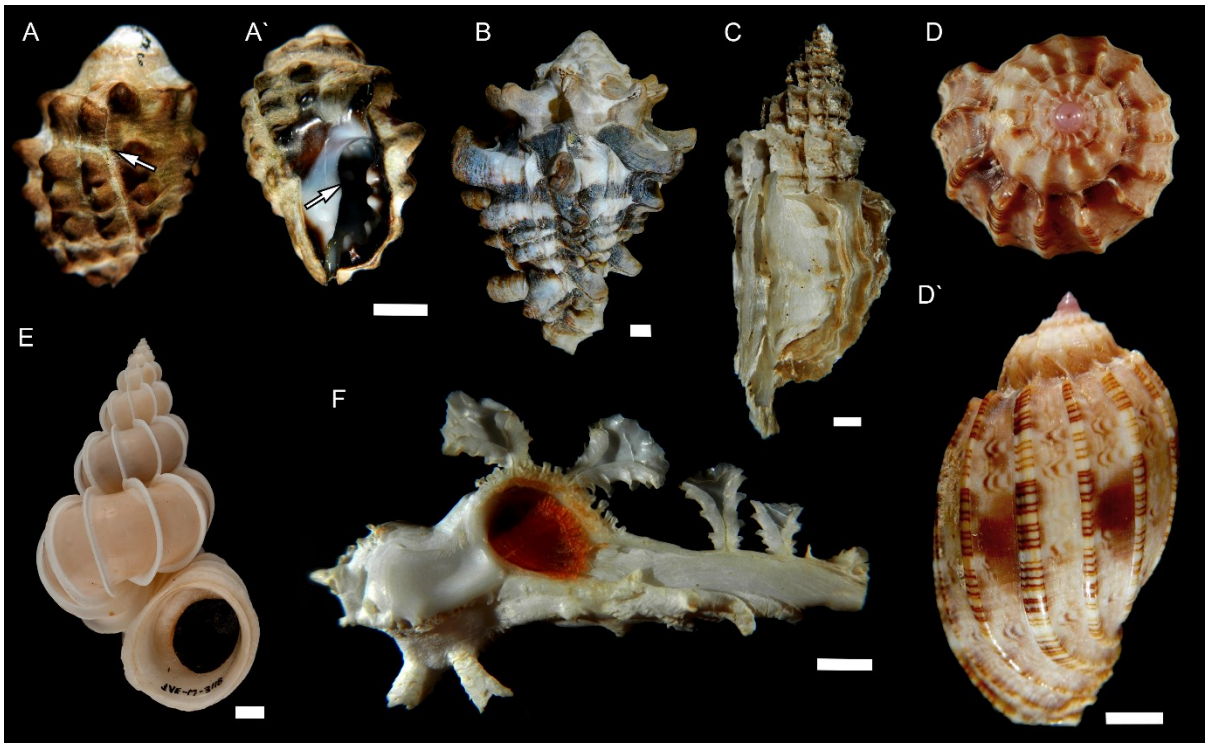

Figure 2.3. Varix-like sculpture not considered to be a true varix. A) Ergalataxinae: *Tenguella granulata* Duclos, 1832, dorsal view, with scar-like rib: arrow. A') Apertural view, previous apertural teeth associated with scar-like rib (arrow, not visible). B) *Vasum turbinellus* L., 1758, dorsal view. C) Trophoninae: *Nipponotrophon stuarti* E. A. Smith, 1880., lateral view. D. Harpidae: *Harpa amouretta* Röding, 1798, apical view. D') Dorsal view. E) Epitoniidae: *Epitonium scalare* L., 1758, JVM3118, apertural view. F) Muricopsinae: *Homalocantha anatomica* Perry, 1811, apertural view. Scale bars = 5 mm; JVM and O represent the University of Alberta collection specimen numbers, specimens without collection numbers come from the Vermeij collection.

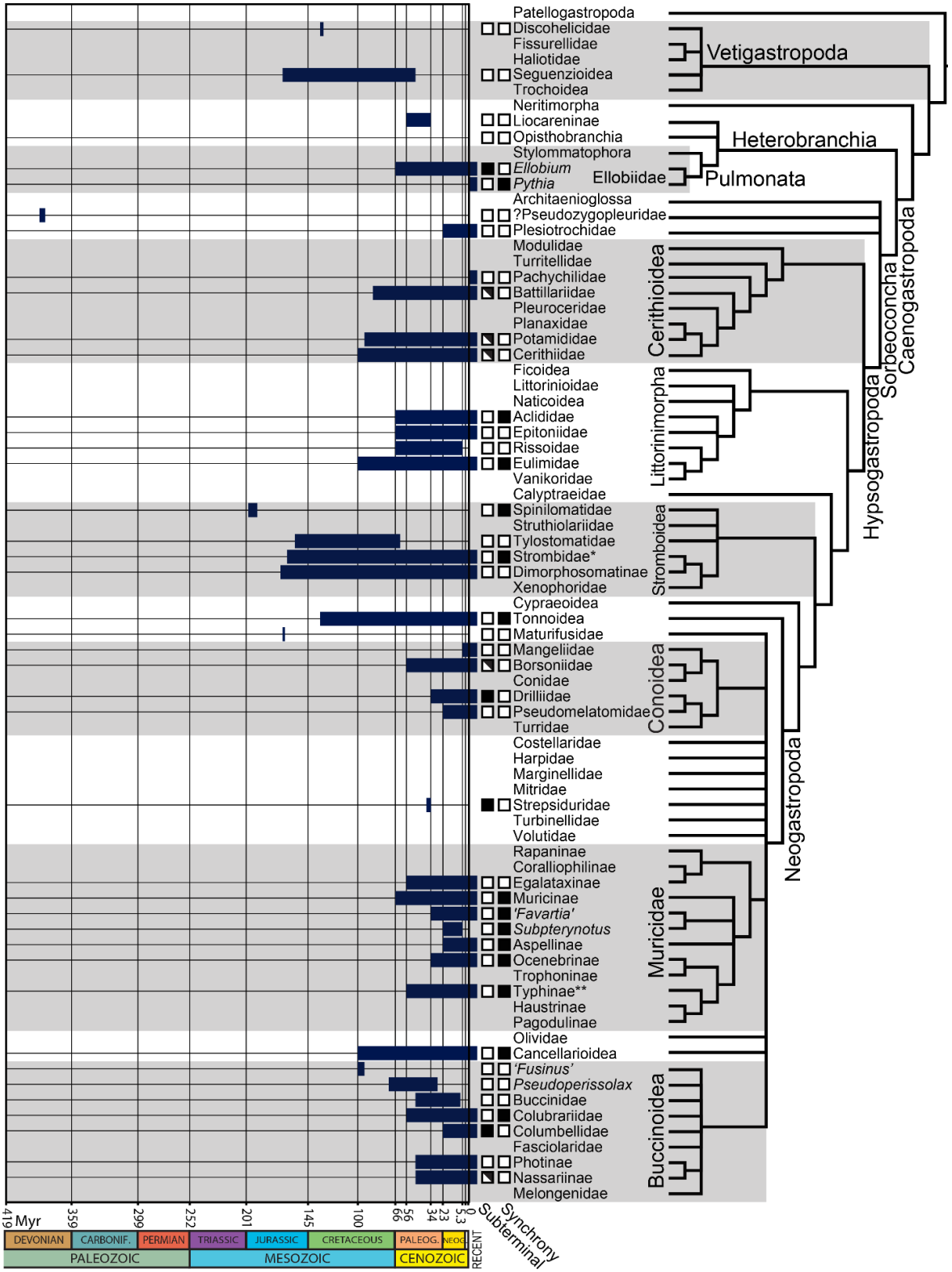
Patellogastropoda
Discohelicidae
Fissurellidae
Haliotidae
Seguenzioidea
Trochoidea
Vetigastropoda
Neritimorpha
Liocareninae
Opisthobranchia
Heterobranchia
Stylommatophora
Ellobium
Pythia
Ellobiidae
Pulmonata
Architaenioglossa
?Pseudozygopleuridae
Plesiotrochidae
Modulidae
Turritellidae
Pachychilidae
Battillariidae
Pleuroceridae
Planaxidae
Potamididae
Cerithiidae
Cerithioidea
Caenogastropoda
Sorbeoconcha
Hypsogastropoda
Ficoidea
Littorinioidae
Naticoidea
Aclididae
Epitoniidae
Rissoidae
Eulimidae
Vanikoridae
Calyptraeidae
Littorinimorpha
Spinilomatidae
Struthiolariidae
Tylostomatidae
Strombidae*
Dimorphosomatinae
Xenophoridae
Stromboidea
Cypraeoidea
Tonnoidea
Maturifusidae
Mangeliidae
Borsoniidae
Conidae
Drilliidae
Pseudomelatomidae
Turridae
Conoidea
Costellaridae
Harpidae
Marginellidae
Mitridae
Strepsiduridae
Turbinellidae
Volutidae
Neogastropoda
Rapaninae
Coralliophilinae
Egalataxinae
Muricinae
'Favartia'
Subpterynotus
Aspellinae
Ocenebrinae
Trophoninae
Typhinae**
Haustrinae
Pagodulinae
Muricidae
Olividae
Cancellarioidea
'Fusinus'
Pseudoperissolax
Buccinidae
Colubrariidae
Columbellidae
Fasciolariidae
Photinae
Nassariinae
Melongenidae
Buccinoidea
419 Myr
359
299
252
201
145
100
66
56
34
23
5.3
0
RECENT
Subterminal
Synchrony
DEVONIAN
CARBONIF.
PERMIAN
TRIASSIC
JURASSIC
CRETACEOUS
PALEOG.
NEOG.
PALEOZOIC
MESOZOIC
CENOZOIC

Figure 2.4. Phylogenetic distribution and relations of varicate Gastropoda. All 41 origins of varices are mapped on a composite phylogeny with large or relevant avaricate clades. Left: The fossil ranges of varicate members of varicate clades (Dark blue) (note that this is not the fossil range of the entire clade). The range is from first to last occurrence, persistence throughout the range was assumed. Right: Cladogram assembled from multiple phylogenies (See 2.2 *Materials and Methods* above). Character state boxes and fossil ranges indicate that varices are present in that lineage. Subterminal; white: absence of subterminal varices, black: clades where all varices are subterminal, half black: a mix of both subterminal and multiwhorl varices are present. Synchrony; white: absence of synchronized varices, black: clades where at least some species show synchronized varices. *Aporrhainae + Strombidae + Rostellariidae, **Typhinae + Trypterotyphinae.

2.3.3 Taxonomic survey of varices

2.3.3.1 Vetigastropoda

Few examples of varices occur in basal gastropods, an observation consistent with the general lack of high relief sculpture, which has been partially attributed to a reduced ability to resorb shell material (Vermeij, 1977). However, two inarguable vetigastropod clades include varicate gastropods — the Seguenzioidea and Discohelicidae (Figure 2.4, Table A1.2).

Three genera within Seguenzioidea are varicate — *Onkospira* from the Middle Jurassic (Bathonian) to the Early Cretaceous and perhaps the Late Cretaceous (Kase, 1984; Das *et al.*, 1999), *Agathodonta* from the Early Cretaceous (Herbert, 2012), and *Calliovarica* from the Early Eocene (Vokes, 1939; Beu and Maxwell, 1990; Hickman and McLean, 1990; Stilwell, 2014). They have been assigned to Eucyclidae (*Onkospira*) or Chilodontidae (*Agathodonta* and *Calliovarica*) and have simple, low rounded varices. Although nothing is known about the phylogeny of these varicate taxa, we take the conservative position that the varicate condition evolved only once in the Seguenzioidea. Significantly, although a terminal varix occurs in several living genera of Chilodontidae (Herbert, 2012), no living Seguenzioidea have multiple varices.

Within the Discohelicidae, *Colpomphalus dupinianus* (d'Orbigny, 1842), from the Hauterivian, is one of the rare cases of varices found on a nearly planispiral shell in gastropods (Kollmann and Fischer, 2005; Ferrari, 2014).

2.3.3.2 Heterobranchia

The near complete lack of varices in heterobranchs is interesting and likely related to their general lack of shell sculpture. In nonmarine groups, this is normally attributed to

reduced predation pressure, with other possible factors being the increased cost of a weighty shell on land and reduced calcium availability (Vermeij, 1987).

2.3.3.2.1 Acteonidae

Varices were just recently described in two genera of Acteonidae, *Hemiauricula* and *Nucleopsis* from the Eocene (Salvador and Cunha, 2016). These consist of weak thickenings and an associated axial scar, with up to three per shell, generally on the last few whorls. These two genera were united as the same members of a redefined Liocareninae. Living acteonids are generally infaunal predators of polychaetes, so thicker varices may be impractical, and their relationship to other heterobranchs is still in flux, although they are generally considered basal (Salvador and Cunha, 2016).

2.3.3.2.2 Ellobiidae

Interestingly, both of the varicate taxa in the Ellobiidae (Pulmonata), the Recent genera *Pythia* and *Ellobium,* co-occur with land crabs in near-shore environments (Raven and Vermeulen, 2007). Neither group has elaborate shell thickenings, and both are placed in different ellobiid clades (Martins, 2007), suggesting separate origins.

In *Pythia,* the varices are similar to those of eulimids, with two axially thickened scars 180° apart, matching the dorsoventral flattening of the shell (Figure 2.2A). The varices of *Ellobium* are quite different, with a dorsal subterminal varix behind the mature aperture, with the same thickened edge (Figure 2.2B). This varix appears in *E. aurisjudae* (L. 1758)*, E. aurismidae* (L. 1758), and *E. scheepmakeri* (Petit de la Saussaye, 1850) but is not present in all individuals. It may be that individuals without varices have not yet reached the appropriate ontogenetic stage, or it could be a polymorphic trait. The earliest *E. olivaeformis* (Briart & Cornet, 1873) from the Early Paleocene is not described with varices (Thorsten, 2002).

2.3.3.3 Caenogastropoda

2.3.3.3.1 ?Pseudozygopleuridae

Spanionema is the earliest known genus with varices, from the Givetian (Middle Devonian). The varices are irregularly placed and relatively pronounced (Knight *et al.*, 1960; Heidelberger, 2001). The relationships of this genus are uncertain, but it clearly represents a separate origin of varices, with no known varicate relatives.

2.3.3.3.2 Campaniloidea

The clade Campaniloidea is mostly free of varicate species, but Harzhauser (2014) noted the presence of varices (one to two per whorl) in the Early Miocene plesiotrochid *Plesiotrochus inopinatus* Cossmann, 1910 from the Quilon Formation of India. A second, Recent species, *Plesiotrochus* aff. *acutangulus* (Yokoyama, 1924) was described by Janssen *et al.* (2011) with very weak varices. These occurrences leave open the possibility that more species in this group will be found to have varices.

2.3.3.3.3 Epitoniidae

The state of varices in this family, which originated in the Cretaceous, is complicated. Most species have a number of axial elements on each whorl that generally align from one whorl to the next. These vary from axial striations to alate lamellae, which we do not consider to be varices (Figure 2.3E). In most cases, we determined these to be ribs or axial lamellae; however, some species, like many *Cirsotrema, Epitonium, Opalia,* and *Amaea* have distinct rounded varices interspersed with the other ribs, the earliest being from the Paleocene (Abbott, 1974; Kilburn, 1985; Lozouet *et al.*, 2001) (Figure 2.2C). These varices are not synchronized, and whether they represent growth stoppages is unknown.

2.3.3.3.4 Eulimidae

The Eulimidae (L. Cretaceous-Recent) are almost exclusively echinoderm parasites, with a generally polished, high-spired shell. The varices of eulimids are atypical of gastropods as a whole. In most species, varices appear as periodic axial scars on the shell associated with an internal thickening. In many cases, they are synchronized between whorls, with only one per whorl, although some have two per whorl, and the degree of synchrony varies (Figure 2.2D). For example, not all specimens of *Melanella martini* (A. Adams in Sowerby, 1854) have synchronized varices (Savazzi and Sasaki, 2004). The varices of eulimids are associated with a growth hiatus and subsequent thickening of the aperture. Interestingly, some eulimids are sequential hermaphrodites, and a varix is associated with the transition from male to female (e.g. *Apicalia*) (Warén, 1983). All eulimids with the characteristic curved shell possess a varix every 360°, although the inverse is not true — not all species with this pattern have curved shells (Savazzi and Sasaki, 2004). The curving of the shell may be accomplished by slight changes to the axis of coiling at each growth hiatus. The internal nature of the varices helps maintain the ultra-smooth texture of the shell while

still providing a thickened aperture during growth stoppages and periodic structural support. Some genera, such as *Auriculigerina, Chileutomia,* and *Oceanida* have more expanded varices, which correspond to a more flaring aperture (Warén, 1983; Lozouet, 1999; Landau and Marquet, 2001; Garilli and Messina, 2006).

2.3.3.3.5 Aclididae

This family is poorly known, but some members of *Aclis* have varices strongly reminiscent of those seen in Eulimidae (Bertolaso and Garilli, 2009). *Aclis aurisparva* Bertolaso & Garilli, 2009 has scar-like varices on the upper whorls, and further down the spire they become more wing-like processes. The placement of this family is uncertain, but it does have an affinity with Eulimidae, although this may be plesiomorphic (Takano and Kano, 2014). Further complicating the matter, the family Aclididae is also not well defined and may be paraphyletic (Warén, 1983).

2.3.3.3.6 Rissoidae

Warén (1983) mentions that 'rissoinids' have internal varices, similar to those of Eulimids, but does not provide details. A single genus *Pseudotaphrus* has occasional varices on its smooth shell, generally on the last whorl (Ponder, 1984). These are similar in appearance to the varices in *Ellobium* in that they appear as a stoppage of growth with associated apertural thickening, followed by a short period of spiral growth to a new aperture. Unlike *Ellobium*, their placement does not appear consistent enough to warrant the label of a dorsal varix.

These four families, Aclididae, Eulimidae, Epitoniidae, and Rissoidae, cluster relatively closely on the phylogeny of Takano and Kano (2014) but phylogenetic relationships remain uncertain. With the exception of Aclididae and Eulimidae, each family differs quite widely in how varices are expressed. This morphological difference supports four separate evolutionary origins, especially considering the rarity of varices in Rissoidae, Epitoniidae, and Aclididae.

2.3.3.3.7 Cerithioidea

Varices appear to have originated four times independently in the Cerithioidea, because the basal-most cerithioideans do not have varices (Strong *et al.*, 2011). Rounded, unsynchronized varices that extend up the spire evolved once in Potamididae (Turonian–

Recent) (Saul and Squires, 2003; Reid *et al.*, 2008) and once in the clade including Cerithiidae, Litiopidae (*Alaba* and *Gibbarissoia*), and Diastomatidae (Paleocene-Recent) (Houbrick, 1981; Strong *et al.*, 2011). In many cases, these varices are lighter in colour compared to rest of the shell. The third origin is in the Batillariidae and the fourth in *Faunus ater* (L. 1758) (Pachychilidae).

Broad, lateral, subterminal varices are also found in many species of Potamididae, Cerithiidae (not Alabininae), Pachychilidae (*Faunus*), and Battilariidae (Figure 2.2E-G). A few cerithiines, including *Clypeomorus* can also have a dorsal subterminal varix (Houbrick, 1985, 1991; Ozawa *et al.*, 2009; Strong *et al.*, 2011).

Many Mesozoic cerithioids are difficult to assign to specific families, so varix origins in these families are unclear. The earliest potamidid with a ventrolateral varix is *Cedrosia pacifica* Saul and Squires 2003 (Late Cretaceous), although many Mesozoic potamidids are also avaricate (Saul and Squires, 2003). The earliest batillariid found was *Pyrazus partschi* (Zekeli, 1852) from the Late Cretaceous, while the first without varices *?Echinobathra* is mid-late Cretaceous (Ozawa *et al.*, 2009). In the paraphyletic Cerithiidae (Ozawa *et al.*, 2009), *Cryptaulax* is found in the Triassic without varices, while the varicate taxon *Hemicerithium? interlinea* (Cragin, 1893) occurs in the Cenomanian (Early Late Cretaceous) (Stephenson, 1952; Sälgeback and Savazzi, 2006).

Faunus ater has a subtle ventrolateral varix not mentioned by Houbrick (1991). *Faunus* is reconstructed as the basal genus, as well as the sole brackish water representative of the freshwater Pachychilidae (Köhler and Glaubrecht, 2010). Earlier fossil pachychilids, including other *Faunus,* do not show varices, so this may be a separate and Recent origin of varices (Pacaud and Harzhauser, 2012).

2.3.3.3.8 Stromboidea

Varices occur widely in the Stromboidea. Most are enlarged rounded ribs, but some are adorned with spines, as in the aporrhaids *Spiniloma* and *Spinigeropsis* (Spinilomatidae) of the Early Jurassic, *Pietteia* (Dimorphosomatinae) of the Middle Jurassic, and *Diempterus* (Aporrhainae) of the Late Jurassic (Gründel *et al.*, 2009; Kollmann, 2009). In most aporrhaids, varices occur at half-whorl intervals, but in some aporrhaids and most strombids, varices are more closely spaced and confined to the spire whorls (Figure 2.2H).

Largely based on Kollmann's (2009) fossil-based evolutionary scenario, we infer three independent origins of varices in the Stromboidea. No varices occur in the oldest member of the group, the genus *Dicroloma* (Aporrhainae) of the Early Jurassic (Sinemurian) (Gründel *et al.*, 2009; Kollmann, 2009). Varices evolved first in *Spiniloma* (Spinilomatidae) during the Sinemurian, separately in *Pietteia* (Dimorphosomatinae) in the Middle Jurassic, and a third time in a lineage of Aporrhainae including the Late Jurassic genera *Dicroloma* and *Diempterus*. According to Kollmann's (2009) scenario, in the Aporrhaidae, the varices of the Early Cretaceous (Barremian) to Recent Arrhoginae (observed in the genera *Arrhoges, Graciliala, Latiala* and *Mexopus*) were inherited from dimorphosomatine ancestors, as were varices in some members of the Anchurinae (*Drepanochilus* and *Helicaulax*), which originated in the Barremian. The varicate Rostellariidae (Campanian Late Cretaceous to Recent) are diphyletic with separate origins in the varicate Arrhoginae (*Graciliala* and *Latiala*). The Strombidae of the Cenozoic are derived via the Rimellinae from the *Calyptraphorus* group of Rostellariidae (Kronenberg and Burger, 2002; Kollmann, 2009).

Finally, varices occur in the Late Mesozoic family Tylostomatidae (genera *Pterodonta* and *Tylostoma*). These varices are visible on the internal moulds (steinkerns), with generally two per whorl (Squires and Saul, 2004). Although Bandel (2007) considers them stromboids, Kollmann (2009) rejects this hypothesis on the grounds that a rostrum and an expanded outer lip, both characteristic of Stromboidea, are absent. Squires and Saul (2004) place this family as Caenogastropoda *incertae sedis*. The phylogenetic placement of Tylostomatidae remains doubtful, but we maintain its placement in the Stromboidea for now and consider their varices to have arisen separately.

Many stromboidean clades lack varices. In Kollmann's (2009) scenario, some of these clades are derived from avaricate Aporrhainae. These include the subfamilies Pterocerellinae and Harpagodinae. A loss of varices apparently occurred in some Dimorphosomatinae and in its derived clade Pugnellinae, as well as groups within the subfamilies Anchurinae and Arrhoginae, and separately in the temperate southern-hemisphere Struthiopterinae, which Kollmann (2009) derives from varicate Anchurinae. Within Strombidae, true varices have been lost in such genera as *Euprotomus*, *Harpago*, *Lambis*, *Lobatus* (some species), *Mirabilistrombus,* and *Tricornis*, but how often the loss of varices occurred in this group or in the Aporrhaidae remains unclear. The living southern-hemisphere family Struthiolariidae

and the Paleocene to Recent tropical Seraphsidae likewise lack varices, but the absence of a phylogenetic hypothesis prevents conclusions about whether this absence is primary or secondary.

2.3.3.3.9 Tonnoidea

Most tonnoid families have varices. In most cases, these follow a synchronized pattern of either varices every 240° (generally in Cassidae, Cymatiinae, Personidae, and some Tonnidae) or 180° (generally in Bursidae and Ranellinae) (Savazzi and Sasaki, 2004). The varices are generally robust, sometimes with a spiny posterior canal as in bursids, true spines as in *Bufonaria echinata* (Link, 1807), alate extensions like *Gyrineum* or *Cymatium,* or associated with a callus as in personids and some cassids. Most are thick and rounded with a prominent adapertural scar (Figure 2.2I). Interestingly, in some tonnoids, such as *Crossata* (Bursidae), the sculpture is not represented by thickenings, but rather by hollowed out distortions that are later filled in (Figure 2.2J). This is seen in bursids and 'ranellids', but not yet observed for personids or cassids. In the Tonnidae, we have identified only a single species, *Malea elliptica* Pilsbry and Johnston 1917 where varices have been observed (Beu, 2010). Interestingly, some families that have been placed as basal tonnoids, Eosassiidae (Aptian-Albian), Mataxidae (Campanian to M. Eocene), and Paladmetidae (L. Cretaceous) do not have strongly synchronized varices, suggesting that synchrony arose after the evolution of varices, although their true affinities are controversial (Sohl, 1964; Beu, 1988; Gründel, 2001; Bandel and Dockery, 2012). A single Early Cretaceous (Hauterivian?) origin of varices in the Tonnoidea seems likely, with subsequent losses within most families. A recent phylogeny found that all tonnoid families are monophyletic, except 'Ranellidae', and supports a monophyletic Tonnoidea with a presumed single origin of varices (Strong *et al.*, 2016). Stephenson (1952) mentions that the holotype of the basal tonnoid *Caveola pinguis* has a varix approximately dorsal, but this is probably not a subterminal varix because later he mentions that varices are occasional in this species.

Laxton (1970) described the growth of varices in some New Zealand 'ranellids', and described a pattern of growth similar to muricids (see 2.3.3.4.4 *Muricidae* below). The shell grows quickly from one varix to the next, leaving a thin sector of shell which is then reinforced during a growth hiatus after the varix has formed. The first occurrence of early varices during growth is related to food availability, with individuals exposed to fewer

resources growing varices on earlier whorls than those with more food. He also noted that although 'adults' did hide and fast while growing intervarical regions, the juveniles did not, presumably to enable faster growth.

As in eulimids, the varices of personids indicate regions where the axis of coiling changes, and in both cases, the ancestral unbent shell is reconstructed as varicate. Causation is unclear, however. If changes in the axis of coiling requires a growth hiatus, varices may simply be a product of the temporary growth arrest.

2.3.3.4 Neogastropoda

2.3.3.4.1 Maturifusidae

The family Maturifusidae comprises one core genus *Maturifusus* (Mid Jurassic to Late Cretaceous) and one or two additional genera according to various interpretations (Guzhov, 2001; Kaim, 2004; Gründel, 2005). All of them have axially sculptured siphonate shells. A single species, *Astandes ticurelatus* (Gründel, 2001), from the Bathonian (Middle Jurassic) of Germany, has some axial ribs enlarged as varices (Gründel, 2001), although these are not evident in the figures of Kaim (2004). The family is interpreted as either a stem group for neogastropods (Guzhov, 2004; Blagovetshenskiy and Shumilkin, 2006) or as ancestral to the clade Latrogastropoda of Riedel (2000), which includes the siphonate Tonnoidea and Neogastropoda as well as Naticoidea, Cypraeoidea, and related clades (for discussion see also Gründel, 2005; Kaim and Beisel, 2005; Bandel and Dockery, 2012). We interpret the appearance of varices in *M. ticurelatus* as separate from that in Tonnoidea and the various neogastropod clades in which varices occur because of the long time-gap between the Bathonian and the earliest varices in undoubted latrogastropods (Hauterivian, Early Cretaceous).

2.3.3.4.2 Strepsiduridae (= Strepturidae Cossmann, 1901)

The neogastropod family Strepsiduridae (Early Eocene to Recent) contains mostly species with a single terminal varix, including species of *Strepsidura* and the Pliocene to Recent genus *Melapium* (Vermeij, 1998). A Late Eocene species from Colombia described as *Peruficus olssoni* by Clark in Clark & Durham (1946) and tentatively assigned to *Streptostyla* by Woodring (1973), has a subterminal varix placed either 180° or 270° from the outer-lip varix in the two specimens of the type lot examined by GJV at the University of California Museum of Paleontology, Berkeley.

2.3.3.4.3 Conoidea

Varices occur only sparsely in the extremely diverse clade Conoidea. *Varicobela* in the Borsoniidae (Eocene-Oligocene), *Tenaturris* in Mangeliidae (Miocene-Recent), and several species of *Inquisitor* (Pseudomelatomidae, Eocene-Recent; Figure 2.2K) have occasional, unsynchronized varices in the form of broader ribs (Powell, 1966; Ladd, 1982). A subterminal dorsal varix is also found in the recent *Darbya* (Borsoniidae). Various tropical West Atlantic drilliids show a dorsal varix: *Agladrillia, Clathrodrillia, Imaclava, Fenimorea,* and *Syntomodrillia* (Powell, 1966; Woodring, 1970; Fallon, 2016) (Figure 2.2L). When comparing species with convincing varices to related species, some sister taxa have near-varices that either cannot be clearly distinguished from ribs, are too close to the aperture to separate from terminal varices, or do not span the whorl to distinguish from a dorsal knob.

This pattern of scattered species bearing varices suggests at least four varix origins within Conoidea, although further phylogenetic analyses will be required to estimate exactly how many. Notably, despite the high spire and regular ribbing in Turridae, Terebridae, Clavatulidae, and Clathurellidae, we identified no members with varices nor within the lower spired but hyperdiverse Conidae. Furthermore, those taxa with varices have remained surprisingly species poor.

2.3.3.4.4 Muricidae

Species of Muricidae bear the most stereotypical and elaborate varices. Muricids are currently divided into eleven subfamilies (Barco *et al.*, 2010, 2012), five of which we consider to be completely lacking varices: Rapaninae, Coralliophilinae, Trophoninae, Haustrinae, and Pagodulinae. All the other subfamilies have at least a few members with varices (Figure 2.2M-P). Many species have axial lamellae rather than varices, such as those in the Trophoninae, with very thin lamellae that lack the robustness, intervarices, and the spacing of varices (Figure 2.3C). The earliest varicate muricid is the Early Paleocene genus *Timbellus* (Merle *et al.*, 2011) with three or four synchronized varices on each whorl. Although the subfamily to which *Timbellus* belongs is unclear, Barco *et al.* (2012) suggests it may fit with the typhines. We estimate seven origins of varices in the Muricidae, but the lack of subfamilial trees makes this a broad estimate at best, with clear evidence of phylogenetic clumping. These seven origins are one each for Muricinae, Ocenebrinae, Ergalataxinae, Typhinae + Tripterotyphinae, and Aspellinae, as well as two origins within the Muricopsinae.

Muricid varices are in most cases synchronized between whorls and, if not, are generally evenly spaced. One of the key features of Muricids is the intervarical ribs. Nearly all varicate species have a regular number of ribs interspersed between varices. This pattern often arises gradually during growth from a juvenile pattern where all axial elements appear as ribs or lamellae. As the snail grows, the elements differentiate into regularly spaced, more elaborate varices, with intervarical ribs (Spight and Lyons, 1974). Although many *Hexaplex* lack intervarical ribs, these ribs are usually present on earlier whorls and are intermittently present on the last whorl (Merle *et al.*, 2011). Generally, muricid varices grow episodically, with short intense spurts of shell growth completing an intervarical region and varix, followed by periods of quiescence where shell growth is limited to reinforcing the new shell segment (MacKenzie, 1961; Inaba, 1967; MacGinitie and MacGinitie, 1968; Spight and Lyons, 1974; Spight *et al.*, 1974; Illert, 1981). Some authors report snails going into hiding and/or not eating during bursts of shell growth (Inaba, 1967; Carriker, 1972; Illert, 1981), but this is not true in the laboratory for muricids (Linsley and Javidpour, 1980), or for *Ceratostoma foliatum* in particular (Pers. Obs., NBW).

Muricid varix morphology has four distinctive features. First is the base of the varix, which can be rounded (as in *Haustellum*) or asymmetrical with a gradual adapertural side and abrupt abapertural side (as in *Typhis* and *Hexaplex*). Second is height variation, from low structures (*Hexaplex*) to extended (most *Timbellus*). Third is margin shape, which ranges from relatively smooth (*Ceratostoma* and *Haustellum*) through varying degrees of spinosity (*Murex*) including branching spines (*Chicoreus*). Last is the degree to which the spiral cords are emphasized in the varix, from very pronounced, forming a corrugated edge (*Ceratostoma*), to low spiral cords that are barely evident (*Siratus*). All of these parameters combine in various ways to describe the full diversity of varices in the Muricidae (Radwin and D'Attilio, 1976). The most common pattern is three varices per whorl, but two, four, and sometimes six per whorl also occur. In an extreme case, the genus *Muricanthus* (Muricinae) can have 12 varices per whorl.

The Ergalataxinae have a few varicate members: *Ergalatax, Cronia,* and *Phrygiomurex*, as well as the fossil taxa *Odontopolys* and *Lyropupura,* which are related to the avaricate *Vitularia,* and *Daphnellopsis* and *Lindapterys* whose relationships are poorly understood (Palmer, 1937; Lozouet *et al.*, 1994; Claremont *et al.*, 2013). The origin of the

Ergalataxinae is difficult to determine, but appears to have been in the Eocene (Vermeij and Carlson, 2000; Claremont *et al.*, 2013), with multiple varicate taxa from that time (*Daphnellopsis, Odontopolys, Morula purulansis* Martin, 1914 and *Lyropupura*). Ergalataxine varices are generally low and rounded, while they are flared in *Lyndapterys* and are mostly synchronized with two per whorl, even in the earliest *L. vokesae* Petuch, 1987 (E. Miocene) (Lozouet *et al.*, 1994). In some taxa, such as *Tenguella* and *Morula spinosa* (H. Adams & A. Adams, 1853), individuals have evidence of a growth stoppage prior to the aperture that resembles a varix. This may be a polymorphic trait in these species or could be due to failed predation events altering shell growth. Some shells show remnants of apertural teeth inside the shell at these locations, which we believe supports the latter hypothesis (Figure 2.3A).

Few Muricopsinae have true varices, despite having some of the most elaborate axial sculpture among muricids. Most species actually have impressively elaborate lamellae like the seemingly impossible branching club lamellae in *Homalocantha anatomica* (Perry, 1811) and its relatives (Figure 2.3F). Three groups show true varices: *Subpterynotus textilis* (Gabb, 1873), with three alate synchronized varices per whorl and identifiable intervarical nodes (E. Miocene-Pliocene) (Vermeij, 2005b). The other varicate genera belong to the *Favartia* complex: *Pygmaepterus menoui* (Houart, 1990), some similar species, and several *Caribiella*. We believe these represent two separate origins, based on the distinct morphology of *Subpterynotus.* This subfamily was deemed polyphyletic by Barco *et al.* (2010), and a great deal of uncertainty about generic placement remains.

Only in the Typhinae, which arose in the Early Eocene, and the very similar Tripterotyphinae, do all members appear to have varices (D'Attilio and Hertz, 1988). These subfamilies have similar large alate varices with a distinct intervarical anal tube. Only the most recent excurrent tube is open; previous ones are filled in during growth of the next varix. Shells in these subfamilies can have two to five varices; *Distichotyphis* for example has two varices per whorl, but most have three to four varices aligned per whorl.

Most Muricinae have varices, and the few exceptions are generally fossil groups that may be more properly considered Muricidae *sensu lato*, or stem muricids (*Attiliosa, Bouchetia, Calotrophon, Crassimurex, Eopaziella, Flexopteron, Nucellopsis, Paziella, Poirieria*). Truly spiny varices, epitomized by *Murex pecten*, only occur within the

muricines. *Bolinus*, with generally five to seven varices on the last whorl, has an interesting trend where the two earliest species, *B. beyrichi* (?L. Eocene – E. Oligocene) and *B. submuticus* (Early-Mid Miocene) (Grateloup, 1846), are the most variable in the number of both varices and intervarical ribs, a pattern that we would expect if varices arise before the canalization of their positioning.

Although the validity of the Aspellinae, whose members all have varices, is contested, we have kept it separate here (Barco *et al.*, 2010; Houart and Héros, 2013). *Aspella* bear two varices per whorl, on the edges of the dorsoventrally flattened shell. This genus arose in the Late Oligocene with *A. subanceps* d'Orbigny, 1852 (Merle *et al.*, 2011). Varix number is more variable in *Dermomurex s.l*, with two to eight varices on the last whorl, depending on the species. On earlier whorls, these are interspersed with intervarical ribs, which fade away gradually, and in some species, the number of varices also gradually decreases (Vokes, 1985). *Viator* has the largest number of varices (eight), while *Gracilimurex* only has two per whorl. The varices are aligned either with previous varices or previous intervarical ribs (Vokes, 1985). *Dermomurex* is the oldest genus, with *Dermomurex s.s, Takia,* and *Viator* extending back to the Early Oligocene (Merle *et al.*, 2011). *Ingensia* has four varices on the last whorl, and is most similar to *Dermomurex,* and no fossils are known (Houart, 2001). These genera are united by a thick intritacalx (an outer calcareous shell layer, above or replacing the periostracum), and low, rounded, smooth varices.

It is difficult to separate the varicate and avaricate Ocenebrinae into clear clades without a broad phylogeny of this morphologically diverse subfamily. The earliest appear in the Early Oligocene, while Ocenebrinae probably arose near the Middle Eocene (Vermeij and Vokes, 1997; Merle *et al.*, 2011). Although two varicate taxa included in the phylogeny of Barco *et al.* (2010), *Eupleura nitida* (Broderip, 1833) and *Ocinebrellus inornata* (Récluz, 1851) (called *Ceratostoma* in Barco *et al.* 2010), were not sister taxa, we feel greater taxon sampling will be required to answer this question. About half of ocenebrine genera have varices, and only *Ocinebrina* and *Ocenebra* appear to have both varicate and avaricate species, with a high degree of variability, even intraspecifically. Interestingly, the only muricid with a subterminal varix that we encountered was *Ocinebrina paddeui* Bonmolo & Buzzurro, 2006*,* which occasionally produces a single dorsal varix, about a half whorl back from the aperture (Bonmolo and Buzzurro, 2006). Ocenebrine varices can vary from low and

rounded in *Ocinebrina edwardsii* (Payraudeau, 1826) (these are only occasional) to the huge alate varices of *Pteropurpura* and *Ceratostoma.* Most have three varices aligned per whorl, except *Eupleura,* with two varices along the plane of the dorsoventrally flattened shell, and *Ceratostoma rorifluum* (Adams & Reeve, 1849), with four.

2.3.3.4.5 Buccinoidea

The relationships of the Buccinoidea are still debated, but we identified six or seven separate origins of varices, one for each of Buccinidae, Colubrariidae, Columbellidae, two in the Nassariidae (Nassarinae and Photinae), as well as a separate origin for *'Fusinus' fluminis* (Stephenson, 1952) from the Cenomanian, which may in fact be a basal neogastropod, and *Pseudoperissolax* (L. Cretaceous – E. Oligocene), whose affinity is still in flux. Squires (2015) placed *Pseudoperissolax* in the Muricinae, but we agree with Beu (Pers. Comm.) and prefer to place this as a buccinoid until further information is available.

Very few members of the Buccinidae possess varices. Only a few fossil species, *Euthria elatior* (Cossman and Pissarro, 1901) from the Middle Eocene and *Euthria varicifera* (Peyrot, 1928) from the Tortonian, showed some irregularly placed varices.

Most members of the Colubrariidae have broad rounded varices, the oldest of which are found in *Metula silvaerupis* (Harris, 1899) from the Early Eocene. Many have nearly to fully synchronized varices between whorls, generally 240° apart, especially in *Colubraria*, *Metula,* and *Cumia*, although the degree of synchrony is variable both within and between species. *Colubraria tortuosa* (Reeve, 1844) is of particular note, as the apex is often twisted or bent, with varices almost 360° apart (Savazzi and Sasaki, 2004) (Figure 2.2Q). As in Eulimidae and Personidae, the twisting line of varices matches closely with the concave portion of the spire's twist.

Most members of the Columbellidae also lack varices. Only some members of the *Strombina* group (Early Miocene–Recent) have dorsal and/or ventrolateral varices (Jung, 1989) (Figure 2.2R).

Although taxonomists have only reported varices in a few members of the Nassariinae, both fossil and Recent, close inspection reveals that many species are varicate. In nearly all cases, a single lateral varix is present, in addition to the terminal one. Species of *Plicarcularia* usually have a dorsal hump, and *Varicinassa* has multiple varices. The earliest varicate nassariine is *Buccitriton* from the M. Eocene, and species with one or more

subterminal varices are clustered in some genera of the recently reorganized Nassariinae: *Buccitriton*, *Nassarius s.s.* from the Indo-West Pacific, and the sister genera *Phrontis* and *Tritia* (Galindo *et al.*, 2016). Although these varicate clades are not perfectly clustered as sister taxa in the phylogeny, we suggest a single origin is appropriate for this subfamily.

Some Photinae bear varices. One is *Tritiaria* from the Middle Eocene, although the oldest, *T. cerralvensis* Gardner 1945 from the Paleocene, which is dubiously attributed to the genus, lacks varices (MacNeil and Dockery, 1984). A few low varices up the spire occur in *Antillophos, Europhos, Cymatophos, Metaphos, Philindophos*, and *Phos* (Figure 2.2S).

Other nassariid subfamilies lack varices altogether: Bulliinae, Buccinanopsinae, Cylleninae, and Dorsaninae. The avaricate condition also applies to stem-group nassariids of the Early Cenozoic in such genera as *Keepingia*, *Molopophorus*, *Colwellia*, *Desorinassa*, *Thanetinassa,* and *Whitecliffia*, some of which may be synonyms of each other, further suggesting that the varicate condition in Nassariidae may have arisen at least twice, once in Photinae and once in Nassariinae.

2.3.3.4.6 Cancellariidae

Many members of the Cancellariidae have varices (Figure 2.2T), including most Plesiotritoninae and a few Cancellariinae, although varices are lacking in Admetinae. The oldest varicate and avaricate species are found in the Maastrichtian Plesiotritoninae (L. Cretaceous), with a general trend of reducing varices in the Recent taxa of this subfamily compared to extinct Cancellariinae (Beu and Maxwell, 1987). Most species of Plesiotritoninae have a few varices scattered up the spire, while a few are at least partially synchronized, as in *Tritonoharpa* (Lozouet *et al.*, 2001; Landau *et al.*, 2006).

2.3.3.5 Lacking varices

A few groups that we consider avaricate have variously been claimed to have varices. One example is the Harpidae, with elaborate ribs, but they generally lack intervarical elements (Figure 2.3D). Recently Merle and Pacaud (2004) described the major and minor varices in *Eocithara,* which we consider to be sharp ribs rather than varices. In the Turbinellidae, the knobby ribs of *Vasum turbinellus* (L. 1758) resemble varices, but again lack the intervarical elements (Figure 2.3B). The elaborate sculpture in the terrestrial caenogastropod family Diplommatinidae we consider lamellae and are generally termed commarginal ribs (Liew *et al.*, 2014).

2.3.3.6 Other molluscs

Although we did not complete a thorough review, we found no clear examples of varices in the other molluscan clades or in brachiopods. However, both ammonoids and bivalves show some sculpture types reminiscent of varices.

2.3.3.6.1 Ammonoidea

Many ammonoids have periodic constrictions — grooves in the shell that appear to cut through other ribs and are sometimes associated with distinct shell thickenings (Arkell *et al.*, 1957). Shell thickenings are also found as internal ridges or pseudo-constrictions, without external structures (Westermann, 1990; Bucher *et al.*, 1996). These periodic shell thickenings are thought to indicate episodic growth and have occasionally been called varices, but are generally called constrictions (Seeley, 1865; Moore *et al.*, 1952; Bucher *et al.*, 1996). Many constrictions clearly share ontogenetic similarity with gastropod varices and could be termed varices. All ammonoid constrictions are regularly spaced — although not necessarily synchronized between whorls — with a set number of inter-ribs. This is almost certainly due to the septa and sutures present in ammonoids, but not in gastropods. Another major form of ammonoid shell sculpture similar to varices is megastriae, distinct radial elements that include a discontinuity in shell secretion (Bucher and Guex, 1990; Bucher *et al.*, 1996). The most intriguing type of megastriae are the parabolae of Phylloceratoidea, Lytoceratoidea, Perisphinctoidea, and the simpler flares of some Lytoceratoidea (Radtke *et al.*, 2016). Although in most cases these structures are worn smooth in the fossils, they were often large, sometimes undulating or spiny extensions of the shell. Cross sections of the shell reveal a discontinuity, a presumed hiatus in growth, and share many features in common with varices, especially those of muricids (Radtke *et al.*, 2016). Interestingly, it appears that these apertural flares were sometimes resorbed altogether, with the outer most edge falling off as an intact ring of shell, as seen in *Lytoceras* (Seilacher and Gunji, 1993; Radtke *et al.*, 2016). Megastriae are not generally synchronous, but may relate to periods of rapid growth (Bucher and Guex, 1990). Just like many muricids, juvenile megastriae are not as complex and may not clearly fit the definition, as they show an ontogenetic progression.

In at least some cases, both ammonoid constrictions and megastriae share sufficient similarities with our definition to be considered varices, although an exhaustive search, and

perhaps a much better understanding of ammonoid shell growth, would be necessary to firmly establish where the boundaries lie.

Some varix-like examples include most members of Ancyloceratidae (E. Cretaceous) showing periodically thickened 'major' ribs interspersed with smaller ribs (Arkell *et al.*, 1957). *Acantholytoceras longispinus* (Uhlig, 1883) (E. Cretaceous, Barremian; Lytoceratidae) has some striking spines on each constriction, although tubercles are found on the constrictions in a few other genera, and in *Hyphantoceras* (L. Cretaceous, Turonian-Santonian; Nostoceratidae), the constrictions are thin and flaring (Arkell *et al.*, 1957).

Several families of Ammonitina with periodic 'major' ribs look like varices, such as Puzosiinae (Hauterivian-Maastrichtian), Holcodiscidae (E. Hauterivian-L. Barremian), and Cheloniceratinae (Barremian-L. Aptian). Several of these ammonite groups show loose or irregular coiling in contrast to gastropods, where no varices are known among groups with loosely coiled shells.

2.3.3.6.2 Bivalvia

Although we will not discuss the entire diversity of bivalve shell sculpture, a few groups of bivalves have sculpture more or less reminiscent of varices. In the Trigoniidae some species, such as *Myophorella montanaensis* (M. Jurassic, Callovian), have sharp commarginal ribs on part of the shell which White (1880) (in Imlay, 1964)) termed varices. These are clearly not varices, however, as they do not extend the breadth of the shell. The Spondylidae have spectacular spiny projections, but these cannot be seen as varices because they do not connect along the growth axis into a single unit and they appear more as separate spines along ribs. A few venerids such as *Hysteroconcha* possess strong commarginal ribs (and spines, but fewer of them), but lack intervarical elements or evidence of periodicity. The sculpture most reminiscent of varices is found in the coarse commarginal nodes of *Swiftopecten swiftii* (Bernardi, 1858) and a few fossil pectinids, which appear as periodic commarginal thickenings, mainly on the right valve; however, these are pleats in the shell rather than thickenings (Hertlein and Grant, 1972) and so do not fit our definition of varices.

2.4 Discussion

2.4.1 Frequency of origin

Given their clear functional advantages (Carter, 1967; Spight & Lyons, 1974; Vermeij, 1974, 1982, 1995;Palmer, 1979; Miller & LaBarbera, 1995; Donovan *et al.*, 1999; Savazzi & Sasaki, 2004; Sälgeback & Savazzi, 2006), it is not surprising that varices have evolved many times in different lineages of gastropods and that many varicate lineages have diversified into large clades. The repeated evolution of adaptive traits, such as the varix, is a recurrent theme in evolution (Vermeij, 2006), reflecting not only a predisposition towards a common constructional mechanism of the trait, but also the wide range of circumstances in which varices confer a survival advantage. As indicated earlier, this advantage derives from the greater resistance of the shell to durophagous predators that break the shell, attack by way of the aperture, or attack an overturned animal that cannot right itself.

The distribution of varicate gastropods in space and time is consistent with the interpretation of varices as passive antipredatory armour. The varicate condition is particularly common and well developed in gastropods from warm shallow marine waters where predation pressure is high. It is rare in temperate, polar, and deep marine habitats, unknown in freshwater, and almost unknown on land. This follows the patterns of other defensive shell features such as small or narrow aperture, thickenings bordering the apertural rim, and a high spire associated with deep retraction of the soft parts. The variety and degree of elaboration of varicate shells greatly expanded from a modest beginning in the mid-Mesozoic. The most elaborate varices (in muricine muricids) arose in the interval from the Oligocene to the Recent. These spatial and temporal patterns may relate to the evolution, specialization, and distribution of predators, especially those that break shells or enter via the shell's aperture (Vermeij, 1977, 1995, 2015a).

Curiously, with the lone exception of the Middle Devonian genus *Spanionema*, the varicate condition did not develop during the Middle and Late Paleozoic. Beginning in the Silurian and continuing episodically in the Mid- and Late-Paleozoic, shell-breaking predators evolved and diversified in many clades (Signor and Brett, 1984). Yet gastropods evolved few of the antipredatory adaptations that became so prominent in Late Mesozoic and Cenozoic times (Vermeij, 2015a). Although the power and diversity of these later predators likely exceeded those of their Paleozoic counterparts (Vermeij, 1977, 1987, 1995), small

gastropods would surely have benefited from effective armour, including varices, even against relatively weak enemies. One possible explanation is that varices could deter a predator visually by clearly displaying its shell defences prior to contact, and that visually hunting, larger predatory fishes and crustaceans did not become important agents of antipredatory selection for bottom-dwelling gastropods until the Late Mesozoic. To test this hypothesis, it will be important to evaluate the sensory capabilities of predators as well as the mechanics of jaws and claws. Another hypothesis is that varices are more effective against peeling predators, while crushing was more common in the Paleozoic. Alternatively, Paleozoic gastropods may not have had the capacity to make varices, or perhaps lacked the ability to remove them efficiently to make way for further shell growth. The sculpture normally found in these groups is either restricted to the last whorl, or the upper part of the whorl, as in many Middle and Late Paleozoic gastropods, where they do not have to be removed to permit further shell growth (Vermeij, 1977).

2.4.2 Evolutionary history of varicate gastropods

I estimate conservatively that shells with non-terminal varices evolved independently 41 times. Many more origins might be inferred as our understanding of gastropod relationships improves, and as new taxa are described. Mapping the varicate condition onto a composite evolutionary tree of gastropods (Figure 2.4) shows that independent origins of varices are highly concentrated in a few large clades, especially in Sorbeoconcha. Multiple origins are known in such relatively restricted clades as Cerithioidea, Stromboidea, Muricidae, Buccinoidea and Conoidea. No cases have come to light in Patellogastropoda, Pleurotomarioidea, and Neritimorpha; and only one each is known for Rissooidea, Vetigastropoda, Campaniloidea, and Heterobranchia. The distribution of varicate gastropods is therefore highly phylogenetically clumped, which may have some interesting implications for the evolution of innovations (Vermeij, 2005a).

As is the case for other minor but functionally beneficial innovations in gastropod shell architecture like shell envelopment (Vermeij, 2005a), labral teeth (Vermeij, 2001), and the siphonal canal (Vermeij, 2007), clades with the varicate condition often remained at low diversity and had a geologically brief tenure. Of the estimated 41 origins of the varicate condition, at least 21 (51%) are represented by three or fewer genera, and at least eight (20%) contain varicate taxa from only one geological stage. Notably, seven of nine (78%) origins of

the varicate condition during or before the Early Cretaceous failed to stimulate diversification. Only two early clades, the Dimorphosomatinae + derived Stromboidea and the Tonnoidea, achieved diversity levels of ten or more genera, always during the Cenozoic.

2.4.3 Geographic distribution of varicate gastropods

Gastropods with the varicate condition are overwhelmingly found in warm shallow marine waters (Figure 2.5). Although a few muricids, epitoniids, ranellids, and bittiine cerithiids occur in cold waters, no varicate clade is known exclusively from or evolved in environments outside the tropics. A survey of Recent gastropod faunas (Table A1.3) revealed a well-defined latitudinal (and therefore temperature) gradient in the incidence of varicate taxa, with the highest frequencies occurring in the tropics (Figure 2.5). The high frequency of varicate taxa in the tropics is due largely to a few diverse clades, especially the Cerithiidae, Tonnoidea, and Muricidae.

With two marginal exceptions, shells with multiple varices are unknown in gastropods living in freshwater or on land. The exceptions are the genus *Faunus* in the cerithioidean family Pachychilidae, which has very weak rounded varices and is found in brackish coastal waters of the Indo-Malayan region; and the genus *Pythia* (Ellobiidae), an Indo-West Pacific group with marine larvae and nearshore terrestrial adult stages. The absence of varicate taxa in freshwater is especially surprising because of the high diversity of freshwater Cerithioidea. This clade has many marine representatives with varices, but no freshwater species — not even those in the Great Lakes of Africa or major river systems around the world — have varices. Whether this absence is primary or derived is not known.

Species with a dorsal knob or hump are exclusively tropical or warm-temperate in distribution, and almost all are sand-dwellers. This distribution is considerably more restricted than that of species with a dorsal varix, as seen in many temperate and tropical rock-dwelling muricids and in the intertidal rocky-shore and mangrove-associated cerithiid genus *Clypeomorus*.

Most varicate gastropods are of Late Mesozoic and Cenozoic age. A single varicate genus, the pseudozygopleurid *Spanionema* from the Givetian stage of the Middle Devonian, is from the Paleozoic. No Late Paleozoic or Triassic varicate gastropods have yet come to light.

Data in Table A1.2, summarized in Figure 2.4, indicate a very low incidence of varicate taxa in the Cretaceous, a slightly higher incidence in the Paleocene, and values reaching modern tropical frequencies by the Late Eocene. The low Cretaceous values generally lie in the range of Miocene to Recent temperate to cold-water faunas. Our data indicates a Paleogene rise in the incidence of antipredatory varices in warm-water faunas which parallels increases in other armour- and speed-related shell traits (Vermeij, 1995).

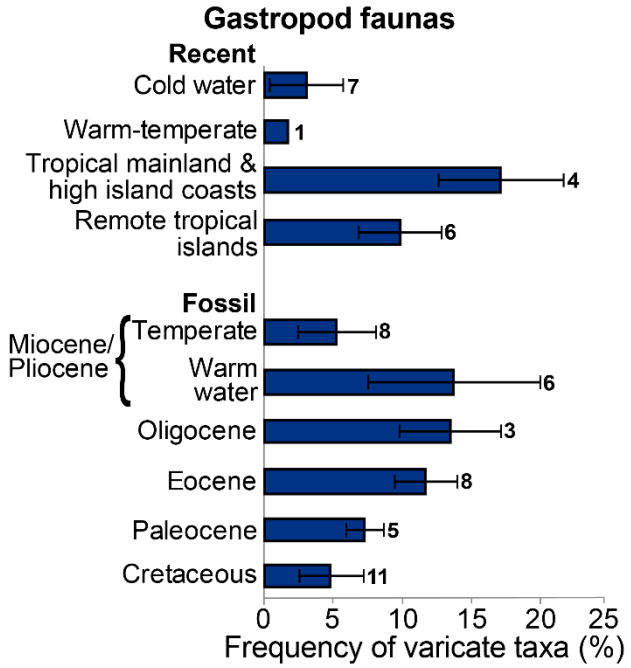

Figure 2.5. Percentage of varicate gastropod species in various faunas. Error bars are SD, numbers indicate number of localities included (see Table A1.1 for specific localities and sources). Miocene and Pliocene were combined to have sufficient samples to examine temperature trends.

2.4.4 Growth hiatus between varices

In many muricids and ranellids, growth stops for a period after a varix is completed, although juveniles appear to grow continuously from one varix to the next (Inaba, 1967; MacGinitie and MacGinitie, 1968; Laxton, 1970; Spight *et al.*, 1974). Varices are generally assumed to be associated with periodic growth in all groups, but this has not been widely tested. The advantage is obvious because they would have a robust apertural defence for a long time. Subterminal varices, whose morphology and placement generally do not suggest a robust aperture, but rather an accessory thickening for the mature last whorl, do not have this advantage.

If the growth of varices is periodic, most specimens should have an apertural varix, as intervarical regions are grown quickly, and the majority of time is spent between growth spurts (Chapter 4, Webster and Palmer, 2016). Two surveys support the idea that juvenile varices may not always be associated with periodic growth. First, we did a small survey of *Cerithium coralium* Keiner, 1841, a species with both rounded varices up the spire (not completely aligned), and a ventrolateral varix. Of 20 juveniles examined from a single population (~15-25 mm shell length), only one specimen had an apertural varix, suggesting that varices are not associated with a significant growth hiatus in this species. In contrast, the related *Cerithideopsis californica* (Haldeman, 1840), with more prominent rounded varices, and no obvious lateral varix, showed a greater tendency toward a growth hiatus. Of 31 juveniles examined (~15-30 mm), 48% had an apertural varix. How and when varices grow during ontogeny appears to vary. We predict that a growth hiatus is related to the degree of synchrony, rate of growth, and the size of varices.

2.4.5 Traits associated with the evolution of varices

Varices occur widely across the Gastropoda, mainly within the Caenogastropoda, and mainly in predatory groups, but also in herbivorous and detritivorous cerithioideans and stromboideans. Varices are found in snails from rocky, sandy, and muddy substrates, as well as in small and large species. Are varices associated with particular forms of shells or other ecological characteristics? Most species with terminal growth have some form of terminal apertural varix, and only these clades show a subterminal varix, although not all do. The majority of species with multiple varices have high-spired shells, but numerous exceptions exist: The Cassidae are a major low-spired, varicate exception, while many groups with the highest spires, Terebridae, Turridae, Turritellidae, Cerithiopsidae, Triphoridae, and Pyramidellidae, lack varices altogether. Withdrawal ability also correlates with the presences of varices. Both a fast and deep withdrawal decrease the effectiveness of shell peeling, and varices can hamper further peeling (Vermeij, 1995). The presence of sculpture on the shell also may increase the chance of evolving varices. If varices are elaborated ribs, ribs must already be present on the shell to develop into varices. Many groups with regular ribs do not have varicate members, such as the Costellariidae, and many of the conoidean families.

Harper (1997) suggested a correlation between a thin periostracum and sculpture in bivalves, and the same correlation may loosely apply in gastropods. Muricids and cassids

have a thin or almost nonexistent periostracum; however, ranellids have a prominent periostracum, and all have prominent varices. Testing this correlation in gastropods would require a more in-depth survey of periostracal properties in relation to shell sculpture.

Curiously, very few land or freshwater snails possess non-terminal varices. This could be due to a number of factors. From a cost perspective, the added shell of a varix would be more costly in these often calcium poor environments (Fournié and Chétail, 1984; Palmer, 1992). Land snails also generally 1) have a thick periostracum, which may limit sculpture formation (Harper, 1997), 2) have less well defended shells, 3) are thought to be under a lower level of predation pressure, and 4) withdraw slowly (Vermeij, 1995). Despite all this, terminal varices are quite common in pulmonate snails. Notably, the two pulmonates with varices are both found near-shore with crab predators (see 2.3.3.2.2 *Ellobiidae* above), and the sole varicate member of the freshwater Pachychilidae is found in brackish water.

2.4.6 Evolutionary origin of varices

Varices could have arisen via two hypothetical trajectories, and both could have occurred among the 41 separate origins. First, varices could have evolved by elaboration of existing periodic shell sculpture in ribbed ancestors. This appears to have occurred in many muricids (and ranellids), where the ratio of varices and intervarical ribs varies through ontogeny or between species, sometimes in clear repeated patterns as in *Hexaplex* or *Dermomurex*. This hypothesis would predict a gradual increase in varix prominence over evolutionary time, and some cerithiids with weak intermittent varices may indicate an early form.

Second, varices could have evolved from repeated production of a single ancestral terminal varix. In this scenario, periodic varices arise via duplication of a terminal varix during development or via a transition from determinate to indeterminate growth, while still maintaining the apertural varix. This would be akin to peramorphy, a form of heterochrony where maturity is delayed and adult structures (the varices) are further developed (in this case repeated) throughout ontogeny (Gould, 1977). This hypothesis follows the morphological 'countdown pattern' explored by Seilacher and Gunji (1993), where a series of iterative structures from the adult shell form prior to the terminal aperture. These structures arise evolutionarily 'backwards', starting at a terminal varix and rewinding ontogenetically. The countdown pattern clearly applies to subterminal varices, but it is less clear which patterns of

multiwhorl varices may have arisen this way. *Ellobium* exhibits a possible ancestral state of this scenario, where a second apertural varix appears to grow after the first, creating an identical dorsally placed varix.

These two hypotheses yield different predictions for the fossil record. The first requires ribbed ancestors, while the second requires heterochrony or a countdown. Varices have arisen independently many times, and both of these origins seem likely in many cases.

2.4.7 Synchrony of varices between adjacent whorls

In many groups, varices are synchronized — aligned with one another in adjacent whorls. This synchronization implies a developmental mechanism to rigidly control varix placement. Clearly, synchrony must have evolved after the origin of varices, but many puzzles remain about how snails maintain the synchrony of varices. Various models have proposed either an activation-inhibition system, a sensory feedback mechanism from previous varices, some way to sense rotation of the shell as the weight of one varix tips the shell balance point, or some combination of these mechanisms (Seilacher and Gunji, 1993; Hammer, 2000; Savazzi and Sasaki, 2004). How the first varix is positioned remains unclear. In many muricids, early whorls have a different sculpture pattern that gradually transitions to the adult form (Spight *et al.*, 1974; Vokes, 1985; Merle *et al.*, 2011), so the synchrony develops gradually. A synchrony of 240° (three varices in two whorls) challenges the tactile/feedback hypothesis because the mantle at the aperture cannot possibly extend back a full whorl to line up a future varix, so other mechanisms must be invoked.

Almost all regular patterns of varix synchrony exist. Some line up on each whorl, whether 360°, 180°, 120°, 90°, or 60° (equivalent to one to six varices per whorl), with three per whorl (120°) being the most common. Some groups alternate whorls, with 240° between varices. Each of these patterns lends itself to specific functions (Savazzi and Sasaki, 2004). Eulimids and colubrariids with one varix per whorl often have a curved columella, and the varix may be a point at which the axis of coiling changes. By keeping the change in inclination to the same part of the whorl, the shell develops a curve rather than wobbling at random between whorls. Similarly, many groups with two varices per whorl are dorsoventrally flattened along the varices (*Pythia, Biplex, Eupleura* and *Aspella*). Three varices per whorl (120°), three per two whorls (240°), and the rare four per whorl (90°) have a similar advantage with a varix always placed laterally to the aperture, similar to a

subterminal lateral varix. Shells with three varices per whorl also always have a dorsal varix, increasing the effective diameter of the shell and aiding in shell righting (Savazzi and Sasaki, 2004). As varix number per whorl increases, synchronization would seem to be less important, as varices are so close together.

For a single dorsal or lateral subterminal varix, synchronization is clearly not an issue; however, the position of single varices is always relative to the aperture, so some mechanism to control their placement is necessary. Presumably some manifestation of the terminal countdown mechanism allows this precise placement of varices (Seilacher and Gunji, 1993).

2.4.8 Conclusions

The term varix encompasses a broad category of shell sculpture that has arisen at least 41 times evolutionarily. As we predicted, these origins of varices were phylogenetically clumped and found mostly in derived gastropods, with most origins occurring during or after the Late Cretaceous. While no single pattern could explain how, when, or where this innovation evolved, a few clear patterns emerged: 1) Like other defensive structures, varices are more common in shallow, warm, marine environments, in which predation is intense. 2) High-spired shells and shells with collabral ribs were more likely to have varices. 3) Although many groups with varices failed to diversify, varices were correlated with diversification in some groups, especially the Tonnoidea. 4) The presumed morphological preadaptations and ecological conditions for varices differed between clades, demonstrating the multitude of pathways to produce this innovation.

Chapter 3 — How do gastropods control synchronized shell sculpture? Experimental shell manipulation of *Ceratostoma foliatum* (Muricidae: Ocenebrinae)

3.1 Introduction

Gastropod shells exhibit some of the most intriguing and beautiful forms in nature (Vermeij, 1995). Their regular geometric shape, and the great variety of relatively discrete elements they exhibit, makes them valuable systems for studying the mechanisms that underlie morphological patterning (Meinhardt, 1984, 2009; Meinhardt and Klingler, 1987). Their evolutionary history is reasonably well known because they are abundant in the fossil record, and their accretionary mode of growth means that nearly the entire growth history of an individual is preserved in its shell (Vermeij, 1995). Despite this, surprisingly little is known about how gastropods control the growth of shell ornamentation: How does a snail control when, where and to what extent periodic shell sculpture is produced?

The helicoid logarithmic spiral form of shells renders them particularly suitable for modeling (Urdy, 2015). In gastropods, shell shape, colour patterns, and to a lesser extent, various forms of shell sculpture have all been modeled geometrically (Thompson, 1917; Raup, 1966; Ackerly, 1989a; b; Morita, 1991a; Stone, 1999; Moulton *et al.*, 2012; Chirat *et al.*, 2013). Such models have been expanded beyond the reaction-diffusion systems of Meinhardt (1984, 2009; Meinhardt and Klingler, 1987) to include neurosecretory models (Saleuddin and Kunigelis, 1984; Ermentrout *et al.*, 1986; Boettiger *et al.*, 2009) and the 'road-holding' hypothesis, where shell expansion and coiling is guided by feedback from previously grown shell and keels (Hutchinson, 1989; Hammer and Bucher, 2005). Although the growth of shell sculpture has been widely observed (Berry, 1962; Gostan, 1966; Inaba, 1967; MacGinitie and MacGinitie, 1968; Laxton, 1970; Spight and Lyons, 1974; Spight *et al.*, 1974; Illert, 1981; Liew *et al.*, 2014), experimental studies of sculpture-growth mechanisms are rare (Checa and Jiménez-Jiménez, 1997; Checa *et al.*, 1998; Webster and Palmer, 2016). Yet to distinguish among various models of sculpture growth, experimental studies are essential.

One common and taxonomically widespread form of axial shell sculpture (sculpture parallel to the growing edge of the shell) is the varix, which can vary in size and complexity from subtle rib-like upliftings to large wing-like flanges or elaborate arrays of spines (Chapter 2, Webster and Vermeij, In Press). Many species produce varices at regular intervals as the shell enlarges, yielding a synchronized pattern of aligned structures between adjacent whorls (turns of the shell; Figure 3.1). The synchronized placement of varices between whorls implies a control mechanism to ensure proper spacing and alignment. Regular placement of sculpture is thought to result from some sensory feedback mechanism, where a varix on a previous whorl provides cues for the location of a new varix (Savazzi and Sasaki 2004). Because previous axial sculpture elements must be removed to produce new living space, they provide an obvious physical cue for where to initiate a new varix (Vermeij and Signor, 1992; Checa *et al.*, 1998). However, other models are possible and have not been tested.

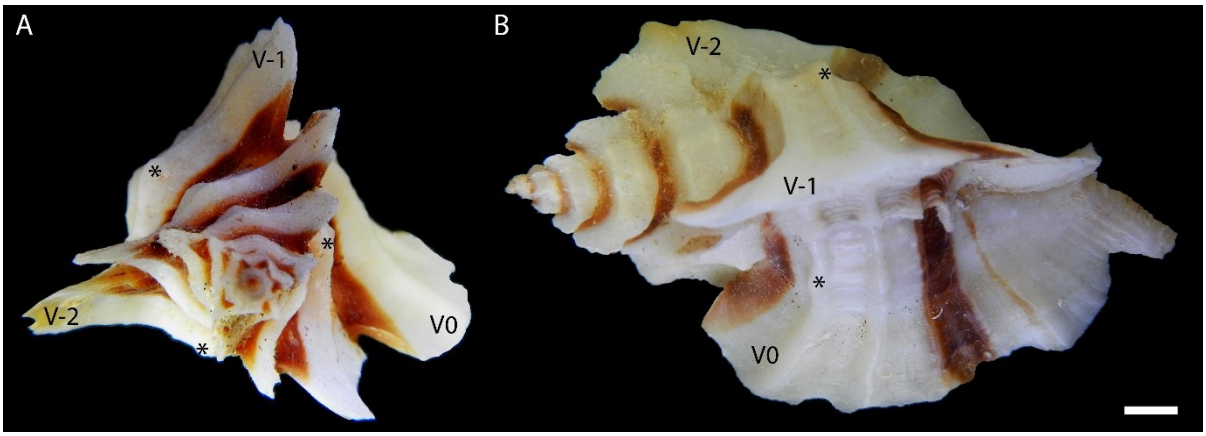

Figure 3.1. Synchronized alate varices of the muricid *Ceratostoma foliatum*, with three varices per whorl, and ~120° between them. A) Apical View. B) Dorsal view. Numbers indicate varix identity: V0: Apertural varix. V-1, Dorsal varix. V-2, Left varix. Asterisk: intervarical node.Scale bar = 5 mm.

Muricid gastropods produce some of the most elaborate forms of varices. *Ceratostoma foliatum* (Gmelin 1791), a predatory marine snail from the West Coast of North America, produces broad alate varices that are regularly spaced around 120° apart, resulting in three slowly spiralling arrays of varices when viewed from the apex, with an intervarical node between each pair of varices (Figure 3.1A). Here I tested the hypothesis that a previous varix provides the physical external cue to position a new varix correctly. I experimentally removed or transplanted varices on the shells of growing *Ceratostoma foliatum* to test

whether the encounter of a previous varix stimulated growth of a new varix as living space was being expanded. Furthermore, I explored experimentally whether, and how quickly, sculpture synchronization is restored following damage to the aperture.

3.2 Materials and methods

3.2.1 Field collections and husbandry

Actively growing *Ceratostoma foliatum* (18 – 44 mm shell length) were collected in Barkley Sound (British Columbia, Canada), both from rocky intertidal shores and by SCUBA, for all experiments (Table A2.1). In 2012 and 2013, snails were maintained in the laboratory in flow-through seawater tables (9 - 12°C) at the Bamfield Marine Sciences Centre (BMSC). Snails were held together in groups of five or six in individual, transparent Ziploc® containers (14 x 14 x 10H cm) perforated with holes. In 2014 snails were suspended from five vertical lines (100 cm apart) off the floating docks at BMSC in opaque Ziploc® containers (sprayed with black spray paint and then dried in the sun for one week to release all volatiles) with four to five containers per line, spread out 30 cm apart, between 50 – 200 cm below the surface. I assumed there would be no difference in growth among those depths. Containers were made opaque because muricids are thought to hide during shell growth, when they are most vulnerable (Carriker, 1972; Illert, 1981), and snail growth rates were low in the 2012-2013 laboratory studies. Snails were held off the docks rather than in seatables to better imitate wild conditions such as lighting. Individual snails were identified by gluing and coating a small printed numbered label on the penultimate whorl with cyanoacrylate glue. Snails were provided with small stones covered in barnacles (*Balanus glandula*) that were changed weekly to allow feeding *ad libitum* unless otherwise noted.

3.2.2 Varix numbering

Varices on all snails were numbered relative to the initial apertural varix at the time of collection (V0) (Fig 1A). Previously grown varices were numbered backwards from the aperture (V-1, V-2. etc.), and newly grown varices were numbered as increasing positive numbers (V+1, V+2. etc.).

3.2.3 Varix spacing in wild-caught snails

Varix spacing was measured for the apertural varix (V-1 to V0) in 130 field-collected *C. foliatum.* Of those, 21 were large individuals (68 - 71 mm shell length) collected from Grappler mouth (1967 and 1971) and stored in the Hazel Jones collection at BMSC. The rest were snails collected from seven different populations including the same area as the Hazel Jones collection (Grappler mouth) across Barkley sound (21 – 51 mm shell length) to capture natural variation in varix spacing (Table A2.1). Many of these snails were then used in the growth experiments described below.

3.2.4 Description of experimental treatments

Varices were removed with a 300 series Dremel grinding tool with 15/16" cutting wheel. Snails were repeatedly cooled (approximately every 20 s) in seawater to prevent overheating.

Snails were exposed to 11 different treatments over three years (2012-2014) (Figure 3.2):

T1. *Control*: no shell manipulation (Figure 3.2A).

T2. *Low Food*: no shell manipulation, with food provided two consecutive days each week; to test whether snails grew slower with less food available.

T3. *Transparent Container*: snails kept in transparent containers, no shell manipulation; to test the effect of opaque containers in 2014.

T4. *Local Cue Removed*: Proceeding varix removed from both the last whorl (left varix (V-2)) and the penultimate whorl (left remnant varix (V-5), contra Miller and LaBarbara (1995)) (Figure 3.2B). This removed the physical cue thought to trigger varix production: if this physical cue is necessary, then the newly grown (V+1) varix should lie ~240° away, rather than ~120° from the apertural edge.

T5. *Two Local Cues Removed*: both left (V-2) and dorsal (V-1) varices were removed (Figure 3.2B, dotted lines), to test whether the lack of multiple physical cues would have the same effect as removing a single local cue.

T6. *Aperture Removed*: the apertural varix (V0), siphonal canal, and as much of the last whorl previous to the aperture were removed without injuring the animal (Figure 3.2C), to test the effect of shell damage on subsequent shell growth. When removing the apertural varix

(V0), the snail was chased into its shell with a paintbrush as far as possible to reduce the risk of injury.

T7. *Aperture and Local Cue Removed*: Apertural varix (V0), left varix (V-2) and left remnant varix (V-5) removed (Figure 3.2D), to test the interaction between physical cue removal and shell damage.

T8. *Moved Varix*: Apertural varix (V0) was removed, and reattached to the shell at the intervarical rib position (V-2.5) before the left varix (V-2) using cyanoacrylate glue (Figure 3.2E), to test the effect of adding a physical cue to the shell, specifically using shell from the same individual. Glue was used the length of the moved varix. If physical cues are sufficient, then the newly grown (V+1) varix should grow adjacent to this transplanted varix.

T9-T10. *Added Varix*: A varix from an empty shell was removed and reattached to a living shell. Due to complications with attaching the added varix precisely, these snails were divided into two categories after gluing: *Added Varix Near* (AVN; T9; angle from aperture < 60°, V>-2.5, Figure 3.2F; solid lines) and *Added Varix Far* (AVF; T10; angle from aperture > 60°, V<-2.5, Figure 3.2F: dotted lines) and based on the angular distance between the added varix and the aperture. These treatments were designed in 2014 to reduce some of the drawbacks discovered in the *Moved Varix* treatment, including glue blocking the aperture and further shell growth (glue was only used where it would not impede further shell growth), and removing the complication of shell damage (the aperture was not removed). Some varices did fall off from the reduced use of glue, but they were reattached within seven days. They were also designed to test whether the location of the cue had an effect on future varix growth. These treatments have the same hypothesis as *Moved Varix*.

T11. *Glued Varix*: left varix (V-2) coated in cyanoacrylate glue along the adapertural side (Figure 3.2A; light blue), to test for artifacts induced by the glue used in *Moved Varix* treatment.

3.2.5 2012-2013 Experimental details

In June 2012, 78 *C. foliatum* (25 – 41 mm shell length) were randomly assigned to seven treatments with a comparable size distribution of snails in each treatment (n =12), except *Glued Varix* (T11, n = 6). Snails were given three weeks to acclimate to the sea tables

after collection, with the experiment starting on July 18, 2012, and ending December 11, 2013 (17 months). Treatments included (see 3.2.4 *Experimental treatments* above): *Control* (T1), *Low Food* (T2), *Local Cue Removed* (T4), *Aperture Removed* (T6)*, Aperture and Local Cue Removed* (T7)*, Moved Varix* (T8), and *Glued Varix* (T11). In May 2013, 60 snails (18 – 43 mm in shell length) were added, with the experiment starting on June 10, 2013, and ending December 11, 2013 (6 months). Treatments included (n = 12): *Control* (T1), *Local Cue Removed* (T4), *Aperture Removed* (T6), *Aperture and Local Cue Removed* (T7), and *Moved Varix* (T8).

Data from the 2012 and 2013 experiments were pooled as all treatments were identical except the duration of the experiment. Snails were photographed and weighed about every three weeks to track growth progress. Snails in 2013 did not get a pre-treatment photo for comparison of the regrown apertural varix (V0) where the aperture was removed. Snails were excluded from analysis if they began growing a new varix before their shell was modified.

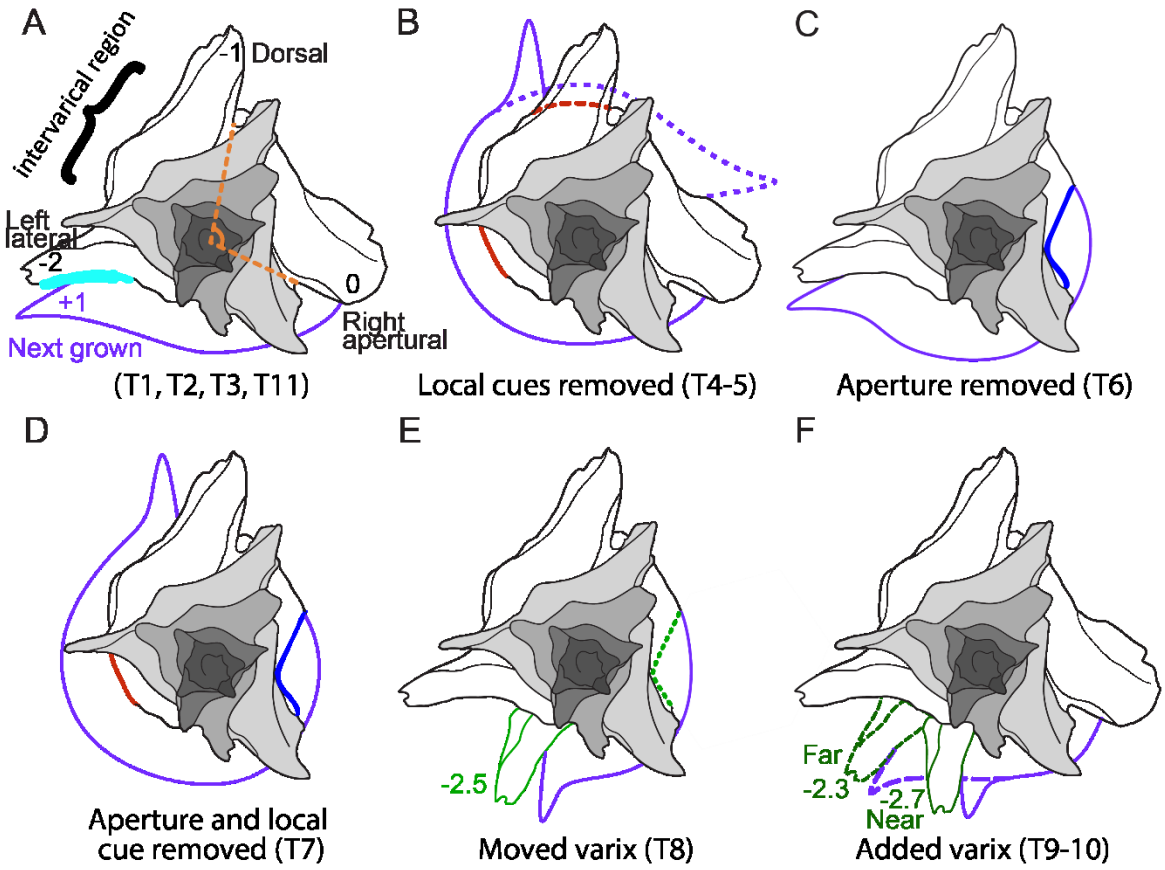

Figure 3.2. Shell-manipulation treatments. A) *Control* (T1, 2012, 2013, 2014). Angular shell measurement shown in orange, from the base of one varix to the base of the next, with the apex as the vertex. Light blue: position of glue in *Glued Varix* treatment (T11, 2012). B) *Local Cue Removed* (T4); left varix (V-2) removed (red marks base of removed varix) (2012, 2013, 2014); in *Two Local Cues Removed* (T5) the dorsal varix (V-1) was also removed (red, dashed lines) (2014). C) *Aperture Removed* (T6); apertural varix (V0, blue) removed (2012, 2013). D) *Aperture and Local Cue Removed* (T7); apertural varix (V0, blue) and left varix (V-2, red) removed (2012; 2013). E) *Moved Varix* (T8); aperture removed (V0) and glued back on in front of aperture (V-2.5, green) (2012, 2013). F) *Added Varix; Added Varix Near* (T9; V>-2.5, solid, green; 2014) or *Far* (T10; V<-2.5, dashed, green; 2014). Purple lines show new shell growth and predicted placement of a new varix assuming that a physical cue on the shell provides the signal for where the new varix should be placed.

3.2.6 2014 Experimental details

In April 2014, 105 *C. foliatum* (21 – 44 mm shell length) were randomly assigned to five treatments with a comparable size distribution of snails in each treatment. Snails were suspended from the BMSC floating dock in opaque (black) containers for over four months (May 13 - Sept. 23, 2014). Treatments included (see 3.2.4 *Experimental treatments* above):

Control (T1, *n* = 20), *Transparent Containers* (T3, *n* = 10), *Local Cue Removed* (T4; *n* = 20), *Two Local Cues Removed* (T5; *n* = 15), *Added Varix Far* (T9; *n* = 22), *Added Varix Near* (T10; *n* = 18). Photos were taken every week to track growth progress, but snails were not weighed repeatedly to avoid disturbing their growth. To measure the speed of varix growth, the aperture was scored from weekly photographs as either 1) Intervarical – shell added spirally in line with the whorl perimeter, 2) Uplifting – added shell was angled away from the whorl perimeter, 3) Filling in – added shell was proceeding towards the whorl perimeter on the apertural face of the varix, or 4) New lip – new lip forming at the base of the new varix. As it was sometimes difficult to determine when a 'new lip' had ended, some snails were excluded from estimates of stage 1 and 4 durations.

3.2.7 Specifics of measurements and analyses

The initial location of the apertural margin was marked with quick-dry nail polish in all snails (Gosselin, 1993). Shell length (apex to tip of siphonal canal) was measured with digital calipers (Mahr, MarCal 16EWR). Angular growth of the shell and the spacing between varices were measured from apical shell images using *ImageJ* (Rasband, 1997). Angular growth was measured from the starting point to the furthest extent of the new shell where it touched the last whorl. Angles were measured using the shell apex as the vertex, varix angles were measured at the base of the varix where it touched the last whorl (Figure 3.2A). Each angle was measured three times successively and blindly from the same image, and the average was rounded to the nearest degree. When the aperture was removed, the angular amount of shell remaining was measured from the dorsal varix (V-1). In some cases, snails did not regrow the removed apertural varix (V0) but did grow the next expected varix (V+1) — they 'skipped' replacing the apertural varix (V0). Here I measured an angle from the dorsal varix (V-1) to the next varix (V+1), producing an angle two times greater than normal. This angle was divided in two for visualization (e.g., Figure 3.8), but not for statistical analyses. Measurement error (mean percent error) was estimated by making blind repeated measurements on different days: a) for angular measurements from the same photographs: ± 5.3% (*n* = 140), b) for measurements of the same shell but from different photographs: ±5.7% (*n* = 40).

Prior to weighing, all epibionts were removed from the shell and any new epibionts were removed during the experiment. A regression of shell weight to immersed weight was

created following Palmer (1982) for *Ceratostoma foliatum* from two pooled populations (n = 31, slope = 1.53, intercept = 0.051, r^2 = .998). Shell weight was calculated from immersed weight (Mettler P153 balance) using this regression for all snails.

Statistical analyses were conducted in RStudio/R (RStudio Team, 2012), figures were created using the beanplot (Kampstra, 2008) and beeswarm (Eklund, 2016) R packages. Images were edited with Adobe Photoshop CS6 (2012 Adobe Systems Inc.) to adjust brightness, contrast, and to clean up the background.

3.3 Results

3.3.1 Varix growth

3.3.1.1 Effect of treatments on growth

Due to the periodic nature of varices, most snails either grew a varix or did not. Even though the 2012 snails grew for 11 extra months compared to 2013, the amount of shell grown in each treatment did not differ significantly between years (Figure 3.3A): (2-way ANOVA (treatment X year), Table A3.1, $F_{1,119} = 2.2$, $p = 0.14$), and there was no interaction between treatment and year ($p = 0.44$). In addition, a comparable number of snails grew a complete varix in both years: 55% of snails in 2012, and 53% of snails in 2013. Treatments did have a significant effect on the amount of angular shell growth (2-way ANOVA (treatment X year), Table A3.1, $F_{6,119} = 4.8$, $p < 0.001$), and data for 2012 and 2013 were pooled for all subsequent statistical tests. Angular shell growth in *Control* snails (T1; 41 ± 11° SE) was significantly less than in snails with the aperture removed: *Aperture Removed* (T6; 129 ± 20° SE), *Aperture and Local Cue Removed* (T7; 94 ± 16° SE), and *Moved Varix* (T8; 84 ± 14° SE). *Moved Varix* snails (T8) grew the least of the three aperture removal treatments (T6-8; Tukey's adjusted $p < 0.03$;Figure 3.3A). Angular growth did not differ significantly between *Control* snails (T1) and *Glued Varix* (T11; 42 ± 12° SE), *Low Food* (T2; 46 ± 19° SE), or *Local Cue Removed* (T4; 59 ± 14° SE) treatments (All Tukey's adjusted $p > 0.9$).

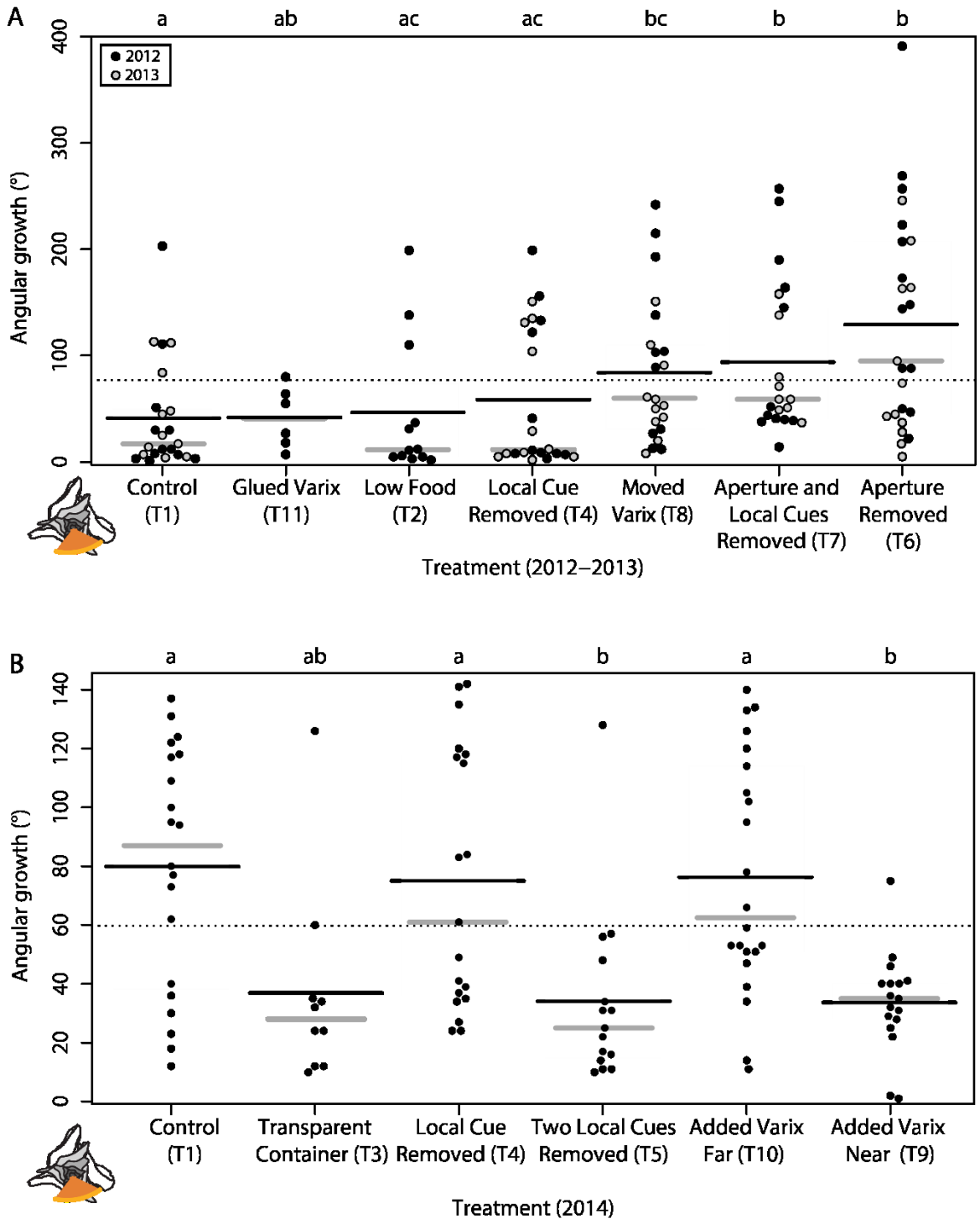

Figure 3.3. Angular growth of snails in all treatments. A) Snails grown in the lab in 2012 (black) and 2013 (grey). B) Snails grown in the field in 2014. Lowercase letters indicate treatments that did not differ significantly from one another (Tukey's adjusted $p < 0.05$). Circles represent individual snails; dotted lines: overall mean; black solid lines: treatment means; grey solid lines: treatment medians; shell diagram: angle measured, from V0 to end of growth (orange).

The 2014 experiments were not directly comparable to 2012-2013 because of the different treatments and the different growth environment (suspended from a floating dock vs. held in laboratory sea-tables). In 2014, treatments also had a significant effect on the amount of shell growth (ANOVA; Table A3.2, $F_{5,97} = 6.5$, $p < 0.001$; Figure 3.3B). Snails where two varices were removed (*Two Local Cues Removed*; T5) grew significantly less (34 ± 8° SE) than both *Control* snails (T1; 80 ± 9° SE) and those with only one varix removed (*Local Cue Removed*; T4; 75 ± 10° SE) (Tukey's adjusted $p < 0.02$; Figure 3.3B). Furthermore, when a varix was added near the aperture (*AVN*; T9; V<-2.5), snails grew significantly less (34 ± 4° SE) than both *Control* snails (T1) and snails with the added varix further away (*AVF*; T10; V>-2.5; (76 ± 9° SE) (Tukey's adjusted $p < 0.005$). Although snails grown in *Transparent Containers* (T3) grew notably less (37 ± 11° SE) than *Control* snails (T1), this difference was not quite significant (Tukey's adjusted $p = 0.06$), and may be due to the small sample size and high variance of the *Transparent Container* treatment (T3; $n = 10$).

3.3.1.2 Speed of varix growth

In 2014, 24 snails (23%) grew a complete varix during the experiment in all treatments. Average time to grow a complete varix, including the intervarical region, was 60 ± 6.7 SE days ($n = 11$). It took an additional 1 - 4 weeks to fully complete the lip and labral tooth after the new varix was started, although this timing was highly variable and subjective because incremental growth sometimes occurs at the lip long after the varix itself is complete. Varix growth occurred in three phases, each of which took about three weeks to complete: Phase 1: Growth of the intervarical region took 24 ± 1.5 SE days ($n = 11$). Phase 2: Uplifting of the new varix once it started (growing up and away from the shell) took 23 ± 2.1 SE days ($n = 23$) to complete, however those snails in the *Added Varix Far* treatment (T10; $n = 9$; *Added Varix Near* (T9) snails grew no varices) took significantly longer to grow the uplift (31 ± 3.7 SE days) than *Control* snails (T1; 17 ± 2.6 SE days, $n = 8$; Tukey's adjusted $p = 0.009$). Phase 3: Filling in the face of the varix and producing a new labral tooth took 16 ± 1.2 SE days ($n = 23$).

3.3.1.3 Varices are eroded from the base

Snails must remove the left varix (V-2) during growth because it impedes further shell growth (Vermeij, 1977). I observed that varix dissolution was part of the general process where the mantle smooths the shell surface in front of the aperture, removing all

sculpture and epibionts. Varices were removed gradually from the base, and generally broke off once thin enough, rather than being completely dissolved (Figure 3.9A). A remnant remained near the apical margin of the previous whorl, and did not impede further shell growth.

3.3.2 Varix spacing

3.3.2.1 Wild varices

In wild-grown varices, spacing varied from 81° to 140° among field-collected snails (mean: 111°, median: 111°). Varix spacing differed significantly between four of the seven populations where more than one snail was collected (ANOVA; Table A3.3, $F_{6,122} = 8.0$, $p < 0.001$; Tukey's adjusted $p < 0.05$; Figure 3.4). BMSC South docks (127 ± 3° SE) and Sandford Island (118 ± 2° SE) had the highest varix spacing angle, and Grappler mouth (106 ± 2° SE) and Nanat/Hosie/Ellis Islands (104 ± 2° SE) with the lowest. Shell length at the time of collection had no effect on varix spacing (ANOVA; $F_{1,119} = 2.0$, $p = 0.16$; data not shown).

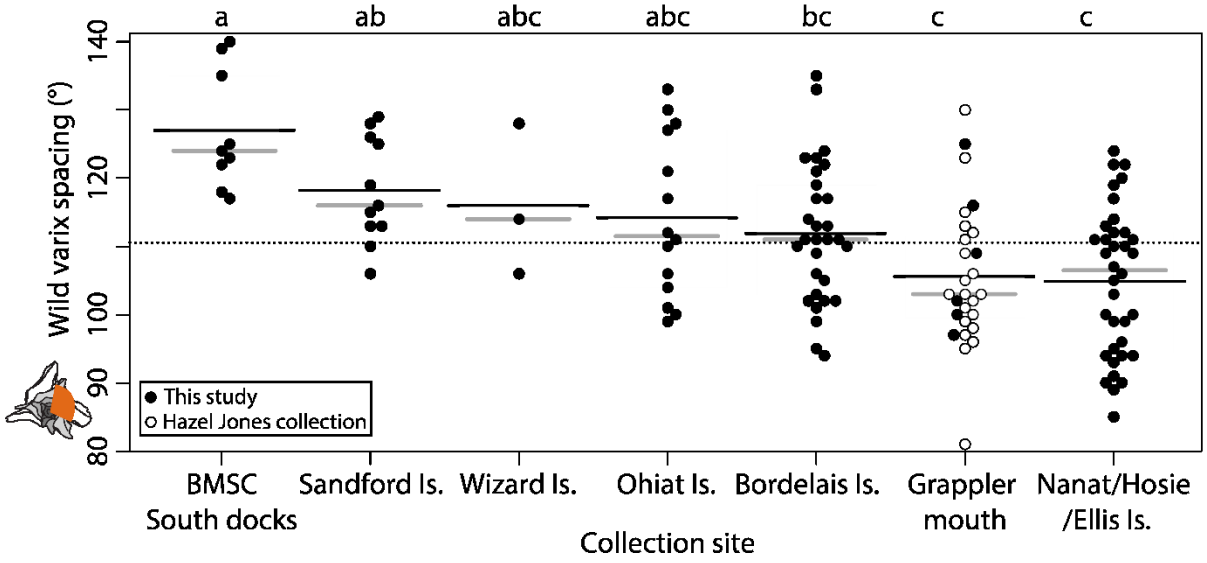

Figure 3.4. Varix spacing in wild populations. Letters indicate samples that did not differ significantly (ANOVA; $p < 0.05$). Circles represent individual snails; white circles: Hazel Jones snails; black circles: snails collected in this study; dotted line: overall mean; black solid lines: sample means; grey solid lines: treatment medians. Collection localities listed in Table A2.1.

3.3.2.2 *Control* snails

In 2012-2013, four out of 24 (17%) *Control* snails (T1) grew a varix, and in 2014, eight out of 20 (40%) *Control* snails (T1; in opaque containers) grew a varix. No *Transparent*

Container (T3; 2014) snails grew a varix. Varix spacing did not differ significantly between the *Control* (T1) snails in 2012-2013 and 2014 ($p = 0.84$), so they were pooled in subsequent analyses. Varix spacing in control snails differed significantly from wild snails, both from the same source population (Bordelais and Nanat/Hosie/Ellis islands; 2-way ANOVA site and treatment; Table A3.4, $F_{1,74} = 8.0$, $p = 0.006$) and from all wild snails pooled (2-way ANOVA site and treatment; Table A3.5, $F_{1,132} = 6.7$, $p = 0.01$) (Figure 3.5), with no interaction effect of treatment in either case ($p > 0.3$). However, the angular spacing of varices grown during the experiment in *Control* snails (T1) did not differ significantly from the previous, wild-grown varix on the same shell, although it was almost significant (Paired t-test; $t_{11} = -2.0$, $p = 0.07$) (Figure 3.6).

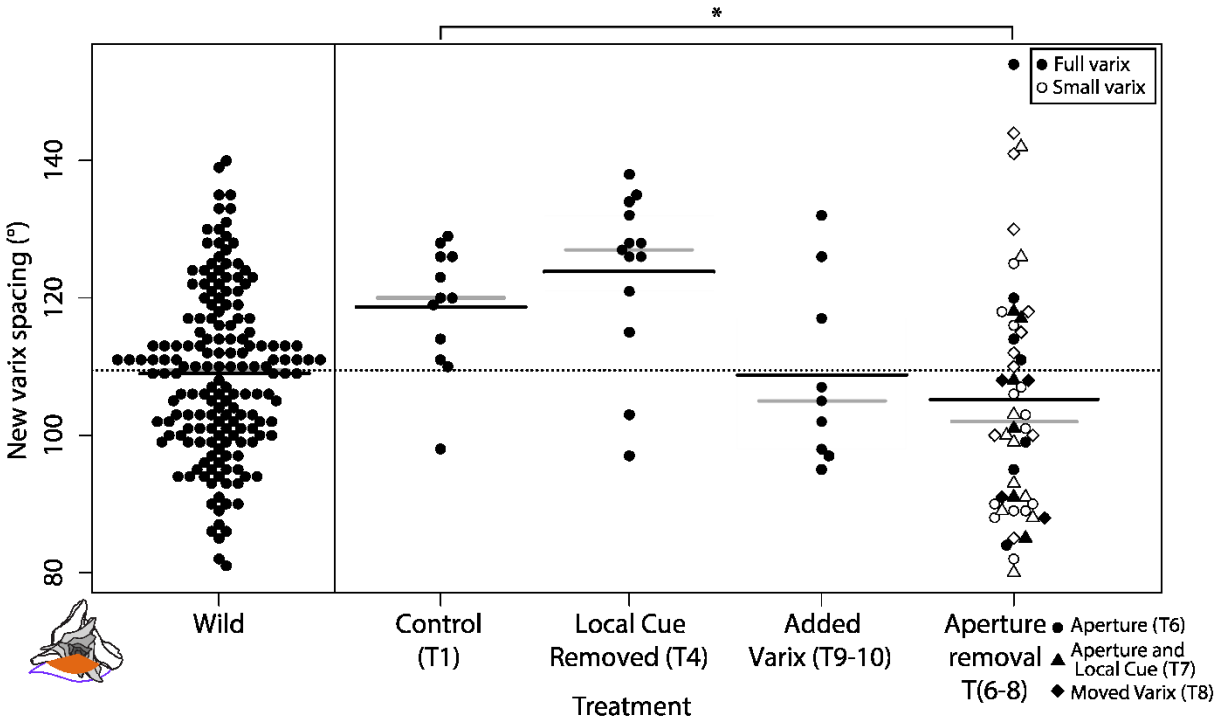

Figure 3.5. Varix spacing of new (experimentally grown) varices in different treatments. Varix spacing was measured as follows: Wild; distance from dorsal (V-1) to apertural varix (V0). *Control* (T1), *Local Cue Removed* (T4) and *Added Varix* (T9-10): distance from apertural (V0) to first grown varix (V+1). Aperture removal (T6-8): Distance from dorsal (V-1) to repaired apertural varix (V0). Symbols indicate individual snails. Aperture removal includes snails from three treatments: *Aperture Removed* (T6; circles), *Aperture and Local Cue Removed* (T7; triangle), and *Moved Varix* (T8; diamond). Open symbols, 'small varix' (See Figure 3.9D). Closed symbol, 'full varix'. Asterisk indicates aperture removal (T6-8) differed significantly from *Control* snails (T1; ANOVA; Table A3.6, $F_{5,78} = 4.4$, $p = 0.001$; Tukey's adjusted $p < 0.05$). Dotted line: overall mean. Black solid lines: treatment means. Grey solid lines: treatment medians. Shell diagram: angle measured, from V0 to V+1 (orange).

3.3.2.3 Effect of *Local Cues Removed*

In 2012-2013, six out of 24 *Local Cue Removed* snails (T4; 25%) grew the next varix (V+1). In 2014, 7 out of 20 *Local Cue Removed* snails (T4; 35%) grew the next (V+1) varix (Figure 3.9B), whereas no snails with *Two Local Cues Removed* (T5) grew the next (V+1) varix. Varix spacing did not differ significantly between 2012-2013, and 2014 so all *Local Cue Removed* treatments (T4) were pooled ($p = 0.5$). Varix spacing in *Control* snails (T1) did not differ significantly from *Local Cue Removed* snails (T4; Tukey's adjusted $p = 0.96$, Figure 3.5). In contrast, spacing of the new varix did differ significantly from that of the previous wild-grown varix on the same shell (Paired t-test; $t_{12} = -5.6$, $p > 0.001$; Figure 3.6).

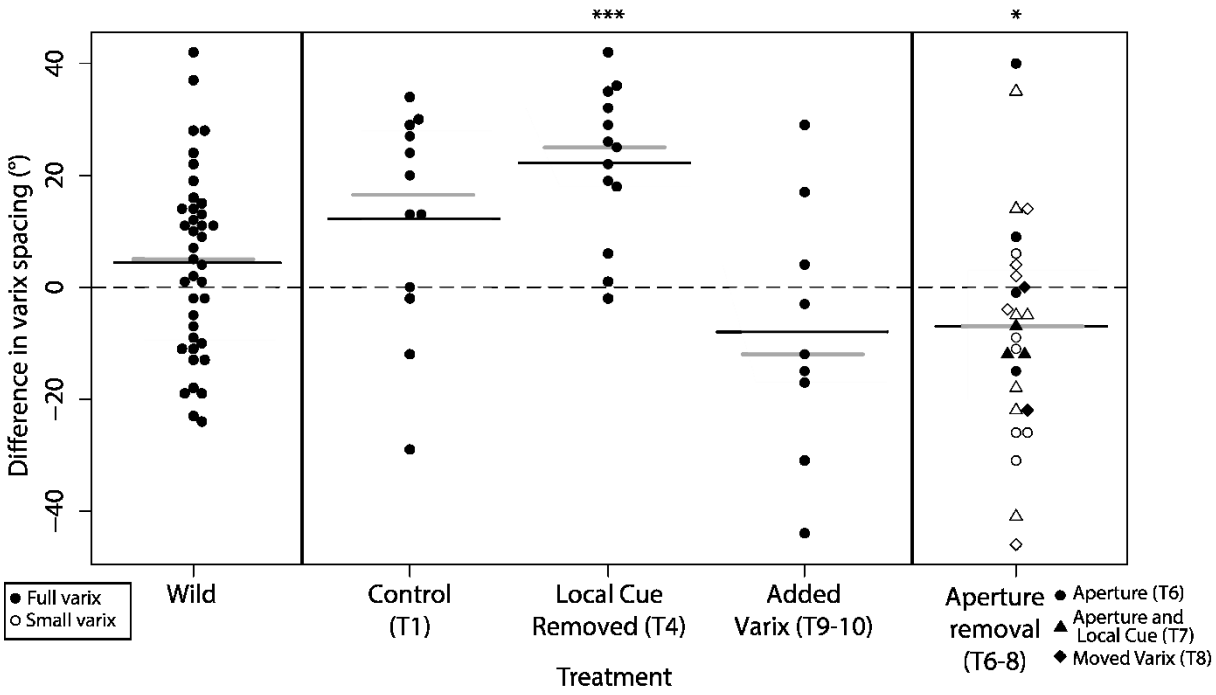

Figure 3.6. Difference in varix spacing between the initial wild-grown varix (V0) and new (experimentally grown) varix on the same shell. Symbols above the dashed line (0) indicate that treatment varices grew further apart than previous wild-grown varix, symbols below indicate treatment varices grew closer together. Aperture removal includes *Aperture Removed* (T6; circles), *Aperture and Local Cue Removed* (T7; triangle), and *Moved Varix* (T8; diamond) snails. Varix spacing of the aperture-removal snails (T6-8) was compared to the placement of the removed apertural varix (V0). Open symbols: 'small varix' (See Fig 3.9D);closed symbols: 'full varix';asterisks indicate significance of a paired T-test *(* $p < 0.05$; *** $p < 0.001$); dashed line: no difference in varix spacing; black solid lines: treatment means; grey solid lines: treatment medians.

3.3.2.4 Effect of aperture removal

When the aperture was removed (T6-8), snails responded in three ways. Either 1) the apertural varix (V0) regrew as a 'full varix' (Figure 3.9C), 2) a small uplifting ('small varix', Figure 3.9D) was produced in place of a complete apertural varix (V0), or 3) no regrowth of any sculpture near the previous varix location was observed ('no varix', Figure 3.9E). The type of varix regrown was affected by the amount of shell removed (ANOVA; Table A3.7, $F_{2,57} = 6.2$, $p = 0.004$). Snails were significantly more likely to regrow a full varix (64 ± 5° SE shell remaining) rather than a small (81 ± 3° SE shell remaining) or no varix (86 ± 6° SE shell remaining) when more of the intervarical region was removed along with the apertural varix (T6-8; V0) (Tukey's adjusted $p < 0.01$). No snails regrew a full apertural varix when more than 81° (about 1/2 of the intervarical region) of shell remained undamaged.

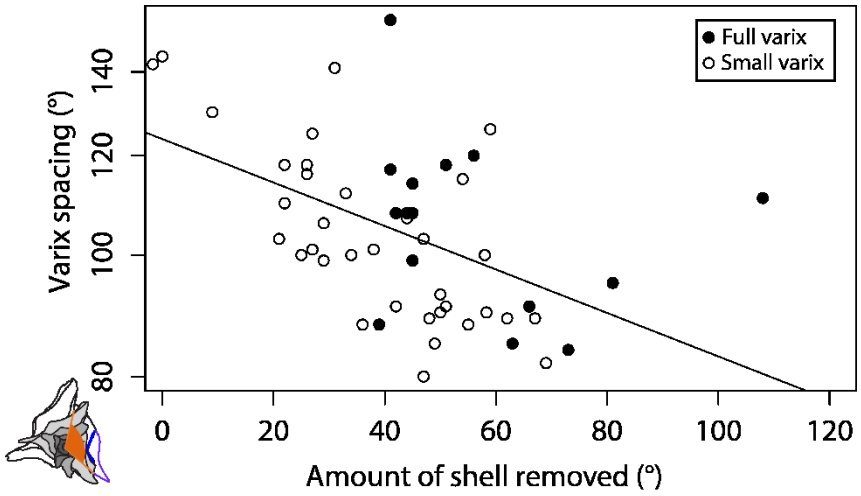

Figure 3.7. The varix spacing of new (replaced) apertural varix (V0) as a function of the amount of shell removed relative to the initial varix (V0). Open symbols: 'small varix'; closed symbol: 'full varix'; solid line: joint regression of small- and full-varix snails ($F_{1,48} = 15.7$, $r^2 = 0.23$, $p < 0.001$); shell diagram: angle measured (orange), from V-1 to new V0 (purple).

The distance to the regrown apertural varix (V0) from the previous dorsal varix (V-1) did not differ significantly between the three aperture removal treatments: *Aperture Removed* (T6; 104 ± 4° SE), Aperture and Local Cue Removed (T7; 101 ± 4° SE), or Moved Varix (T8; 111 ± 5° SE) (2-way ANOVA (treatment X type of varix grown); Table A3.9, $F_{2,44} = 1.1$, $p = 0.35$), and the interaction was not significant ($p = 0.10$). Nor did the varix spacing differ between full (107 ± 5° SE) and small (105 ± 3° SE) varices (2-way ANOVA (treatment X type of varix grown); Table A3.8, $F_{1,44} = 0.2$, $p = 0.70$), and the interaction was not

significant ($p = 0.10$). The three treatments and the two types of varices (full or small) were therefore pooled in all tests to examine how the apertural varix (V0) regrew following removal. The regrown aperture's varix spacing was significantly smaller than both the varix spacing in *Control* snails (T1; Tukey's adjusted $p < 0.04$, Figure 3.5), and original apertural varix (V0) spacing (Paired t-test; $t_{26} = 2.1$, $p = 0.046$; Figure 3.6). However, individually, the three aperture removal treatments (T6-8) did not differ significantly from *Control* snails (T1; Tukey's adjusted $p > 0.06$, Figure 3.5) or the previous varix ($p > 0.2$). The varix spacing of the regrown aperture decreased as more shell was removed along with the aperture ($F_{1,48} = 15.7$, $r^2 = 0.23$, $p < 0.001$, Figure 3.7).

3.3.2.5 Effect of *Aperture and Local Cue Removed*

Angular shell growth did not differ qualitatively or quantitatively between *Aperture Removed* snails (T6) and *Aperture and Local Cue Removed* (T7), either for the regrowth of the apertural varix (V0) (Figure 3.5), or growth of the next varix (V+1) (Figure 3.8).

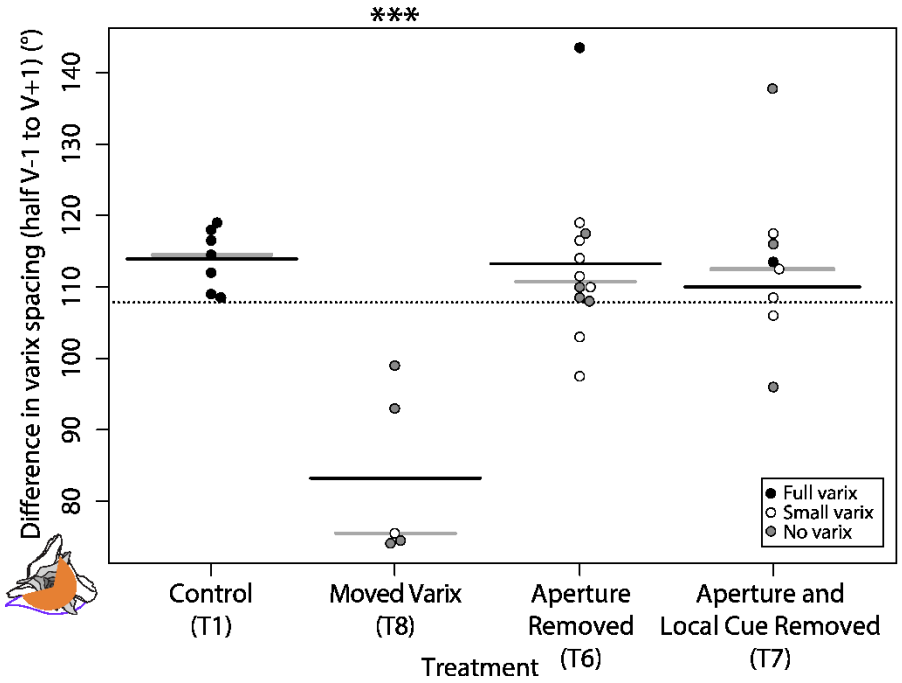

Figure 3.8. Difference in varix spacing for next varix (V+1). Measured relative to the dorsal (V-1) varix, then divided by two to include snails that grew no apertural varix (~120° expected). Points indicate individual snails. Colour indicates state of apertural varix (V0): Black, 'full varix'; white, 'small varix'; grey, 'no varix'. Asterisks indicate a significant difference from all other treatments (ANOVA; Table A3.10, $F_{3,27} = 13.8$, $p < 0.001$); dotted line: overall mean; black solid lines: treatment means; grey solid lines: treatment medians; shell diagram: measured angle (orange), from V-1 to V+1 (purple).

3.3.2.6 Effect of *Moved Varix*

The spacing of new varices (V+1) produced by *Moved Varix* snails (T8; 83 ± 5° SE) differed significantly from all other aperture-removal treatments (Tukey's adjusted $p < 0.001$): *Control* (T1; 114 ± 2° SE), *Aperture Removed* (T6; 113 ± 3° SE), and *Aperture and Local Cue Removed* (T7; 110 ± 3° SE) (ANOVA; Table A3.10, $F_{3,27} = 13.8$, $p < 0.001$, Figure 3.8).

Qualitatively, of the eight snails that grew far enough, one grew its next varix (V+1) in the wild location adjacent to the left varix (V-2) (Figure 3.9F). Only two clearly grew the next varix (V+1) adjacent to the moved varix (V-2.5) (Figure 3.9G), while five could not be scored definitively.

Some *Moved Varix* snails (T8) also grew a second (V+2) varix. All three of these snails grew abnormally, with the second varix (V+2) growing midway between two varices (Figure 3.9G). Two grew varices adjacent to the moved varix (V-2.5) and one skipped growing a next varix (V+1) altogether. Of the seven *Aperture Removed* snails (T6) that grew a second (V+2) varix, five grew the second varix (V+2) in the wild location, adjacent to the original left lateral varix (V-2) and two grew the second varix (V+2) midway along the intervarical region. Of these, one skipped the next (V+1) varix altogether, and the other did not.

3.3.2.7 Effect of *Added Varix*

In 2014, nine out of 39 (23%) snails from the *Added Varix* treatments (T9-10) grew a complete varix, all of which were *Added Varix Far* snails (T10; Figure 3.9H). The closer the varix was glued to the aperture, the less shell was grown (Regression; df = 37, $r^2 = 0.24$, $p < 0.001$, data not shown). Varix spacing in *Control* snails (T1) did not differ significantly from snails with an added varix (Tukey's adjusted $p = 0.7$, Figure 3.5). Varix spacing also did not differ significantly from the previous wild-grown varix on the shell (Paired; $t_8 = 1.2$, $p = 0.269$, Figure 3.6).

Qualitatively, six out of nine snails that grew a next varix (67%; V+1) grew it past the added varix (V-2.3) on the shell, while three appeared to grow it adjacent to the added varix (V-2.3).

3.3.2.8 Effect of *Glued Varix*

Shells where the left varix (V-2) was coated in glue (*Glued Varix;* T2) grew strangely, with a stuttering growth pattern. Only one out of six (17%) grew a next varix (V+1), which was obliquely angled and the left varix did not dissolve, forcing the snail to squeeze out a small opening (Figure 3.9I). The snails were incapable of removing the glue, although some managed to dissolve some of the shell beneath it.

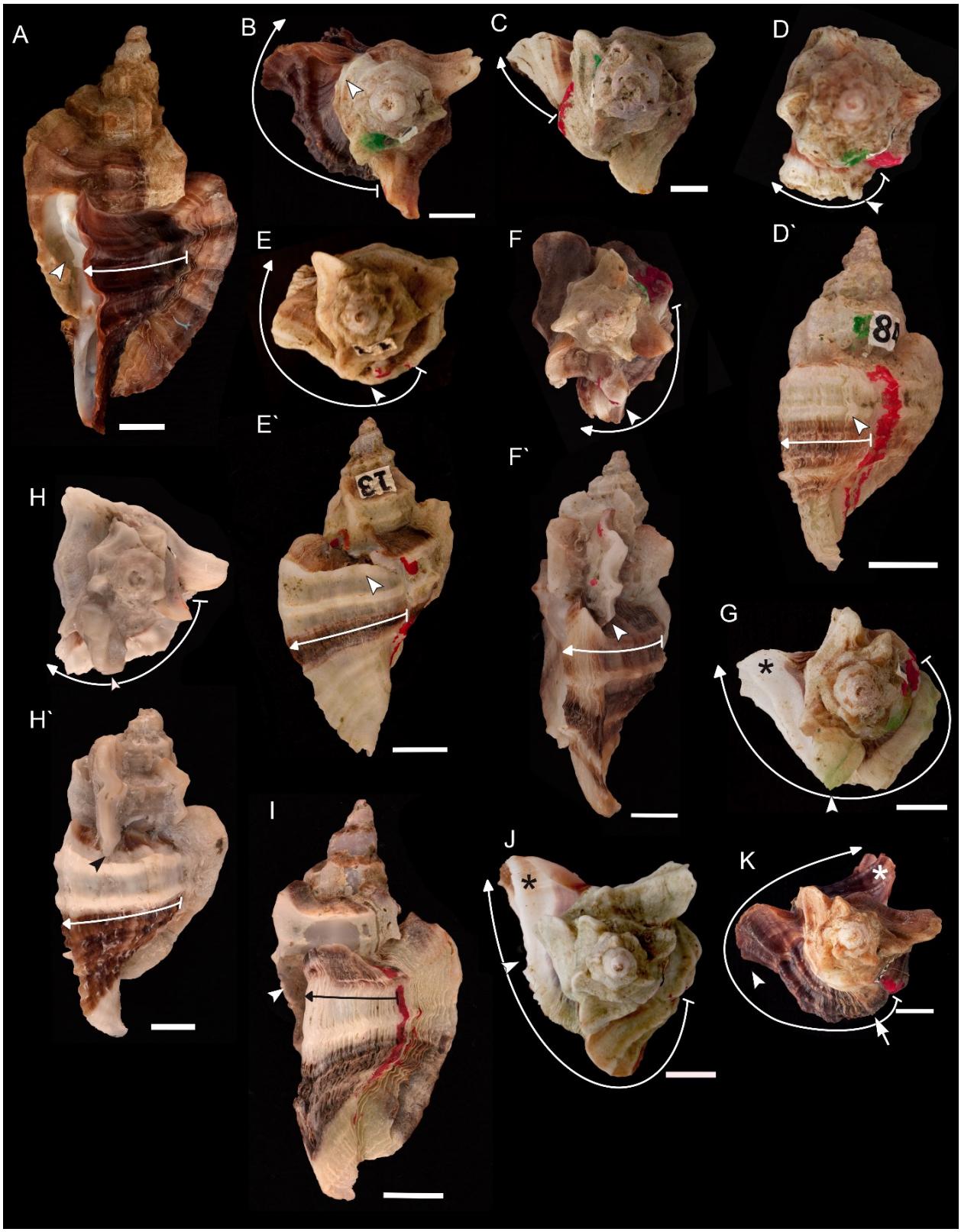
A
B
C
D
E
F
D`
E`
F`
H
G
H`
I
J
K

Figure 3.9. Growth of varices. A) Previous varix (V-2) starting to be dissolved at the base (arrowhead), lateral view. B) New varix (V+1) grown slightly past the expected location (arrowhead) in *Local Cue Removed* treatment (T4), apical view. CDE) Regrown apertural varix (V0). C) Full varix regrown, apical view. D-D') Small varix regrown (arrowhead), apical view (D), lateral view (D'). E-E') No varix regrown at expected location (arrowhead), apical view (E), lateral view (E'). FG) Location of next varix (V+1) grown in *Moved Varix* treatment (T8). F-F') New varix skipped moved varix location (arrowhead) and grew in wild location, next to V-2 varix, apical view (F), lateral view (F'). G) Varix grown adjacent to moved varix (arrowhead), second (V+2) varix grown midway along intervarical region (*), apical view. H-H') Varix skipped added varix location (V-2.3, arrowhead), and grew adjacent to wild (V-2) cue, apical view (H), lateral view (H'). I) *Glued Varix* treatment (T11) caused the next varix (V+1) to grow at an odd angle, and without dissolving the left varix (V-2; arrowhead), lateral view. J) *Aperture Removed* snail (T6) with fully repaired apertural varix that skipped the next varix (V+1; arrowhead) and grew an abnormal second (V+2) varix (*), apical view. K) *Aperture Removed* snail (T6) with 'small' regrown apertural varix (arrow), normal next varix (V+1; arrowhead) and grew an abnormal second (V+2) varix (*), apical view. For all paired images of the same shell, the shell was rotated 90° from the apical view to the lateral view keeping the aperture position relative to the viewer and the axis of coiling the same. White curved arrows show growth during the experiment that terminated at the aperture. Scale bars = 5 mm.

3.3.3 Shell malformation and anomalous growth

The most common form of anomalous growth we termed stuttering growth, where the shell did not grow smoothly but instead grew in a series of thick, bunched striations, each associated with a labral tooth (Figure 3.10A). This was distinct from normal varices and was especially common in aperture removal snails (T6-8). The cause of this is unclear, and these snails were excluded from varix-spacing analyses. In 2014, many snails (60%) in all treatments stopped growing suddenly between varices and grew a labral tooth. This coincided with a red tide in Bamfield, and these snails did not grow a varix (Figure 3.10B). In 2014, the difference between *Control* snails (T1) and *Transparent Container* snails (T3) would have been significant if all snails midway through a varix had completed them rather than stopping abnormally due to the red tide.

Two other snails grew anomalously in groups without shell manipulation. A *Low Food* (T2) snail and *Transparent Container* (T3) snail grew their next (V+1) varix past the left (V-2) varix cue (Figure 3.10C). The *Transparent Container* (T3) snail showed previous aligment errors on the shell, probably due to shell damage, but no obvious cause could be associated with the *Low Food* (T2) snail. Growth in captivity was clearly not identical to wild conditions, but the experimental design, controls, and general observations still shed light on how snails control shell sculpture patterning.

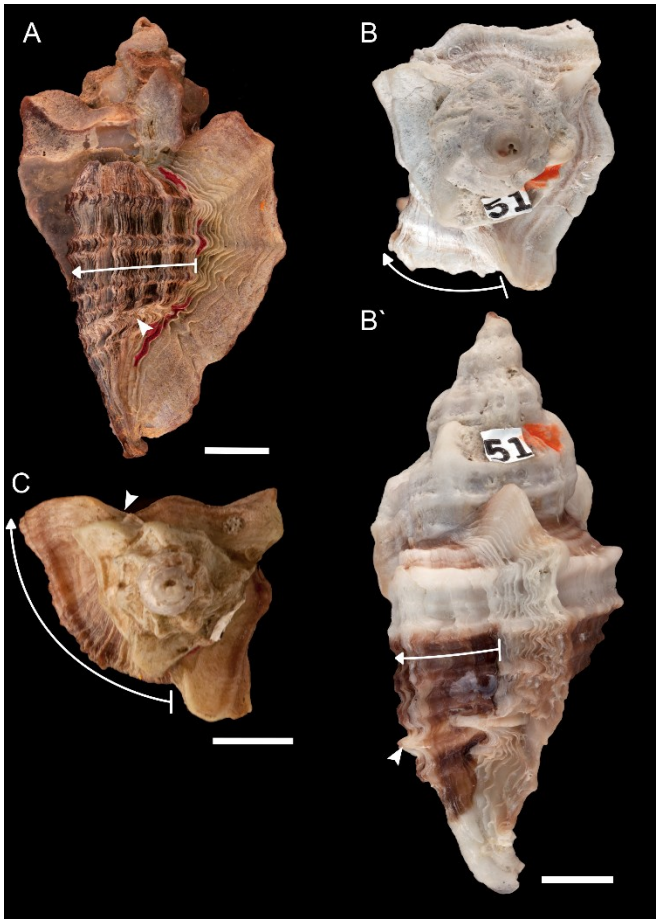

Figure 3.10. Snails with unusual growth not associated with a particular treatment. A. Stuttering growth with multiple apertural teeth (arrowhead) and ridges in *Glued Varix* snail (T11), lateral view. B,B'. Interrupted growth, probably due to a red tide in a *Control* snail (T1), with an labral tooth in the middle of an intervarical region (arrowhead) but no varix, apical view (B), lateral view (B'). C. *Low Food* snail (T2) that grew a varix past the left (V-2) varix cue (arrowhead), apical view. White curved arrows show growth during the experiment that terminated at the aperture. Lateral and apical view of the same shell (B,B') oriented as in Figure 3.9 ; scale bars = 5 mm.

3.4 Discussion

3.4.1 Varix spacing in wild snails

Varix spacing varied rather more than expected among wild populations, which might be due either to genetic or environmental effects. *Ceratostoma foliatum* has direct development with no pelagic stage (Spight *et al.*, 1974), which might facilitate genetic divergence among populations due to genetic drift (Palumbi, 1994). However, *C. foliatum* may not have been established in the region long enough for genetic drift to take effect because the last glacial maximum covered this region with ice. The related, direct developing

Nucella species in the region show two different genetic trends. *Nucella ostrina* exhibits a lack of population structure due, at least in part, to rapid range expansion from the south. In contrast, *N. lamellosa* does show population divergence, possibly due to refugia populations (Grant and Utter, 1988; Marko, 2004).

Environmental factors are a more likely cause of this natural variation in varix spacing, suggesting that varix spacing may be partially affected by phenotypic plasticity. The BMSC south docks and Grappler mouth populations were only 300-600m apart and yet showed significant differences in varix spacing (Figure 3.4), possibly associated with different microhabitats; the south docks snails, with widely-spaced varices, were living on dock pilings above a sandy bottom while the Grappler mouth snails with more closely-spaced varices, were living on intertidal rocks. Additional samples would be required to test associations between various differences between microhabitats — like predation and food availability — and varix spacing.

3.4.2 Treatment effects on angular shell growth

Due to the periodic nature of varix growth, most snails either grew a varix or did not and the likelihood of growing a new varix was affected by different experimental treatments. Aperture removal (T6-8) triggered a shell-damage response, and all those snails grew either a full varix or an immediate small varix. In contrast, varix removal decreased the amount of angular shell growth, but only if two varices (V-1 and V-2) were removed. The vibration and heat of dremelling may have stressed the snails, but it did not affect angular growth when a single varix (V-2) was removed, suggesting that shell removal itself was not a problem. Instead I suspect that removing the dorsal varix (V-1) had a larger effect because the heat and vibration was centered directly over the retracted mantle and head of the snail. Alternatively, the effect from removing two varices was sufficiently disruptive to be significant, while the effect of a single varix removal was not.

Adding a varix to the shell (T8-10) also affected the likelihood of producing a varix. Varices glued too close to the aperture may have prevented addition of new shell at the lip, perhaps by obstructing the aperture (Figure 3.3B). This would also explain why *Moved Varix* snails (T8) seemed to grow less than the other aperture removal treatments (T6-7; Figure 3.3A), although this was not significant statistically.

Muricids are thought to hide during shell growth when they are most vulnerable (Carriker, 1972; Illert, 1981), although Linsley and Javidpour (1980) disagree. So, snails in transparent containers may have felt less protected and therefore delayed shell growth, although this result was also not significant statistically. However, I did observe *Ceratostoma foliatum* feeding during intervarical growth in both the laboratory and in the wild, so feeding does not appear to be suppressed during intervarical growth.

The time to produce a varix in *C. foliatum* was considerably longer than Inaba (1967) reported for the muricid *Chicoreous asianus* Kuroda, 1942, which has varices that are spinier and require less shell material, and also lives in warmer water, all of which should decrease the time to grow a varix (Vermeij, 1995).

3.4.3 Shell repair and varix spacing

The process of shell repair is generally considered similar to normal shell growth, especially when repair occurs at the aperture (Watabe, 1983). However, depending on the location and severity of the injury, shell layers and crystalline structure may be disrupted in the repaired shell (Watabe, 1983; Fleury *et al.*, 2008). Several authors have based assumptions of shell sculpture control mechanisms by examining 'natural experiments' of wild damaged and repaired shells (Savazzi and Sasaki, 2004; Hammer and Bucher, 2005). However, here I showed that shell repair does not necessarily follow the same pattern as normal growth, and perhaps some caution should be used when interpreting shell repair as normal growth. Nonetheless, snails with less specific sculptural spacing may be less disrupted by apertural damage.

When the aperture was removed, *C. foliatum* quickly repaired the missing shell, and in most cases grew a new apertural varix (V0), either full size or a small thickening. This varix was positioned significantly closer to the dorsal varix (V-1) than to either the previous apertural varix (V0) or to the position for a new varix (V+1) in *Control* snails (T1; Figure 3.5, 3.6). The apertural varix was therefore not replaced with another synchronized varix. This response might be a defence mechanism, where a snail quickly grows a replacement varix to defend the aperture (Vermeij, 1987) sooner than wild varix positioning would allow. Snails that had more shell removed did grow their varix further back (closer to both the dorsal varix (V-1) and the shell damage), supporting this hypothesis. Other factors may affect how quickly or at what size a repaired varix is grown, including the snail's current energy

reserves or the presence of predator cues (Palmer, 1981; Appleton and Palmer, 1988). Most snails returned to normal varix spacing after repairing the apertural varix (V0), but a few grew the next varix too far along the whorl, suggesting that varix spacing could be disrupted more long-term (Figure 3.9J,K). I did observe disrupted varix-spacing rarely in the wild, but only on shells showing clear shell damage scars (Pers. Obs. NBW). These observations and results suggest that shell damage temporarily disrupts varix patterning, and in some cases can cause long term de-synchronization. So, because the shell-repair response seems to override normal shell growth, it is hard to infer how snails maintain sculpture patterning by damaging shells.

3.4.4 Control of shell sculpture synchronization

Two possible types of mechanism could explain the synchronous positioning of axial sculptural elements across adjacent whorls in mollusc shells: 1) a physical cue feedback system, where a new varix is triggered by physical detection of a previous varix, or 2) an endogenous molecular feedback or clock mechanism tracks angular growth to signal a new varix location. My results are most consistent with the second hypothesis, with some limited additional feedback from the shell.

3.4.4.1 Physical cue feedback hypothesis

The synchronized placement of axial sculpture is generally thought to be guided by the position of sculpture elements on previous shell whorls (Elder and Sibatani, 1991; Savazzi and Sasaki, 2004). However, this hypothesis cannot be a general one for regular varix placement. First, it does not easily apply to shells with widely spaced varices, such as two varices every three whorls (240°), which is common in many non-muricid gastropod groups (Chapter 2, Webster and Vermeij, In Press). Although such varices are formed in a regular pattern, they are not aligned between adjacent whorls, so one varix cannot act as a cue for positioning a new varix. Second, juvenile snails often lack varices (Chapter 2, Webster and Vermeij, In Press), so the first varices must be positioned without reference to any prior sculpture. For example, *C. foliatum* juveniles initially produce many narrow axial ribs that are gradually spaced further apart and increase in size until they achieve the adult pattern of three varices per whorl with intervarical nodes (smaller axial sculpture elements, see 2.3.1 *Type and variation of varices*, above) placed mid-way between each varix (Spight and Lyons, 1974). The adult synchronous pattern is not fully established until shells reach a

size of 4-5 whorls, at around 30 mm shell length, although this is highly variable (Pers. Obs. NBW). So, placement of new varices during this transition from asynchronous to synchronous axial sculpture in juvenile snails does not depend on the position of earlier varices.

Contrary to the hypothesis, external physical cues are not the sole guide for the synchronized spacing of varices in *Ceratostoma foliatum*. Previous varices were neither sufficient (*Added Varix*, T9-10, and *Moved Varix*, T8; Figures 3.5, 3.6) nor necessary (*Local Cue Removed*, T4, Figure 3.5) to induce a new varix near the expected location.

Nonetheless, physical cues do appear to help position varices more precisely. In the absence of a local cue varix (T4, T5, T7; V-2), varices grew significantly further along the whorl (about 20°) than the previous wild-grown varix (Figure 3.6), although overall this spacing did not differ significantly from *Control* snails (T1). Whether adding varices to the shell affected new varix placement is less clear, due to some unforeseen complications. The *Moved Varix* treatment (T8) had a significant effect; these snails grew the next varix (V+1) significantly closer to the aperture than snails with only the *Aperture Removed* (T6) or *Control* snails (T1; Figure 3.8). However, snails seemed unable to dissolve the glue used to attach the moved varix, which prevented further growth – as seen in the *Glued Varix* treatment (T11; Figure 3.3). So, this treatment effect was likely due to the glue preventing additional growth rather than a positioning cue provided by the location of the glued-on varix.

In 2014, I changed to the *Added Varix* treatments (T9-10), where the aperture was not removed and glue was only used to attach the added varix to the penultimate whorl, where it could not impede shell growth. Unfortunately, this reduced the fit of the added varix cue against the shell, which might have limited its effectiveness as a physical cue to trigger new varix formation. Despite or because of these corrections, *Added Varix* snails (T9-10) in 2014 did not grow varices significantly closer to the aperture as expected if the added physical cues affected varix placement. Two possibilities exist: 1) Added physical cues do affect future varix placement. In this case, the *Moved Varix* treatment (T8) shows the true effect, while the *Added Varix* (T9-10) results were not significant because the added varices did not contact the last whorl sufficiently to trigger a change in varix placement. 2) Added physical cues do not affect future varix placement. In this case, the glue disrupted varix positioning in

the *Moved Varix* treatment (T8), and the *Added Varix* (T9-10) results more accurately reflect the true signaling system.

Most aspects of shell growth — shape, coiling, color, sculpture — require some way for the snail to know its relative size and position to ensure proper shell growth. Physical feedback from the shell may provide cues for other aspects of shell growth. The road holding hypothesis states that snails control their coiling pattern – aligning one whorl of the shell relative to previous whorls — by 'following' cues on the previous whorl to maintain aperture position during growth (Hutchinson, 1989). This is a separate component of shell-growth patterning where the shell is hypothesized to act as a physical cue. Experiments with *Sphincterochila* support the road-holding hypothesis. A lower, silicone keel (parallel to shell growth), resulted in a change to the axis of coiling, showing that a physical cue was sufficient to change the axis of coiling (Checa *et al.*, 1998). In contrast, when the false keel was placed above the natural (and worn off) keel, very little, if any change in coiling was detected, suggesting the physical cue provided by the keel was not necessary for maintaining the axis of coiling. I have two hesitations about the robustness of these conclusions. First, the silicone itself might have disrupted shell growth, as the glue did in this study, by physically preventing the snail from following the natural keel, rather than by acting as a guide. Second, most snails in Checa *et al.* (1998) had their apertures removed, which could cause a damage response and disrupt the pattern of shell growth, as seen in several specimens they reported (their Figure 2E-H). So, whether local cues from the previous whorl guide the positioning of the mantle during normal spiral growth remains uncertain.

Weight distribution is another possible mechanism that might facilitate synchronous placement of varices. Snails are capable of changing shell coiling in response to balance disruptions. Checa and Jiménez-Jiménez (2003) observed that unbalanced weighting affected shell growth in members of the Planorbidae. The shell's coiling angle changed to counter a weight attached to one side of the shell so as to maintain an upright shell. This adds credence to Bunji Tojo's hypothesis (Savazzi and Sasaki, 2004) as well as Okamoto's (1988b) model to explain shell orientation in heteromorph ammonoids. As a snail's shell grows from one varix to the next, the position of each varix — each of which contributes significant mass to a shell – shifts, forcing the snail to adjust how its shell is held in position above the body. Shifts in balance could induce a snail to produce a properly positioned varix even when

varices do not abut one another. In juvenile snails, mass distribution would not change much as the shell grows until the sculpture reaches a large enough size to cause detectable changes in mass distribution, which could then cause a transition from a ribbed to a synchronous pattern. My results are at least partly consistent with this hypothesis. Removal of the local cue (T4, T5, T7; V-2) caused the next varix (V+1) to be placed slightly further along the shell in such a way that might correct for a weight imbalance caused by varix removal (Figure 3.6). Such placement of the next (V+1) varix would return the shell to its previous weight distribution. However, not all evidence from my experiments supports this hypothesis. For example, if a varix is added (T9-10; e.g., at V-2.5), this 'balance' hypothesis predicts that a new varix should be placed further than normal along the whorl periphery to counterbalance the added weight. I did not see such a shift (Figure 3.6), although the confounding effect of glue in the *Added Varix* treatment (T9-10) renders these results hard to interpret. Overall, I expect that weight balance does affect shell growth, but perhaps not the specific alignment of varices.

3.4.4.2 Molecular feedback hypothesis

Other organisms produce regularly spaced structures where the molecular mechanism is better understood, such as the somites of vertebrates or the regular branching patterns of plants. For example, vertebrate somites are regularly produced during development, where Hes/Her family gene expression oscillates regularly within cells using a negative feedback loop, and Notch acts to maintain synchrony between cells. A regular division of presomitic mesoderm is created, which produces regularly spaced somites (Soza-Ried *et al.*, 2014). Similarly, many plants have regularly branching roots, with a putative two-phase activation system (Norman *et al.*, 2013). First, a 6h oscillation associated with DR5 primes the cells for root branching. Then, bending of the root, a separate event, causes a stretch-receptor response to initiate development of the root branch and to determine the side (Norman *et al.*, 2013).

The growth of shells is fundamentally different from other developmental systems because the same cells of the mantle secrete the shell throughout life. In vertebrate somites (Soza-Ried *et al.*, 2014) and plant meristems (Norman *et al.*, 2013), mitosis constantly moves the stem cells forward, leaving behind differentiating cells that produce structures. Also, in

both examples, the molecular clocks oscillate in a matter of hours, whereas varices are produced months apart, and it is the spacing, not the timing that is regular.

Our results emphasize that something more than physical feedback is necessary to produce synchronized sculpture. Several theoretical models have suggested endogenous regulatory systems like local excitation with lateral inhibition models (LALI) may control shell growth, either through reaction-diffusion models (Meinhardt, 2009) or neurosecretory systems (Boettiger *et al.*, 2009). Models like these assume that snails control shell growth through some internal clock, where both a) how much shell has grown, and b) where the aperture is relative to other shell features, is tracked internally (Savazzi and Sasaki, 2004; Boettiger *et al.*, 2009). Unfortunately, these models are difficult to test experimentally without a much better understanding of the signaling systems involved in shell formation. Although modelling these hypotheses generally does not account for such widely-spaced structures as synchronized varices, more complex cascades of reaction-diffusion molecules are capable of signaling over longer distances by using a complex cascade of molecules (Heller and Fuchs, 2015), and neurosecretory systems should be able to act over sufficiently large spatial and temporal scales.

3.4.5 Conclusions

Our results reveal that 1) shell repair can temporarily disrupt the normal synchronized growth pattern, 2) *C. foliatum* can be induced to form a new varix as a response to shell damage, and 3) physical cues, like the encounter of a previous varix during spiral growth, are not the main mechanism used to position new varices relative to older ones. Varix synchrony must therefore arise via some other mechanism, possibly a LALI-based system (Boettiger *et al.*, 2009; Meinhardt, 2009), with some additional fine-tuning feedback from previous shell sculpture.

Chapter 4 — Shaving a shell: Effect of manipulated sculpture and feeding on shell growth and sculpture development in *Nucella lamellosa* (Muricidae: Ocenebrinae)[2]

4.1 Introduction

Gastropod shell sculpture offers a potentially intriguing tool to study morphological patterning. Shell sculpture is highly variable, yet made up of relatively discrete elements. As a snail grows, it must control when, where, and to what extent sculpture is produced. Although shell shape and, to a much lesser extent, shell sculpture have been modeled computationally and studied geometrically (Ackerly, 1989a; Hammer and Bucher, 2005; Meinhardt, 2009; Chirat *et al.*, 2013), the factors affecting sculpture growth have not been studied experimentally.

For spiral sculpture, which is oriented parallel to the direction of shell growth, a sculpture pattern could be set at the shell lip initially, and remain fixed for the rest of a snail's life; the shape of the mantle, which secretes the shell, does not need to vary over time to maintain sculpture patterning (Meinhardt, 2009). The potential mechanism is more complicated for axial sculpture, where ribs, varices, or lamellae are oriented perpendicularly to the direction of shell growth (parallel to the apertural margin). The mantle's form or positioning must vary over time to produce axial sculpture periodically. The degree of regularity in axial sculpture varies greatly. Varices — periodic thickenings of the aperture that uplift from the shell surface — are usually regularly spaced (Webster and Vermeij, In Press; Vermeij, 1995; Savazzi and Sasaki, 2004). This spacing yields a synchronized pattern in which each newly produced varix lines up with one on the previous whorl. Previous varices on the shell are thought to provide a cue for the location of these new varices (Savazzi and Sasaki, 2004). Varices are also thought to be associated with episodic shell growth, where shell length does not increase for some time after the growth of a varix, even though reinforcement of existing shell can occur, and the body may continue to expand to fill

[2] A version of this chapter has been published as: **Webster NB, Palmer AR. 2016**. Shaving a shell: Effect of manipulated sculpture and feeding on shell growth and sculpture development in *Nucella lamellosa* (Muricidae: Ocenebrinae). *The Biological Bulletin* **230**: 1–14.

the new living space. This hiatus between periods of shell growth often produces a thickened apertural lip, and can last for several months (MacKenzie, 1961; Inaba, 1967; MacGinitie and MacGinitie, 1968; Spight and Lyons, 1974; Spight *et al.*, 1974; Illert, 1981).

No hypothesis exists to explain how snails control less regular patterns of axial sculpture. *Nucella lamellosa* (Gmelin, 1791) is an intertidal muricid gastropod from the Pacific coast of North America and is best known for its highly plastic shell morphology, and its ability to change shell form adaptively in response to predators (Kincaid, 1957; Spight, 1973; A. R. Palmer, 1985; Appleton and Palmer, 1988). In the presence of crab predators, *N. lamellosa* grow a thicker shell, with minimal shell sculpture, and more well developed apertural teeth (Appleton and Palmer, 1988). Where crab predation is less of a threat, *N. lamellosa* generally exhibit the frilled form, even in the lab with low water flow (Figure 4.1). This thin-shelled, frilled form bears semi-regular axial sculpture, variously called 'foliate ribs' or 'lamellose ridges' (Webster and Vermeij, In Press; Kincaid, 1957; Abbott, 1974), but which we will refer to as lamellae. These axial lamellae resemble the varices of other muricids. Although they are thinner and more variable, they may have a similar function in shell defence (Palmer, 1979; Miller and LaBarbera, 1995; Donovan *et al.*, 1999) The axial lamellae of *N. lamellosa* are thought to reflect a trade-off between the slow-growing but well defended thick form, and a thin-shelled, faster-growing alternative, where lamellae may provide some reinforcement of the lip (Spight and Lyons, 1974; Palmer, 1981; A. R. Palmer, 1985). Similar lamellae occur in many other muricids (Radwin and D'Attilio, 1976).

Elaborate sculpture is possible only because most gastropods can dissolve shell material that might otherwise impede subsequent shell growth (Vermeij, 1977). As a snail grows, it must first remove sculpture from the previous whorl that may obstruct the aperture. The cost of such resorption in energy or time is unknown. Resorption of sculpture could impose additional energetic costs, or constrain the maximal rate of shell growth, by requiring more time to remove pre-existing sculpture.

Here we describe in detail — for the first time — the growth of axial lamellae in *N. lamellosa.* We explored the factors that affect lamellar growth, and how lamellae differ in form from varices: Are lamellae associated with a growth hiatus? Is the spacing between axial lamellae regular? How quickly are lamellae produced? Does feeding rate affect lamellar

spacing or shell growth rate? Do existing lamellae affect body growth rate or the addition of new lamellae?

4.1.1 Measurements and analyses

The starting location of shell growth was marked by painting the margin of the aperture with nail polish (Gosselin, 1993). Shell weight was calculated from immersed weight (Mettler P153 balance; Toledo Intl., Inc., Columbus, OH) following Palmer (1982). Shell length (apex to tip of siphonal canal) was measured with digital calipers (Mahr, MarCal 16EWR; Mahr GmbH, Göttingen, Germany). Shell diameter was measured, using digital calipers, on the body whorl starting at the aperture, and excluding lamellae (Figure 4.1A). Angular growth of the aperture and angular lamellar spacing were measured from apical shell images using *ImageJ* (Rasband, 1997). Using the apex as the center point, the angles were measured at the suture between the body whorl and the penultimate whorl. Angular lamellar spacing was measured from where the edge of the lamellae contacted the body whorl. This point was determined by drawing lines along the edge of each lamella from the shoulder (P1) to the suture (Figure 4.1A) to account for shell curvature. Linear distances along the arc of the shell — to report spiral growth of the aperture and lamellar spacing (distance between two adjacent lamellae) — was calculated from the angular distance using the following equation: $arc = \pi d*\theta/360°$, where arc = the linear distance, d = shell diameter (mm), and θ = angular distance (degrees). Forty *N. lamellosa* were measured in order to calculate the relationship between shell diameter and shell length (diameter (mm) = 0.380 * shell length (mm) + 3.323; $r^2 = 0.81$).

Measurement error (mean percent error) was estimated by taking blind repeated measurements on different days: shell length: ± 0.8% (n = 30); shell diameter: ± 2.5% (n = 40); lamellar angles, same photos +/- 16.6% (n = 28); lamellar angles, different photos +/- 6.9% (n = 28).

The state of apertural sculpture was scored in two stages. First, apertures were scored according to the state of the axial lamella: ‘no lamella’ (no outward bend of the aperture edge), ‘incipient lamella’ (evidence of some outward bending of the aperture), or ‘full lamella’ (a complete lamella was clearly present; see inset drawing, Figure 4.2). Lamellae were considered distinct when their tips at the primary shoulder cords (P1; Figure 4.1) were not touching. Second, the aperture was scored for the presence or absence of a ‘frill’ —

where multiple were lamellae stacked closely together; (Figure 4.1C). A frill was defined as axial sculpture at least three times as thick as other lamellae on the shell, and apparently made up of multiple lamellae stacked together.

When quantifying the timing of lamellar growth, frills were considered to be single lamellae, and the time to grow a lamella was counted from the start of one 'no lamella' phase to the beginning of the next 'no lamella' phase.

Statistics were run in RStudio/R (RStudio Team, 2012); the package 'Least-square means' (Lenth, 2014) was used to compute the mean response for each treatment at a standardized body size from the ANCOVA. Least-square means were calculated only when the slopes did not differ significantly among treatments (all cases). Images were edited with Adobe Photoshop CS6 (2012 Adobe Systems Inc.) to adjust brightness, contrast, and to clean up the background.

4.2 Materials and methods

4.2.1 Field collections and husbandry

Small to medium-sized 'frilled' *Nucella lamellosa* (15 - 36 mm shell length; Figure 4.1) were collected from the Ross Islets, Barkley Sound, B.C., Canada (48.8722, -125.1618) for all experiments. Snails reared in the laboratory were maintained in flow-through seawater tables (9 - 12°C) at the Bamfield Marine Sciences Centre. Six to ten snails were held together in perforated individual Ziploc® containers. For food, snails were provided with small stones covered in barnacles (*Balanus glandula*) that were changed weekly.

4.2.2 Feeding experiment

In June 2012, 36 *N. lamellosa* (16 - 27 mm in length) were collected and separated into three feeding treatments, with a comparable size distribution of snails in each treatment. Snails were acclimatized to laboratory conditions for two months. Those receiving the 'High' feeding treatment received *ad libitum* barnacles; those given the 'Medium' feeding treatment received barnacles for four consecutive days each week; snails receiving the 'Low' feeding treatment were given barnacles for two consecutive days each week. A bare rock was placed in the cage when snails were not being fed. Snails were grown for 112 days (almost 4

months). Immersed weight, shell length, number of axial lamellae, and spiral growth of the aperture were measured approximately every three weeks.

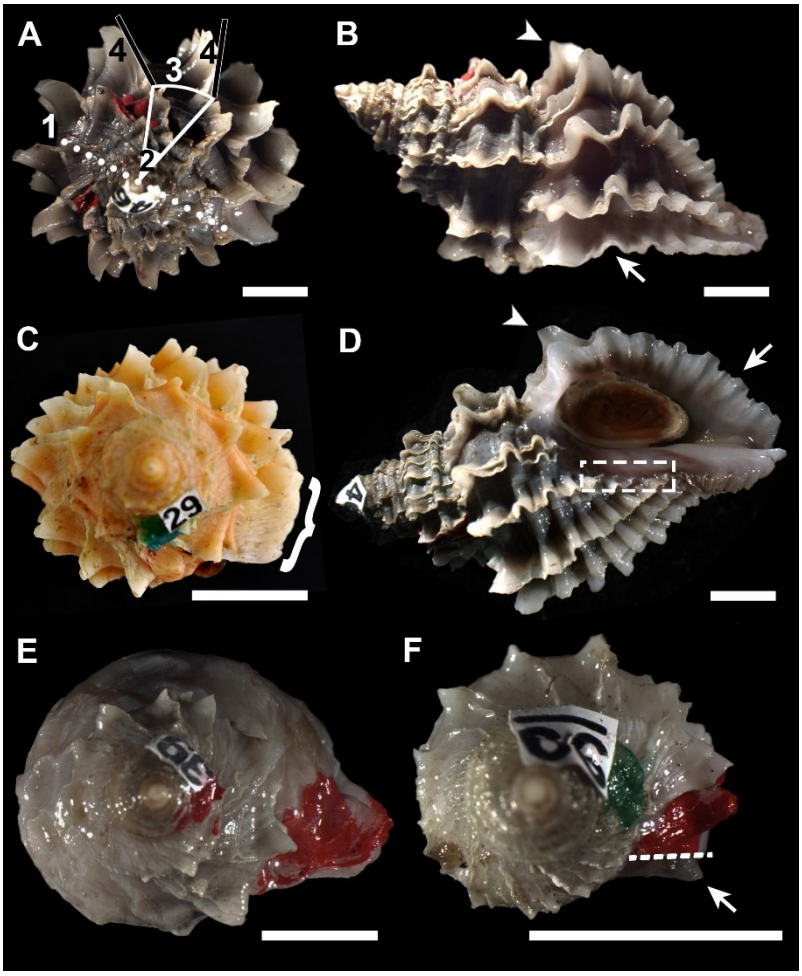

Figure 4.1. 'Frilly' *Nucella lamellosa*.Apex view, no shell manipulation, showing shell measurements: 1) shell diameter (mm) from aperture, across apex, to opposite side of whorl, excluding lamellae (dotted line). 2) Angular spacing of lamellae from apex to the points where individual lamellae touch the suture (white triangle; degrees). 3) Spiral lamellar spacing, calculated using shell diameter and angular lamellar spacing (white curve; mm). 4) Line along the edge of each lamella extended to the suture between ultimate and penultimate whorls, to mark the joining point of each lamella to the whorl (black lines). B) Side view of shell in panel A. C) Apex view showing apertural frill, made up of multiple lamellae (white brace: }). D) Apertural view showing previous lamellae being resorbed in front of the aperture to allow for continued shell growth (dashed box). E-F) Sculpture removal treatments: a 'shaved' shell with all lamellae (except the apertural lamella) of the last whorl removed, with no damage to the body whorl E); aperture removed (arrow): only the single lamella at the apertural margin was removed, including a portion of the body whorl F). Scale bars = 5 mm. Arrowhead: shoulder cord (P1); arrow: apertural lamella.

4.2.3 Sculpture growth-rate

To quantify the rates of addition of new lamellae and spiral shell growth, 33 *N. lamellosa* (16 - 36 mm shell length) were collected in April 2014 and grown for 56 days in individual containers. The number of barnacles eaten was scored weekly by counting empty tests (stones were cleared of all empty tests before being placed in the cage), and the state of apertural sculpture was scored every one to two days for two periods of 22 days each (the first and second time periods) separated by 12 days, during which there was no scoring.

4.2.4 Field sculpture-growth

In April 2014, 148 *N. lamellosa* were scored in the field for shell length and state of apertural sculpture to document the proportion of each stage found in the field.

4.2.5 Sculpture-removal experiment

In April 2013, 90 *N. lamellosa* (15 - 33 mm shell length) were collected and separated into three treatments, each with an even size distribution. Snails were acclimatized to laboratory conditions for one month. 'Lamellae removed' snails had all shell sculpture except the apertural lamella removed with a Dremel grinding tool (300 Dremel series; Robert Bosch Tool Corp., Anaheim, CA). This did not damage the body whorl or otherwise harm the snail. (Figure 4.1E). 'Aperture removed' snails had the apertural lamella removed including the portion of the body whorl extending to the penultimate lamella (Figure 4.1F). 'Control' snails experienced no shell manipulation. Snails were grown for 141 days (more than 4 months), during which, immersed weight, shell length, number of axial lamellae, and angular growth were measured at three times.

4.3 Results

4.3.1 Are lamellae associated with a growth hiatus?

Nucella lamellosa of all sizes showed evidence of recent spiral growth in the field: 50% - 70% of snails of all size classes were observed without a complete apertural lamella. The proportion of 'growing' snails did not differ significantly among size classes ($\chi^2 = 5.9$, df = 6, $p = 0.44$; Figure 4.2). Frills, areas where many lamellae were grown all together, were found only in snails larger than 20 mm in shell length. The proportion of snails with frills increased with shell size (Figure 4.2).

4.3.2 Is the spacing between axial lamellae regular?

The spacing between adjacent lamellae varied from 0.4 to 9.0 mm (mean = 4.0 ± 0.05 mm, n = 888; Figure 4.3A). The level of variation in lamellar spacing differed among snails, with the standard deviation of lamellar spacing in an individual ranging from 0.55 to 2.1 mm (mean = 1.3 ± 0.035 mm, n = 87; Figure 4.3B). Qualitatively, some individuals had fairly regularly spaced lamellae, with each lamella approximately lining up to one on the previous whorl (Figure 4.3C); others clearly had an irregular arrangement of lamellae (Figure 4.3D).

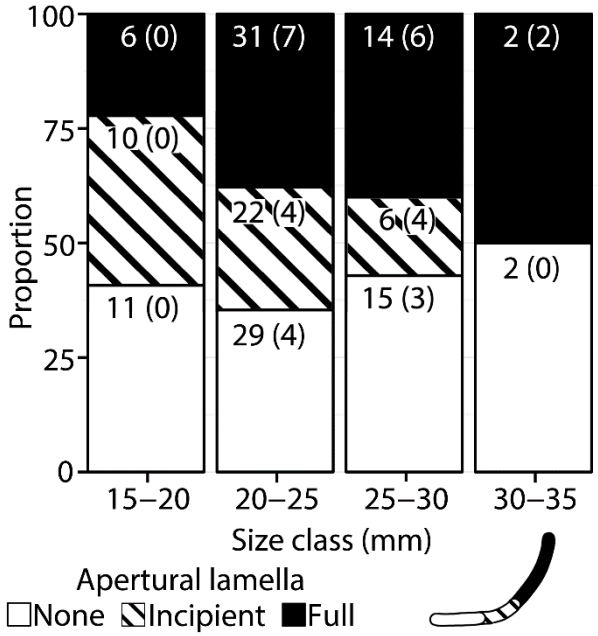

Figure 4.2. State of the apertural lamella for different size classes of *N. lamellosa* scored in the field. Numbers denote the total number of snails; numbers in parentheses indicate the subset in which the most recent lamella was a frill rather than a solitary lamella. Diagram (lower right corner) shows a cross-section of a lamella, indicating the three states scored

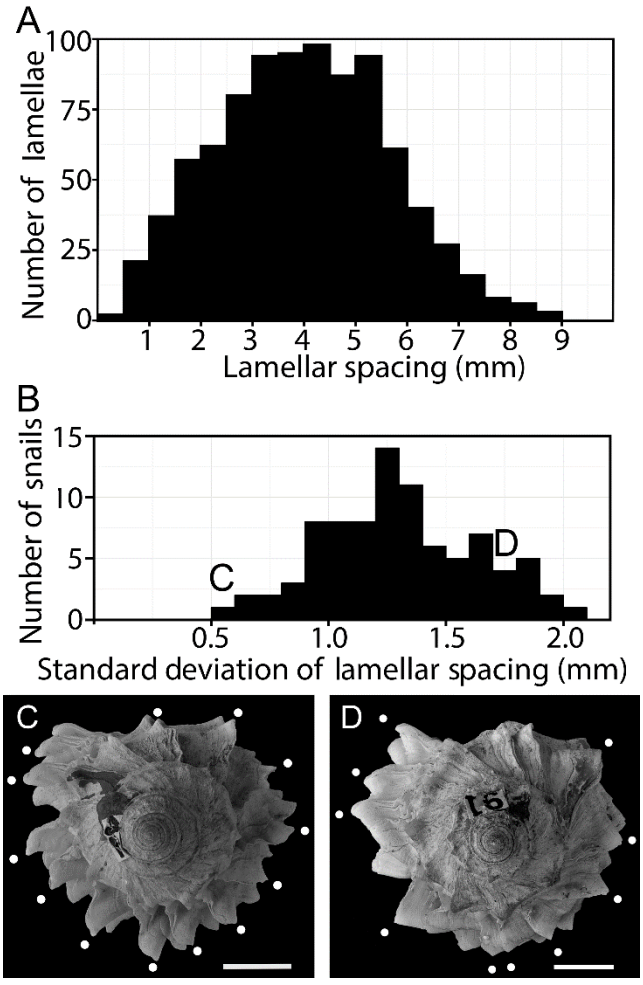

Figure 4.3. Spacing between newly grown lamellae in the sculpture removal experiment. A) Histogram of the distance between all adjacent pairs of lamellae on all snails in all treatments (*n* = 888). B) Histogram of the standard deviation (SD) of lamellar spacing for each individual snail (*n* = 87). (C-D) illustrate snails (that grew more than three quarters of a whorl) showing unusually low (C: shell length = 24.1 mm; mean lamellar spacing = 2.8 mm) or high growth (D: shell length = 20.8 mm; mean lamellar spacing = 3.1 mm) (SD), as indicated by C and D in panel B. White dots, location of individual lamellae grown during the experiment on last whorl at shoulder cord (P1). Note that the spacing between lamellae was measured at the point where the lamellae contacted the suture of the body whorl, not at the lamellar tips where the dots are located (see Figure 4.1A). Scale bar = 5 mm.

4.3.3 How quickly are lamellae produced?

All 33 snails in the sculpture growth-rate experiment grew at least one lamella. One snail took longer than the duration of the experiment to grow a single lamella (>51 days) and was excluded from the analysis. Two snails took longer than 22 days to grow a lamella (30 and 31 days) and were considered outliers (more than 3 SD away from the mean). Overall,

the average time to grow one complete lamella, including the intervening flat portion of shell, was 9.46 ± 0.6 SE days (median = 8 days, mode = 8 days), or 8.3 ± 0.4 SE days with data from outliers removed (Figure 4.4A). During the growth of a lamella, the 'no lamella' phase took an average of 1.9 ± 0.2 SE days (excluding outliers). The 'incipient lamella' phase was much more subjective to score, but took a similar length of time to complete. It took an average of 5.5 ± 0.4 days SE, excluding outliers, from the end of the 'incipient lamella' phase to complete the axial sculpture and begin the next 'no lamella' phase. This time period would include any pause in growth between lamellae where no shell growth occured.

The spacing between adjacent lamellae generally declined with increasing time to grow a lamella, but this relationship was not statistically significant unless outliers were included (Figure 4.4B). When outliers were included, lamellae that took less time to grow were spaced further apart. No small snails (smallest third of the group; < 25 mm shell length) required more than ten days to grow a lamella.

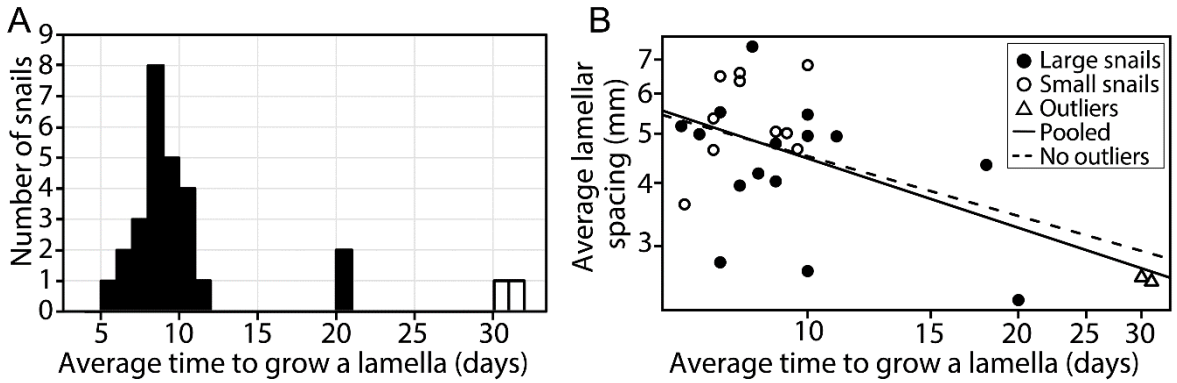

Figure 4.4. Lamellar growth and spacing in laboratory-reared snails. A) Histogram of the average time to grow one lamella. Lamellae grown during the second time-period of the feeding treatment were averaged for each snail (white bars indicate outliers). B) Average lamellar spacing as a function of the average time to grow a lamella on log-transformed axes. Each point represents a single snail; small snails were less than 26 mm in shell length, and large snails were 26 mm or longer in shell length. Regression including outliers (solid line: df = 25, r^2 = 0.32, p = 0.001); regression excluding outliers (dashed line: df = 23, r^2 = 0.09, p = 0.07).

4.3.4 How does feeding rate affect shell sculpture and growth rate?

For shell length, shell weight, and spiral growth, snails in the 'High' feeding treatment grew significantly, although not surprisingly, more than snails in the 'Low' feeding treatment (P < 0.007; Figure A4.1A,B; data for growth in shell length and weight not shown).

4.3.5 Lamellar spacing

When compared to initial shell length, the spacing between lamellae decreased in larger snails (Figure A4.1C, D). 'High' feeding-rate snails had significantly greater spacing between lamellae than 'Low' feeding-rate snails when adjusted for size ($p = 0.03$). In contrast, relative to daily spiral shell growth, lamellar spacing increased in snails that grew more (Figure 4.5A) and did not differ between feeding treatments after standardizing for the amount grown (Figure 4.5B).

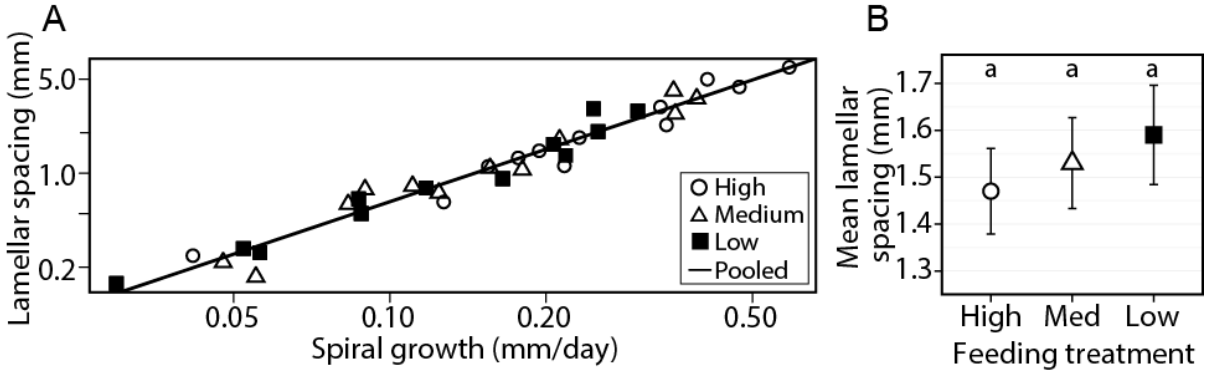

Figure 4.5. Lamellar spacing in the feeding rate treatments. A) Lamellar spacing compared to daily spiral growth on log-transformed axes. Black line shows pooled regression (df = 10, r^2 = 0.96, $p < 0.0001$); slopes did not differ significantly among treatments, $p > 0.7$. B) Lamellar spacing in the 3 feeding treatments using least-squares means from ANCOVA for data shown in panel A ($p > 0.68$). Error bars (SE); treatments sharing the same letter did not differ significantly ($p > 0.68$).

4.3.6 Time to grow a lamella

The average time to grow a lamella increased in larger snails (Figure A4.1E, F), and decreased in snails that grew more. 'High' feeding-rate snails took 16.3 ± 3.8 days, 'Medium' feeding-rate snails took 19.8 ± 2.8 days, and 'Low' feeding-rate snails took 23.0 ± 3.9 days, on average, to grow a lamella. When adjusted for body size, 'High' snails grew lamellae significantly faster than 'Low' snails ($p = 0.02$). The time needed to grow a lamella was approximated by dividing the time by the number of lamellae grown. These numbers cannot be compared to the daily measurement of lamellar growth (4.3.3 *How quickly are lamellae produced?* above) because they are simply averaged over the entire growth period, with no consideration for outliers or snail size.

4.3.7 Feeding rate

Snails ate more barnacles later in the sculpture growth-rate experiment (second time period compared to the first: Wilcoxon test W = 65, $p = 0.0001$), and larger snails ate more

barnacles than did smaller snails (second time period; Figure A4.2A). The number of barnacles eaten in one week correlated significantly with the number of lamellae grown in the same week (Spearman's correlation: $r_s = 0.21$, $p = 0.003$; Figure A4.2B). Of the 33 snails, 20 completed more lamellae when more barnacles were eaten, whereas only seven snails completed more lamellae when fewer barnacles were eaten. When the total number of lamellae grown was compared to the average feeding rate, the relationship was not significant ($p = 0.28$). Although more lamellae were grown, snails that ate more barnacles did not grow lamellae significantly faster (Spearman's correlation: $r_s = -0.02$, $p = 0.84$; Figure A4.2C).

4.3.8 Do existing lamellae affect shell growth rate or growth of new lamellae?

Neither removal of the apertural lamella nor removal of all body-whorl lamellae had a significant effect on the subsequent shell growth rate of *N. lamellosa* or on the spacing and number of lamellae produced. This was true with log-log regressions against shell length, as well as when least-square means were calculated to account for body size (see 4.3.9 *Shell growth rate* below). All analyses of this experiment were therefore pooled to look at growth rate trends.

4.3.9 Shell growth rate

Larger snails grew more slowly than smaller snails both in shell-length change (df = 10, $r^2 = 0.46$, $p < 0.0001$; data not shown) and spiral growth (Figure 4.6A). Snails whose shell length larger than 29 mm appeared to grow more slowly, although the change in slope was not significant for length ($p < 0.077$) or spiral growth ($p < 0.17$); few snails in the experiment were that large. Neither removal of lamellae nor removal of the aperture had a significant effect on change in shell length ($p > 0.98$; data not shown) or spiral growth (Figure 4.6B).

Increase in shell weight did not vary significantly with initial shell length when all snails were included ($p = 0.77$; data not shown). However, when only the snails whose initial weight was less than 1.8 g were included, larger snails increased in mass slightly faster than the smaller snails ($r^2 = 0.05$, $p = 0.023$; data not shown). The sculpture-removal treatment had no effect on rate of shell weight gain (data not shown).

4.3.10 Time to grow a lamella

The time to grow a lamella was approximated by dividing the total time in the treatment by the number of lamellae grown. The average time taken to grow a lamella was 14.3 days ± 0.5 SE (13.7 days ± 0.4 SE with snails smaller than 29 mm). It increased with initial shell length (Figure 4.6C) and decreased with the amount of spiral growth (df = 85, r^2 = 0.62, $p < 0.0001$; data not shown). These numbers cannot be compared to the daily measurement of lamellar growth (4.3.3 *How quickly are lamellae produced?* above) because they are simply averaged over the entire growth period, with no consideration for outliers or snail size.

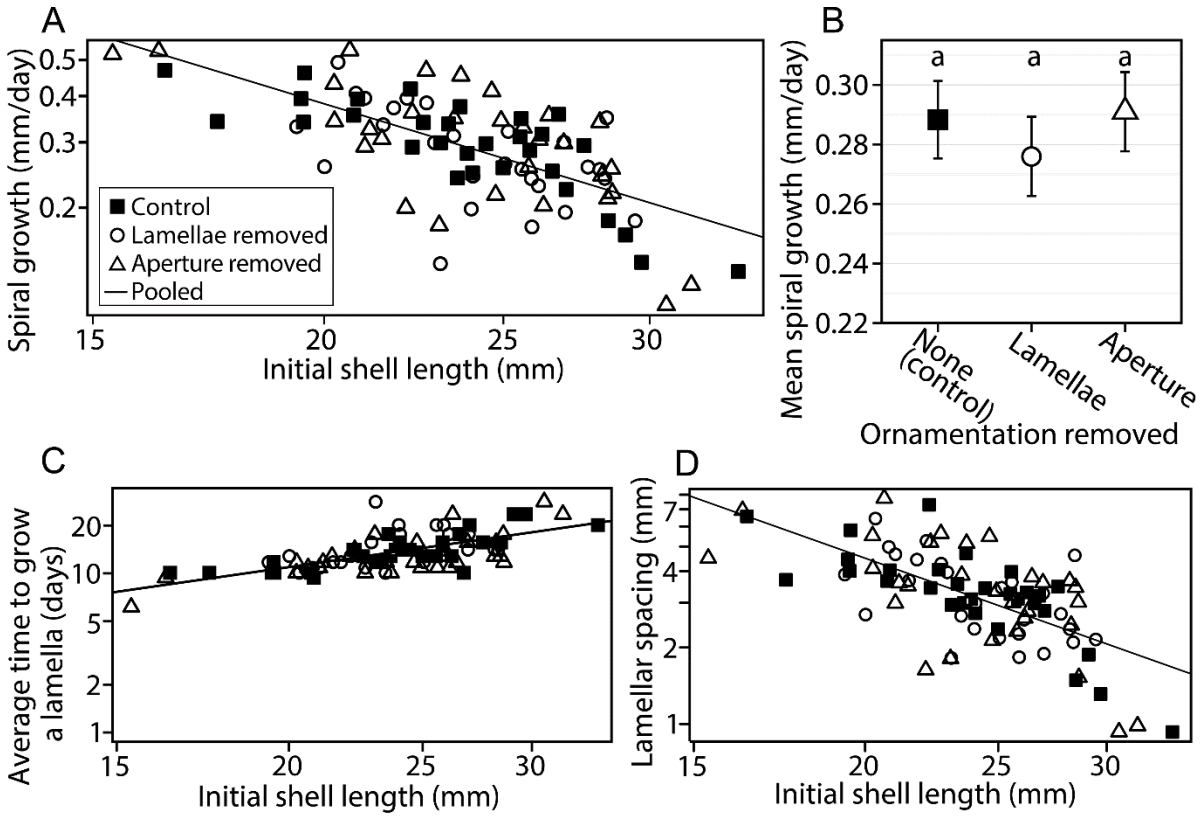

Figure 4.6. Spiral shell growth and lamellar growth relative to initial shell length in the sculpture removal experiment. A) Daily spiral shell growth versus initial shell length on log-transformed axes. Larger snails exhibited less spiral growth (pooled: df = 10, r^2 = 0.45, p < 0.0001; slopes did not differ significantly among treatments, p = 0.83). B) Least-squares means of data shown in panel A, from ANCOVA. Error bars are standard error; treatments sharing the same letter did not differ significantly (p > 0.7). C) Average time to grow a lamella by an individual snail as a function of initial shell length, on log-transformed axes. Black line shows pooled regression (df = 85, r^2 = 0.45, p < 0.0001; slopes did not differ significantly among treatments, p = 0.97). D) Average spacing between lamellae as a function of initial length on log-transformed axes. Black line shows pooled regression (df = 85, r^2 = 0.43, p < 0.0001; slopes did not differ significantly among treatments, p = 0.8).

4.3.11 Lamellar spacing

Lamellar spacing decreased in larger snails, (Figure 4.6D) and increased with rate of spiral growth (df = 85, $r^2 = 0.87$, $p < 0.0001$; data not shown). Lamellar spacing did not differ significantly between treatments in the sculpture-removal experiment (data not shown).

4.4 Discussion

Growth rate (increase in shell length) was the primary determinant of lamellar growth dynamics in this study. Across the various experiments, neither feeding rate, nor presence of past lamellae, had any direct effect on the rate of lamellar production or on lamellar spacing. As expected, increased size and decreased feeding rate were generally associated with lower rates of shell length increase (Spight, 1981). However, in our experiments, there was no evidence of an interactive effect of these factors on the rate of lamellar growth. Shell manipulation (removal of shell sculpture or the aperture) had no effect on overall shell growth rate, and did not change the spacing or timing of lamellae.

4.4.1 Are lamellae associated with a growth hiatus?

Although lamellae in *Nucella lamellosa* resemble axial varices in other muricid shells, and a growth hiatus is typically observed after completion of a varix (MacKenzie, 1961; Inaba, 1967; MacGinitie and MacGinitie, 1968; Spight and Lyons, 1974; Spight *et al.*, 1974; Illert, 1981), we observed no evidence of a growth hiatus after completion of a lamella. If spiral growth paused significantly between lamellae in *N. lamellosa*, we would predict that in a static sample of snails from the field, most would bear a complete apertural lamella at the apertural lip, and few snails would be observed between lamellae. Larger snails would also be expected to spend more time paused due to their slower overall growth rate. Most *N. lamellosa* of all size classes collected from the field were in the process of growing a lamella (Figure 4.2), a finding that suggests significant pauses are not associated with lamellar growth, unlike varices.

4.4.2 Lamellar spacing and lamellar growth rate

In most varix-bearing muricids, varices are regularly spaced and aligned with previous varices on the preceding shell whorl (Webster and Vermeij, In Press; Vermeij, 1995; Savazzi and Sasaki, 2004); however, such regular spacing and alignment between

whorls were not apparent in the lamellae of *N. lamellosa*. The spacing between lamellae was highly variable within individuals, and variability also differed among individuals (Figure 4.3B). Although some snails showed fairly regular lamellar spacing (Figure 4.3C), no snail showed a complete whorl in which lamellae were aligned with those on the previous whorl. Therefore, the developmental control of lamellar placement appears to differ quite significantly from the presumed mechanism for varices (Vermeij, 1995; Savazzi and Sasaki, 2004; Seilacher and Gishlick, 2014).

Overall shell growth rate clearly affected lamellar spacing. Larger snails, as well as snails that were fed less, had lower rates of shell-length increase, resulting in lamellae grown at a slower rate, and lamellae that were closer together, on average. Lamellar spacing was directly related to spiral growth (growth rate; Figure 4.5A) in the feeding experiment, but there was no additional effect of feeding treatment (Figure 4.5). Snails that were fed more did grow lamellae further apart when compared to initial shell length, a proxy for body size (Figure A4.1D); the feeding rate indirectly changed lamellar spacing by affecting the spiral growth rate.

Although shell growth has been modeled geometrically in many types of shells (Ackerly, 1989a; Hammer and Bucher, 2005; Meinhardt, 2009; Chirat *et al.*, 2013), these models have not been tested for biological relevance. Surprisingly little is known about how the rate of lamellar accretion compares to normal spiral accretionary growth. When fed *ad libitum*, *N. lamellosa* grew a new lamella in approximately one to two weeks. Over this cycle from one lamella to the next, we observed that about a third of the time was spent growing intervening shell ('no lamella' and 'incipient lamella'; Figure 4.2 inset), and the other two thirds was devoted to growing the lamella itself, including any possible pause in growth. This finding corresponded roughly to a linear accretion rate of 1.6 ± 0.1 SE mm/day in between lamellae, and 0.8 ± 0.08 SE mm/day when growing a lamella (n = 27, measured at the P1 shoulder cord).

The lamellar accretion rate may be significantly lower than the spiral accretion rate (Paired t-test; t = 3.89, df = 26, p = 0.0006) for many possible reasons. 1) A short growth hiatus may be associated with completion of a lamella, although not nearly as long as seen for varices. 2) The relative thickness of the lamella compared to the body whorl may differ. 3) The growing margin of a lamella is greatly expanded, with added corrugation not seen

between lamellae (Figure 4.1). These undulations increase the total length of the secretory edge, as well as the length and marginal area of the mantle during lamellar growth; time may be required to physically expand the mantle, then shorten it again for the next phase. This last point is consistent with Chirat *et al.*'s (2013) models, in which they showed that wavy or spiny edges could arise from excessive marginal growth (expansion of the mantle). It would be interesting to document how the mantle expands then retracts during successive iterations of lamellar growth. Mantle expansion may not be simply a muscle-driven stretching. Individuals relaxed in $MgCl_2$ had much shorter (perpendicular to the growth edge) mantles when they were between lamellae than when they were mid-lamella (Pers. Obs. NBW). Instead, the mantle may be physically expanding, but exactly how it expands remains unclear.

Even though individuals were held under the same conditions, the time taken to grow a lamella varied widely (Figure 4.4A). A few snails took much longer (e.g. one snail required more than 51 days) but these were likely outliers due to extreme natural variation, a slowing of growth with increasing size, or some other factor. Such wide, among-individual variation is not uncommon even under controlled conditions (Spight, 1981; Koehn and Shumway, 1982; Burrows and Hughes, 1990).

The time taken to grow a lamella did appear to depend, at least weakly, on its distance from the previous one. The more rapidly grown lamellae were generally spaced more widely (Figure 4.4B), although this relationship was not quite statistically significant if outliers were excluded. The weakness of this association, at least in part, was that lamellae were scored only once per day. So, in an extreme case, if a lamella was completed after 4.1 days, it would be scored as 5 days, which is a difference of 18%. This overestimate of time taken would be more pronounced among faster-growing snails, which would artificially decrease the slope in Figure 4.4B.

Finally, lamellar growth rate and spacing likely depend on how close snails are to maturity. The size at which snails reach maturity varies greatly even within species (Spight 1973), and some of the variation we observed may have arisen from some snails reaching maturity at smaller sizes. *N. lamellosa*, like many other snails (Spight, 1981), drastically decrease growth rate with maturity, even though growth is not determinate (Spight 1973). Maturity also appeared to have an effect on lamellar spacing in *N. lamellosa*. Many larger

snails stopped producing separate lamellae and instead grew a terminal frill (Figure 4.1C). This frill appears to be the result of lamellae being grown closer together when the spiral growth rate is reduced at larger sizes. However, not all large snails grew a frill, nor were all frills terminal, and no snails were dissected to confirm sexual maturity.

4.4.3 Effect of existing lamellae on shell growth rate and growth of new lamellae

Previously produced axial sculpture is a potential impediment to subsequent shell growth because it must be reabsorbed before additional spiral growth may proceed (Carriker, 1972; Vermeij, 1977). We therefore expected that removal of *N. lamellosa* lamellae would affect either spiral growth rate or the spacing of new lamellae. However, despite thoroughly shaving the shells, neither removing the aperture (damaging the shell), nor removing all remaining lamellae from the body whorl had any effect on any metric of shell or sculpture growth. We therefore reject the hypothesis that the rate of spiral growth or placement of new lamellae is affected by previous lamellae.

This result was surprising. Prominent shell sculpture necessarily impedes further growth if it is not removed from in front of the aperture, although nothing is known about the costs of this process (Vermeij, 1977). This suggests a relatively low cost of sculpture removal, and does not contradict the findings of Palmer (1981) who reported that the deposition rate of the shell is the rate limiting step, not energy, somatic growth, or sculpture resorption. Muricids use a system of shell removal to drill their prey (Carriker, 1981), and a similar mechanism may aid in the removal of sculpture in front of the expanding aperture. The ability to dissolve shell sculpture appears to be derived in gastropods, as internal shell remodeling is absent in most basal groups except the Neritidae (Vermeij, 1973). More basal lineages of gastropod taxa generally do not have elaborate shell sculpture, probably due to an inability to resorb it efficiently (Vermeij, 1977). We therefore predict that more basal snails bearing sculpture grow faster when shell sculpture is removed experimentally.

4.4.4 Comparing lamellae and varices

Muricid varices, whether blade-like or an array of spines, are typically regularly spaced and exhibit a fixed angle within species (Webster and Vermeij, In Press; Vermeij, 1995; Savazzi and Sasaki, 2004). The lamellae of *N. lamellosa* do not follow this stereotypical growth pattern, and have relatively plastic positioning. Lamellae and blade-like

varices appear superficially similar and are thought to be primarily defensive (Vermeij *et al.*, 1981; Carefoot and Donovan, 1995; Miller and LaBarbera, 1995; Donovan *et al.*, 1999). But the varices of other muricids are associated with periodic bursts of shell growth. In larger specimens with the mature arrangement of varices, long pauses of up to several months occur between bursts of fast growth from one varix to the next (Inaba, 1967; MacGinitie and MacGinitie, 1968; Spight and Lyons, 1974; Illert, 1981). Lamellar growth in *N. lamellosa*, on the other hand, was completed in one to two weeks and was not associated with any such hiatus. In addition, varices are also associated with a period of shell thickening (Inaba, 1967; Carriker, 1972) and a stereotypical lip, but neither was present in *N. lamellosa* (Laxton, 1970). Thus, we predict that in muricids with varices, factors influencing shell growth rate affect the length of the pause between varices, but not the time taken to grow the varix itself, nor their spacing; some muricids do not eat during shell growth (Carriker, 1972). We feel that these differences in growth between the axial sculpture of *N. lamellosa* differ sufficiently from the stereotypical varix pattern to warrant the separate term lamellae. See Chapter 2 for an in-depth discussion on the origin and evolution of varices, including clarification on the different forms of axial sculpture (Chapter 2, Webster and Vermeij, In Press).

4.4.5 Growth and development of lamellae

Most shell sculpture is thought to have a defensive function (Vermeij, 1987, 1995), and the alignment of varices appears to add to their functionality (Spight and Lyons, 1974; Carefoot and Donovan, 1995; Donovan *et al.*, 1999). But what about lamellae? Our results suggest that the rate at which lamellae are produced depends mostly on factors that affect shell growth rate. When spiral growth rate is relatively constant, the spacing and timing of lamellae should also be relatively constant. The variation in sculpture patterning suggests that the spacing of lamellae is neither a priority, nor regulated by some higher-level control mechanism. If a particular lamellar spacing was adaptive, then it should be constant regardless of shell growth rate. However, lamellae appear to be added in a pattern in which the likelihood of having an apertural lamella at a given point in time remains relatively constant. When conditions are good, growth is fast, and the snail generally adds lamellae faster, yet further apart. When growth is slow, *N. lamellosa* places lamellae closer together. The likelihood of producing an apertural lamella, therefore, appears to remain relatively constant regardless of environmental conditions and may ensure that apertural reinforcement

does not depend on external factors, such as variation in food availability or water temperature.

Nucella lamellosa shell form is known to be quite plastic, changing readily between thin-shelled with frilly lamellae and thick-shelled with few/no lamellae (Appleton and Palmer, 1988). This plasticity would not be possible if new lamellae depended on physical cues from previous lamellae for positioning. Furthermore, a mechanism to control lamellar spacing might be difficult to evolve under these circumstances. If snails regularly transition to a form without lamellae, the opportunity for selection of coordinated lamellar placement would be lessened. It is unclear how actively the plastic shell responds to predator cues, and the apparently passive plasticity of axial lamellar growth interact with one another. Even though shell plasticity is not uncommon (Trussell, 2000; Hoverman and Relyea, 2009; Pascoal *et al.*, 2012), our understanding of the role of plasticity in evolution is just beginning (Laland *et al.*, 2014; Forsman, 2015).

In snails, larger juveniles generally grow more quickly than smaller snails, but growth rate then drops off again with maturity (Spight, 1981). If rate of production of lamellae is correlated with growth rate, then similar trends should be seen for lamellar spacing. Diplommatinid land snails bear sharp axial sculpture, termed 'ribs', that are quite similar to axial lamellae. One species, *Plectostoma retrovens* (Tomlin, 1938), reportedly grows ribs nightly, and will grow faster if it is kept in the dark (Berry, 1962). Another species, *Plectostoma concinnum* (Fulton, 1901), grows ribs more slowly, and the spacing of ribs correlates with shell growth rate (Liew *et al.*, 2014). Rib spacing increases with increased growth rate initially, then begins to decrease again with maturity; diplommatinids have determinate growth. Similarly, Taylor *et al.* (2004) examined the spacing of lamellae in the bivalve *Lucina pensylvanica* (L., 1758). Within individuals, lamellae grew further apart as the bivalve grew larger, up to a length corresponding to sexual maturity, then lamellar spacing decreased with an increase in variability. In *N. lamellosa*, larger snails had lamellae closer together, but this was an intraspecific pattern, and did not include very small snails. When the distance between all measurable lamellae (including those grown prior to collection) on an individual snail was measured, the general trend in *N. lamellosa* followed that of *P. concinnum* and *L. pensylvanica*: increased lamellar spacing with increasing juvenile size, followed by an irregular decrease as maturity approached (Figure A4.3). The

variation in spacing is much higher in *N. lamellosa* than in these other two mollusc species, and the size at which lamellar spacing begins to decrease also varies. The most distinct period when lamellar spacing increased occurred prior to collection, which explains why we did not detect it during our experiments. Interestingly, Figure A4.3 shows no obvious difference in lamellar spacing between the laboratory-grown and the previous wild-grown lamellae. That such disparate species, with different shell sculpture, exhibit such a similar growth pattern strongly suggests a conserved process, which may be widespread among mollusc taxa bearing axial sculpture. Without a specific and separate mechanism to regulate the spacing of such sculpture, though, the underlying pattern seems to be to produce lamellae at more or less regular time intervals, which results in a spacing that depends on the rate of spiral shell growth.

Parallel color patterns on shells have been modeled based on reaction-diffusion, and neurosecretory models (Ermentrout *et al.*, 1986; Boettiger *et al.*, 2009; Meinhardt, 2009). Similar mechanisms may also apply to the control of axial sculpture. Although several theoretical mechanisms have been proposed (Hammer, 2000; Moulton *et al.*, 2012; Chirat *et al.*, 2013), the actual biological processes responsible for the growth of axial sculpture remain poorly studied from either an experimental or developmental point of view. Both morphological and physiological changes to the mantle are theoretically required each time a lamella is produced, leaving room for developmental plasticity to affect each lamella separately and adding to the overall variability in shell sculpture growth. Clearly, much remains to be learned about the signaling pathways and mantle feedback mechanisms underlying the control of shell sculpture (Urdy, 2015). If we can understand how the mantle grows a shell, we can begin to understand how the striking diversity of gastropod shells evolved.

Chapter 5 — Connecting pattern to process: How snails grow spiral shell sculpture in *Nucella ostrina* (Muricidae: Ocenebrinae)

5.1 Introduction

The great variety of forms in gastropod shells is truly an example of 'endless forms most beautiful' (Darwin, 1859). But much is not known about how the diversity of forms arose evolutionarily, and how they develop. Because of their geometric simplicity, and our basic understanding of shell biomineralization, gastropod shells make an ideal system to examine the developmental mechanics underlying different skeletal phenotypes.

Mollusc shells are secreted by the mantle, a thin flexible tissue layer that lines the shell's opening (aperture). The mantle secretes the main mineral components, primarily calcium carbonate, and a diverse array of macromolecules including proteins, polysaccharides, and lipids into the extrapallial space (Marin *et al.*, 2012; Marie *et al.*, 2013; Gaume *et al.*, 2014). The extrapallial space is the small fluid-filled gap bounded by the mantle on one side and the periostracum on the other, although recent work suggests the mantle may directly abut the shell (Addadi *et al.*, 2006; Marie *et al.*, 2012). The periostracum is a thin, cross-linked, proteinaceous layer secreted by the distal margin of the mantle fold (Bevelander and Nakahara, 1970), and forms the outermost shell layer. The underlying calcareous layers of the shell are secreted by the outer mantle epithelium (OME) that lines the inside of the shell (Bevelander and Nakahara, 1970; Kniprath, 1972; Marxen *et al.*, 2003; Jackson *et al.*, 2006). Current theories suggest a complex, extracellular matrix-mediated, self-assembly process ultimately yielding the shell itself (Furuhashi *et al.*, 2009).

Terminology for mantle features varies with differences in morphology between species. The periostracum is generally secreted by the periostracal groove (PG), although this structure lacks a groove in *Littorina littorea* (Linnaeus, 1758) (Bevelander and Nakahara, 1970; Marxen *et al.*, 2003). In general, the OME, can be divided into several secretion-specific zones depending on the species, all of which can be separated into at least two regions. Region 1 is the distal-most OME, adjacent to the periostracal groove, and is a thickened region of tall columnar cells sometimes termed the belt. The distal-most portion of the belt is thought to help secrete the periostracum, while more proximal portions of the belt secrete the outermost mineral shell layers (Bevelander and Nakahara, 1970; Kniprath, 1972).

Proximally, the epithelial thickness of the belt diminishes abruptly through a transition zone into Region 2. This proximal OME is made up of shorter cells thought to be responsible for secreting the inner shell layers. A number of enzymes have been identified as playing a role in shell formation, and have been examined in multiple species to help identify these OME regions, especially a) alkaline phosphatase (AP), which is present in the more proximal OME, b) acid phosphatase (AcP), which is present in the distal OME, and c) Peroxidase (PO), which is thought to be involved in periostracum formation (Marxen *et al.*, 2003).

Understanding how shell sculpture is produced at the tissue level is an important step to completing the picture of shell development. Although much is known about how biomineralization occurs, most studies have focused mainly on how organic components are involved in guiding mineral precipitation to form hard parts of the shell – not on how the process varies to produce different shell morphologies (Furuhashi *et al.*, 2009). Although this generalized mechanism of shell formation is understood, almost nothing is known about how the changes in the mantle produce variation in shell form — except for the pigment gene Somesuke in *Haliotis* (Jackson *et al.*, 2006). To study this, I examined a simple difference in shell morphology, smooth shell vs spiral ribs, within a single polymorphic species to assess what corresponding variation in the mantle might produce this difference.

The muricid *Nucella ostrina* (Gould, 1852) has a noticeable dimorphism in shell sculpture: smooth-shelled or spirally ribbed. Genetic crosses have confirmed that this dimorphism is largely controlled by two alleles at a single locus (A. Richard Palmer, 1985). This species is ideal to study the production of shell sculpture, as adjacent regions with and without ribs are easily compared. Also, spiral ribs, which grow perpendicular to the apertural margin, are produced more or less continuously throughout life, as opposed to the episodic temporal variation that characterizes axial ribs.

How does the portion of the mantle that produces spiral ribs differ a) from the intervening mantle that produces inter-ribs and b) from the mantle of smooth individuals? Does the mantle in these different regions differ at a tissue, cellular, or molecular level? Because changing shell thickness to produce a rib seems like a relatively straightforward difference, I predict that tissue level changes in the mantle are responsible for differences between ribbed and smooth forms, due to changes in either the number or distribution of cells, rather than differences in the molecular and cellular components involved.

5.2 Materials and methods

5.2.1 Animal collection

Live *Nucella ostrina* were collected from various locations in Barkeley Sound (B.C., Canada), mainly Grappler Inlet (48.8319, -125.1187), Grappler Mouth (48.8379, -125.1349), and the Ross Islets (48.8722, –125.1618), and anaesthetized in 7% $MgCl_2$ in distilled H_2O for 24h at 4°C (Rouse and Pleijel, 2001). Mantles were extracted by crushing the shell apex with pliers, dislodging the columellar muscle, and dissecting out the mantle fold. This kept the shell aperture and body whorl intact for comparison between the mantle and the shell.

5.2.2 Shell morphology

5.2.2.1 Shell sections

To determine the shell layers responsible for rib formation and which forms of calcite were in the shell, I sectioned shells of *N. ostrina*. For shell sectioning, the snail body was removed, the shell soaked in 3% sodium hypochlorite (bleach) for 2h, and then rinsed thoroughly to remove the remaining soft tissue. Shells were left to dry overnight and then embedded in Epoxy resin (Epothin, Buehler). Embedded shells were sectioned, polished, and mounted on glass slides by the Thin Section Laboratory (Department of Earth and Atmospheric Sciences, University of Alberta). Some sections were partially stained with Feigl's stain to differentiate aragonite from calcite (Friedman, 1959).

5.2.2.2 Shell SEM

Shell microstructure was examined using scanning electron microscopy (SEM). Shells were dried in a 65°C oven overnight, fractured with pliers, and etched in 500 mM EDTA (ethylenediaminetetraacetic acid) for 15 min to reveal the microcrystalline structure. Shells were mounted onto metal stubs using adhesive tape and nail polish, then sputter coated with an Au-Pd alloy before viewing on a FEI (XL30) Scanning Electron Microscope.

5.2.3 Mantle morphology and histochemistry

5.2.3.1 Histology

Mantles were fixed in 4% PFA (paraformaldehyde) in PBS (phosphate buffered saline) overnight at 4°C, then dehydrated through a graded ethanol series. Tissue was then either dehydrated through 100% toluene and embedded in wax, or embedded in JB-4 resin

(Electron Microscopy Sciences) following the manufacturer's protocol. One complete hatchling *N. ostrina* (2 mm shell length) was also fixed in the shell in 4% PFA overnight, then treated with 5% EDTA in PBS for 3h to partially degrade the shell prior to embedding in JB-4 and sectioning. Serial sections (7 µm wax, 4 µm JB-4) were used for histological staining and 3D reconstructions. Sections were stained with Masson's trichrome (Humason, 1962; Cerri & Sasso-Cerri, 2003).

5.2.3.2 Cryosections

The cryosectioning protocol was modified from Barthel and Raymond (1990). Briefly, tissue was fixed overnight in 4% PFA in PBS with 5% sucrose, then gradually washed through to 1:1 20% sucrose:Tissue-Tek® O.C.T. Compound (VWR) over 24h. Tissue was then embedded in 1:1 20% sucrose:OCT in a mold and set at -80°C. 20µm sections were made with a CM1850 (Leica) cryostat and placed on Superfrost glass slides (Thermo Fisher Scientific).

5.2.3.3 3D reconstruction

Serial paraffin sections (7 µm) were photographed under a light microscope (Zeiss Axio Imager M2) and white balanced (Adobe Photoshop CS6) prior to both an automated alignment using the ImageJ plugin StackReg (Rasband, 1997; Thévenaz *et al.*, 1998) and a manual alignment with Reconstruct (SynapseWeb, v1.1). Manual alignment incorporated multiple reference points including the periostracal groove, right efferent pallial vein (hereafter pallial vein) (Bekius, 1971), and the mantle outline. Stacked sections were then imported into Imaris (Bitplane) for reconstruction (smooth, $n = 2$; ribbed, $n = 2$).

5.2.3.4 Histochemistry

Fresh, unfixed, mantle tissue was stained for peroxidase (PO; smooth, $n = 2$; ribbed, $n = 1$), alkaline phosphatase (AP; smooth, $n = 4$; ribbed, $n = 5$) (Hohagen and Jackson, 2013), or acid phosphatase (AcP; smooth, $n = 3$; ribbed, $n = 3$) (Gruber *et al.*, 1988), all enzymes known to be involved in the shell secretion process with expected expression patterns from other gastropods (Timmermans, 1969; Ulrich Bielefeld *et al.*, 1993; Marxen *et al.*, 2003; Hohagen and Jackson, 2013). Following staining, tissue was fixed, dehydrated, wax-embedded, sectioned (see 5.2.5 *Histology* above), and counterstained with eosin for 5 s, except for tissue samples stained to detect AcP. Staining was lost after embedding and

sectioning for all three histochemical stains, probably due to the dehydration process. Staining was too weak on AcP sections to determine stain location or to counterstain, and much of the AP expression was lost during the embedding process, leaving only weak traces along the apical edge of the OME.

For alkaline phosphatase on cryosections, sections were washed in 3x 3 min 0.01M PBS, 3x 3min 50mM tris (hydroxymethyl) aminomethane (Tris) buffer (pH 9.5), then 30 min in colour buffer from Hohagen and Jackson (2013). The tissue was then dehydrated to 100% ethanol, stained for 2min in Eosin, then dehydrated through Toluene and coverslipped.

For Acid phosphatase staining of cryosections, sections were washed in 3x 3 min 0.01M PBS, 30min Acetate buffer (pH 5.0), 2h in hexazotized pararosanilin with napthol AS-TR phosphate (Gruber et al., 1988), 2x 3min PBS, 30s in Hemotoxylin, 5x H_2O, air dried at 37°C and coverslipped.

5.2.3.5 TEM

Mantle ultrastructure was examined using TEM (transmission electron microscopy). TEM fixation was modified from Lacalli (1981) and Harris and Shaw (1984). In short, tissue was preserved in 1:1 sea water: 4% glutaraldehyde in a 10% sodium acetate (NaAc) buffer (pH 7.6) for 3 min then post-fixed in 1% OsO_4 in 10% NaAc for 30 min, then replaced with fresh fixative and fixed at 4°C overnight. Specimens were embedded in Spurr resin (Sigma-Aldrich) and thick and thin sections were cut on an ultramicrotome. Thick sections (0.6 µm) were stained with Richardson's stain (Richardson *et al.*, 1960) to verify angle and position. Thin sections (70 nm) were mounted on CuPd grids (smooth, $n = 2$; ribbed, $n = 2$) and stained with 4% uranyl acetate for 20 min and lead citrate for 7 min. Sections were viewed on a Philips/FEI (Morgagni 268) TEM.

5.2.4 Measurements

Measurements were made of several features on histological sections using ImageJ (Rasband, 1997). Cell heights in the OME were measured along the long axis of the cell (Figure 5.3B,C): Across from the pallial vein, 1 mm proximally from the periostracal groove, and at the distalmost occurrence of AP activity. Lengths along the OME were measured using a segmented line that traced the contour of the OME, starting from the proximal border of the periostracal groove, along the apical edge of the epithelium to either the pallial vein or to the distal-most AP activity (see Figure 5.3A). Measurement error (mean percent error) was

estimated by taking blind, repeated measurements on different days: cell height: ± 1.9% (n = 45); OME length: ± 1.9% (n = 45). Measurements were repeated three times on each image, in two smooth and two ribbed snails, except AP activity, which was only measured in one ribbed snail. All measurements were of fixed tissue, with no correction for shrinkage.

Images were edited with Adobe Photoshop CS6 (2012 Adobe Systems Inc.) to adjust brightness, contrast, and to clean up the background.

5.3 Results

5.3.1 Shell morphology

The shell of *N. ostrina* was made up of two distinct shell layers, an outer prismatic calcite layer and a thinner, inner aragonite layer (Figure 5.1A). The calcite had irregular crystals, perhaps homogenous, while the aragonite had two separate and orthogonal simple crossed lamellar layers (Chateigner *et al.*, 2000). The inner-most aragonite layer appeared much further back along the shell (Figure 5.1B). The aragonite layer was the same thickness in rib and inter-rib regions as well as in smooth shells, while the calcite layer was thicker in ribbed regions (Figure 5.1A-D). The border between the calcite and aragonite layers was relatively straight in both ribbed and smooth shells, with a short and raggedly heterogeneous transition zone (Figure 5.1H,I).

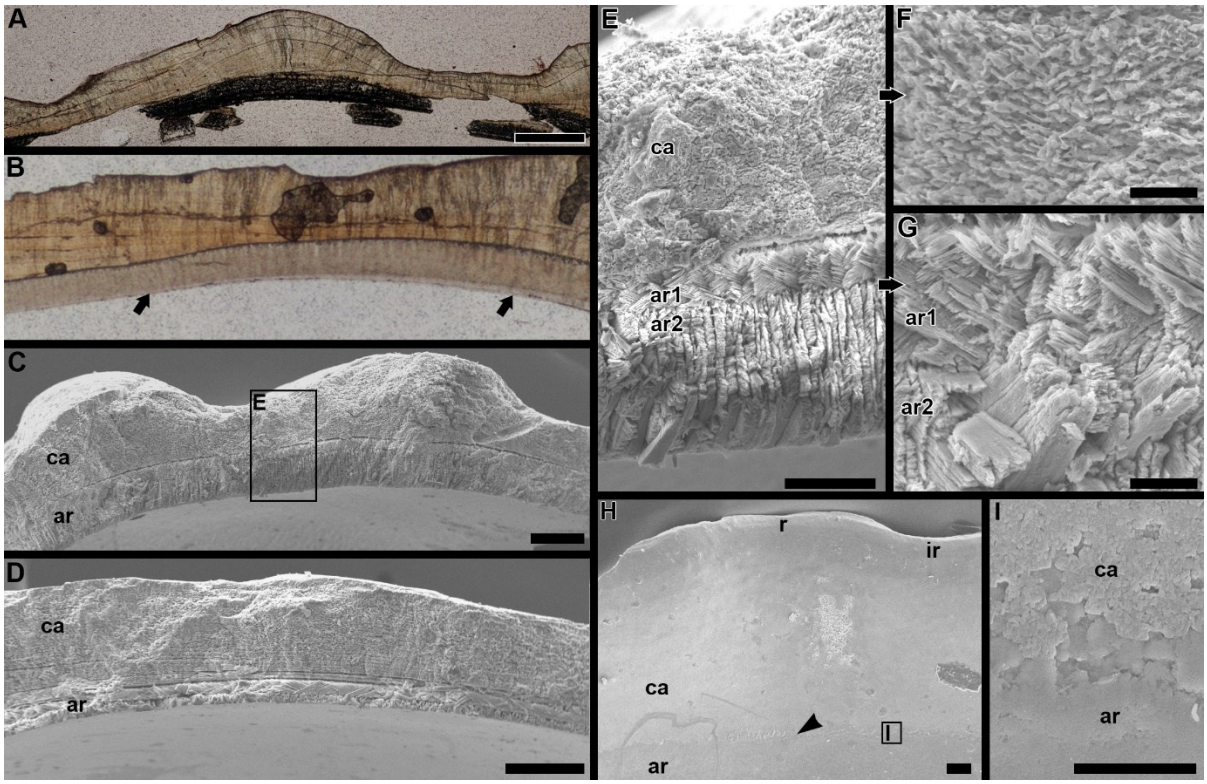

Figure 5.1. Shell layers in *N. ostrina*. A) Shell thin-section, parallel to aperture margin of ribbed *N. ostrina* showing the single upper outer calcite layer, and the two inner aragonite layers stained Feigl's stain (black) (shell length = 19.0 mm). B) Shell thin-section, perpendicular to aperture margin of ribbed *N. ostrina* showing all three shell layers, including the start of the second inner aragonite layer ~1/3 whorl back from the aperture (arrow) (shell length = 18.7 mm). C) SEM of ribbed shell section, perpendicular to aperture margin, showing that inner layers maintain an even thickness. D) SEM of a smooth shell section, perpendicular to aperture margin with same three layers visible. E) Inset of C, showing three separate shell layers, outer prismatic calcite (ca) and two orthogonal inner crossed lamellar aragonite layers (ar1 and ar2). F) Outer prismatic calcite layer. G) Inner crossed-lamellar aragonite layers. H) View of shell surface interior, aperture up, showing straight boundary between the inner and outer shell layers (arrowhead). I) Inset of H, showing variation in the border between calcite layer and the start of the aragonite layer. ar1- outer aragonite layer; ar2- inner aragonite layer; ca- calcite layer; ir- inter-rib region; r- rib. A,B,C,D,H, scale bars = 250 µm; E, scale bar = 100 µm; F,G,I scale bars = 25 µm.

5.3.2 Mantle morphology

The distal-most portion of the mantle fold was relatively thick and robust, but proximally it gave way to a much thinner epithelium with regional specializations including a gill, osphradium, and hypobranchial gland (Figure 5.2). Near the distal edge was the pallial vein, which was a relatively straight vessel running parallel to the mantle margin in both

smooth and ribbed shell individuals (Figure 5.2B,C) (Fretter and Graham, 1962; Bekius, 1971). The mantles of ribbed and smooth individuals could easily be distinguished by their overall shape. Snails with ribbed shells had mantles with a scalloped margin — the tissue periodically extended distally from the mantle margin, while snails with smooth shells had smooth, curved mantle margins. The extent of scalloping generally corresponded to the thickness of the spiral ribs. Both ribbed and smooth mantles did show some ruffling — where the mantle margin curled dorsally, but this was inconsistent. Although the difference between mantles of ribbed and smooth snails was clear in overview, I could not determine whether an individual cross-section of the mantle (x.s., perpendicular to aperture margin) belonged to a ribbed or smooth individual.

When examined in cross-section, the mantle of *N. ostrina* appeared quite similar to the mantles of other gastropods, especially *Littorina littorea* (Bevelander and Nakahara, 1970) (Figure 5.3). The inner mantle epithelium (IME) lined the inner side of the mantle, facing the mantle cavity, and was made up of large cells intermixed with mucous-filled globe cells that were covered in long cilia and microvilli. The interior of the mantle fold was composed mostly of haemocoel spaces (h), along with a few isolated muscle filaments (m), and some connective tissue (c). The majority of the tissue lined the base of the epithelia, especially around the distal margin of the mantle fold. A few hemocoelic channels were also present, including a distinctive pallial vein (a) that ran parallel to the mantle margin, adjacent to the IME. The outer mantle epithelium (OME) was made up of densely packed cells, whose outline undulated irregularly in wrinkles. Distally, the cells of the OME were tall and columnar, packed so tightly that they were difficult to distinguish individually, and generally had irregular borders (Figure 5.3B). These cells gradually shortened proximally into cuboidal cells that were easier to identify individually, with straighter lateral margins, with no clear zone between the two cell morphologies (Figure 5.3C). The periostracal groove lacked a ‘groove’, and consisted of a small group of cells that sat below the distal OME, with extensions through to the outside between the OME and IME, (Figure 5.3D).

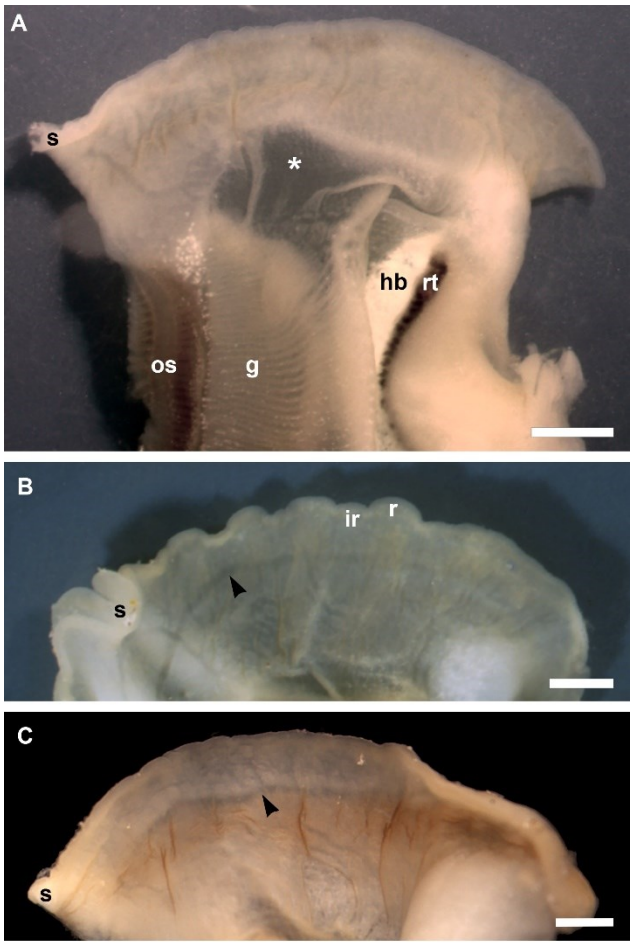

Figure 5.2. Gross mantle morphology and overview of the OME, aperture up. A) The mantle of a snail with a smooth shell, with a smooth mantle margin. Thin tissue (*) lies between the mantle and other organs attached to the mantle epithelium such as the gill (g), hypobranchial gland (hb), osphradium (os), and rectum (rt) (19.3 mm shell length). B) Mantle of a snail with a ribbed shell showing a scalloped edge (upper margin) with ribbed (r) and inter-rib (ir) portions, and a straight pallial vein (arrowhead) (14.6 mm shell length). C) Mantle of a smooth-shelled snail showing proximal mantle pigmentation from a grey shell (brown) and a straight pallial vein (arrowhead) (20.5 mm shell length). Siphon (s), Scale bars = 1 mm.

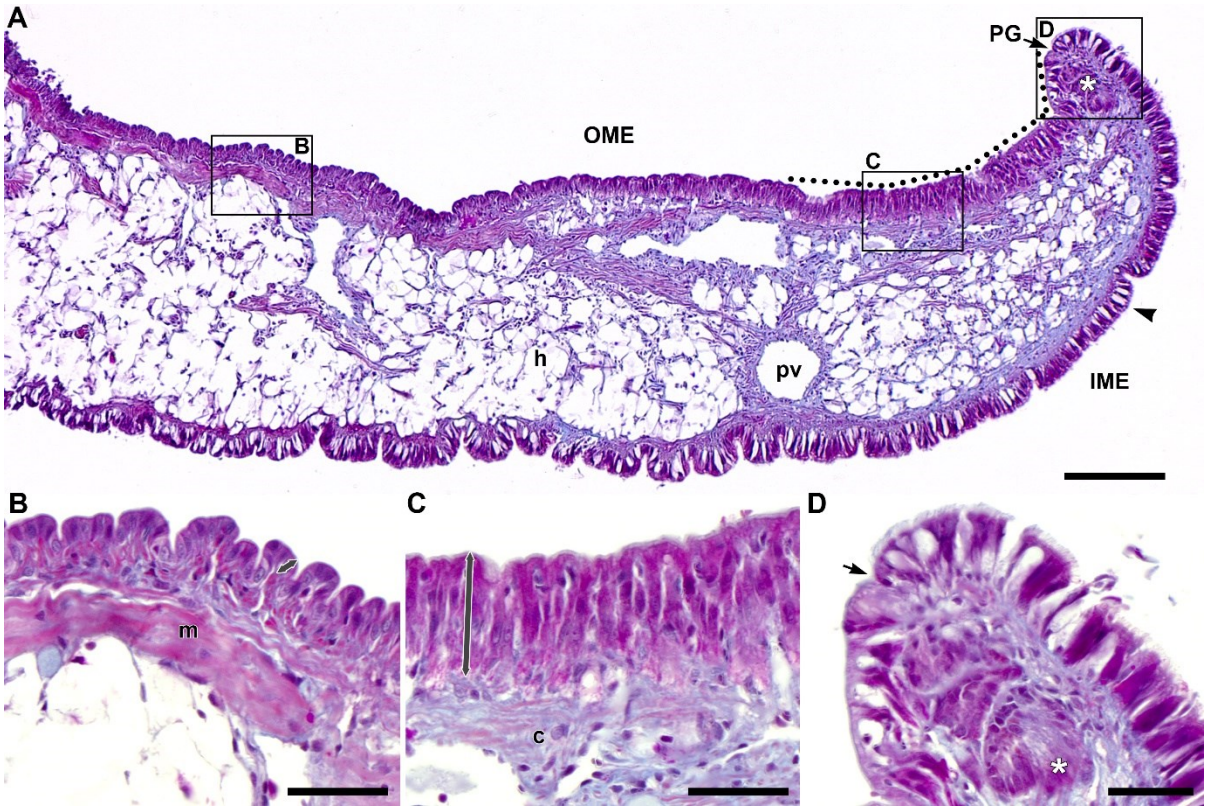

Figure 5.3. Mantle x.s. stained with Masson's Trichrome (7 µm paraffin section; 26.7 mm shell length).A) Mantle margin. Dotted line: proximo-distal OME length from periostracal groove to pallial vein. B) proximal OME, inset of A. C) distal OME, inset of A. D) Periostracal groove, inset of A. Double-headed arrow (grey): cell height measurement; pv: pallial vein, used in 3D reconstructions and measurements; c: connective tissue; h: haemocoel; IME: inner mantle epithelium; m: muscle fibres; OME: Outer mantle epithelium; PG: periostracal groove (*); arrow: exit of periostracal groove; arrowhead: globe cell. A, scale bar = 200 µm; B,C,D scale bar = 50 µm.

The mantle of hatchling snails differed from larger individuals, primarily in the OME (Figure 5.4). The periostracal groove (pg) had a clear groove, with a periostracum (P), clearly emanating from within the periostracal groove. Proceeding proximally along the OME was a curved region of medium columnar cells along which the periostracum thickened, then a belt of tall cells (B), and lastly the cells shortened dramatically into cuboidal cells through a transition zone (tz).

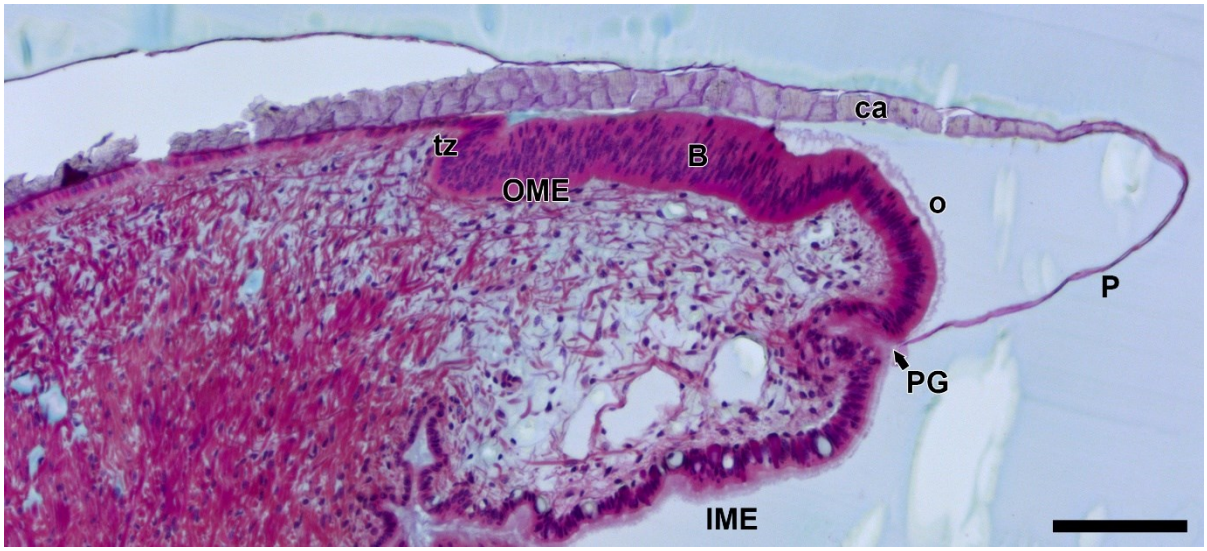

Figure 5.4. Cross-section (parallel to shell growth) through the mantle of a partially decalcified hatchling *N. ostrina* showing a different morphology than older snails, with a thick belt (B) and obvious transitional zone (tz) in the OME. JB-4 section (4 µm) stained with Masson's trichrome. ca – calcium carbonate shell remnant; IME – inner mantle epithelium; o – remnant organic matrix; OME – outer mantle epithelium; P – periostracum; PG – periostracal groove. Scale bar = 100 µm.

5.3.3 Ultrastructure of the OME and periostracal groove

The cells of the proximal cuboidal (Figure 5.5D) and distal columnar OME (Figure 5.5A, C) were generally similar, with large nuclei, many mitochondria, an extensive rough endoplasmic reticulum, as well as a highly convoluted apical edge. Distal OME cells were more stratified, with a denser basal cytoplasm, and more, larger apical vesicles than proximal OME cells. Proximal OME cells were generally less tightly packed, with straighter, more obvious cell membranes, and a less dense cytoplasm. The periostracal groove (Figure 5.5B) connected to the external surface with long, thin cellular processes that expanded out into secretory vesicles. The distal edge of the periostracal 'groove' was lined with cilia, reminiscent of true periostracal groove. Cells of all three epithelia, the IME, OME, and the periostracal groove all had a dense cytoplasm full of ribosomes, mitochondria, and vesicles (data not shown).

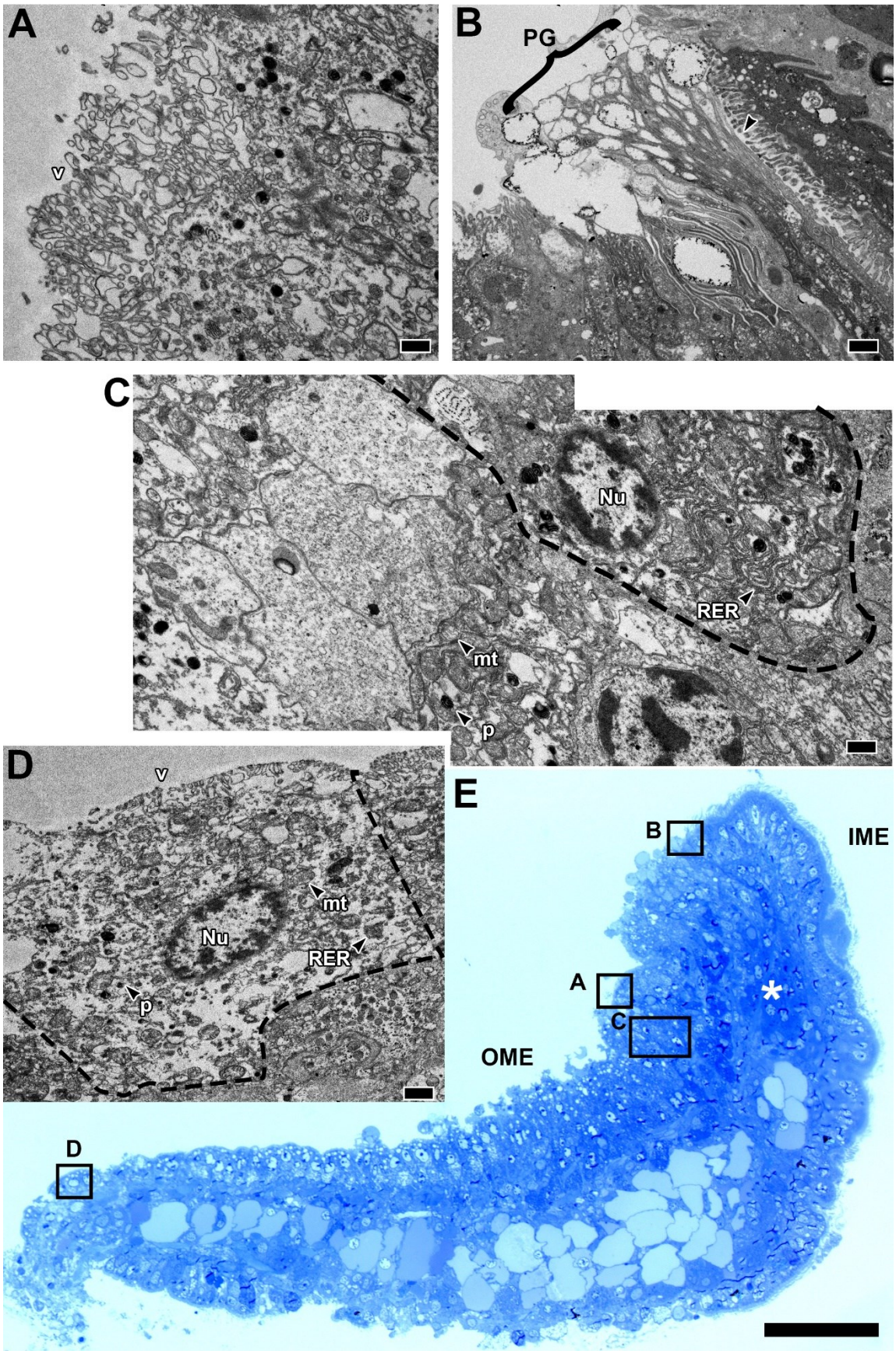
A
v
B
PG
C
Nu
RER
mt
p
D
v
mt
Nu
RER
p
E
B
IME
A
C
OME
D

Figure 5.5. Mantle ultrastructure of *N. ostrina*. A) Inset of E showing the apical border of distal OME cells. B) Inset of E showing the cellular projections along the distal border of the periostracal groove (arrowhead). C) Inset of E showing some distal OME cells, apical is left. D) Inset of E showing a proximal OME cell with border (dashed line). E) Thick section of *N. ostrina* mantle x.s. asterisk – periostracal groove; mt – mitochondria; Nu – nucleus; RER – rough endoplasmic reticulum; p – pigment granule; PG – periostracal groove; v – apical vesicles. A,B,C,D, Scale bar = 1 µm; E, Scale bar = 50 µm.

5.3.4 Enzyme activity in the OME and periostracal groove: alkaline phosphatase, acid phosphatase, and peroxidase

In the OME, Alkaline phosphatase (AP) activity was in the apical region of the proximal epithelial cells (Figure 5.6A,C). The start of AP expression in the OME appeared to coincide with the change from columnar to cuboidal epithelial cells, although that transition is gradual (Figure 5.7B). AP activity was also observed in the apical border of the IME, and in the connective tissue at the base of epithelia, mostly at the distal tip and proximal thin regions of the mantle (Figure 5.7A). Acid phosphatase (AcP) activity was strongest in the more distal OME (Figure 5.6B,D), although more precise localization was difficult because in section, the staining only showed a weak apical AcP activity in the OME (Figure 5.7D,E,F). Peroxidase activity was limited to some, but not all cells of the periostracal groove, as well as the apical region and some globe cells of the IME (Figure 5.8).

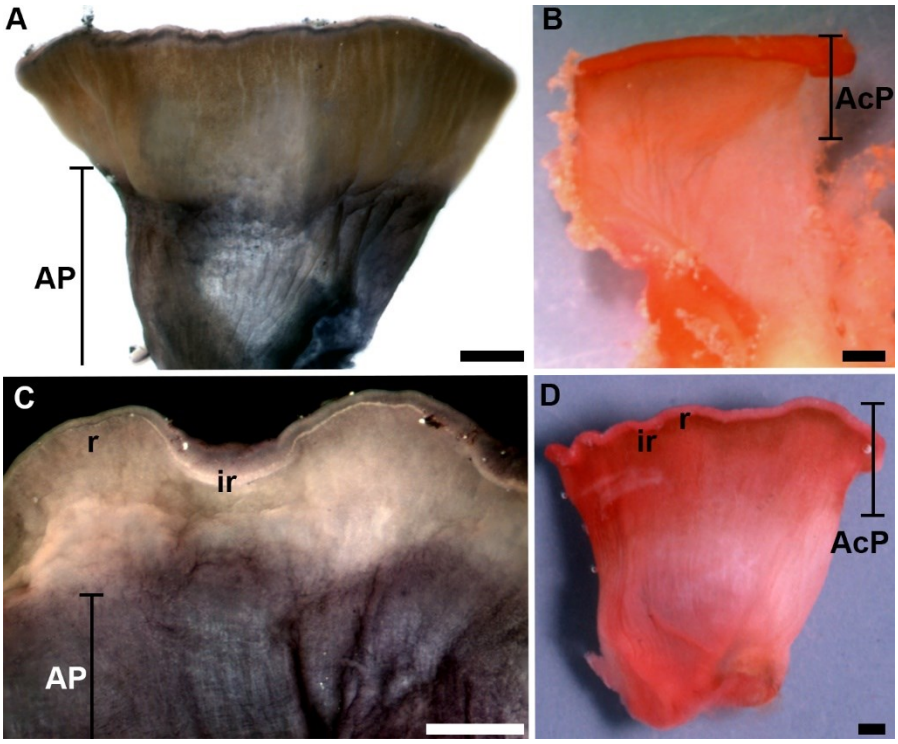

Figure 5.6. Enzymatic activity in mantles of smooth and ribbed *N. ostrina*. Aperture is up, OME view. Smooth mantle (A,B) and ribbed mantle (C,D) were labeled for AP activity (A,C, purple stain), and AcP activity (B,D, pink stain). Shell length: A, 12.2 mm; B, 14.7 mm; C, 14.9 mm; D, 15.5 mm. r – ribbed; ir – inter-rib; scale bars = 500 µm.

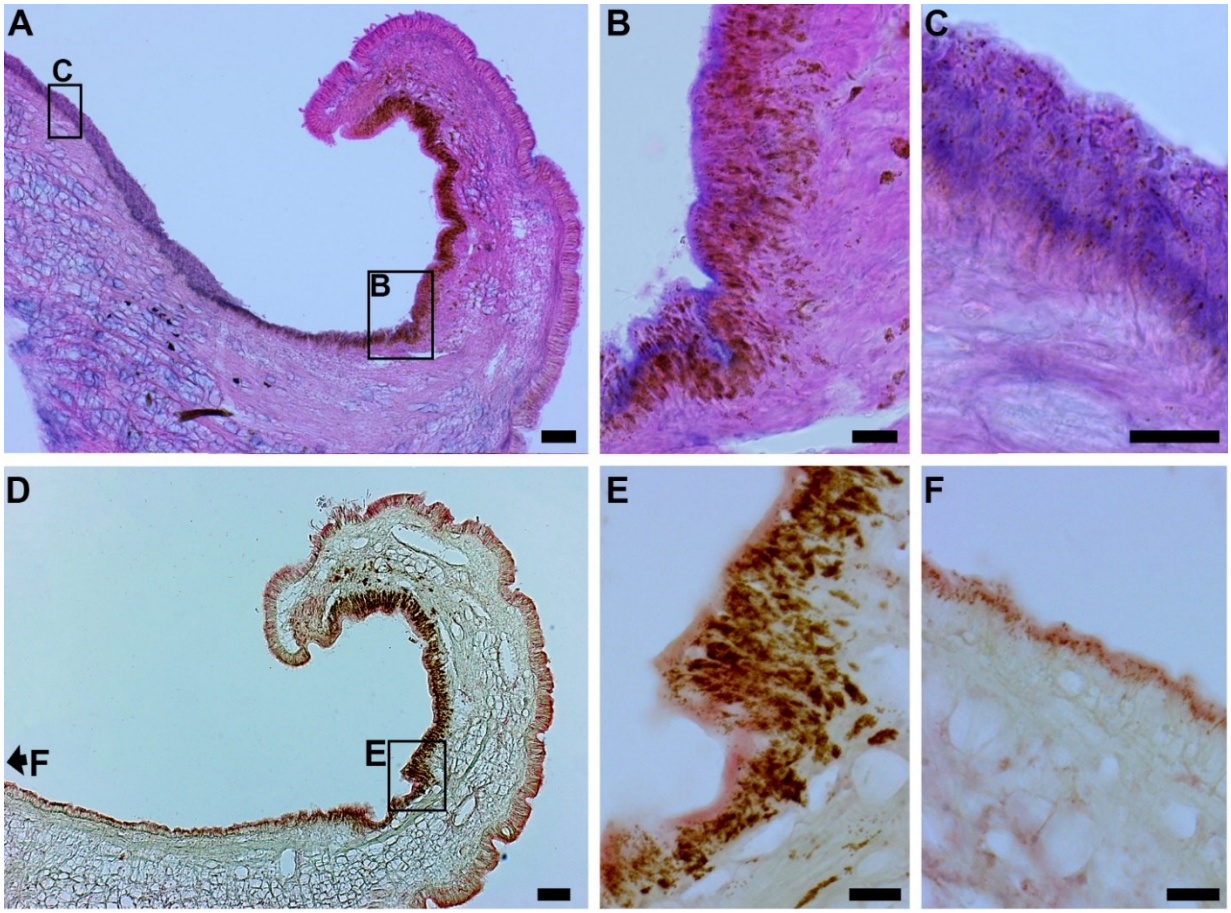

Figure 5.7. Mantle histochemistry: AP and AcP activity in *N. ostrina.* Mantle x.s. cryosections (20um thick; shell length 16.0 mm). Brown colour shows shell pigments of black shell A) Overview of AP (purple) in the apical edge of the proximal OME B) Inset of A showing distal edge of AP expression in the OME. C) Inset of A showing AP expression in the proximal OME. D) Overview of AcP (pink) in the apical edge of the OME E) Inset of D showing AcP expression in the distal OME. F) Inset of D showing AcP expression in the proximal OME. A,D Scale bar = 100 µm; B,C,E,F Scale bar = 25 µm.

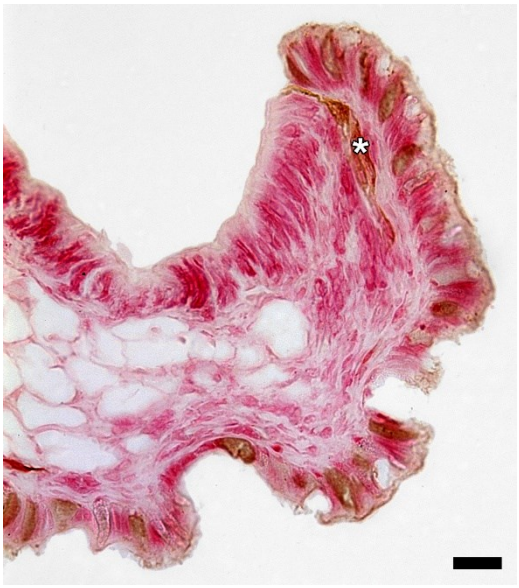

Figure 5.1 Mantle histochemistry: PO activity in *N. ostrina*. Mantle paraffin x.s. (7µm thick, shell length 16.1 mm). Peroxidase (brown) present in the distal part of the periostracal groove (*) and the mucous globe cells and apical border of the IME. Scale bar = 25 µm.

5.3.5 Difference in OME between ribbed and smooth mantles

Serial cross-sections were needed to recognize whether a particular cross-section was from either a smooth or ribbed individual, or whether it was a ribbed or inter-rib region of a ribbed individual. Size and shape of cells along the OME differed between ribbed and inter-rib sections and remained relatively constant in smooth mantles. At a fixed distance proximally from the periostracal groove (1 mm), cell height varied in ribbed mantles but not in smooth mantles (Figure 5.9A, B, blue triangles). Similarly, relative to a landmark (the pallial vein), cell height also varied in both ribbed and smooth mantles, in association with mantle ribbing (Figure 5.9A, B, red circles). The extensions of the mantle seen in the scalloped margin of a ribbed mantle appear to be distal extensions the length of the OME as the relatively straight pallial vein was further from the mantle margin at a rib rather than in an inter-rib location (Figure 5.9C, E). AP expression showed the same result, where the distance between the periostracal groove and start of AP expression was longer in ribbed compared to inter-ribbed mantle sections, while the cell height remained relatively constant at the border of AP expression (Figure 5.6C, Figure 5.9A, C). Put altogether, these measurements show that the cells of the distal OME are taller in ribbed rather than inter-rib sections (Figure 5.10), a pattern not seen in smooth mantles. In contrast, the more cuboidal proximal OME cells are of similar heights, such as at the beginning of AP activity.

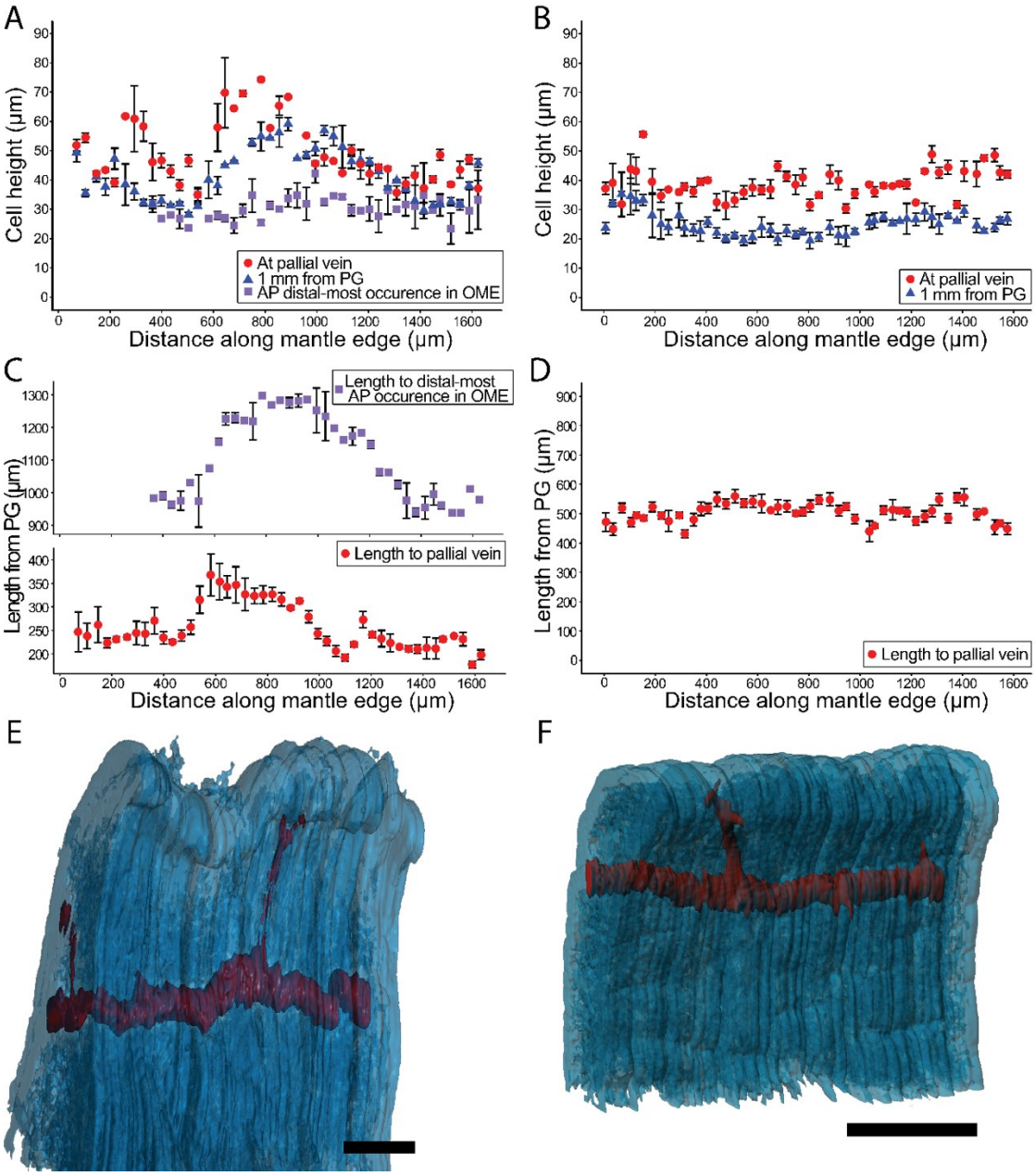

Figure 5.9. Morphometric differences in the OME between ribbed and smooth mantles of *N. ostrina*. A,B) OME cell heights at various locations: Across from the pallial vein (red), 1 mm proximally from the periostracal groove (blue), and at the distal-most occurrence of AP in the OME (purple). C,D) Proximo-distal length along the OME from the periostracal groove to the pallial vein (red), or to the distal-most occurrence of AP in the OME (purple) (Shell length, 20.2 mm). A,C,E) Ribbed mantle, B,D,F) Smooth mantle. Error bars- Standard Error, *n* = 3. E, F) 3D reconstruction of mantle tissue (blue) from a smooth (E) and ribbed (F) snail with the pallial vein reconstructed (red), oblique OME-side view. E) Not the same snail as A or C. F) Same snail as in B and D. Measurements illustrated in Figure 5.3. Shell length: A,C, 15.7 mm; B,D,F, 14.7 mm; D, 26.7 mm. Scale bars = 500 µm.

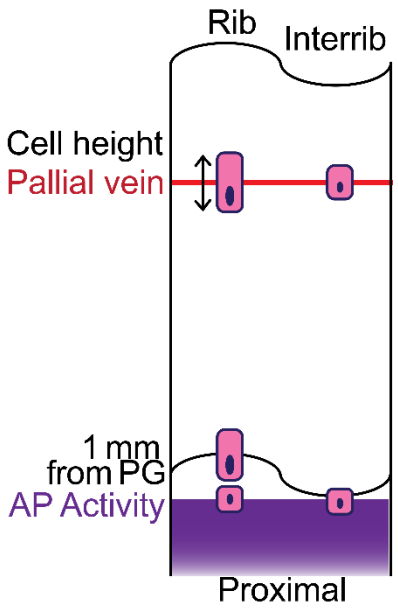

Figure 5.10 Diagram of relative cells heights in ribbed *N. ostrina* from Figure 5.9A,C. Cells heights (pink) are to scale. The distances between the pallial vein (red), 1 mm from periostracal groove (black), and the distal most edge of AP activity (purple) are also to scale, but a different scale.

5.4 Discussion

5.4.1 Rib formation in Nucella ostrina

Overall, rib formation in *Nucella ostrina* appears to be a relatively straightforward process. In smooth-shelled individuals, the length of the distal OME was relatively constant. In contrast, the length of the distal OME of ribbed individuals was longer in the regions secreting ribs than in inter-rib regions (Figure 5.9). The overall difference in mantle shape confirms this difference; mantle from a ribbed individual had a scalloped margin, while mantle from a smooth-shelled individual had a correspondingly smoothly curved margin (Figure 5.2). Three-dimensional reconstructions and measurements of serial sections showed that the pallial vein, generally parallel to the mantle margin, was further from the mantle margin at the rib compared to the inter-rib regions of the same mantle, as was the border of AP activity (Figure 5.9), suggesting that the distal region of the OME was longer in ribbed regions. The columnar cells of the OME were so tightly packed it was difficult to determine, but neither cell width nor density (although neither can be easily compared, even in TEM) differed in any obvious way, so I assume that the OME was extended by increasing the

number of cells. I believe that the thicker shell associated with a rib is produced by a longer OME, relative to the thinner shell of adjacent inter-rib regions, which have a shorter OME. This increased secretion may be enhanced by the taller cells seen in the distal OME in ribbed vs inter-rib regions of the distal OME, which would further increase the amount of shell material secreted to form the thicker spiral rib (Figure 5.10). In general, snails with less pronounced ribs also had less wavy mantle margins, further supporting this hypothesis. If the results seen in *N. ostrina* are applicable to shell growth more generally, then shell thickness should at least partially correlate with the length (parallel to the growth direction) of the mantle surface responsible for secreting that shell layer.

5.4.2 Rib formation in other molluscs

5.4.2.1 Mantle morphology

The mechanism of spiral rib formation proposed here may be applicable to other molluscs. Unfortunately, almost nothing is known about how shell sculpture is formed in other species. Young *Haliotis*, which produce spiral ribs, also have a mantle margin with small projections along the mantle margin that line up with the ribs, suggesting a similar mechanism for rib formation (see Figure 4B,D in Jackson *et al.*, 2006). The mantle of *Hexaplex trunculus* (Linnaeus, 1758), another muricid, is quite different from the mantle in *N. ostrina*, but the changes to produce sculpture appear similar (Urdy, 2015). The mantle has an outer fold and periostracal groove, more like *Haliotis* and pulmonates (Figure 5.11), with a short inner fold. Unfortunately the images in Urdy (2015) are not detailed enough to determine the cell types in the OME, but when secreting a spine or spiral rib, the outer fold is longer than adjacent inter-rib mantle sections, and bent upwards (Urdy, 2015).

Bivalve shell rib production does seem to differ from that of *N. ostrina*. In some shells with radial ribs, like *Aequipecten opercularis* (Linnaeus, 1758), the mantle has a distinct 3D morphology where the upper surface is ruffled, but the mantle margin is not scalloped as in *N. ostrina*. These raised portions of the outer mantle surface, called *corpora spinosa*, are responsible for rib formation (Checa & Jiménez-Jiménez, 2003). In some species, these ribs are not shell thickenings but ruffles in both the inner and outer shell surfaces (Tunnell *et al.*, 2010), seemingly formed by the shape of the *corpora spinosa*. Some gastropods like *Tonna* (Tonnidae) also have spiral ribs that are not thickenings (Tunnell *et al.*, 2010), so perhaps their mantle also shows *corpora spinosa.* Some oysters, which have a

different form of spiral sculpture called anti-marginal ribs (Checa & Jiménez-Jiménez, 2003), have shell thickenings only in the inner shell layer. The outer shell layer is ruffled, but uniformly thick (Figure A5.1D), but the mantle lacks any apparent scalloping of the mantle margin (Checa & Jiménez-Jiménez, 2003).

Although the evidence is quite sparse, spiral ribs appear to be formed in at least three different ways. 1) Ribs may be formed as thickenings of the outer shell layer, where they are presumably secreted by extensions of the scalloped distal OME, with a uniformly thick inner shell layer, as in *N. ostrina*. 2) Ribs of uniform thickness may be secreted by ruffled folds in the mantle (*corpora spinosa*), perhaps like in *A. opercularis*. 3) Thickened ribs may be formed as a ruffled outer shell layer that is then filled in by the inner shell layer to create a smooth inner surface — seen in oysters, although the mechanism is unclear. This inner shell layer may be secreted by extensions of the more proximal OME that do not affect the mantle margin. Clearly more information is needed to differentiate and confirm these different possible mechanisms.

5.4.2.2 Shell morphology

Rib formation solely in the outer shell layer is widely distributed in gastropods. The spiral ribs in *Calliostoma ligatum* (Gould, 1849) (Calliostomatidae), *Turbo* sp. (Turbinidae), and *Turritella* sp. (Turritellidae) were also only evident in the outer shell layers (Figure A5.1). If the pattern of shell layers is consistent between multiple species with spiral ribs, then it stands to reason that the mechanism of rib formation is also relatively conserved.

The outer calcite irregular layer and two inner crossed-lamellar aragonite layers seen in *N. ostrina* fits well with the pattern described for many muricids, and for ocenebrines in particular (Petitjean, 1965), but it is uncommon in Caenogastropoda (Taylor and Reid, 1990) as a whole. Unfortunately, too little information is available to say how similar shell secretion and sculpture formation is in other gastropods.

5.4.3 Mantle morphology in Gastropoda

The fine structure of the mantle appears to differ quite a bit among gastropod groups (Figure 5.11). The mantle of adult *N. ostrina* most closely resembles that of another marine caenogastropod, *Littorina littorea*, in having a periostracal groove that lacks a ‘groove’. Unfortunately, Bevelander and Nakahara (1970) did not describe the OME of *L. littorea* in sufficient detail for further comparison. In all other snails, the freshwater heterobranchs

Biomphalaria glabrata (Say, 1818) and *Lymnaea stagnalis* (L., 1758), the freshwater caenogastropod *Pomacea bridgesi diffusa* (Blume 1957), and the marine *Haliotis*, the OME shape is quite different. A clear division exists between the two OME regions, with further subdivisions that can be identified primarily by zones of gene expression (Timmermans, 1969; Marxen *et al.*, 2003; Jolly *et al.*, 2004; Jackson *et al.*, 2006). Fisher (1904) illustrated the mantle of *Lottia gigantea* Gray in G. B. Sowerby I, 1834 showing two zones in the OME, a distal uniform 'sense stripe' and a wrinkled proximal zone, although cell height did not appear to differ substantially between zones. Here I have used the term distal OME, and although the morphologies are not identical, I assume that this region generally corresponds to the belt and possibly transition zone of many other gastropods. What I have termed the proximal OME presumably corresponds to the zone 5 OME described for pulmonates (Marxen *et al.*, 2003). Similarly, for *Haliotis,* the distal and proximal OME regions correspond to the distal/anterior/tubular and proximal/posterior sections of the outer fold, respectively (Figure 5.11C) (Sud *et al.*, 2002; Jackson *et al.*, 2006; McDougall *et al.*, 2011). *Budd et al.* (2014) also briefly examined the mantles of *Stomatella impertusa* (Burrow, 1815), with a similar structure to *Haliotis*, and *Diodora* sp., whose mantle is reminiscent of bivalves with three lobes.

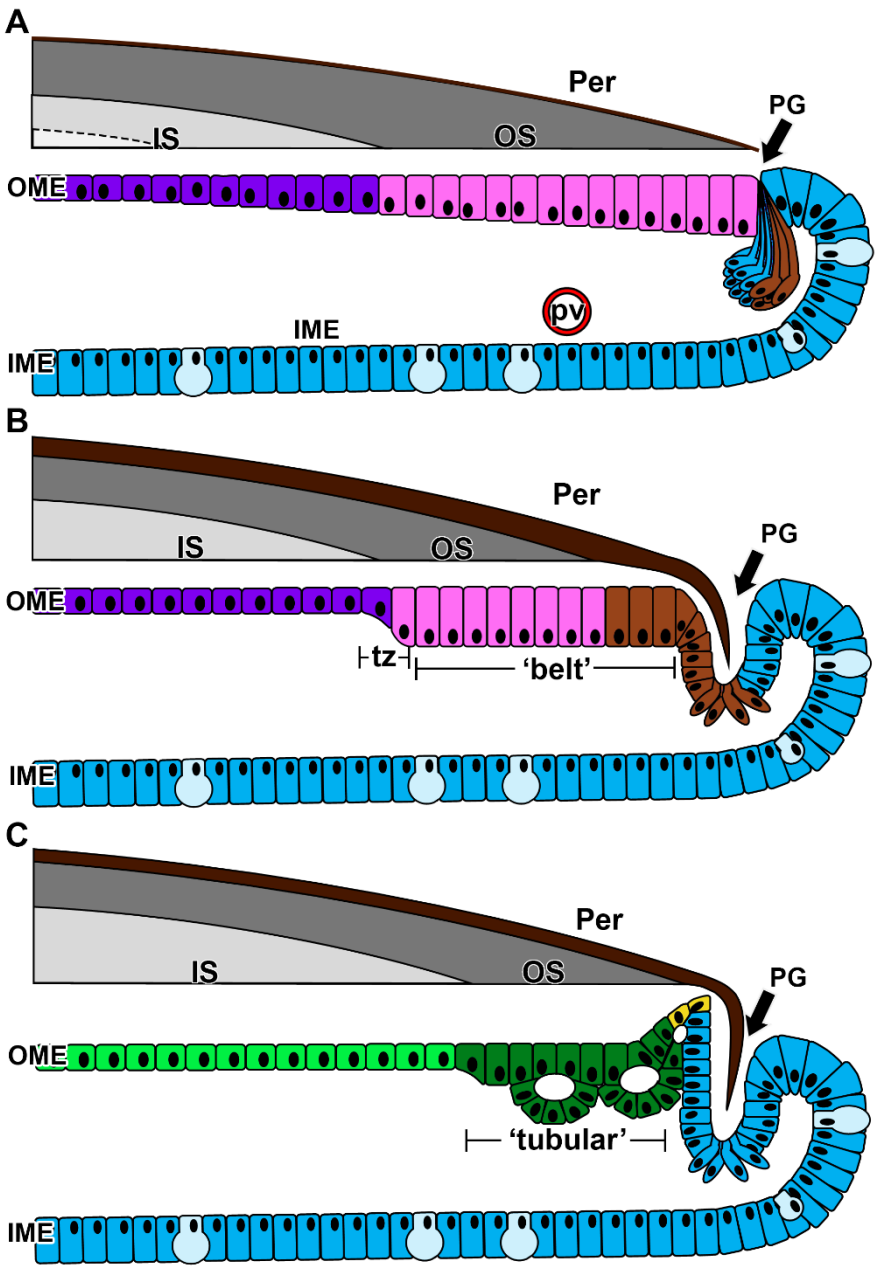

Figure 5.11. Generalized mantle x.s. diagrams showing shells layers and the mantle zones responsible, as well as known expression patterns of key enzymes. A) Mantle of mature *N. ostrina* and *L. littorea*, with periostracal 'groove' secreting the periostracum and a gradually decreasing height of OME cells proximally. B) Generalized mantle of *P. bridgesi, L. stagnalis, B. glabrata,* and hatchling *N. ostrina* with a periostracal groove secreting the periostracum, a thickened 'belt', short transition zone (tz), and cuboidal proximal OME cells. C) Mantle of juvenile *Haliotis* with periostracal groove, thick 'tubular' zone, and shorter cells in the proximal OME. Expression zones determined in Jackson *et al.* (2006): 'posterior zone of outer fold' = proximal OME (light green); 'anterior zone of outer fold = distal OME (dark green) (also region of MSI60/MSI31 expression (Jolly *et al.* 2004); 'anterior edge of outer fold' (yellow). pv: pallial vein; AP expression: purple; AcP expression: pink; IS: inner shell layer (light grey); OS: outer shell layer (dark grey); PG: periostracal groove; Per: periostracum (dark brown); peroxidase expression: brown. Not to scale.

5.4.4 Mantle ontogeny and seasonality

The OME morphology of hatchling *N. ostrina* (Figure 5.4) offers some intriguing insights into both the ontogeny and evolution of the mantle in muricids. Hatchling mantle morphology differed considerably from the larger snails I sampled. Rather than a gradual transition in cell shape along the OME, a clear periostracal groove was present (from which the periostracum emerged), followed by a thick belt, a short transition zone, and then a thinner cuboidal OME proximally. Mantles in other gastropods, including another caenogastropod, *Pomacea,* closely resemble this morphology (Timmermans, 1969). A similar ontogeny is found in *Haliotis*, where juvenile snails have a much larger distal OME, while adults may lack that region altogether (Sud *et al.*, 2002). However, this pattern varies seasonally in *Haliotis* (Jolly *et al.*, 2004). Seasonal variation also occurs in *Lymnaea stagnalis,* where the mantle of hibernating snails maintains a similar OME morphology, but expression of key shell-secretion enzymes is significantly reduced (Timmermans, 1969). I suspect that the distinctive belt morphology of juvenile *N. ostrina* relates to fast shell secretion in newly hatched individuals, and that mantle morphology gradually transitions to the adult morphology as shell secretion rates slow. Bevelander and Nakahara (1970) studied mature *L. littorea*, so this mantle morphology and ontogeny may occur more broadly.

5.4.5 Enzymatic activity

Enzyme activity in *N. ostrina* was similar to other gastropods. Peroxidase activity, which is involved in cross-linking the amino acids of the proteinaceous periostracum (Hohagen and Jackson, 2013), was limited in the mantle of *N. ostrina*, and consistent with the thin periostracum in larger *N. ostrina* (Figure 5.7). I am unsure why only some of the periostracal groove showed peroxidase expression, as the entire periostracal groove is thought to be used in periostracum formation in *Littorina littorea*. However, the mantle of *L. littorea* is much thicker than that of *N. ostrina* (Bevelander and Nakahara, 1970). *Lymnaea stagnalis*, with a thick periostracum, shows peroxidase activity throughout the periostracal groove and the majority of the belt (Timmermans, 1969).

Although the exact role of alkaline phosphatase in shell secretion is unclear, the expression pattern seen here matches that of other molluscs. AP activity was found in the apical region of the more proximal cells of the OME, as well as in the IME and connective tissue (Timmermans, 1969; U. Bielefeld *et al.*, 1993; Marxen *et al.*, 2003; Hohagen and Jackson,

2013). Acid phosphatase expression, whose function in biomineralization is also unclear, was similar between *N. ostrina* and other snail species, with a low background expression but with increased activity in the more distal OME (Timmermans, 1969; Marxen *et al.*, 2003). These two enzymes appear to divide the OME into two regions, which may reflect the transition between secretion of the inner and outer shell layers. The outer shell layer is secreted by the more distal OME cells, which are columnar, and express upregulated AcP activity. The inner shell layer is secreted by the more proximal, cuboidal OME cells with AP activity. McDougall *et al.* (2011) proposed a similar theory for the two shell layers of *Haliotis* based on different secretions seen in SEM images of the different regions of the OME. This subdivision is further supported by the different mantle zones identified by Jackson *et al.* (2006) with *in situ* hybridization. The separate expression patterns of two shell matrix protein genes, MSI31 and MSI60 in *Pinctada* (Sudo *et al.*, 1997) were thought to mark the two shell layers in these species, however the pattern was much more complicated in *Haliotis* (Jolly *et al.*, 2004). In *Haliotis,* both MSI60 and MSI31 were expressed in the periostracal groove, tubular zone, and some of the proximal OME in overlapping regions, and their expression also varied seasonally. *Haliotis* has an outer prismatic layer comprised of both calcite and aragonite, which may help explain this complicated expression pattern, but no exclusive nacreous expression was seen like that in *Pinctada*.

5.4.6 Conclusions

A few papers have modeled shell ornamentation (Checa, 1994; Checa & Jiménez-Jiménez, 2003; Chirat *et al.*, 2013), but how such ornamentation is produced by the mantle remains a puzzle. I compared the mantle and shell morphologies of ribbed and smooth-shelled *N. ostrina* with multiple techniques; histological, ultrastructural, 3D reconstructions, and a histochemical investigation of some key marker enzymes. Altogether these observations revealed a simple mechanism, most features were similar in mantles from ribbed and smooth-shelled individuals, which is perhaps not surprising given the different sculpture types are controlled by a single-locus, two-allele polymorphism (A. Richard Palmer, 1985). Only the length of the OME and distal OME cells heights appeared to change to produce spiral ribs in *N. ostrina.* Meagre evidence from other gastropods suggests that the pattern seen in *N. ostrina* may be more generally applicable in gastropods, but that remains to

be tested. My model offers a straightforward mechanism for the development of spiral shell sculpture that would be worth testing in other gastropods.

Numerous transcriptomic and genetic surveys suggest that the molecular pathways and signaling for shell secretion is complicated, and some sections are not very conserved (reviewed in Kocot *et al.*, 2016). However, as modern tools and mollusc sampling improves, our ability to understand the formation and evolution shell morphology, both in terms of shell sculpture and shell colour (Williams, 2016) improves.

Chapter 6 — Discussion

6.1 Summary

This thesis addresses some major questions that have not yet been widely explored: 'How did shell sculpture evolve?' and 'How is shell sculpture built?' (Judson, 1979). The results from each chapter have implications for gastropod biology and how gastropods control the growth of shell sculpture. In particular, I tried to answer four separate questions about the development and evolution of gastropod shell sculpture.

1) What is the evolutionary history of a distinctive type of axial shell sculpture in gastropods: the varix (Chapter 2)? I observed that the same structural innovation evolved at least 41 times (Webster and Vermeij, In Press), although it is not clear whether these varices are functionally significant in all cases. In many cases varix origins appeared to be phylogenetically clumped, suggesting that certain preconditions – genetic or ecological – increased the likelihood of those origins. Some patterns emerged about when, where, and from what preconditions, varices might evolve. Most notably, they appear to have evolved in snails with high spired shells with axial ribs found in environments prone to high predation levels – shallow, warm, marine environments. These results re-affirm the value of gastropod shells for studying the evolution of novel morphologies.

2) What is the mechanism that synchronizes varix placement between adjacent shell whorls (Chapter 3)? I investigated the intricacies of a complex developmental program and the possibly simple mechanism behind it in a species with highly periodic and synchronized axial sculpture. By shaving off different varices, I confirmed that *Ceratostoma foliatum* does not simply use physical cues from prior sculpture to position a new varix. Rather, an endogenous system appears to be involved in regulating shell growth into periodic, aligned varices. Furthermore, I showed that normal synchronized shell growth can be disrupted during shell repair, which can induce an apertural varix outside of the normal positioning. Shell secretion differs from other patterns of morphological development. The structure produced is nonliving, and grows in an accretionary fashion from the same cells. More work on the developmental mechanics of gastropod shell sculpture has the potential to reveal valuable clues about the evolution and development of skeletons produced by accretionary growth in other mollusc classes, and in other groups like brachiopods, tube-dwelling

polychaete annelids (e.g., Serpulidae) and hemichordates (e.g., Pterobranchia and their extinct graptolite kin).

3) How does previous shell sculpture affect future shell growth, and what affects the growth and spacing of axial sculpture in species with non-synchronized sculpture (Chapter 4)? I showed that the position of previous lamellae does not affect the placement of future lamellae or affect shell growth rate in *Nucella lamellosa*, suggesting that no significant cost to shell dissolution exists during growth (Webster and Palmer, 2016). Specifically, lamellar spacing was affected solely by shell growth rate, which was in turn affected by body size and feeding rate. These conclusions support the suggestion (Chapter 2) that lamellae are different structures from varices. From a broader perspective, these results demonstrated the great variation in both feeding and shell growth parameters in this highly plastic species, opening up the potential to test the effect of extrinsic factors on shell and sculpture growth as a model for the complex factors that affect plasticity in many organisms.

4) What changes in the mantle are responsible for producing spiral ribs (Chapter 5)? I described the basic morphological changes in the mantle that allow *Nucella ostrina* to secrete spiral ribs. By extending the proximo-distal length of the mantle and increasing the cell height of those cells, more shell is secreted, leading to a thicker shell at the location of a rib. Some observations from the literature suggest that this may be a conserved mechanism for controlling shell thickness in general. This relatively simple mechanism, studied with a rapidly expanding combination of tools, could be a viable direction to add to our understanding of the development of form, and its molecular underpinnings.

This research also revealed several technical challenges to the study of gastropod shell-sculpture development (Appendix 6): more work is required to develop successful protocols for *in situ* hybridization, and many intricacies of snail husbandry are underappreciated.

6.2 Synchronized shell sculpture growth

The ability to precisely position shell sculpture elements is not rare in gastropods. Fourteen of 41 origins of varices showed at least some species with synchronization of varix growth, six of which are in the Muricidae (Chapter 2, Webster and Vermeij, In Press). Many other shell forms require precise positioning during shell growth. Many gastropods and

ammonoids exhibited a morphogenetic countdown, where a specific temporal series of structures form (e.g., changes to the sculpture or coiling axis) prior to the terminal aperture (Chapter 2, Webster and Vermeij, In Press; Seilacher and Gunji, 1993). Examples include the unusual coiling of heteromorph ammonites (Figure 6.1A) (Seilacher and Gunji, 1993), the recurved 'sinistroid' tuba of some diplommatinid land snails (Figure 6.1C) (Webster *et al.*, 2012), and the nine separate origins of subterminal varices (Chapter 2, Webster and Vermeij, In Press). The precise positioning of these countdown structures during growth requires the same level of control as for synchronized varices. The Xenophoridae show a more unusual example of 'sculpture' alignment, where bits of shell or debris are regularly attached to the shell during growth (Figure 6.1B) (Ponder, 1983). All of these examples require some mechanism where the relative position of shell features is known, and are found in diverse clades. Either this ability is highly conserved, or it has evolved multiple times.

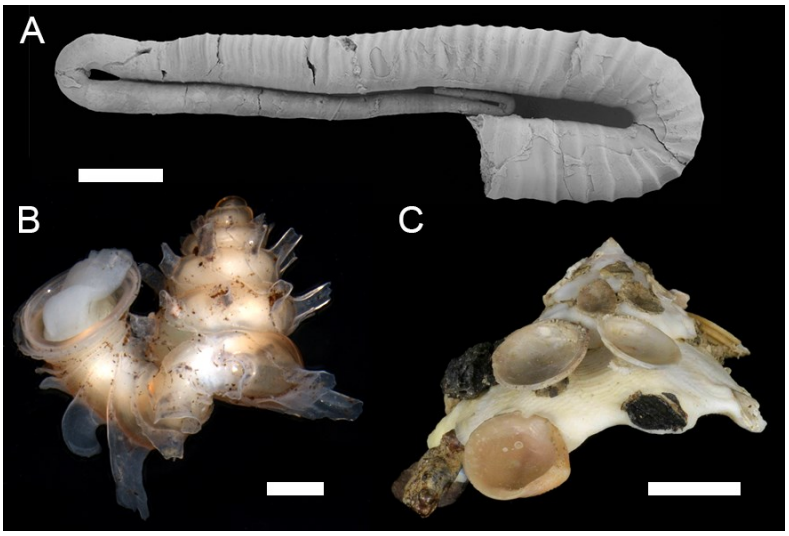

Figure 6.1. Examples of specific positioning of shell features other than varices. A) Heteromorph ammonite; *Polyptychoceras pseudogaultinum* Yokoyama 1890. Scale bar = 10 mm, modified from (Ikuno and Hirano, 2015). B) 'Sinistroid' diplommatinid; *Opisthostoma fraternum* E. A. Smith, 1905 RMNH.MOL.119824. Scale bar = 0.5 mm C) Xenophoridae. *Xenophora crispa* (König, 1825) USNM 1197251. Scale bar = 1 cm, modified from http://collections.nmnh.si.edu/.

Shell features are rarely, if ever, randomly distributed on the shell. Colour, as well as both axial and spiral sculpture, may not always be precisely positioned, but are generally produced in a regular or semi-regular pattern. For example, the lamellae of *N. lamellosa* appear superficially regular, despite the high degree of variation in lamellar spacing (Chapter 4, Webster and Palmer, 2016), suggesting that shell growth is normally regular and regulated.

If the conserved mechanism of shell secretion includes normal positioning of shell features, even if somewhat imprecisely, then the mechanism behind synchronized sculpture growth is likely similar across gastropods.

6.3 Variability and extrinsic factors affecting shell growth

The research presented here revealed a great, although unsurprising, variability in growth in snails, from the intraspecific variation in varix presence in some families (Chapter 2, Webster and Vermeij, In Press) to the different growth forms of *C. foliatum* as a result of shell manipulation (Chapter 3). The most obvious case is *N. lamellosa*, which exhibited a great deal of variation in shell growth rates, feeding rates, and lamellar spacing among individual snails (Chapter 4, Webster and Palmer, 2016). Although previous shell sculpture had little effect on subsequent shell growth, the factors inducing lamellar growth and spacing (other than shell growth rate) remain unclear. Lamella formation simply may not be a strongly regulated system (Chapter 4, Webster and Palmer, 2016). However, factors must affect their placement, and identifying those factors could help explain why these lamellae are so variable, when most other shell sculpture forms appear more regular (see 6.2 *Synchronized shell sculpture growth* above). Careful observation of other species will be required to test this hypothesis, perhaps demonstrating a higher level of sculpture variability across Gastropoda. Any number of biotic or abiotic factors could affect the spacing of lamellae, from water temperature, to food quality, or predation pressure. Most of these factors will also affect shell growth rate, and increased shell growth rate appears to increase lamellar spacing (Chapter 4, Webster and Palmer, 2016). Snail behavior can correlate with shell features, such that 'bolder' *Radix balthica* have thicker shells than snails that are more 'shy' (Ahlgren *et al.*, 2015). Because lamellae are assumed to be a defensive structure, their spacing may relate to snail behavior; other *N. lamellosa* shell features have been shown to vary with predator presence (Appleton and Palmer, 1988).

Field-collected snails grow their shell differently than snails grown in the laboratory (A. Richard Palmer, 1985). Laboratory-raised *N. ostrina* had a strongly bimodal distribution of rib formation, but field-collected snails had more intermediate rib heights, even after growing in the lab. The past effect of environmental cues therefore appears to persist in future shell growth. If the study of *N. lamellosa* sculpture growth (Chapter 4) had been done

with fully laboratory-raised snails, the results might have been less variable, and possibly clearer.

6.4 Parietal and siphonal shell secretion

The mantle is a continuous sheet of tissue that rings the entirety of the shell aperture. In addition to the aperture and associated shell sculpture, this tissue also secretes the parietal (columellar) side of the aperture and the siphon (when present). To my knowledge, all studies of shell secretion have focused on the apertural side of the mantle — the largest area of tissue — which secretes the majority of the shell.

New shell is also secreted by the parietal mantle. It produces a thin, smooth layer over top of the previous body whorl, which ultimately yields the columella, and keeps the boundaries of the living space smooth (Carriker, 1972). The parietal mantle has an additional function. It is responsible for partly dissolving the outer surface of the previous whorl, smoothing away sculpture (Fretter and Graham, 1962; Carriker, 1972) and sometimes removing epibionts (Pers. Obs. NBW) in front of the aperture. As noted in Chapter 3, an entire layer of shell is smoothed away, not just sculpture (although not in all snails, see Carriker, 1972).

How this dual function affects the morphology of the parietal mantle is unclear. I would predict a few differences when compared to the apertural mantle region: 1) The shell can be secreted directly onto the previous whorl, so neither a periostracum, or periostracal groove, is required. 2) Shell dissolution would occur prior to shell deposition, so the distal-most region of the mantle should be responsible for shell dissolution. This region would likely have many similarities to the ABO (Accessory Boring Organ), a tissue responsible for the chemical dissolution during prey drilling (Clelland and Webster, 2016). 3) Thin-sections of the shell (Figure 6.2) suggest that only the inner shell layer is secreted along the columella, so no tall columnar cells would be present to secrete the outer shell layer. A cuboidal inner shell layer-secreting epidermis should therefore lie proximal to the shell dissolution region.

These hypotheses about the morphology of the parietal mantle can easily be tested using histological sections to compare the morphology to the pallial mantle and ABO tissue. Furthermore, it would be most interesting to determine how shell dissolution is achieved, and

if the mechanism is similar to that of the ABO (Clelland and Webster, 2016). More derived gastropods may use a more efficient method of smoothing the shell in front of the aperture. If true, it might support the hypothesis (Chapter 4) that elaborate shell sculpture could arise more easily once an efficient mode of shell dissolution arose, possibly in conjunction with a drilling mode of predation (Clelland and Webster, 2016; Webster and Palmer, 2016), as the cost of removing shell sculpture was prohibitive in ancestral gastropods.

A third region of the mantle must produce the siphon. The siphon primarily guides the incurrent flow into the mantle cavity, which includes oxygenated water and chemosensory cues, although it may also have chemoreceptors itself (Emery, 1992). Most likely, the external epithelium that produces the siphonal canal is similar to the apertural and parietal mantle regions, secreting the siphonal canal directly, although the shell covering the siphon is much thinner, and may lack inner shell layers. Chapter 2 posited that the typical periodic growth of varices may be advantageous to species with siphonal canals, especially for infaunal snails with bent siphons, as this would prevent the need for constant remodeling of the siphonal canal, and may allow the snail to close (cover over) the siphonal canal (Webster and Vermeij, In Press).

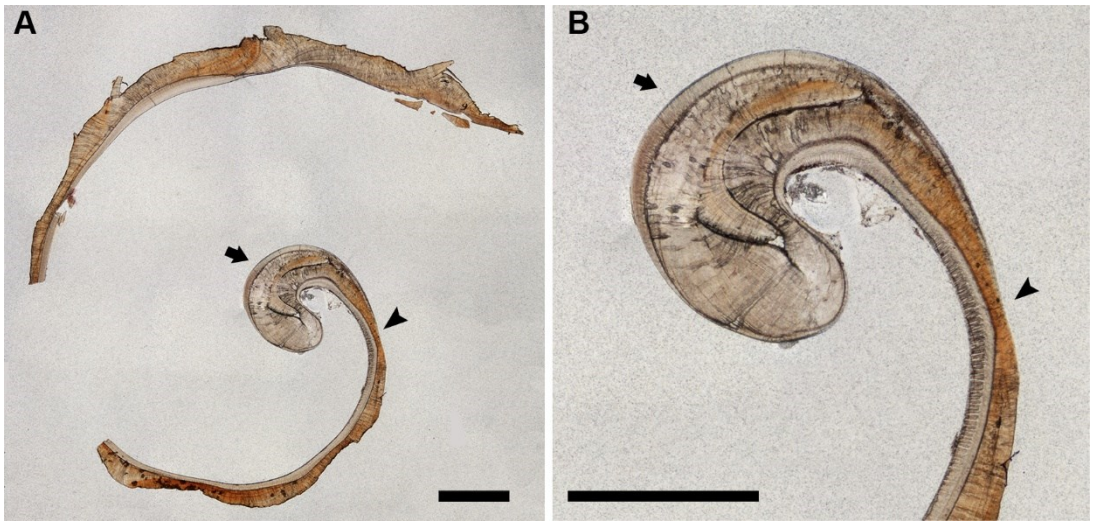

Figure 6.2. Ribbed *N. ostrina* shell x.s. showing parietal shell dissolution and secretion. A) Entire shell section, aperture on right. B) Inset of columella and parietal side of the aperture. parietal shell dissolution: arrowhead; secretion of crossed-lamellar inner layer: arrow. Scale bar = 1 mm.

6.5 Mantle flexibility and spine formation

The mantle fold of gastropods is basically a flexible hydrostatic skeleton (Savazzi, 1990) that must be able to retract with the snail body, and re-extend into position for shell secretion. During shell secretion, mantle shape is constrained by the shell it is pressed against during shell secretion and the mantle musculature. During normal shell secretion, the mantle is thought to grow and extend simultaneously with shell secretion, continually extending the apertural margin (Chirat *et al.*, 2013). Chirat *et al.* (2013) modeled spine formation using a continuously growing, elastic mantle edge that gradually curves into itself as it grows up a spine, by conforming to the shape of the previously deposited shell. A similar mechanism seems reasonable for the growth of any axial sculpture, with the mantle gradually expanding up and out from the shell, secreting the axial element. However, this has been neither modeled nor tested. In addition, no attempt has been made to model the rest of the process of mantle deformation during sculpture growth.

What happens when the deposition of a spine is complete, and the mantle returns to growing the body whorl? Two possible mechanisms might explain how the mantle grows and shrinks during the production of axial sculpture. 1) The mantle expands through mitosis and shrinks through apoptosis. Indeed, the mantle must reduce in size to grow down the front face of the varix to fill it in (Chapter 3). This is also the presumed mechanism of spine formation in *Hysteroconcha* (Bivalvia) (Carter, 1967). In both *N. lamellosa* and *C. foliatum*, when relaxed (in $MgCl_2$), the mantle covers the entirety of the lamella or varix at its peak height, but also only covers the apertural edge in between axial elements (Pers. Obs. NBW). The large varices of *C. foliatum* or the almost impossibly elongate spines of the venus comb murex (*Murex pecten*) seem so large that they would require mitosis. 2) Alternatively, the mantle expands elastically and contracts plastically to grow axial sculpture. It seems energetically wasteful to repeatedly grow and shrink the mantle through apoptosis after each axial element. In the case of lamellae, or some spines, where growth starts again from the base (Chapter 4, Webster and Palmer, 2016), how does apoptosis shrink the mantle so quickly? Lamellae are produced repeatedly and constantly (see Chapter 4), unlike the long pauses between varices. Experiments will be required to determine the biological mechanism for mantle expansion and contraction during axial sculpture growth. It would be interesting to see how this mechanism differs among different types of sculptures.

6.6 Other forms of shell sculpture

The research presented here focused on the growth of three major types of shell sculpture: varices, lamellae, and spiral ribs. However, a great diversity of other forms of shell sculpture exist that were not examined here (Abbott and Dance, 1982). Spiral sculpture essentially represents local shell thickenings or undulations in the shell edge. Whether the mechanism of spiral rib growth seen in *N. ostrina* is conserved in other species remains to be seen (Chapter 5), but if so, it should apply to spiral sculpture in general. Questions still remain about the growth of different types of axial sculpture – mainly varices, lamellae, and ribs, and how the mantle expands and contracts to secrete them and how their spacing is maintained. Most beads, knobs or nodes could be seen simply as discontinuous spiral ribs, or as a combination of mechanisms of spiral and axial sculpture.

Less clear are sculpture types that do not align with the direction of growth, such as the peculiar oblique subterminal varices in some Nassaridae (Chapter 2, Webster and Vermeij, In Press), which would require a signal that varies along the length of the aperture with shell growth. Many colour morphs of gastropods also exhibit oblique patterns. Although untested, most authors assume that the signaling that regulates colour pattern or a sculpture pattern are similar (Boettiger *et al.*, 2009; Meinhardt, 2009; Williams, 2016).

The callus is a form of shell sculpture that covers the body whorl in front of the aperture (Radwin and D'Attilio, 1976), either periodically (e.g. *Distorsio*) or terminally (Cypraeidae), which could be grown by a temporary expansion of the parietal mantle, similar to the expansion of the apertural mantle required to produce a varix. This is not to be confused with what occurs in some families with external shells that are covered and smoothed constantly by a highly expansive foot or mantle (e.g. Cypraeidae, Olividae) (Vermeij, 1995). Investigation of the presence of mantle-like abilities in the foot of such species, and how that arose evolutionarily, would be worth exploring.

One unusual type of sculpture is internal sculpture — a variable array of folds or teeth grown inside the aperture, mostly for defence purposes, although they have not been well investigated (Price, 2003; Vermeij, 2015b). These structures are probably only produced by the inner shell layer, generally as terminal structures, and it would be interesting to see how similar the process is to secreting external sculpture.

One final form of shell sculpture encountered during this thesis is the labral tooth, a spiral projection from the aperture in many predatory species, generally used in feeding (Vermeij, 2001). Normally in *Ceratostoma. foliatum*, the labral tooth is only formed in association with a varix (i.e., it is not present during intervarical growth). During its growth hiatus, *C. foliatum* gradually grows the lip of the varix, including the labral tooth, although why they continue to grow slowly is unclear. It may be that the labral tooth can become worn or easily broken during feeding (Vermeij, 2001), and this slow growth can maintain it, or it could be due to a low level of constant shell secretion of gastropods, even in the absence of food (Palmer, 1981). Interestingly, several *C. foliatum* individuals exhibited a stuttered growth pattern, potentially caused by either obstruction by glue or interruption of growth by a red tide (Chapter 3). In these cases, the apertural margin progressed very slowly forward, producing a labral tooth. The production of this tooth suggests that the snail has specifically stopped growing, rather than simply being impeded.

6.7 Molecular aspects of sculpture growth

With decreasing financial costs and increasing interest in the molecular biology of non-model systems, it has rapidly become more feasible to understand the molecular aspects of shell secretion, and how they are used to modify shell shape and colour. For instance, it now seems feasible to identify the single gene responsible for rib formation in *N. ostrina* by collecting and comparing mantle transcriptomes of ribbed and smooth-shelled snails. The problem is not that simple however. 1) Rather than a single gene, regulation could instead be a tightly linked set of genes that act as a single unit (Palmer, 1985), like the colour supergenes seen in several land snails (Murray and Clarke, 1976; Cook, 1998; Asami and Asami, 2008). 2) The gene may only be active for a short period. Spiral ribs are grown consistently throughout life after metamorphosis, and rib formation starts at the transition from the protoconch (larval shell) to the teleoconch (adult shell). 3) The genetic difference between ribbed and smooth actually involves rib suppression. Upon hatching, all *N. ostrina* start growing ribs, which then gradually fade to a smooth shell after a couple of whorls of growth, so all individuals grow ribs initially, but ribbing is somehow suppressed later in life in smooth-shelled snails. 4) Rib formation is at least partially a plastic process. Although sculpture in laboratory-grown snails is relatively dimorphic, field-collected snails exhibit

intermediate degrees of spiral sculpture, even after being brought into the lab (Palmer, 1985). This suggests that other signalling pathways may modulate the degree of rib formation based on environmental cues. A set of transcriptomes should be able to identify the gene(s) responsible, or at least its downstream targets; it would identify the process to stop rib formation, rather than start it.

Once the functional genes are identified, we can begin to unravel the mechanism of control for shell sculpture. Where are these genes expressed? Do they cause differential growth of the mantle, specifically the distal OME (Chapter 5)? Are there connections to some form of neurosecretory pathway that could support one popular model of shell secretion (Boettiger *et al.*, 2009)?

6.8 Using models to predict biological mechanisms

Although the main physical-feedback hypothesis for how *C. foliatum* controls synchronization of varix position was rejected (Chapter 3), the actual mechanism underlying regular varix spacing is still unknown. However, an endogenous signaling mechanism seems most likely. Further experimentation on the effects of disrupting synchronized shell growth should give greater insight into how this mechanism works. Experimenting with a faster growing species, one with more varices per whorl (e.g., *Hexaplex*), or one with greater changes correlating with synchronization of varix growth (e.g. the bizarre undulating coiling axis of *Distorsio* or some Eulimidae; Chapter 2, Webster and Vermeij, In Press) might provide further clues about what can disrupt normal shell growth, and thus what is involved in regulating sculpture position.

Although model systems have given us examples of a range of cellular and molecular mechanisms underlying morphogenesis and developmental patterning (Heller and Fuchs, 2015), two main models have been proposed for the control of sculpture growth: A reaction-diffusion model (Meinhardt, 2009) where the interaction between diffusing activation and inhibition molecules control patterning, and a neurosecretory model (Boettiger *et al.*, 2009) where patterning is under nervous control, including the patterning of activation and inhibiting neurohormoes. Both models have been shown to affect development in other organisms. The activator/inhibitor pair Nodal/Lefty interact according to reaction-diffusion models in zebrafish development (Müller *et al.*, 2012). Neurohormones are also known to be

involved in triggering multiple developmental events in both vertebrates and invertebrates, including metamorphosis (Klowden, 2003).

The same logic applied mainly to modeling shell colour patterns should apply to shell sculpture. Both Meinhardt (2009) and Boettiger (2009) were able to replicate a remarkable diversity of sculpture patterns along with shell coiling and colour patterns. Overall the two models are fundamentally similar in how they function, termed local activation with lateral inhibition models (LALI) (Boettiger *et al.*, 2009), where spatial or temporal arrangements of activating and inhibiting molecules interact to form specific patterns. Alternatively, the two systems could work together to produce shell morphology and patterns. Although a LALI type mechanism seems feasible for most cases of shell sculpture, none have modeled shells on the much larger spatiotemporal scale required in the case of varices, which might be 240° or 360° apart. This widely spaced type of sculpture does not exclude either model. Furthermore, there is no indication of what specific molecules or neurohormones might be involved. However, studies in other organisms have shown that reaction-diffusion systems are capable of signaling over longer distances by using a complex cascade of molecules (Heller and Fuchs, 2015). Also, the mantle epithelium is interconnected by nerves, allowing a long range effect of neurosecretory signaling (Saleuddin and Dillaman, 1976; Budd *et al.*, 2014). There are also major problems with these models. Current computer models do not attempt to incorporate a realistically variable growth rate, whether periodic or due to extrinsic factors, like season. These could disrupt the crucial synchronization pattern of the signaling in a way not predicted in the model. Perhaps more importantly for our understanding of the actual mechanisms, reaction-diffusion models do not provide predictions that can be tested without in depth knowledge of the signaling molecules involved. As a result, we cannot easily use them to guide future work.

Overall I favour the neurosecretory model (Saleuddin and Kunigelis, 1984; Ermentrout *et al.*, 1986; Boettiger *et al.*, 2009). 1) This model is more directly based in biology and mantle morphology. 2) It allows for direct input from the brain that could modify shell sculpture based on other factors, such as the detection of predators (Appleton and Palmer, 1988). 3) This model could incorporate the evidence that some physical feedback is capable of modifying shell secretion, either in synchronized varices (Chapter 3), or correcting coiling angle (Checa and Jiménez-Jiménez, 1997; Checa *et al.*, 1998). 4) This model may be

testable. Sophisticated techniques could measure differences in nerve signaling or neurohormone secretions across the mantle spatially or temporally, although this may not be simple or feasible. The neurosecretory model does not exclude possible contributions from reaction-diffusion elements, possibly to maintain a pattern set by neurosecretions.

6.9 Future directions

As is typical of any research endeavour, my thesis has produced more questions than it has answered. Throughout this discussion and the previous chapters I have suggested several possible ideas for follow up experiments to try and pose a number of new questions raised by my conclusions. In general, repeating these experiments with more diverse taxa would test the robustness and universality of my results. Knowing how conserved the patterns of shell sculpture growth and control are will help us understand how they evolved. Other ideas involve more expensive or involved techniques that I did not have a chance to try, and which, in future, will be better directed based on the knowledge I present here.

6.10 Conclusions

My thesis examined multiple aspects of gastropod shell sculpture development and evolution, a topic that is not yet well understood. I examined the repeated evolution of varices, a shell sculpture innovation, and demonstrated both the correlations and variations associated with its origins and defined varices separately from other forms of shell sculpture (Chapter 2, Webster and Vermeij, In Press). I also rejected the main physical feedback hypothesis for how synchronized shell sculpture is maintained in *C. foliatum*, and suggest that the mechanism is more complex and probably endogenous (Chapter 3). I investigated the growth of axial lamellae in *N. lamellosa,* establishing that lamellae grow continuously, previous shell sculpture does not slow shell secretion, and lamellar spacing increases with shell growth rate (Chapter 4, Webster and Palmer, 2016). Finally, I observed mantle morphology in *N. ostrina,* which suggests that spiral rib formation is due to increased and larger secreting cells producing the thicker ribs in the distal OME. Although we might never map out the entire complex system responsible for shell sculpture, further study of this system would be worthwhile as an example of a different type of development, the accretionary growth of hard parts. This has arisen multiple times in earth's history, in

molluscs, brachiopods, polychaete annelids, foraminiferans, and corals. I believe lines of inquiry like the ones presented here can give us a different perspective on the development and evolution of novel forms of organisms.

References

Aartsen, J. van, H. Menkhorst and E. Gittenberger. **1984**. The marine Mollusca of the Bay of Algeciras, Spain, with general notes on *Mitrella*, Marginellidae and Turridae. *Basteria Suppl* **2**: 1–135.

Abbott, R. T. 1974. *American Seashells*, 2nd ed. Litton Educational Publishing, Inc., New York.

Abbott, R. T. and S. P. Dance. **1982**. *Compendium of Seashells: A Full-color Guide to More Than 4,200 of the World's Marine Shells*. E. P. Dutton, New York.

Ackerly, S. C. 1989a. Kinematics of accretionary shell growth, with examples from brachiopods and molluscs. *Paleobiology* **15**: 147–164.

Ackerly, S. C. 1989b. Shell coiling in gastropods: Analysis by stereographic projection. *Palaios* **4**: 374–378.

Addadi, L., D. Joester, F. Nudelman and S. Weiner. **2006**. Mollusk shell formation: A source of new concepts for understanding biomineralization processes. *Chem. – Eur. J.* **12**: 980–987.

Adegoke, O. S. 1977. Stratigraphy and paleontology of the Ewekoro Formation (Paleocene) of southwestern Nigeria. *Bull. Am. Paleontol.* **71**: 1–379, 50pl.

Ahlgren, J., B. B. Chapman, P. A. Nilsson and C. Brönmark. **2015**. Individual boldness is linked to protective shell shape in aquatic snails. *Biol. Lett.* **11**: 20150029.

Aktipis, S. W. and G. Giribet. **2011**. Testing relationships among the vetigastropod taxa: A molecular approach. *J. Molluscan Stud.* **78**: 12–27.

Aldea, C. and C. Valdovinos. **2005**. Moluscos del intermareal rocoso del centro-sur de Chile (36° - 38°s): Taxonomia y clave de identificacion. *Gayana Concepc.* **69**: 364–396.

Andree, K. B. and M. A. López. **2013**. Species identification from archived snail shells via genetic analysis: A method for DNA extraction from empty shells. *Molluscan Res.* **33**: 1–5.

Appleton, R. D. and A. R. Palmer. **1988**. Water-borne stimuli released by predatory crabs and damaged prey induce more predator-resistant shells in a marine gastropod. *Proc. Natl. Acad. Sci. U. S. A.* **85**: 4387–4391.

Arkell, W. J., B. Kummel and C. W. Wright. **1957**. Mesozoic Ammonoidea. In: *Treatise on Invertebrate Paleontology, Part L, Mollusca 4, Cephalopoda, Ammonoidea.* (R. C. Moore, ed), pp. 80–465. The Geological Society of America and The University of Kansas Press, Lawrence, Kansas.

Asami, T. and N. Asami. **2008**. Maintenance mechanism of a supergene for shell colour polymorphism in the terrestrial pulmonate *Bradybaena similaris*. *Basteria* **72**: 119–127.

Bandel, K. 2007. About the larval shell of some Stromboidea, connected to a review of the classification and phylogeny of the Strombimorpha (Caenogastropoda). *Freib. Forschungshefte C* **524**: 97–206.

Bandel, K. and D. T. Dockery. **2012**. Protoconch characters of Late Cretaceous Latrogastropoda (Neogastropoda and Neomesogastropoda) as an aid in the reconstruction of the phylogeny of the Neogastropoda. *Paläontol. Stratigr. Fazies 20 Freib. Forschungshefte* **C 542**: 93–128.

Barco, A., M. Claremont, D. G. Reid, R. Houart, P. Bouchet, S. T. Williams, C. Cruaud, A. Couloux and M. Oliverio. **2010**. A molecular phylogenetic framework for the Muricidae, a diverse family of carnivorous gastropods. *Mol. Phylogenet. Evol.* **56**: 1025–1039.

Barco, A., S. Schiaparelli, R. Houart and M. Oliverio. **2012**. Cenozoic evolution of Muricidae (Mollusca, Neogastropoda) in the Southern Ocean, with the description of a new subfamily. *Zool. Scr.* **41**: 596–616.

Barthel, L. K. and P. A. Raymond. **1990**. Improved method for obtaining 3-microns cryosections for immunocytochemistry. *J. Histochem. Cytochem.* **38**: 1383–1388.

Bekius, R. 1971. The Circulatory System of Lymnaea Stagnalis (L.). *Neth. J. Zool.* **22**: 1–58.

Berry, A. J. 1962. The growth of *Opisthostoma (Plectostoma) retrovertens* Tomlin, a minute cyclophorid from a Malayan limestone hill. *Proc. Malacol. Soc.* **35**: 46–49.

Bertolaso, L. and V. Garilli. **2009**. Description of *Aclis aurisparva* n. sp. (Gastropoda, Aclididae) from the Pliocene of Emilia Romagna (N. Italy). *Boll. Della Soc. Paleontol. Ital.* **48**: 15–19.

Beu, A. G. 1988. Taxonomy of gastropods of the families Ranellidae (=Cymatiidae) and Bursidae, part 5. Early history of the families, with four new genera and recognition

of the family Personidae. In: *Professor Tamio Kotaka commemorative volume on molluscan paleontology* (Grant-Mackie, J.A., Masuda, K., and Mori, K., eds), pp. 69–96. Saito Gratitude Foundation, Sendai.

Beu, A. G. 2010. Neogene tonnoidean gastropods of tropical and South America: Contributions to the Dominican Republic and Panama paleontology projects and uplift of the Central American Isthmus. *Bull. Am. Paleontol.* **377**–**378**: 1–550.

Beu, A. G. and P. A. Maxwell. **1987**. A revision of the fossil and living gastropods related to Plesiotriton Fischer, 1884 (Family Cancellariidae, Subfamily Plesiotritoninae n. subfam). With an Appendix: Genera of Buccinidae Pisaniinae related to Colubraria Schumacher, 1817. *N. Z. Geol. Surv. Paleontol. Bull.* **54**: 1–140.

Beu, A. G. and R. C. Maxwell. **1990**. *Cenozoic Mollusca of New Zealand*. New Zealand Geological Survey.

Bevelander, G. and H. Nakahara. **1970**. An electron microscope study of the formation and structure of the periostracum of a gastropod, *Littorina littorea*. *Calcif. Tissue Res.* **5**: 1–12.

Bielefeld, Ulrich, K. H. Körtje, H. Rahmann and W. Becker. **1993**. The Shell-Forming Mantle Epithelium of *Biophalaria Glabrata* (pulmonata): Ultrastructure, Permeability and Cytochemistry. *J. Molluscan Stud.* **59**: 323–338.

Bielefeld, U., W. Peters and W. Becker. **1993**. Ultrastructure and cytochemistry of periostracum and mantle edge of *Biomphalaria glabrata* (Gastropoda, Basommatophora). *Acta Zool.* **74**: 181–193.

Blagovetshenskiy, I. V. and I. A. Shumilkin. **2006**. Gastropod mollusks from the Hauterivian of Ulyanovsk (Volga Region): 2. Genera *Khetella* Beisel, 1977 and *Cretadmete* gen. nov. *Paleontol. J.* **40**: 143–149.

Boettiger, A., B. Ermentrout and G. Oster. **2009**. The neural origins of shell structure and pattern in aquatic mollusks. *Proc. Natl. Acad. Sci. U. S. A.* **106**: 6837–6842.

Bonmolo, G. and G. Buzzurro. **2006**. Description of a new muricid for the Mediterranean Sea: *Ocinebrina paddeui* (Mollusca, Gastropoda, Muricidae, Ocenebrinae). *Triton* **13**: 1–4.

Brito-Manzano, N. and D. Aldana-Aranda. **2013**. Effect of photoperiod and feeding schedule on growth and survival of larvae of the fighting conch *Strombus pugilis* Linné, 1758 (Mollusca, Gastropoda). *Aquaculture* **408**–**409**: 47–50.

Bucher, H. and J. Guex. **1990**. Rythmes de croissance chez les ammonites triasiques. *Bull. Société Vaudoise Sci. Nat.* **80**: 191–209.

Bucher, H., N. H. Landman, S. M. Klofak and J. Guex. **1996**. Mode and rate of growth in Ammonoids. In: *Ammonoid Paleobiology* (N. H. Landman, K. Tanabe, and R. A. Davis, eds), pp. 407–461. Springer US.

Budd, A., C. McDougall, K. Green and B. Degnan. **2014**. Control of shell pigmentation by secretory tubules in the abalone mantle. *Front. Zool.* **11**: 62.

Burrows, M. T. and R. N. Hughes. **1990**. Variation in growth and consumption among individuals and populations of dogwhelks, *Nucella lapillus*: A link between foraging behaviour and fitness. *J. Anim. Ecol.* **59**: 723–742.

Campbell, L. D. 1993. *Pliocene Molluscs from the Yorktown and Chowan River Formations in Virginia*. Commonwealth of Virginia, Department of Mines, Minerals, and Energy, Division of Mineral Resources.

Cantera, J. R. and P. Arnaud. **1984**. Les gastéropodes prosobranches des Îles Kerguelen et Crozet (sud de l'Océan Indien): Comparaison écologique et particularités biologiques. *Com. Natl. Fr. Rech. Antarct.* **56**: 1–169.

Carefoot, T. H. and D. A. Donovan. **1995**. Functional-significance of varices in the muricid gastropod *Ceratostoma foliatum*. *Biol. Bull.* **189**: 59–68.

Carriker, M. R. 1972. Observations on removal of spines by muricid gastropods during shell growth. *Veliger* **15**: 69–74.

Carriker, M. R. 1981. Shell penetration and feeding by naticacean and muricacean predatory gastropods: A synthesis. *Malacologia* **20**: 403–422.

Carter, R. M. 1967. The shell ornament of *Hysteroconcha* and *Hecuba* (Bivalvia): A test case for interefential functional morphology. *Veliger* **10**: 59–71.

Cerri, P. S. and E. Sasso-Cerri. **2003**. Staining methods applied to glycol methacrylate embedded tissue sections. *Micron* **34**: 365–372.

Chateigner, D., C. Hedegaard and H.-R. Wenk. **2000**. Mollusc shell microstructures and crystallographic textures. *J. Struct. Geol.* **22**: 1723–1735.

Checa, A. G. 1994. A model for the morphogenesis of ribs in ammonites inferred from associated microsculptures. *Palaeontology* **37**: 863–888.

Checa, A. G. and A. P. Jiménez-Jiménez. **1997**. Regulation of spiral growth in planorbid gastropods. *Lethaia* **30**: 257–269.

Checa, A. G. and A. P. Jiménez-Jiménez. **2003**. Rib fabrication in Ostreoidea and Plicatuloidea (Bivalvia, Pteriomorphia) and its evolutionary significance. *Zoomorphology* **122**: 145–159.

Checa, A. G., A. P. Jiménez-Jiménez and P. Rivas. **1998**. Regulation of spiral coiling in the terrestrial gastropod *Sphincterochila*: An experimental test of the road-holding model. *J. Morphol.* **235**: 249–257.

Checa, A. G., T. Okamoto and H. Keupp. **2002**. Abnormalities as natural experiments: A morphogenetic model for coiling regulation in planispiral ammonites. *Paleobiology* **28**: 127–138.

Chirat, R., D. E. Moulton and A. Goriely. **2013**. Mechanical basis of morphogenesis and convergent evolution of spiny seashells. *Proc. Natl. Acad. Sci.* **110**: 6015–6020.

Claremont, M., R. Houart, S. T. Williams and D. G. Reid. **2013**. A molecular phylogenetic framework for the Ergalataxinae (Neogastropoda: Muricidae). *J. Molluscan Stud.* **79**: 19–29.

Clark, B. L. and J. W. Durham. **1946**. Eocene Faunas from the Department of Bolivar, Colombia. *Geol. Soc. Am. Mem.* **16**: 1–116.

Clelland, E. and N. B. Webster. **2016**. Drilling into hard substrate by naticid and muricid gastropods: A chemo-mechanical process involved in feeding. In: *Physiology of Molluscs: A Collection of Selected Reviews* (S. Saleuddin and S. Mukai, eds), pp. 77–112. Apple Academic Press, New Jersey.

Colgan, D. J., W. F. Ponder, E. Beacham and J. Macaranas. **2007**. Molecular phylogenetics of Caenogastropoda (Gastropoda: Mollusca). *Mol. Phylogenet. Evol.* **42**: 717–737.

Collins, T. M., K. Frazer, A. R. Palmer, G. J. Vermeij and W. M. Brown. **1996**. Evolutionary history of northern hemisphere *Nucella* (Gastropoda, Muricidae): Molecular, morphological, ecological, and paleontological evidence. *Evolution* **50**: 2287–2304.

Conway Morris, S. 2003. *Life's Solution: Inevitable Humans in a Lonely Universe*. University of Cambridge, Cambridge, UK.

Cook, L. M. 1998. A two–stage model for *Cepaea* polymorphism. *Philos. Trans. R. Soc. Lond. B Biol. Sci.* **353**: 1577–1593.

Cossman, M. and G. Pissarro. **1901**. Faune Éocénique du Cotentin (mollusques). 2é article. *Bull. Société Géologique Normandie* **20**: 11–90, 7-15pls, figs 1-4.

Danko, J. P. 2002. Studies on the defensive role of shell ornamentation in the marine gastropod *Ceratostoma foliatum*. University of British Colombia, Vancouver.

Darwin, C. 1859. *The Origin of Species*. Random House, Inc., New York.

Das, S. S., S. Bardhan and T. C. Lahiri. **1999**. The Late Bathonian gastropod fauna of Kutch, western India-a new assemblage. *Paleontol. Res.* **3**: 268–286.

D'Attilio, A. and C. Hertz. **1988**. An illustrated catalogue of the family Typhidae Cossmann, 1903. *Festivus* **20 Supplement**: 1–73.

Dayrat, B., M. Conrad, S. Balayan, T. R. White, C. Albrecht, R. Golding, S. R. Gomes, M. G. Harasewych and A. M. de Frias Martins. **2011**. Phylogenetic relationships and evolution of pulmonate gastropods (Mollusca): New insights from increased taxon sampling. *Mol. Phylogenet. Evol.* **59**: 425–437.

Dockery, D. T. 1977. Mollusca of the Moodys Branch Formation, Mississippi. *Miss. Geol. Econ. Topogr. Surv.* **120**: 7–211.

Dockery, D. T. 1998. Molluscan faunas across the Paleocene/Eocene series boundary in the North American Gulf Coastal Plain. In: *Late Paleocene-Early Eocene Climatic and Biotic Events in the Marine and Terrestrial Records* (M.-P. Aubry, S. Lucas, and W. A. Berggren, eds), pp. 296–322. Columbia University Press, New York.

Dolin, L., C. Dolin and J. Le Renard. **1980**. Inventaire systématique des Mollusques de l'Auversien à «Faciès charrié» de Baron (Oise), et remarques paléontologiques. *Bull. Inf. Géologues Bassin Paris* **17**: 26–48.

Donovan, D. A., J. P. Danko and T. H. Carefoot. **1999**. Functional significance of shell sculpture in gastropod molluscs: Test of a predator-deterrent hypothesis in *Ceratostoma foliatum* (Gmelin). *J. Exp. Mar. Biol. Ecol.* **236**: 235–251.

Eklund, A. 2016. *R package beeswarm: The Bee Swarm Plot, an Alternative to Stripchart [Online]. Available: https://CRAN.R-project.org/package=beeswarm [2016, May 25]*.

Elder, D. and A. Sibatani. **1991**. Holistic molluscs and entrainment. *Riv. Biol. - Biol. Forum* **84**: 113–120.

Emery, D. G. 1992. Fine structure of olfactory epithelia of gastropod molluscs. *Microsc. Res. Tech.* **22**: 307–324.

Ermentrout, B., J. Campbell and G. Oster. **1986**. A model for shell patterns based on neural activity. *Veliger* **28**: 369–388.

Fallon, P. J. J. 2016. Taxonomic review of tropical western Atlantic shallow water Drilliidae (Mollusca: Gastropoda: Conoidea) including descriptions of 100 new species. *Zootaxa* **4090**: 1–363.

Ferrari, S. M. 2014. Patellogastropoda and Vetigastropoda (Mollusca, Gastropoda) from the marine Jurassic of Patagonia, Argentina. *Hist. Biol.* **26**: 563–581.

Fisher, W. K. 1904. The anatomy of *Lottia gigantea* Gray. *Zool. Jahrb. Abt. Für Anat. Ontog. Tiere* **20**: 66.

Fleury, C., F. Marin, B. Marie, G. Luquet, J. Thomas, C. Josse, A. Serpentini and J. M. Lebel. **2008**. Shell repair process in the green ormer *Haliotis tuberculata*: A histological and microstructural study. *Tissue Cell* **40**: 207–218.

Foin, T. C. 1989. Significance of shell thickness in cowries (Mesogastropoda: Cypraeidae). *Bull. Mar. Sci.* **45**: 505–518.

Forsman, A. 2015. Rethinking phenotypic plasticity and its consequences for individuals, populations and species. *Heredity* **115**: 276–284.

Fournié, J. and M. Chétail. **1984**. Calcium dynamics in land gastropods. *Am. Zool.* **24**: 857–870.

Fretter, V. and A. Graham. **1962**. *British Prosobranch Molluscs: Their Functional Anatomy and Ecology*. Ray Society, London.

Friedman, G. M. 1959. Identification of carbonate minerals by staining methods. *J. Sediment. Res.* **29**.

Furuhashi, T., C. Schwarzinger, I. Miksik, M. Smrz and A. Beran. **2009**. Molluscan shell evolution with review of shell calcification hypothesis. *Comp. Biochem. Physiol. B Biochem. Mol. Biol.* **154**: 351–371.

Galindo, L. A., N. Puillandre, J. Utge, P. Lozouet and P. Bouchet. **2016**. The phylogeny and systematics of the Nassariidae revisited (Gastropoda, Buccinoidea). *Mol. Phylogenet. Evol.* **99**: 337–353.

García-Esquivel, Z., S. Montes-Magallón and M. A. González-Gómez. **2007**. Effect of temperature and photoperiod on the growth, feed consumption, and biochemical content of juvenile green abalone, *Haliotis fulgens*, fed on a balanced diet. *Aquaculture* **262**: 129–141.

Garilli, V. and R. Messina. **2006**. The genus *Chileutomia* (Gastropoda: Eulimidae) in the Pliocene to Recent Mediterranean area. *Boll.-Soc. Paleontol. Ital.* **45**: 195.

Garvie, C. L. 1996. The Molluscan Macrofauna of the Reklaw Formation, Marquez Member (Eocene, Lower Claibornian), in Texas. *Bull. Am. Paleontol.* **111**: 1–123.

Garvie, C. L. 2013. Additions to the molluscan macrofauna of the Reklaw Formation (Eocene: Lower Claibornian) and two new taxa from the middle Claibornian in Texas. *Bull. Am. Paleontol.* **384**: 131–162.

Gaume, B., F. Denis, A. Van Wormhoudt, S. Huchette, D. J. Jackson, S. Avignon and S. Auzoux-Bordenave. **2014**. Characterisation and expression of the biomineralising gene Lustrin A during shell formation of the European abalone *Haliotis tuberculata*. *Comp. Biochem. Physiol. B Biochem. Mol. Biol.* **169**: 1–8.

Glibert, M. 1973. Révision des Gastropoda du Danien et du Montien de la Belgique. **173**: 1–116, XI.

Gosselin, L. A. 1993. A method for marking small juvenile gastropods. *J. Mar. Biol. Assoc. U. K.* **73**: 963–966.

Gostan, G. 1966. Aspects cycliques de la morphogenese de la coquille de *Rissoa parva* (da Costa)(Gasteropode: Prosobranche). *Vie Milieu A* **17**: 9–107.

Gould, S. J. 1977. *Ontogeny and Phylogeny*. Belknap Press of Harvard University Press, Cambridge, MA.

Grant, W. S. and F. M. Utter. **1988**. Genetic heterogeneity on different geographic scales in *Nucella lamellosa* (Prosobranchia, Thaididae). *Malacologia* **28**: 275–287.

Grateloup, J.-P. S. de. **1846**. *Conchyliologie Fossile des Terrains Tertiaires du Bassin de L'Adour (environ de Dax). Tome 1. Univalves.* Lafargue, Bordeaux.

Gruber, H. E., G. J. Marshall, L. M. Nolasco, M. E. Kirchen and D. L. Rimoin. **1988**. Alkaline and acid phosphatase demonstration in human bone and cartilage: Effects of fixation interval and methacrylate embedments. *Biotech. Histochem.* **63**: 299–306.

Gründel, J. 2001. Neritimorpha und weitere Caenogastropoda (Gastropoda) aus dem Dogger Norddeutschlands und des nordwestlichen Polens. *Berl. Geowiss. Abh. Reihe E* **36**: S. 45-99.

Gründel, J. 2005. Die Gattung *Discohelix* Dunker, 1847 (Gastropoda) und zur Fassung der Discohelicidae Schröder, 1995. *Neues Jahrb. Für Geol. Paläonologie Monathshefte* **12**: 729–748.

Gründel, J., A. Nützel and C. Schulbert. **2009**. *Toarctocera* (Gastropoda, Aporrhaidae): A new genus from the Jurassic (Toarcian/Aalenian) of South Germany and the early evolutionary history of the family Aporrhaidae. *Paläontol. Z.* **83**: 533–543.

Guzhov, A. E. 2001. To the revision of some Jurassic gastropods from central Russia: 1. Genus *Plicacerithium*. *Paleontol. J.* **36**: 338–342.

Guzhov, A. V. 2004. Jurassic gastropods of European Russia (orders Cerithiiformes, Bucciniformes, and Epitoniiformes). *Paleontol. J.* **38**: 457–562.

Habe, T. 1958. The fauna of Akkeshi Bay-XXV. Gastropoda. *Publ. Akkeshi Mar. Biol. Stn.* **8**: 1–39.

Hammer, Ø. 2000. A theory for the formation of commarginal ribs in mollusc shells by regulative oscillation. *J. Molluscan Stud.* **66**: 383–392.

Hammer, Ø. and H. Bucher. **1999**. Reaction-diffusion processes: Application to the morphogenesis of ammonoid ornamentation. *Geobios* **32**: 841–852.

Hammer, Ø. and H. Bucher. **2005**. Models for the morphogenesis of the molluscan shell. *Lethaia* **38**: 111–122.

Hardy. **2016**. Hardy's Internet Guide to Marine Gastropods [Online]. Available: http://www.gastropods.com/ [2016, March 15].

Harper, E. M. 1997. The molluscan periostracum: An important constraint in bivalve evolution. *Palaeontology* **40**: 71–97.

Harris, G. D. 1899. The Lignitic stage, part II, Scaphopoda, Gastropoda, Pteropoda and Cephalopoda. *Bull. Am. Paleontol.* **3**: 1–128.

Harris, P. and G. Shaw. **1984**. Intermediate filaments, microtubules and microfilaments in epidermis of sea urchin tube foot. *Cell Tissue Res.* **236**: 27–33.

Harzhauser, M. 2014. A seagrass-associated Early Miocene Indo-Pacific gastropod fauna from South-West India (Kerala). *Palaeontogr. Abt. A* **1**–**6**: 73–178.

Hawk, H. L. 2010. Historic genetic diversity of the endangered white abalone (*Haliotis sorenseni*). California State University, Monterey Bay.

Heidelberger, D. 2001. Mitteldevonische (Givetische) Gastropoden (Mollusca) aus der Lahnmulde (südliches Rheinisches Schiefergebirge). *Geol. Abh. Hess.* **106**: 1–291.

Heller, E. and E. Fuchs. **2015**. Tissue patterning and cellular mechanics. *J. Cell Biol.* **211**: 219–231.

Herbert, D. G. 2012. A revision of the Chilodontidae (Gastropoda: Vetigastropoda: Seguenzioidea) of southern Africa and the south-western Indian Ocean. *Afr. Invertebr.* **53**: 381–502.

Hertlein, L. G. and U. S. Grant. **1972**. The geology and paleontology of the marine Pliocene of San Diego, California (Paleontology: Pelecypoda). *Mem. San Diego Soc. Nat. Hist.* **2**: 134–409.

Hickman, C. S. 1980. Paleogene marine gastropods of the Keasey Formation in Oregon. *Bull. Am. Paleontol.* **78**: 1–112.

Hickman, C. S. and J. H. McLean. **1990**. Systematic revision and suprageneric classification of trochacean gastropods. *Sci. Ser. Nat. Hist. Mus. Los Angel. Cty.* **35**: 1–169.

Hohagen, J. and D. J. Jackson. **2013**. An ancient process in a modern mollusc: Early development of the shell in *Lymnaea stagnalis*. *BMC Dev. Biol.* **13**: 1–14.

Høsæter, T. 1986. An annotated check-list of marine molluscs of the Norwegian coast and adjacent waters. *Sarsia* **71**: 73–145.

Houart, R. 2001. *Ingensia* gen. nov. and eleven new species of Muricidae (Gastropoda) from New Caledonia, Vanuatu, and Wallis and Futuna Islands. *Mém. Muséum Natl. Hist. Nat.* **185**: 243–269.

Houart, R. and V. Héros. **2013**. Description of new Muricidae (Mollusca: Gastropoda) collected during the ATIMO VATAE expedition to Madagascar "Deep South." *Zoosystema* **35**: 503–523.

Houbrick, R. S. 1981. Anatomy of *Diastoma melanioides* with remarks on the systematic position of the family Diastomatidae (Prosobranchia: Gastropoda). *Proc. Biol. Soc. Wash.* **94**: 598–621.

Houbrick, R. S. 1985. Genus *Clypeomorus* Jousseaume (Cerithiidae: Prosobranchia). *Smithson. Contrib. Zool.* **403**: 1–131.

Houbrick, R. S. 1991. Anatomy and systematic placement of *Faunus* Montfort 1810 (Prosobranchia: Melanopsinae). *Malacol. Rev.* **24**: 35–54.

Hoverman, J. T. and R. A. Relyea. **2009**. Survival trade-offs associated with inducible defences in snails: The roles of multiple predators and developmental plasticity. *Funct. Ecol.* **23**: 1179–1188.

Humason, G. L. 1962. *Animal Tissue Techniques.* W.H. Freeman, San Francisco.

Hutchinson, J. M. C. 1989. Control of gastropod shell shape; the role of the preceding whorl. *J. Theor. Biol.* **140**: 431–444.

Ikuno, K. and H. Hirano. **2015**. Nomenclatural review of *Polyptychoceras* and 18 related taxa (Ammonoidea: Diplomoceratidae). *Swiss J. Palaeontol.* **134**: 227–232.

Illert, C. 1981. The growth and feeding habits of a South Australian *Murex*. *Sea Shore* **12**: 9–10.

Illert, C. 1987. Formulation and solution of the classical seashell problem. I. Seashell geometry. *Il Nuovo Cimento* **9**: 791–814.

Illert, C. 1989. Formulation and solution of the classical seashell problem. II. Tubular three-dimensional sheashell surfaces. *Il Nuovo Cimento* **11**: 761–780.

Illert, C. 1990. *Nipponites mirabilis*—a challenge to seashell theory? *Il Nuovo Cimento D* **12**: 1405–1421.

Imlay, R. W. 1964. Marine Jurassic pelecypods from central and southern Utah. *USGS Prof. Pap.* **483–C**: 1–42, pl 1-4.

Inaba, A. 1967. The growth of *Chicoreus asianus*. *Venus* **26**: 5–7.

Jackson, D. J., C. McDougall, K. Green, F. Simpson, G. Wörheide and B. M. Degnan. **2006**. A rapidly evolving secretome builds and patterns a sea shell. *BMC Biol.* **4**: 40.

Janssen, A. W. 1984. *Mollusken Uit Het Mioceen Van Winterswijk-Miste: Een Inventarisatie, Met Beschrijvingen En Afbeeldingen Van Alle Aangetroffen Soorten*. Koninklijke Nederlandse Natuurhistorische Vereniging, Leiden.

Janssen, R. 1978. Die Mollusken des Oberoligozäns (Chattium) im Nordseebecken. 1. Scaphopoda, Archaeogastropoda, Mesogastropoda. *Arch. Für Molluskenkd.* **109**: 137–227.

Janssen, R. 1979. Die Mollusken des Oberoligozäns (Chattium) im Nordseebecken. 2. Neogastropoda, Euthyneura, Cephalopoda. *Arch. Für Molluskenkd.* **109**: 227–376.

Janssen, R., M. Zuschin and C. Baal. **2011**. Gastropods and their habitats from the northern Red Sea (Egypt: Safaga): Part 2: Caenogastropoda: Sorbeoconcha and Littorinimorpha. *Ann. Naturhistorischen Mus. Wien Ser. Für Mineral. Petrogr. Geol. Paläontol. Anthropol. Prähistorie* **113**: 373–509.

Jolly, C., S. Berland, C. Milet, S. Borzeix, E. Lopez and D. Doumenc. **2004**. Zona localization of shell matrix proteins in mantle of *Haliotis tuberculata* (Mollusca, Gastropoda). *Mar. Biotechnol.* **6**: 541–551.

Judson, H. F. 1979. *The Eighth Day of Creation: Makers of the Revolution in Biology*. Simon and Schuster, New York.

Jung, P. 1989. Revision of the *Strombina*-group (Gastropoda: Columbellidae), fossil and living: Distribution, biostratigraphy, and systematics. *Schweiz. Palaeontol. Abh.* **111**: 1–298.

Kaim, A. 2004. The evolution of conch ontogeny in Mesozoic open sea gastropods. *Palaeontol. Pol.* **62**: 3–183.

Kaim, A. and A. L. Beisel. **2005**. Mesozoic gastropods from Siberia and Timan (Russia). Part 2: Neogastropoda and Heterobranchia. *Pol. Polar Res.* **26**: 41–64.

Kaiser, K. L. 2007. The recent molluscan fauna of Île Clipperton (tropical eastern Pacific). *The Festivus.* **39 suppl.**: 1–162.

Kampstra, P. 2008. Beanplot: A boxplot alternative for visual comparison of distributions. *J. Stat. Softw. Code Snippets* **28**: 1–9.

Kase, T. 1984. Early Cretaceous marine and brackish-water Gastropoda from Japan. *Natl. Sci. Mus. Monogr.* **1**: 1–189.

Kay, E. A. 1979. *Hawaiian Marine Shells*. Bishop Museum Press.

Kay, E. A. and S. Johnson. **1987**. Mollusca of Enewetak Atoll. In: *The Natural History of Enewetak Atoll. Volume II Biogeography and Systematics*, pp. 105–146.

Kennedy, W. J. and H. A. Kollmann. **1979**. Lower Albian ammonites from the Tannheim Formation near Losenstein, Upper Austria. *Beitr. Zur Paläontol. Von Österr.* **6**: 1–25.

Kensley, B. and J. Pether. **1986**. Late Tertiary and Early Quaternary fossil Mollusca of the Hondeklip area, Cape Province, South Africa. *Ann. South Afr. Mus.* **97**: 141–225.

Kilburn, R. N. 1985. The family Epitoniidae (Mollusca: Gastropoda) in southern Africa and Mozambique. *Ann. Natal Mus.* **27**: 239–337.

Kincaid, T. 1957. *Local Races and Clines in the Marine Gastropod* Thais lamellosa *Gmelin. A population study*. The Calliostoma Company, Seattle.

Klowden, M. J. 2003. Contributions of insect research toward our understanding of neurosecretion. *Arch. Insect Biochem. Physiol.* **53**: 101–114.

Knight, J. B., L. R. Cox, A. M. Keen, A. G. Smith, R. L. Batten, E. L. Yochelson, N. H. Ludbrook, Robert Robertson, C. M. Yonge and R. C. Moore. **1960**. Part I, Mollusca 1. In: *Treatise on Invertebrate Paleontology* (R. C. Moore, ed), p. xxiii + 351 pp. Geological Society of America and University of Kansas Press, Lawrence.

Kniprath, E. 1972. Formation and structure of the periostracum in *Lymnaea stagnalis*. *Calcif. Tissue Int.* **9**: 260–271.

Kocot, K. M., F. Aguilera, C. McDougall, D. J. Jackson and B. M. Degnan. **2016**. Sea shell diversity and rapidly evolving secretomes: Insights into the evolution of biomineralization. *Front. Zool.* **13**: 23.

Koehn, R. K. and S. E. Shumway. **1982**. A genetic/physiological explanation for differential growth rate among individuals of the American oyster, *Crassostrea virginica* (Gmelin). *Mar. Biol. Lett.* **3**: 35–42.

Köhler, F. and M. Glaubrecht. **2010**. Uncovering an overlooked radiation: Molecular phylogeny and biogeography of Madagascar's endemic river snails (Caenogastropoda: Pachychilidae: *Madagasikara* gen. nov.). *Biol. J. Linn. Soc.* **99**: 867–894.

Kollmann, H. A. 1978. Gastropoden aus den Losensteiner Schichten der Umgebung von Losenstein (Oberösterreich). Zweiter Teil: Naticidae, Colombellinidae, Aporrhaidae,

Ceritellidae, Epitoniidae (Mesogastropoda). *Ann. Naturhistorischen Mus. Wien* **81**: 183–201.

Kollmann, H. A. 1979. Gastropoden aus den Losensteiner Schichten der Umgebung von Losenstein (Oberösterreich). Dritter Teil: Cerithiacea (Mesogastropoda). *Ann. Naturhistorischen Mus. Wien* **82**: 11–51.

Kollmann, H. A. 1982. Gastropoden aus den Losensteiner Schichten der Umgebung von Losenstein (Oberösterreich).Vierter Teil: Archaeogastropoda und allgemeine Bermerkung zur Fauna. *Ann. Naturhistorischen Mus. Wien* **84**: 13–56.

Kollmann, H. A. 2009. A Late Cretaceous Aporrhaidae-dominated gastropod assemblage from the Gosau Group of the Pletzach Alm near Kramsach (Tyrol, Austria). With an appendix on the taxonomy of Mesozoic Aporrhaidae and their position in the superfamily Stromboidea. *Ann. Naturhistorischen Mus. Wien Ser. Für Mineral. Petrogr. Geol. Paläontol. Anthropol. Prähistorie* **111A**: 33–72.

Kollmann, H. A. and J.-C. Fischer. **2005**. *Révision Critique de la "Paléontologie Française" d'Alcide d'Orbigny: Incluant la Réédition de l'Original Volume III, Gastropodes Crétacés*. Backhuys Publishers, Leiden.

Kollmann HA, Summesberger H. 1982. Excursions to Coniacian-Maastrichtian in the Austrian Alps. Working Group on the Coniacian-Maastrichtian stages. 4th Meeting Gosau Basins in Austria: 3–105.

Kozloff, E. N. 1987. *Marine Invertebrates of the Pacific Northwest*. University of Washington Press, Seattle.

Kronenberg, G. C. and A. W. Burger. **2002**. On the subdivision of recent *Tibia*-like gastropods (Gastropoda: Stromboidea) with the recognition of the family Rostellariidae, Gabb, 1868 and a note on the type species of *Tibia* Röding, 1798. *Vita Malacol.* **1**: 39–48.

Lacalli, T. C. 1981. Structure and development of the apical organ in trochophores of *Spirobranchus polycerus, Phyllodoce maculata* and *Phyllodoce mucosa* (Polychaeta). *Proc. R. Soc. Lond. B Biol. Sci.* **212**: 381–402.

Ladd, H. S. 1982. Cenozoic fossil mollusks from western Pacific islands; gastropods (Eulimidae and Volutidae through Terebridae). *USGS Prof. Pap.* **1171**: 1–100, 41pls.

Laland, K., T. Uller, M. Feldman, K. Sterelny, G. B. Müller, A. Moczek, E. Jablonka, J. Odling-Smee, G. A. Wray, H. E. Hoekstra, *et al.* 2014. Does evolutionary theory need a rethink? *Nature* **514**: 161–164.

Landau, B. M. and C. M. da Silva. **2010**. Early Pliocene gastropods of Cubagua, Venezuela: Taxonomy, palaeobiogeography and ecostratigraphy. *Palaeontos* **19**: 221.

Landau, B. M., M. Harzhauser, Y. Islamoglu and C. M. da Silva. **2013**. Systematics and palaeobiogeography of the gastropods of the middle Miocene (Serravallian) Karaman Basin, Turkey. *Cainozoic Res.* **11**–**13**: 1–584.

Landau, B. M., R. La Perna and R. Marquet. **2006**. The early Pliocene Gastropoda (Mollusca) of Estepona, southern Spain 6: Triphoroidea, Epitonioidea, Eulimoidea. *Palaeontos* **10**: 1–96.

Landau, B. M. and R. Marquet. **2001**. The first fossil record of the genus *Chileutomia* (Eulimidae: Gastropoda) in the Mediterranean Neogene. *Boll. Malacol.* **37**: 223–224.

Landau, B. M., C. M. da Silva, A. Heitz and A. W. Janssen. **2016**. Systematics of the gastropods of the lower-middle Miocene Cantaure Formation, Paraguaná Peninsula, Venezuela. *Bull. Am. Paleontol.* **389**: 1–581.

Laxton, J. H. 1970. Shell growth in some New Zealand Cymatiidae (Gastropoda: Prosobranchia). *J. Exp. Mar. Biol. Ecol.* **4**: 250–260.

Leighton, L. R. 2002. Inferring predation intensity in the marine fossil record. *Paleobiology* **28**: 328–342.

Lenth, R. V. 2014. *R package lsmeans: Least-squares means [Online]. Available: http://CRAN.R-project.org/package=lsmeans [2015, August 29].*

Liew, T.-S., A. C. M. Kok, M. Schilthuizen and S. Urdy. **2014**. On growth and form of irregular coiled-shell of a terrestrial snail: *Plectostoma concinnum* (Fulton, 1901) (Mollusca: Caenogastropoda: Diplommatinidae). *PeerJ* **2**: e383.

Linsley, R. M. and M. Javidpour. **1980**. Episodic growth in Gastropoda. *Malacologia* **20**: 153–160.

Long, P. E. and J. A. Zalasiewicz. **2011**. The molluscan fauna of the Coralline Crag (Pliocene, Zanclean) at Raydon Hall, Suffolk, UK: Palaeoecological significance reassessed. *Palaeogeogr. Palaeoclimatol. Palaeoecol.* **309**: 53–72.

Lozouet, P. 1999. Nouvelles espèces de gastéropodes (Mollusca: Gastropoda) de l'Oligocène et du Miocène inférieur de l'Aquitaine (Sud-Ouest de la France). Partie 2. *Cossmanniana* **6**: 1–68.

Lozouet, P., L. Dolin, P. Maesterati and R. Favia. **2001**. Un site exceptionnel du Miocène Inférieur (Aquitanien): La "Carrière Vives"; (Meilhan, Landes, France). *Cossmanniana* **8**: 47–67.

Lozouet, P., D. Ledon and J.-F. Lesport. **1994**. Le Genre *Lindapterys* (Neogastropoda, Muricidae): Un exemple de disjonction de distribution en domaine tropical marin. *Geobios* **27**: 39–50.

MacGinitie, G. E. and N. MacGinitie. **1968**. *Natural History of Marine Animals*, 2nd ed. McGraw-Hill, New York.

MacKenzie, C. L., Jr. 1961. Growth and reproduction of the oyster drill *Eupleura caudata* in the York River, Virginia. *Ecology* **42**: 317–338.

MacNeil, F. S. and D. T. Dockery. **1984**. Lower Oligocene Gastropoda, Scaphopoda, and Cephalopoda of the Vicksburg group in Mississippi. *Miss. Dep. Nat. Resour. Bur. Geol.* **124**: 415.

Macpherson, E. 1971. The marine molluscs of Arctic Canada: Prosobranch gastropods, chitons and scaphopods. *Natl. Mus. Can. Publ. Biol. Oceanogr.* **3**: 1–149.

Maes, V. O. 1967. The littoral marine mollusks of Cocos-Keeling Islands (Indian Ocean). *Proc. Acad. Nat. Sci. Phila.* **119**: 93–217.

Marie, B., D. J. Jackson, P. Ramos-Silva, I. Zanella-Cléon, N. Guichard and F. Marin. **2013**. The shell-forming proteome of *Lottia gigantea* reveals both deep conservations and lineage-specific novelties. *FEBS J.* **280**: 214–232.

Marie, B., C. Joubert, A. Tayale, I. Zanella-Cleon, C. Belliard, D. Piquemal, N. Cochennec-Laureau, F. Marin, Y. Gueguen and C. Montagnani. **2012**. Different secretory repertoires control the biomineralization processes of prism and nacre deposition of the pearl oyster shell. *Proc. Natl. Acad. Sci.* **109**: 20986–20991.

Marin, F., N. Le Roy and B. Marie. **2012**. The formation and mineralization of mollusc shell. *Front. Biosci.* **4**: 1099–1125.

Marko, P. B. 2004. "What's larvae got to do with it?" Disparate patterns of post-glacial population structure in two benthic marine gastropods with identical dispersal potential. *Mol. Ecol.* **13**: 597–611.

Marquet, R. 1995. Pliocene gastropod faunas from Kallo (Oost-Vlaanderen, Belgium): Part 1. Introduction and Archaeogastropoda. *Contrib. Tert. Quat. Geol.* **32**: 53–85.

Marquet, R. 1997a. Pliocene gastropod faunas from Kallo (oost-Vlaanderen, Belgium). Part 3. Caenogastropoda, Aporrhaidae to Muricidae, and Part 4. Buccinidae to Helicidae. *Contrib. Tert. Quat. Geol.* **34**: 69–149.

Marquet, R. 1997b. The Pliocene turrid gastropods of Belgium. 1: Drilliidae, Turridae, Conidae (genus *Bela*). *Bull. Inst. R. Sci. Nat. Belg. Sci. Terre* **67**: 119–151.

Marquet, R. 2001. A study of some Neogene European species of Seilinae (Cerithiopsidae, Gastropoda). *Bull. Inst. R. Sci. Nat. Belg. Sci. Terre* **71**: 195–208.

Martins, A. M. F. 2007. Morphological and anatomical diversity within the Ellobiidae (Gastropoda, Pulmonata, Archaeopulmonata). *Vita Malacol.* **4**: 1–28.

Marxen, J. C., P. E. Witten, D. Finke, O. Reelsen, M. Rezgaoui and W. Becker. **2003**. A light- and electron-microscopic study of enzymes in the embryonic shell-forming tissue of the freshwater snail, *Biomphalaria glabrata*. *Invertebr. Biol.* **122**: 313–325.

Maxwell, P. A. 1992. Eocene mollusca from the vicinity of McCulloch's Bridge, Waihao River, South Canterbury, New Zealand: Paleoecology and systematics. *N. Z. Geol. Surv. Bull. Paleontol. Bull.* **65**: 1–280.

McDougall, C., K. Green, D. J. Jackson and B. M. Degnan. **2011**. Ultrastructure of the mantle of the gastropod *Haliotis asinina* and mechanisms of shell regionalization. *Cells Tissues Organs* **194**: 103–107.

Meinhardt, H. 1984. Models for positional signalling, the threefold subdivision of segments and the pigmentation pattern of molluscs. *Development* **83**: 289–311.

Meinhardt, H. 2009. *The Algorithmic Beauty of Sea Shells*. Springer, Berlin; London.

Meinhardt, H. and M. Klingler. **1987**. A model for pattern formation on the shells of molluscs. *J. Theor. Biol.* **126**: 63–89.

Merle, D., B. Garrigues and J.-P. Pointier. **2011**. *Fossil and Recent Muricidae of the World: Part Muricinae*. ConchBooks, Hackenheim.

Merle, D. and J.-M. Pacaud. **2004**. New species of *Eocithara* Fischer, 1883 (Mollusca, Gastropoda, Harpidae) from the Early Paleogene with phylogenetic analysis of the Harpidae. *Geodiversitas* **26**: 61–87.

Miller, D. J. and M. LaBarbera. **1995**. Effects of foliaceous varices on the mechanical properties of *Chicoreus dilectus* (Gastropoda: Muricidae). *J. Zool.* **236**: 151–160.

Moore, R. C., C. G. Lalicker and A. G. Fischer. **1952**. *Invertebrate Fossils*. McGraw-Hill New York.

Morita, R. 1991a. Finite element analysis of a double membrane tube (DMS-tube) and its implication for gastropod shell morphology. *J. Morphol.* **207**: 81–92.

Morita, R. 1991b. Mechanical constraints on aperture form in gastropods. *J. Morphol.* **207**: 93–102.

Morita, R. 1993. Development mechanics of retractor muscles and the "Dead Spiral Model" in gastropod shell morphogenesis. *Neues Jahrb. Geol. Palaontologie-Abh.* **190**: 191–218.

Morita, R. 2003. Why do univalve shells of gastropods coil so tightly? A head-foot guidance model of shell growth and its implication on developmental constraints. In: *Morphogenesis and Pattern Formation in Biological Systems* (T. Sekimura, S. Noji, N. Ueno, and P. K. Maini, eds), pp. 345–354. Springer Japan.

Moulton, D. E., A. Goriely and R. Chirat. **2012**. Mechanical growth and morphogenesis of seashells. *J. Theor. Biol.* **311**: 69–79.

Müller, P., K. W. Rogers, B. M. Jordan, J. S. Lee, D. Robson, S. Ramanathan and A. F. Schier. **2012**. Differential diffusivity of nodal and lefty underlies a reaction-diffusion patterning system. *Science* 1221920.

Murray, J. and B. Clarke. **1976**. Supergenes in polymorphic land snails. I. *Partulae taeniata*. *Heredity* **37**: 253–269.

Myhre, J. L., J. A. Hills, K. Prill, S. L. Wohlgemuth and D. B. Pilgrim. **2014**. The titin A-band rod domain is dispensable for initial thick filament assembly in zebrafish. *Dev. Biol.* **387**: 93–108.

Noda, H. 1988. Molluscan fossils from the Ryukyu Islands, southwest Japan Part 2. Gastropoda and Pelecypoda from the Shinzato Formation in the middle part of Okinawa-jima. *Sci. Rep. Inst. Geosci. Univ. Tsukuba* **9**: 29-85 pls 5–19.

Norman, J. M. V., W. Xuan, T. Beeckman and P. N. Benfey. **2013**. To branch or not to branch: The role of pre-patterning in lateral root formation. *Development* **140**: 4301–4310.

Nudelman, F. 2015. Nacre biomineralisation: A review on the mechanisms of crystal nucleation. *Semin. Cell Dev. Biol.* **46**: 2–10.

Nützel, A. 1998. Über die Stammesgeschichte der Ptenoglossa (Gastropoda). *Berl. Geowiss. Abh. Reihe E* **26**: 1–229.

Okamoto, T. 1988a. Analysis of heteromorph ammonoids by differential geometry. *Palaeontology* **31**: 35–52.

Okamoto, T. 1988b. Changes in life orientation during the ontogeny of some heteromorph ammonoids. *Palaeontology* **31**: 281–294.

Oliverio, M. and M. V. Modica. **2010**. Relationships of the haematophagous marine snail *Colubraria* (Rachiglossa: Colubrariidae), within the neogastropod phylogenetic framework. *Zool. J. Linn. Soc.* **158**: 779–800.

Olsson, A. A. 1934. 1934, Contributions to the paleontology of northern Peru; the Cretaceous of the Amotape region: Bull. *Bull. Am. Paleontol.* **20**: 1–104.

Olsson, A. A. 1944. Contributions to the paleontology of northern Peru: Part VII. The Cretaceous of the Paita Region. *Bull. Am. Paleontol.* **28**: 163–305.

Olsson, A. A. 1964. *Neogene Mollusks from Northwestern Ecuador*. Paleontological Research Institution, Ithaca, N.Y.

Ozawa, T., F. Köhler, D. G. Reid and M. Glaubrecht. **2009**. Tethyan relicts on continental coastlines of the northwestern Pacific Ocean and Australasia: Molecular phylogeny and fossil record of batillariid gastropods (Caenogastropoda, Cerithioidea). *Zool. Scr.* **38**: 503–525.

Pacaud, J.-M. and M. Harzhauser. **2012**. *Jponsia, Moniquia* et *Eginea*, trois nouveaux genres de Pachychilidae (Gastropoda, Caenogastropoda) du Paléogène Européen. *Ann. Muséum Hist. Nat. Nice* **27**: 105–153.

Palmer, A. R. 1977. Function of shell sculpture in marine gastropods: Hydrodynamic destabilization in *Ceratostoma foliatum*. *Science* **197**: 1293–1295.

Palmer, A. R. 1979. Fish predation and the evolution of gastropod shell sculpture: Experimental and geographic evidence. *Evolution* **33**: 697–713.

Palmer, A. R. 1981. Do carbonate skeletons limit the rate of body growth? *Nature* **292**: 150–152.

Palmer, A. R. 1982. Growth in marine gastropods: A non-destructive technique for independently measuring shell and body-weight. *Malacologia* **23**: 63–73.

Palmer, A. R. 1985. Adaptive value of shell variation in *Thais lamellosa*: Effect of thick shells on vulnerability to and preference by crabs. *Veliger* **27**: 349–356.

Palmer, A. Richard. **1985**. Quantum changes in gastropod shell morphology need not reflect speciation. *Evolution* **39**: 699–705.

Palmer, A. R. 1992. Calcification in marine molluscs: How costly is it? *Proc. Natl. Acad. Sci. U. S. A.* **89**: 1379–1382.

Palmer, K. V. W. 1937. The Claibornian Scaphopoda, Gastropoda, and dibranchiate Cephalopoda of the Southern United States. *Bull. Am. Paleontol.* **7**: 1–730.

Palumbi, S. R. 1994. Genetic divergence, reproductive isolation, and marine speciation. *Annu. Rev. Ecol. Syst.* **25**: 547–572.

Pascoal, S., G. Carvalho, S. Creer, J. Rock, K. Kawaii, S. Mendo and R. Hughes. **2012**. Plastic and heritable components of phenotypic variation in *Nucella lapillus*: An assessment using reciprocal transplant and common garden experiments. *PLoS ONE* **7**: e30289.

Paul, C. R. C. 1981. The function of the spines in *Murex (Murex) pecten* Lightfoot and related species (Prosobranchia: Muricidae). *J. Conchol.* **30**: 285.

Paulay, G. 1989. Marine invertebrates of the Pitcairn Islands: Species composition and biogeography of corals, molluscs, and echinoderms. *Atoll Res. Bull.* **326**: 1–28.

Peterson, T. and G. B. Müller. **2013**. What is evolutionary novelty? Process versus character based definitions. *J. Exp. Zool. B Mol. Dev. Evol.* **320**: 345–350.

Petitjean, M. 1965. *Structures Microscopiques, Nature Minéralogique Et Composition Chimique De La Coquille Des Muricidés (Gastéropodes Prosobranches). Importance Systématique De Ces Caractères.* Université de Paris, Paris.

Petuch, E. J. 1998. A new gastropod fauna from an Oligocene back-reef lagoonal environment in west central Florida. *Nautilus* **110**: 122–138.

Peyrot, A. 1928. Conchologie Néogénique de L'Aquitaine, (Suite). *Actes Société Linn. Bordx.* **79 Supplement**: 5–264, pls 5-14.

Ponder, W. F. 1983. A revision of the recent Xenophoridae of the world and of the Australian fossil species (Mollusca: Gastropoda). *Aust. Mus. Mem.* **17**: 1–126.

Ponder, W. F. 1984. A review of the genera of the Rissoidae (Mollusca: Mesogastropoda: Rissoacea). *Rec. Aust. Mus.* **Suppl. 4**: 1–221.

Ponder, W. F. and D. R. Lindberg. **2008**. *Phylogeny and Evolution of the Mollusca*. University of California Press, Berkeley, CA.

Powell, A. W. B. 1966. The molluscan families Speightiidae and Turridae: An evaluation of the valid taxa, both recent and fossil, with lists of characteristic species. *Bull. Auckalnd Inst. Mus.* **5**: 1–184.

Price, R. M. 2003. Columellar muscle of neogastropods: Muscle attachment and the function of columellar folds. *Biol. Bull.* **205**: 351–366.

Puillandre, N., Y. I. Kantor, A. Sysoev, A. Couloux, C. Meyer, T. Rawlings, J. A. Todd and P. Bouchet. **2011**. The dragon tamed? A molecular phylogeny of the Conoidea (Gastropoda). *J. Molluscan Stud.* **77**: 259–272.

Radtke, G., R. Hoffmann and H. Keupp. **2016**. Form and formation of flares and parabolae based on new observations of the internal shell structure in lytoceratid and perisphinctid ammonoids. *Acta Palaeontol. Pol.* **61**: 503–517.

Radwin, G. E. and A. D'Attilio. **1976**. *Murex Shells of the World: An Illustrated Guide to the Muricidae*. Stanford University Press, Stanford, CA.

Raines, B. K. 2007. New molluscan records from Easter Island, with the description of a new Ethminolia. *Visaya* **2**: 70–88.

Rasband, W. S. 1997. *ImageJ*. U. S. National Institutes of Health, Bethesda, MD.

Raup, D. M. 1966. Geometric analysis of shell coiling: General problems. *J. Paleontol.* **40**: 1178–1190.

Raven, H. and J. J. Vermeulen. **2007**. Notes on molluscs from NW Borneo and Singapore. 2. A synopsis of the Ellobiidae (Gastropoda, Pulmonata). *Vita Malacol.* **4**: 29–62.

Rehder, H. A. 1980. *The Marine Mollusks of Easter Island (Isla De Pascua) and Sala Y Gómez*. Smithsonian Institution Press.

Reid, D. G., P. Dyal, P. Lozouet, M. Glaubrecht and S. T. Williams. **2008**. Mudwhelks and mangroves: The evolutionary history of an ecological association (Gastropoda: Potamididae). *Mol. Phylogenet. Evol.* **47**: 680–699.

Rice, S. H. 1998. The bio-geometry of mollusc shells. *Paleobiology* **24**: 133–149.

Richardson, K. C., L. Jarrett and E. H. Finke. **1960**. Embedding in epoxy resins for ultrathin sectioning in electron microscopy. *Stain Technol.* **35**: 313.

Riedel, F. 2000. Ursprung und Evolution der "höheren" Casenogastropoda: Eine paläobiologische Konzeption. *Berl. Geowiss. Abh. Reihe E* **32**: 1–240.

Rouse, G. and F. Pleijel. **2001**. *Polychaetes*. Oxford University Press.

RStudio Team. **2012**. *RStudio : Integrated Development for R. RStudio, Inc. [Online]. RStudio. Available: http://www.rstudio.org/ [2015, August 28].* RStudio, Boston, MA.

Saleuddin, A. S. M. and S. C. Kunigelis. **1984**. Neuroendocrine control mechanisms in shell formation. *Am. Zool.* **24**: 911–916.

Saleuddin, D. A. S. M. and R. M. Dillaman. **1976**. Direct innervation of the mantle edge gland by neurosecretory axons in *Helisoma duryi* (Mollusca: Pulmonata). *Cell Tissue Res.* **171**: 397–401.

Sälgeback, J. and E. Savazzi. **2006**. Constructional morphology of cerithiform gastropods. *Paleontol. Res.* **10**: 233–259.

Salvador, R. B. and C. M. Cunha. **2016**. Taxonomic revision of the fossil genera *Bulimactaeon* , *Hemiauricula* (= *Liocarenus*) and *Nucleopsis*, with description of a new Recent genus and species (Gastropoda: Heterobranchia: Acteonidae). *J. Molluscan Stud.* **82**: 472–483.

Saul, L. R. and R. L. Squires. **2003**. New Cretaceous cerithiform gastropods from the Pacific Slope of North America. *J. Paleontol.* **77**: 442–453.

Savazzi, E. 1990. Biological aspects of theoretical shell morphology. *Lethaia* **23**: 195–212.

Savazzi, E. 1991. Constructional morphology of strombid gastropods. *Lethaia* **24**: 311–331.

Savazzi, E. and T. Sasaki. **2004**. Synchronized sculpture in gastropod shells. *Am. Malacol. Bull.* **18**: 87–114.

Schilthuizen, M. 2003. Sexual selection on land snail shell ornamentation: A hypothesis that may explain shell diversity. *Bmc Evol. Biol.* **3**.

Schnetler, K. I. 2005. The Mollusca from the stratotype of the Gram Formation (late Miocene, Denmark). *Palaeontos* **7**: 62–189.

Schnetler, K. I. and C. Beyer. **1987**. A Late Oligocene (Chattian B) mollusc fauna from the clay-pit of Galten Brickworks at Nørre Vissing, Jylland, Denmark. *Meded. Werkgr. Voor Tert. En Kwartaire Geol.* **24**: 193–224.

Seeley, H. 1865. On Ammonites from the Cambridge Greensand. *Ann. Mag. Nat. Hist. Zool. Bot. Geol. Inc. J. Bot.* **16**: 225–246.

Seilacher, A. and A. D. Gishlick. **2014**. *Morphodynamics*. CRC Press, Boca Raton, FL.

Seilacher, A. and Gunji. **1993**. Morphogenetic count-downs in heteromorph shells. *Neues Jahrb. Geol. Palaontologie Abh.* **190**: 237–265.

Signor, P. W. and C. E. Brett. **1984**. The mid-Paleozoic precursor to the Mesozoic marine revolution. *Paleobiology* **10**: 229–245.

Simone, L. R. L. 2011. Phylogeny of the Caenogastropoda (Mollusca), based on comparative morphology. *Arq. Zool.* **42**: 83–323.

Sohl, N. F. 1960. Archaeogastropoda, Mesogastropoda, and stratigraphy of the Ripley, Owl Creek and Prairie Bluff Formations. *USGS Prof. Pap.* **331**–**A**: 151p 18pls.

Sohl, N. F. 1964. Neogastropoda, Opisthobranchia, and Basommatophora from the Ripley, Owl Creek, and Prairie Bluff Formations. *USGS Prof. Pap.* **331 B**: 153-344 pl 19–52.

Soza-Ried, C., E. Öztürk, D. Ish-Horowicz and J. Lewis. **2014**. Pulses of Notch activation synchronise oscillating somite cells and entrain the zebrafish segmentation clock. *Development* **141**: 1780–1788.

Spight, T. M. 1973. Ontogeny, environment, and shape of a marine snail *Thais lamellosa* Gmelin. *J. Exp. Mar. Biol. Ecol.* **13**: 215–228.

Spight, T. M. 1981. The ecology of body growth: Environmental influences on the growth of marine snails. *Ecosynthesis* **1**: 257–344.

Spight, T. M., C. Birkeland and A. Lyons. **1974**. Life histories of large and small murexes (Prosobranchia: Muricidae). *Mar. Biol.* **24**: 229–242.

Spight, T. M. and A. Lyons. **1974**. Development and functions of the shell sculpture of the marine snail *Ceratostoma foliatum*. *Mar. Biol.* **24**: 77–83.

Squires, R. L. 1987. Eocene molluscan paleontology of the Whitaker Peak area, Los Angeles and Ventura counties, California. *LACM Contrib. Sci.* **388**: 135.

Squires, R. L. 2015. Northeast Pacific record of the Paleogene genus *Pseudoperissolax* (Neogastropoda: Muricidae: Muricinae) and its paleobiogeography. *J. Paleontol.* **89**: 576–588.

Squires, R. L. and L. R. Saul. **2004**. Uncommon Cretaceous naticiform gastropods from the Pacific slope of North America. *Veliger* **47**: 21–37.

Stephenson, L. W. 1952. Larger invertebrate fossils of the Woodbine formation (Cenomanian) of Texas. *USGS Prof. Pap.* **242**: 1–226, pl 8-59.

Stilwell, J. D. 2014. Expansion of the rare trochid *Calliovarica* (Mollusca: Gastropoda) into eastern Zealandian waters during the late Paleocene–early Eocene thermal event. *Alcheringa Australas. J. Palaeontol.* **38**: 239–244.

Stone, J. R. 1996. The evolution of ideas: A phylogeny of shell models. *Am. Nat.* **148**: 904–929.

Stone, J. R. 1999. Using a mathematical model to test the null hypothesis of optimal shell construction by four marine gastropods. *Mar. Biol.* **134**: 397–403.

Strong, E. E., D. J. Colgan, J. M. Healy, C. Lydeard, W. F. Ponder and M. Glaubrecht. **2011**. Phylogeny of the gastropod superfamily Cerithioidea using morphology and molecules. *Zool. J. Linn. Soc.* **162**: 43–89.

Strong, E. E., N. Puillandre, M. Castelin, A. G. Beu and P. Bouchet. **2016**. A molecular phylogeny of the Tonnoidea. *Proc. 82nd Am. Malacol. Soc. 12-16 June Ensenada Baja Calif. Mex.* 148.

Sud, D., J. M. Poncet, A. Saihi, J. M. Lebel, D. Doumenc and E. Boucaud-Camou. **2002**. A cytological study of the mantle edge of *Haliotis tuberculata* L.(Mollusca, Gastropoda) in relation to shell structure. *J. Shellfish Res.* **21**: 201–210.

Sudo, S., T. Fujikawa, T. Nagakura, T. Ohkubo, K. Sakaguchi, M. Tanaka, K. Nakashima and T. Takahashi. **1997**. Structures of mollusc shell framework proteins. *Nature* **387**: 563–564.

Takano, T. and Y. Kano. **2014**. Molecular phylogenetic investigations of the relationships of the echinoderm-parasite family Eulimidae within Hypsogastropoda (Mollusca). *Mol. Phylogenet. Evol.* **79**: 258–269.

Taylor, J. D., E. A. Glover, M. Peharda, G. Bigatti and A. Ball. **2004**. Extraordinary flexible shell sculpture: The structure and formation of calcified periostracal lamellae in *Lucina pensylvanica* (Bivalvia: Lucinidae). *Malacologia* **46**: 277–294.

Taylor, J. D. and D. G. Reid. **1990**. Shell microstructure and mineralogy of the Littorinidae: Ecological and evolutionary significance. *Hydrobiologia* **193**: 199–215.

Thévenaz, P., U. E. Ruttimann and M. Unser. **1998**. A pyramid approach to subpixel registration based on intensity. *IEEE Trans. Image Process.* **7**: 27–41.

Thompson, D. W. 1917. *On Growth and Form*. Cambridge University Press, London.

Thorson, G. 1944. The Zoology of East Greenland: Marine Gastropoda Prosobranchiata. *Medeleser Om Grönland* **121**: 1–181.

Thorsten, K. O. W. 2002. Systematic revision of Palaeocene brackish water Gastropoda from Mons, Belgium, based on their early ontogenetic shells. *Bull. Inst. R. Sci. Nat. Belg. Sci. Terre* **72**: 111–134.

Timmermans, L. P. 1969. Studies on shell formation in molluscs. *Neth. J. Zool.* **19**: 413–523.

Tracey, S. 2010. Gastropods. In: *Fossils of the Gault Clay* (J. R. Young, A. S. Gale, R. I. Knight, and B. A. Smith, eds), pp. 106–155. London.

Trussell, G. C. 2000. Phenotypic clines, plasticity, and morphological trade-offs in an intertidal snail. *Evolution* **54**: 151–166.

Tunnell, J. W., J. Andrews, N. C. Barrera and F. Moretzsohn. **2010**. *Encyclopedia of Texas Seashells: Identification, Ecology, Distribution, and History*. Texas A&M University Press, Texas.

Urdy, S. 2015. Theoretical modelling of the molluscan shell: What has been learned from the comparison among molluscan taxa? In: *Ammonoid Paleobiology: From Anatomy to Ecology*, pp. 207–251. Springer, New York.

Urdy, S., N. Goudemand, H. Bucher and R. Chirat. **2010a**. Allometries and the morphogenesis of the molluscan shell: A quantitative and theoretical model. *J. Exp. Zoolog. B Mol. Dev. Evol.* **314B**: 280–302.

Urdy, S., N. Goudemand, H. Bucher and R. Chirat. **2010b**. Growth-dependent phenotypic variation of molluscan shells: Implications for allometric data interpretation. *J. Exp. Zoolog. B Mol. Dev. Evol.* **314B**: 303–326.

Vermeij, G. 2001. Innovation and evolution at the edge: Origins and fates of gastropods with a labral tooth. *Biol. J. Linn. Soc.* **72**: 461–508.

Vermeij, G. J. 1973. Adaptation, versatility, and evolution. *Syst. Biol.* **22**: 466–477.

Vermeij, G. J. 1974. Marine faunal dominance and molluscan shell form. *Evolution* **28**: 656–664.

Vermeij, G. J. 1977. The mesozoic marine revolution: Evidence from snails, predators and grazers. *Paleobiology* **3**: 245–258.

Vermeij, G. J. 1978. *Biogeography and Adaptation Patterns of Marine Life*. Harvard University Press, Harvard.

Vermeij, G. J. 1982. Phenotypic evolution in a poorly dispersing snail after arrival of a predator. *Nature* **299**: 349–350.

Vermeij, G. J. 1987. *Evolution and Escalation: An Ecological History of Life*. Princeton University Press, Princeton, NJ.

Vermeij, G. J. 1995. *A Natural History of Shells*. Princeton University Press, Princeton, NJ.

Vermeij, G. J. 1998. Generic revision of the neogastropod family Pseudolividae. *Nautilus* **111**: 53–84.

Vermeij, G. J. 2005a. Shells inside out: The architecture, evolution and function of shell envelopment in molluscs. In: *Evolving Form and Function: Fossils and Development: Proceedings of a Symposium Honoring Adolf Seilacher for His Contributions to Paleontolog, in Celebration of His 80th Birthday: April 1-2* (A. Seilacher and D. E. G. Briggs, eds), pp. 197–221. Peabody Museum of Natural History, Yale University, New Haven, Connecticut.

Vermeij, G. J. 2005b. One-way traffic in the western Atlantic: Causes and consequences of Miocene to early Pleistocene molluscan invasions in Florida and the Caribbean. *Paleobiology* **31**: 624–642.

Vermeij, G. J. 2006. Historical contingency and the purported uniqueness of evolutionary innovations. *Proc. Natl. Acad. Sci. U. S. A.* **103**: 1804–1809.

Vermeij, G. J. 2007. The ecology of invasion: Acquisition and loss of the siphonal canal in gastropods. *Paleobiology* **33**: 469–493.

Vermeij, G. J. 2014. Molluscan marginalia: Serration at the lip edge in gastropods. *J. Molluscan Stud.* **80**: 326–336.

Vermeij, G. J. 2015a. Fossil predation: Did some clavilithine fasciolariid gastropods employ valve-wedging to feed on bivalves? *Vita Malacol.* **13**: 27–30.

Vermeij, G. J. 2015b. Gastropod skeletal defences: Land, freshwater, and sea compared. *Vita Malacol.* **13**: 1–25.

Vermeij, G. J. and S. J. Carlson. **2000**. The muricid gastropod subfamily Rapaninae: Phylogeny and ecological history. *Paleobiology* **26**: 19–46.

Vermeij, G. J., A. R. Palmer and D. R. Lindberg. **1990**. Range limits and dispersal of mollusks in the Aleutian Islands, Alaska. *Veliger* **33**: 346–354.

Vermeij, G. J., D. E. Schindel and E. Zipser. **1981**. Predation through geological time: Evidence from gastropod shell repair. *Science* **214**: 1024–1026.

Vermeij, G. J. and P. W. Signor. **1992**. The geographic, taxonomic and temporal distribution of determinate growth in marine gastropods. *Biol. J. Linn. Soc.* **47**: 233–247.

Vermeij, G. J. and E. H. Vokes. **1997**. Cenozoic Muricidae of the western Atlantic region. Part XII—The subfamily Ocenebrinae (in part). *Tulane Stud. Geol. Paleontol.* **29**: 69–118.

Villanea, F. A., C. E. Parent and B. M. Kemp. **2016**. Reviving Galápagos snails: Ancient DNA extraction and amplification from shells of probably extinct endemic land snails. *J. Molluscan Stud.* **82**: 449–456.

Vokes, E. H. 1985. The genus *Dermomurex* (Mollusca:Gastropoda) in Australia. *J. Malacol. Soc. Aust.* **7**: 45–65.

Vokes, H. E. 1939. Molluscan faunas of the Domengine and Arroyo Hondo formations of the California Eocene. *Ann. N. Y. Acad. Sci.* **38**: 1–246.

Warén, A. 1983. A generic revision of the Family Eulimidae (Gastropoda, Prosobranchia). *J. Molluscan Stud.* **49**: 1–96.

Watabe, N. 1983. Shell Repair. In: *The Mollusca* (K. M. Wilbur and A. S. M. Saleuddin, eds). Academic Press.

Watters, G. T. 2016. Digital *Murex* [Online]. Available: http://www.biosci.ohio-state.edu/~molluscs/test3/index.html [2016, March 15}.

Webster, N. B. and A. R. Palmer. **2016**. Shaving a shell: Effect of manipulated sculpture and feeding on shell growth and sculpture development in *Nucella lamellosa* (Muricidae: Ocenebrinae). *Biol. Bull.* **230**: 1–14.

Webster, N. B., T. J. M. Van Dooren and M. Schilthuizen. **2012**. Phylogenetic reconstruction and shell evolution of the Diplommatinidae (Gastropoda: Caenogastropoda). *Mol. Phylogenet. Evol.* **63**: 625–638.

Webster, N. B. and G. J. Vermeij. **In Press**. The varix: Evolution, distribution, and phylogenetic clumping of a repeated gastropod innovation. *Zool. J. Linn. Soc.*

Westermann, G. E. G. 1990. New developments in ecology of Jurassic-Cretaceous ammonoids. In: *Atti II Convegno Internazionale. Fossili. Evoluzione. Ambiente. Pergola 1987* (G. Pallini, F. Cecca, S. Cresta, and M. Santantonio, eds), pp. 459–478. Technostampa, Ostra Vetere.

White, C. A. 1880. Contributions to invertebrate paleontology, Nos. 2-8. *Twelfth Annu. Rep. U. S. Geol. Geogr. Surv. Territ. Year 1878* 5–171.

Wieneke, U., H. Stoutjesdijk, P. Simonet and V. Liverani. **2016**. Gastropoda Stromboidea. {Online} Available: http://www.stromboidea.de/ [2016, March 15].

Williams, S. T. 2016. Molluscan shell colour. *Biol. Rev.* **In Press**.

Woodring, W. P. 1970. Geology and paleontology of Canal Zone and adjoining parts of Panama; description of Tertiary mollusks (Gastropods: Eulimidae, Marginellidae to Helminthoglyptidae). *USGS Prof. Pap.* **306**–**D**: 299–452, pl 48-66.

Woodring, W. P. 1973. Affinities of Miocene marine molluscan faunas on Pacific side of Central America. *Inst. Centroam. Investig. Tecnol. Ind. Publicaciónes Geol.* **4**: 179–187.

Zekeli, L. F. 1852. *Die Gasteropoden der Gosaugebilde in den Nordöstlichen Alpen*. K.K. Hof- und Staatsdruckerei, Vienna.

Zou, S., Q. Li and L. Kong. **2011**. Additional gene data and increased sampling give new insights into the phylogenetic relationships of Neogastropoda, within the caenogastropod phylogenetic framework. *Mol. Phylogenet. Evol.* **61**: 425–435.

Appendix 1 — Phylogentic data sources, varicate clades and geological occurrences

Table A1.1. List of phylogenetic references used to create supertree.

Taxa	Source	Molecular/Morphological	Fossil/Recent
Gastropoda/Caenogastropoda	Ponder and Lindberg, 2008	Molecular/Morphological	Recent
Vetigastropoda	Aktipis and Giribet, 2011	Molecular	Recent
Ptenoglossa	Nützel, 1998	Morphological	Fossil/Recent
Hypsogastropoda	Takano and Kano, 2014	Molecular	Recent
Pulmonata	Dayrat et al., 2011	Molecular	Recent
Caenogastropoda	Colgan et al., 2007	Molecular	Recent
Caenogastropoda	Simone, 2011	Morphological	Recent
Cerithioidea	Strong et al., 2011	Molecular/Morphological	Recent
Neogastropoda	Zou et al., 2011	Molecular	Recent
Conoidea	Puillandre et al., 2011	Molecular	Recent
Muricidae	Barco et al., 2010	Molecular	Recent
Neogastropoda/Buccinoidea	Oliverio and Modica, 2010	Molecular	Recent
Buccinoidea/Nassariidae	Galindo et al., 2016	Molecular	Recent

Table A1.2. List of varicate clades including varix types, synchrony present, and time ranges in each presumed separate origin. See Chapter 2 for terms.

Clade	Superfamily	Family	Subfamily	Genus	Varix type	Synchrony	Time Range
Vetigastropoda	**Seguenzioidea**	Chilodontidae / Eucyclidae			multi-whorl	none	M. Jurassic: Eocene
	Porcellioidea	Discohelicidae		*Colpomphalus dupinianus*	multi-whorl	none	E. Cretaceous
Heterobranchia	**Acteonoidea**	Acteonidae	Liocareninae	*Hemiauricula, Nucleopsis*	multi-whorl	none	Eocene
Pulmonata	**Ellobioidea**	Ellobiidae		*Pythia*	internal	2/whorl	Paleocene: Recent
				Ellobium	subterminal: dorsal	NA	Holocene: Recent
Caenogastropoda		?Pseudozygopleuridae		*Spanionema*	multi-whorl	none	M. Devonian
	Campaniloidea	Plesiotrochidae		*Plesiotrochus*	multi-whorl	none	E. Miocene: Recent
	Epitonioidea	Epitoniidae			multi-whorl	none	Paleocene: Recent
	Vanikoroidea	Eulimidae			internal/multi-whorl	some 1-2/whorl	L. Cretaceous: Recent
		Aclididae			internal/multi-whorl	2 or 4/whorl	Paleocene: Recent
	Rissooidea	Rissoidae		*Pseudotaphrus*	internal/multi-whorl	none	Paleocene: Miocene
	Cerithioidea	Batillariidae			multi-whorl and/or subterminal: lateral	none	L. Cretaceous- Recent
		Cerithiidae /Diastomatidae /Litiopidae			multi-whorl and subterminal: lateral and/or dorsal	none	M. Cretaceous: Recent
		Potamididae			multi-whorl and/or subterminal: lateral	none	L. Cretaceous: Recent
		Pachychilidae		*Faunus ater*	multi-whorl	none	Recent
	Stromboidea	Aporrhaidae	Aporrhainiae / Strombidae / Rostellariidae		multi-whorl	3/whorl	L. Jurassic-Recent
			Dimorphosomatinae	*Pietteia*	multi-whorl	none	M. Jurassic to recent
		Spinilomatidae		*Spiniloma, Spinigeropsis*	multi-whorl	2/whorl	E. Jurassic
		Tylostomatidae		*Pterodona, Tlostoma*	internal/multi-whorl	none	L. Jurassic-E. Paleocene
	Tonnoidea				multi-whorl	most 2-2/3whorl	E. Cretaceous: Recent

Clade	Superfamily	Family	Subfamily	Genus	Varix type	Synchrony	Time Range
Neogastropoda		Maturifusidae		*Astandes ticurelatus*	multi-whorl	none	M. Jurassic
		Strepsiduridae		*Peruficus olssoni*	subterminal: lateral or dorsal	NA	L. Eocene
	Connoidea	Drilliidae			subterminal: dorsal	none	E. Oligocene: Recent
		Pseudomelatomidae		*Inquisitor*	multi-whorl	none	E. Miocene: Recent
		Borsoniidae		*Darbya, Varicobela*	multi-whorl /subterminal: dorsal	none	M. Eocene: Recent
		Mangeliidae		*Tenaturris*	multi-whorl	none	Pliocene-Recent
	Muricoidea	Muricidae	Aspellinae		multi-whorl	2-8/whorl	E. Miocene: Recent
			Ergalataxinae		multi-whorl	none	E. Eocene: Recent
			Muricinae		multi-whorl	3-7/whorl	E. Paleocene: Recent
			Muricopsinae	*Favartia* complex	multi-whorl	2-3/whorl	Oligocene: Recent
				Subpterynotus	multi-whorl	3/whorl	E. Miocene: Pliocene
			Ocenebrinae		multi-whorl	2-4/whorl	E. Oligocene: Recent
			Typhinae / Trypterotyphinae		multi-whorl	2-5/whorl	E. Eocene: Recent
	Buccinoidea	Buccinidae		*Euthria*	multi-whorl	none	M. Eocene: L. Miocene
		Colubrariidae			multi-whorl	1 or 2/3 per whorl	E. Eocene: Recent
		Columbellidae		*Strombina group*	subterminal: lateral or dorsal	NA	E. Miocene-Recent
		Nassariidae	Nassariinae		multi-whorl and/or subterminal: lateral	none	M. Eocene: Recent
			Photinae		multi-whorl	none	M. Eocene: Recent
				Fusinus fluminis	multi-whorl	none	M. Cretaceous
				Pseudoperissolax	multi-whorl	none	L. Cretaceous: E. Oligocene
	Cancellaroidea	Cancellariidae			multi-whorl	some	L. Cretaceous: Recent

Table A1.3. Incidence of varicate species in various faunas.

Time	Number of species	Number of varicate species	Frequency of Varices	References
Cretaceous				
Albian, France	63	1	1.6%	(Kollmann and Fischer, 2005)
Cenomanian, France	51	2	3.9%	(Kollmann and Fischer, 2005)
Gault Clay, England (Albian)	62	3	4.8%	(Tracey, 2010)
Hauterivian, France	49	2	4.1%	(Kollmann and Fischer, 2005)
Hiraiga Formation (Late Aptian)	69	6	8.7%	(Kase, 1984)
Losenstein Formation (Late Albian)	92	2	2.2%	(Kollmann, 1978, 1979, 1982; Kennedy and Kollmann, 1979; Kollmann and Summesberger, 1982)
Maastrichtian, Peru	59	1	1.7%	(Olsson, 1934, 1944)
Owl Creek Formation, Campanian	75	5	6.7%	(Sohl, 1960, 1964)
Prairie Bluff Formation, Campanian	59	4	6.8%	(Sohl, 1964, 1960)
Ripley Formation, Maastrichtian	266	15	5.6%	(Sohl, 1964, 1960)
Tanohata Formation (Early Albian)	29	2	6.9%	(Kase, 1984)
Paleocene				
Bashi Marl	135	8	5.9%	(Dockery, 1998)
Bells Landing Member	55	4	7.3%	(Dockery, 1998)
Ewekoro Formation	138	12	8.7%	(Adegoke, 1977)
Greggs Landing Member	67	4	6.0%	(Dockery, 1998)
Mons, Early Paleocene of Belgium	214	18	8.4%	(Glibert, 1973)
Eocene				
Baron, Auversian, Late Eocene	488	62	12.7%	(Dolin *et al.*, 1980)
Keasey Formation, Late Eocene	70	9	12.9%	(Hickman, 1980)
Late Eocene, Colombia	83	9	10.8%	(Clark and Durham, 1946)
McCulloch's Bridge, Kaiatan Late Eocene	173	19	11.0%	(Maxwell, 1992)
Moodys Branch Formation, Late Eocene	180	19	10.6%	(Dockery, 1977)
Reklaw Formation, Middle Eocene	164	17	10.4%	(Garvie, 1996, 2013)
Suwannee Formation, Late Eocene	74	12	16.2%	(Petuch, 1998)
Whittaker Peak, Juncal and Matilija Formations, Early to Middle Eocene	56	5	8.9%	(Squires, 1987)

Time	Number of species	Number of varicate species	Frequency of Varices	References
Oligocene				
Early Oligocene, Mississippi	360	35	9.7%	(MacNeil and Dockery, 1984)
Late Oligocene, Nörre Vissing, Denmark	88	15	17.0%	(Schnetler and Beyer, 1987)
Late Oligocene, North Sea Basin	324	44	13.6%	(Janssen, 1978, 1979)
Miocene				
Cantaure Formation, Mexico (Early Miocene)	335	54	16.1%	(Landau *et al.*, 2016)
Gram Formation, Denmark (Late Miocene)	90	6	6.7%	(Schnetler, 2005)
Karaman, Turkey (Middle Miocene)	434	50	11.5%	(Landau *et al.*, 2013)
Miste Beds, Netherlands (Middle Miocene)	344	25	7.3%	(Janssen, 1984)
Quilon Formation, India (Early Miocene)	104	12	11.5%	(Harzhauser, 2014)
Pliocene				
Coralline Crag, United Kingdom	116	6	5.2%	(Long and Zalasiewicz, 2011)
Cubagua Formation, Venezuela	129	27	20.9%	(Landau and da Silva, 2010)
Hondeklip 50m, South Africa	56	2	3.6%	(Kensley and Pether, 1986)
Kattendijk Formation, Belgium	77	2	2.6%	(Marquet, 1995, 1997a; b, 2001)
Kruisschans Member, Lillo Formation, Belgium	60	2	3.3%	(Marquet, 1995, 1997a; b, 2001)
Onzole Formation, Ecuador	113	21	18.6%	(Olsson, 1964)
Oorderen Member, Lillo Formation, Belgium	113	3	2.7%	(Marquet, 1995, 1997a; b, 2001)
Shinzato Formation, Japan	149	16	10.7%	(Noda, 1988)
Zone 2, Yorktown Formation, Virginia	278	10	3.6%	(Campbell, 1993)

Time	Number of species	Number of varicate species	Frequency of Varices	References
Recent tropical				
Clipperton Atoll	207	17	8.2%	(Kaiser, 2007)
Cocos-Keeling	431	40	9.3%	(Maes, 1967)
Easter Island	106	16	15.1%	(Rehder, 1980; Raines, 2007)
Enewetak Atoll	883	89	10.1%	(Kay and Johnson, 1987)
Guam	482	62	12.9%	Vermeij collection
Hawaiian Islands	800	48	6.0%	(Kay, 1979)
Palau	300	46	15.3%	Vermeij collection
Pitcairn Islands	147	15	10.2%	(Paulay, 1989)
western Florida	68	16	23.5%	Vermeij collection
western Panama	240	40	16.7%	Vermeij collection
Recent cold water				
Akkeshi Bay, Japan	74	4	5.4%	(Habe, 1958)
Aleutian Islands	71	2	2.8%	(Vermeij *et al.*, 1990)
Arctic Canada	104	0	0.0%	(Macpherson, 1971)
Bay of Algeciras, Spain	277	15	5.4%	(Aartsen *et al.*, 1984)
East Greenland	84	0	0.0%	(Thorson, 1944)
Kerguelen and Crozet	139	2	1.4%	(Cantera and Arnaud, 1984)
Norway	327	7	2.1%	(Høsæter, 1986)
south-central Chile	58	4	6.9%	(Aldea and Valdovinos, 2005)
Recent, cool water				
Washington State	238	4	1.7%	(Kozloff, 1987)

Appendix 2 — Collection localities of *Ceratostoma foliatum*

Table A2.1. Collection localities of *Ceratostoma foliatum* for Chapter 3.

Site	Latitude (°)	Longitude (°)	Collection method	Depth (m)	Collection date
Bordelais Island	48.817	-125.232	low tide	1 to 0	2012-07-24, 2012-08-02, 2013-05-01, 2014-05-01
Edward King Island	48.826	-125.223	low tide	1 to 0	2014-04-30
Ellis Islet*	48.862	-125.108	SCUBA	0 to -20	2012-05-11
Grappler mouth	48.838	-125.135	SCUBA	0 to -20	2014-05-17
Helby Island	48.855	-125.169	low tide	1 to 0	2013-05-07
Hosie Islands*	48.909	-125.039	SCUBA	0 to -20	2012-05-11
Nanat Island*	48.885	-125.078	SCUBA	0 to -20	2012-05-11
Ohiat Island	48.856	-125.184	SCUBA	0 to -20	2012-05-10
Sandford Island	48.868	-125.168	SCUBA	0 to -20	2014-05-17
South Docks	48.833	-125.137	SCUBA	0 to -20	2014-04-24
Wizard Island	48.858	-125.160	SCUBA	0 to -20	2014-05-02

*Populations were mixed prior to labelling, so wild population data was lost

Appendix 3 — ANOVA tables for Chapter 3

ANOVA tables for Chapter 3, see text for details. Df: degrees of freedom; Sum Sq.: Sum of squares; Mean Sq: mean sum of squares. Significant P values are bolded ($p < 0.05$)

Table A3.1. 2012-2013 Angular growth

	Df	Sum Sq	Mean Sq	F value	P
Year (2012,2013)	1	10845	10845	2.163	0.1440
Treatment	6	145449	24241	4.836	**0.0002**
Interaction	4	19123	4781	0.954	0.4357
Residuals	119	596535	5013		

Table A3.2. 2014 Angular growth

	Df	Sum Sq	Mean Sq	F value	P
Treatment	5	20.51	4.102	6.548	**<0.0001**
Residuals	97	60.77	0.626		

Table A3.3. Varix spacing in wild populations

	Df	Sum Sq	Mean Sq	F value	P
Population	6	5172	862	7.98	**<0.0001**
Residuals	122	13179	108		

Table A3.4. Varix spacing in control snails compared to wild source population

	Df	Sum Sq	Mean Sq	F value	P
Population	1	1001	1001.4	9.271	**0.0032**
Treatment (wild, control)	1	858	858.3	7.946	**0.0062**
Interaction	1	82	81.9	0.759	0.3866
Residuals	74	7993	108		

Table A3.5. Varix spacing in control snails compared to all wild snails

	Df	Sum Sq	Mean Sq	F value	P
Treatment (wild, control)	1	711	710.8	6.663	**0.0109**
Population	6	5093	848.8	7.956	**<0.0001**
Interaction	1	82	81.9	0.768	0.3824
Residuals	132	14083	106.7		

Table A3.6. Varix spacing in treatments

	Df	Sum Sq	Mean Sq	F value	P
Treatment	5	5148	1029.6	4.375	**0.00146**
Residuals	78	18355	235.3		

Table A3.7. Type of apertural varix grown, compared to the amount of shell removed from the aperture

	Df	Sum Sq	Mean Sq	F value	P
Apertural varix (full, small, none)	2	3868	1934	6.239	**0.0036**
Residuals	57	17670	310		

Table A3.8. Treatment compared to the apertural angle

	Df	Sum Sq	Mean Sq	F value	P
Treatment	2	622	311.2	1.071	0.3515
Apertural varix (full, small, none)	1	43	42.5	0.146	0.7038
Interaction	2	1416	708	2.436	0.0992
Residuals	44	12788	290.6		

Table A3.9. Type of apertural varix grown, compared to the apertural angle grown

	Df	Sum Sq	Mean Sq	F value	P
Apertural varix (full, small)	1	44	43.6	0.15	0.7003
Treatment	2	621	310.7	1.069	0.3521
Interaction	2	1416	708	2.436	0.0992
Residuals	44	12788	290.6		

Table A3.10. Spacing of next varix (V+1) compared to treatment

	Df	Sum Sq	Mean Sq	F value	P
Treatment	3	14697	4899	13.78	**<0.0001**
Residuals	27	9600	356		

Appendix 4 — Effects of feeding on shell growth and lamellar spacing in *Nucella lamellosa*

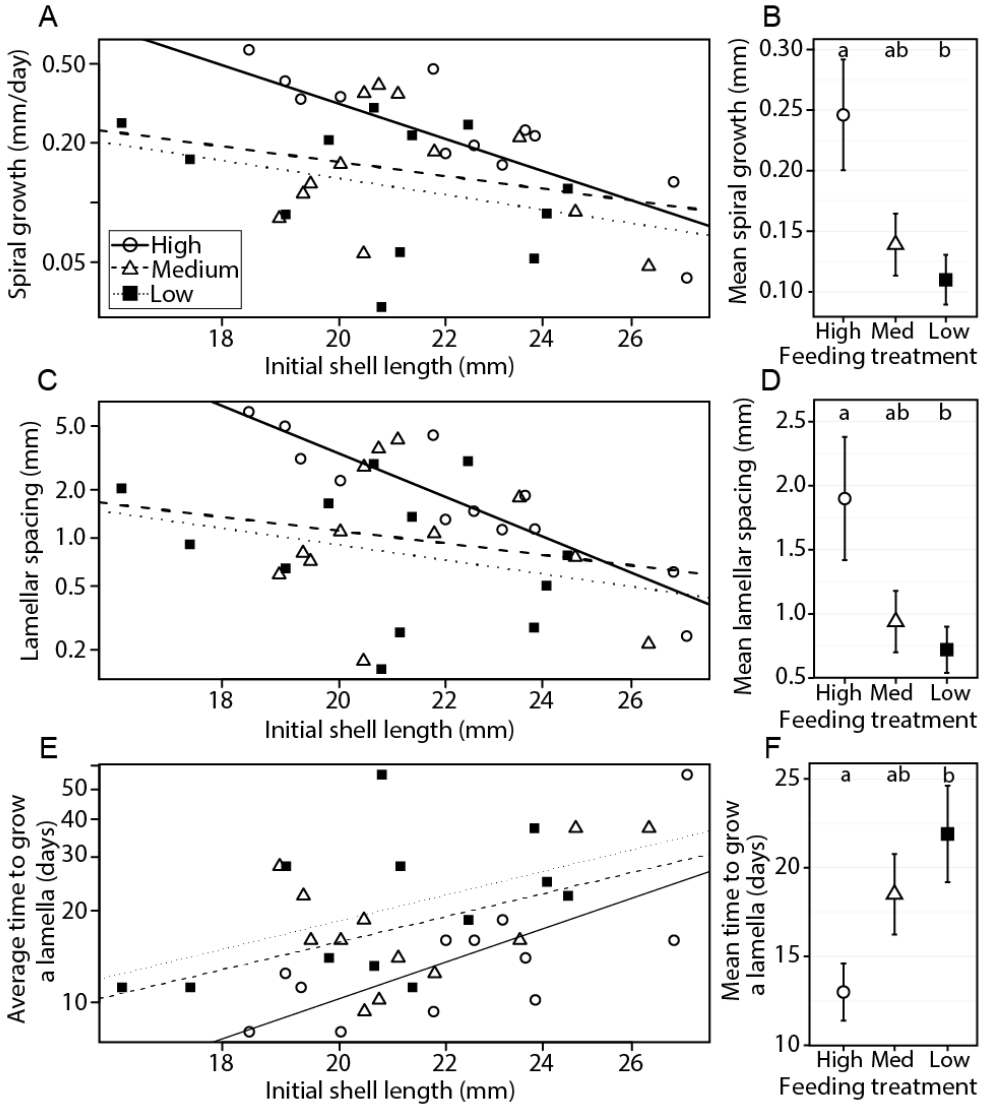

Figure A4.1. Shell and sculpture growth relative to initial shell length in the feeding rate treatments. A) Daily spiral shell growth versus initial shell length on log-transformed axes. Larger snails grew less than small snails (High, $r^2 = 0.71$, df = 10, $p = 0.0003$); slopes did not differ significantly among treatments, $p > 0.3$. B) Mean daily spiral growth (least-squares means from ANCOVA of data in panel A; High:Low, $p = 0.01$). C) Average lamellar spacing versus initial shell length on log-transformed axes (High, df = 10, $r^2 = 0.80$, $p < 0.0001$); slopes did not differ significantly among treatments, $p > 0.2$. D) Average lamellar spacing in the 3 feeding rate treatments (least-squares means of data in panel C; High:Low, $p = 0.03$). E) Average time to grow a lamella as a function of initial shell length on log-transformed axes. Larger snails grew lamellae closer together than smaller snails (High, $r^2 = 0.45$, df = 10, $p = 0.01$); slopes did not differ significantly among treatments, $p > 0.8$. F) Average time to grow a lamella (least-squares means of data in panel E; High:Low, $p = 0.02$). Error bars (SD); letters indicate groups that did not differ significantly.

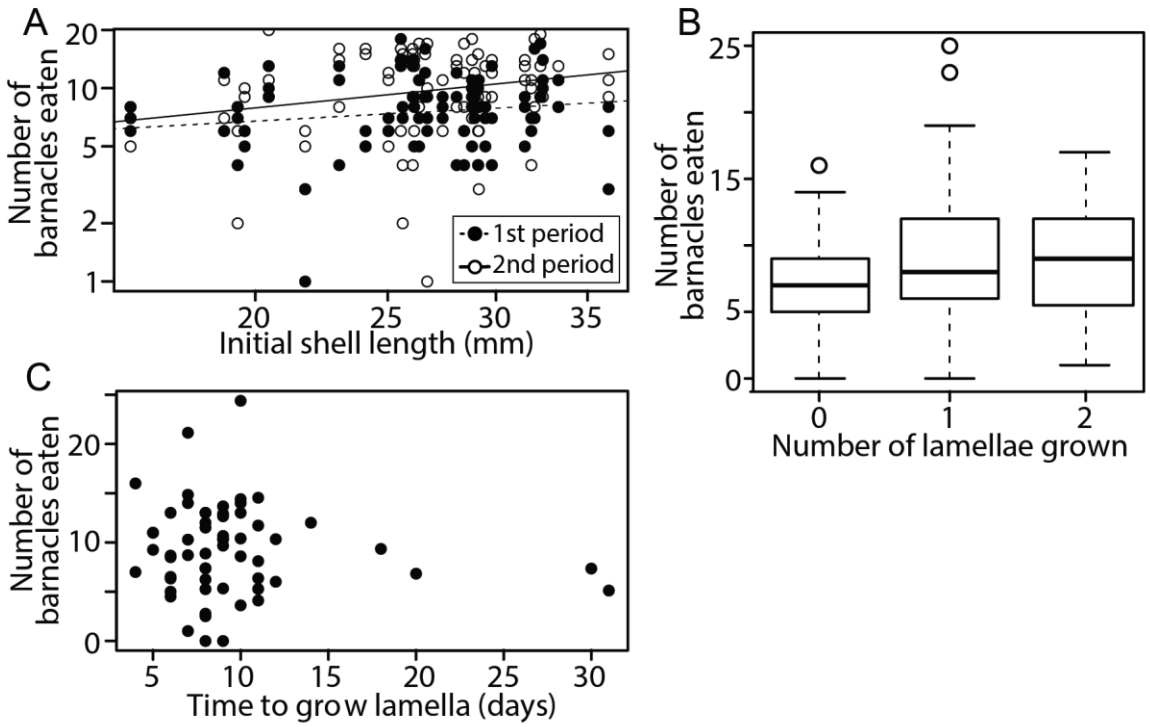

Figure A4.2. Number of barnacles eaten during the sculpture growth rate experiment. A) Average number of barnacles eaten each week as a function of initial shell length on log-transformed axes (first time period, dashed line: $p = 0.1$; second time period, solid line: df = 97, $r^2 = 0.048$, $p = 0.02$). B) Boxplot of the total number of barnacles eaten each week as a function of the number of lamellae completed in the same week. Solid middle line, median; box, data between the 25th and 75th percentiles; dashed whiskers (error bars), data within 1.5 the interquartile range; circles, individual data points outside that range. C) Total number of barnacles eaten during growth of a single lamella as a function of the time taken to grow that lamella; each point represents an individual lamella.

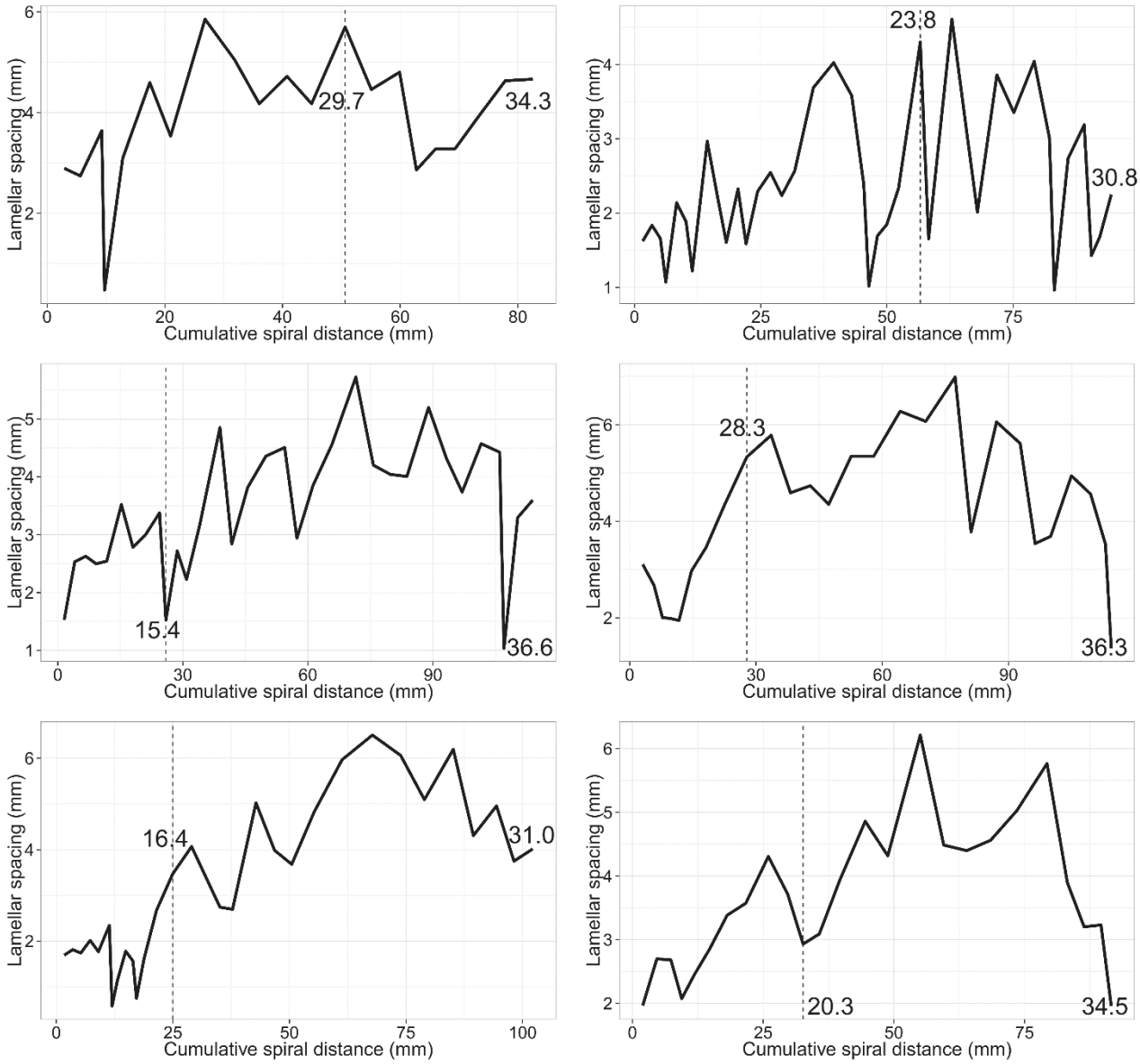

Figure A4.3. Lamellar spacing of the entire shell for six *N. lamellosa*. Distance was measured linearly from one lamella to the next, on the outermost edge of the whorl, from an apex photograph using ImageJ (Rasband, 1997). The first lamella measured was the first prominent lamella in a sequential series, and not the first lamella on the first teleoconch whorl. Cumulative spiral distance is the total cumulative spacing between lamellae. Dashed line indicates the point at which the snail was collected: lamellae to the left of the dashed line were produced in the field; those to the right, in the laboratory. Numbers indicate shell length (mm) at collection (dashed line) and at the end of the experiment.

Appendix 5 — Spiral ribs in other molluscs

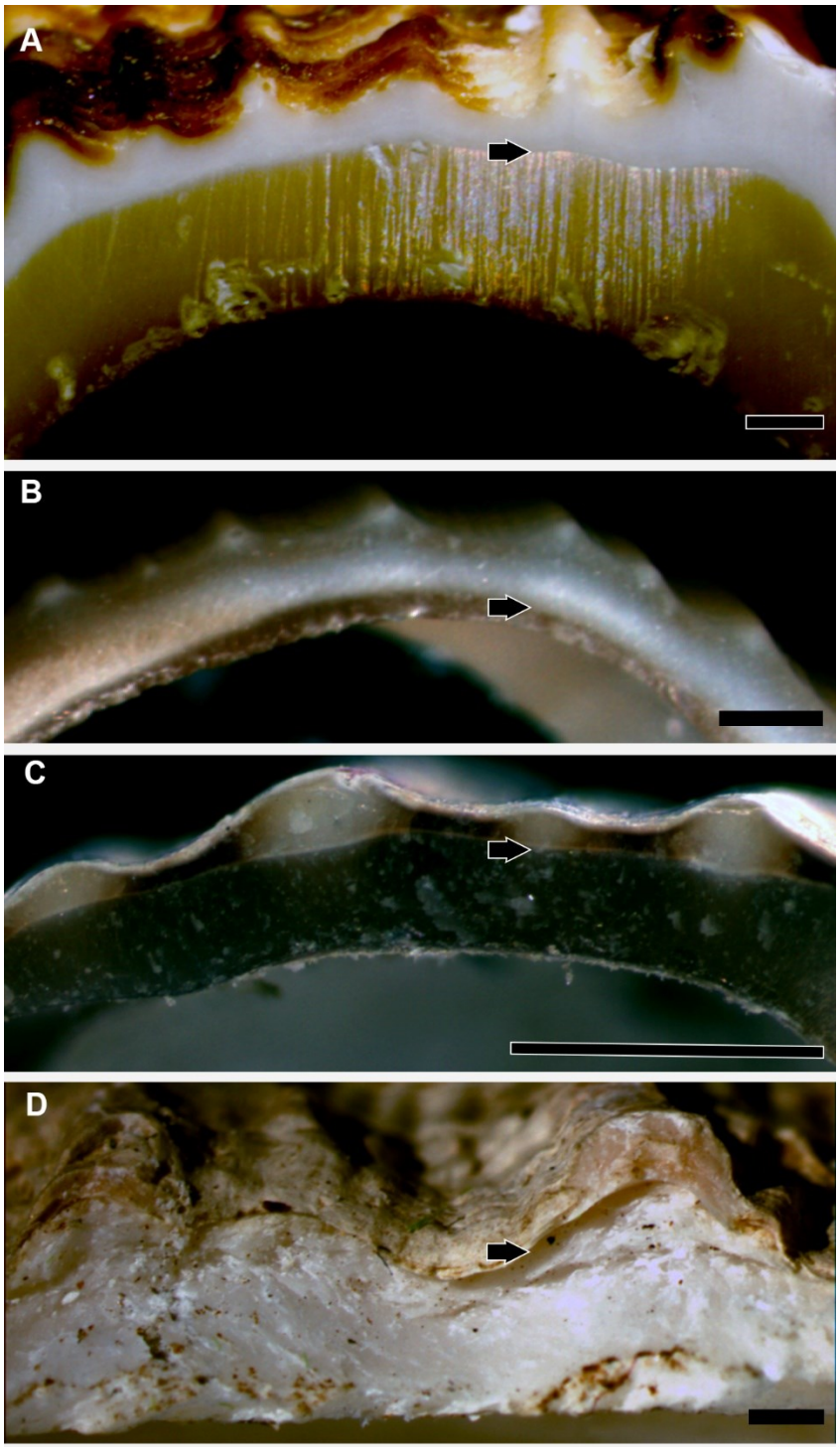

Figure A5.1. Spiral ribs in other molluscs. A) *Turbo* sp. (Turbinidae) B) *Turritella* sp. (Turritellidae) C) *Calliostoma ligatum* (Calliostomatidae). D) *Ostrea* sp. Arrow: division between shell layers. Scale bars = 1 mm.

Appendix 6 — *In situ* methods and snail husbandry

A6.1 In-situ *hybridization*

A6.1.1 Methods

A6.1.1.1 RNA extraction and cDNA synthesis

A *Nucella ostrina* cDNA library was created from a mixture of snails. Mantles from both ribbed and smooth adults and juveniles, as well as entire hatchling snails (<3 mm shell length) were flash frozen in liquid nitrogen, homogenized, and RNA was extracted with a TRIzol extraction (Life Technologies). RNA concentration was standardized and then reverse transcribed with SuperScript III kit (Invitrogen). cDNA library was diluted, and quality was confirmed with a Bioanalyzer (Agilent 2100). Degenerate primers were designed for MSI60, MSI31, and lustrin (Table A5.1) based on published sequences of gastropods (*Haliotis* spp., *Patella vulgata*, and *Lottia gigantea*) and bivalves (*Pinctada*). Actin positive control primers were derived from Colgan *et al.* (2007).

A6.1.1.2 Sequencing

DNA was amplified with PCR and sequencing was performed by MBSU (Molecular Biology Service Unit, University of Alberta). Resulting sequences were compared to GenBank to confirm identity. Only lustrin provided a successful sequence. PCR products were cloned into the pGEM-T cloning vector (Promega) following manufacturer's instructions.

Table A6.1. Lustrin primers and *N. ostrina* lustrin sequence.

Sequence name	Sequence (5'→3')	Source
Lustrin degenerate primer F	AARCCNGGNWSNTGYCC	Genbank sequences from *Haliotis, Patella, and Lottia**
Lustrin degenerate primer R	AARTGYTGYWSNAAYGGNTG	
Lustrin primer F	CCCAAACGGAAGAAGTGCTG	*N. ostrina*
Lustrin primer R	GTGTGGACGGAAAGTGTGTT	*N. ostrina*
Lustrin sequence including primers (120bp)	CCCAAACGGAAGAAGTGCTGTAGAGTGGGCTGCAAAACCTCCATATGT GTGACCCCGCTGCCGCCTTGTGCCGTTGTGCGCTGCAGCAGTGGACAC GTTTGTGTGGACGGAAAGTGTGTT	

*Accession numbers: ABC00197.1, AAB95154.1, AAB95154.1, AAB95154.1, AAB95154.1, AAB95154.1, AAB95154.1, AAB95154.1, AAB95154.1, AAB95154.1, AAB95154.1. ADM52208.2, ADM52208.2, CCJ09595.1, XP_009051424.1

A6.1.1.3 Probe creation

Both sense and anti-sense probes were synthesized using SP6 and T7 RNA polymerase for lustrin and actin. Probe quality was confirmed using a dot-blot test and Nano-drop.

A6.1.1.4 *In situ* hybridization

Whole mount *in-situ* hybridization followed Zebrafish protocols (Myhre *et al.*, 2014), Briefly, tissue was rehydrated through to PBST, then a 25 min digestion in 30 µg/mL proteinase K (10 min for hatchlings), and post-fixed in 4% PFA for 20 min. Tissue was pre-hybridized for 1h at 65°C, and hybridized overnight (0.5 ng/uL of probe). Tissue was washed and blocked in BSA for 1h, and overnight in 1:5000 anti-DIG at 4°C. Then the tissue was washed, buffered, and incubated in NBT-BCIP at room temperature until colour appeared, or left overnight at 4°C with fresh NBT-BCIP.

A6.1.2 Results

Despite attempts with both cryo-sections and whole mounts of hatchling and juvenile *N. ostrina* mantles (foot tissue was also attempted for actin), all *in-situs* yielded the same non-specific staining in sense and anti-sense probes of actin and lustrin. Multiple probe concentrations and proteinase K digestions were tried, on both freshly fixed and methanol-stored tissue.

A6.2 Snail husbandry

Throughout this thesis I grew all three of these species (*C. foliatum, N. lamellosa,* and *N. ostrina*) in the laboratory. In all cases they fed and grew in sea water flow-through tables at BMSC. All the species needed to be kept in lidded containers to stop them from crawling out of the water and dehydrating.

A6.2.1 Nucella *reproduction and hatching*

Both *Nucella* grew quickly and easily in the lab, while regularly laying fertilized eggs. These eggs developed very slowly in the cold water of the sea tables, while wild eggs seemed to hatch faster in the intertidal. Although the eggs developed faster in smaller containers held at warmer temperatures, they were at a greater risk, and the water needed to be replaced very regularly.

Once hatched, hatchlings thrived when given sufficient food and protected from small predators. The easiest I found was to collect newly settled mussels (<2 mm), mostly found along docks. Although they would also eat barnacles of the same size, these were much harder to find, and rarely on portable rocks. Without sufficient food, many of the snails cannibalized each other. A small mesh size (<1 mm openings) was needed to keep the hatchlings in their containers, which limited water flow. To mitigate this, I regularly drained and refilled the container, even though it was already in a free flow sea table. Once the snails were large enough to be seen easily and not escape a large mesh, they were transferred to a container with better water flow and larger food.

In *N. lamellosa,* growth rates were relatively steady throughout the summer and early fall, and seemed to drop as the temperature outside dropped, as would be expected in wild populations (Spight, 1973). The water and lab temperature remained relatively steady, with no external light, so they probably detected the season change from the quality of their barnacle prey or from chemical cues. Barnacles were harvested regularly from the intertidal; it was too work intensive to maintain a large, healthy populations in the lab as they would need to be regularly manually fed by turning off the flow.

A6.2.2 Growing Ceratostoma

Chapter 2 suggested that angular shell growth was fastest in *C. foliatum* kept in opaque containers rather than transparent ones while suspended in the ocean (hanging from lines on the

docks). I predict that the different would have been significant if a red tide had not disturbed the experiment.

In June 2014, a red tide of *Noctulica* sp. killed most of the barnacles feeding the *Ceratostoma*. This lead to an abrupt growth halt, even for snails in the middle of growing their intervarical region. These snails quickly produced a labial tooth and stopped shell growth, and growth did not resume over the next month before the experiment was terminated. It is unclear what caused the snails to stop growing, but it seems likely that consuming the toxins in the barnacles poisoned them. No snails died during this period, but the experiment was quickly terminated. Palmer (1981) suggested that shell secretion is rate limited, not resource limited; shell growth occurs even in the absence of food. Accordingly, *C. foliatum* should have continued to deposit shell, completing the varix, during the red tide if it was only a lack of food. Likely then the snails were sickened from eating the toxins which disrupted normal shell growth.

Unfortunately, no control was made to differentiate whether snails grew faster in the laboratory over the same time period because there was a lack of suitable specimens for the main purpose of the experiment – to look at varix spacing and growth. In the laboratory, snails were grown in a communal space with inconsistent lighting. Juvenile abalone (García-Esquivel *et al.*, 2007), larval conch (Brito-Manzano and Aldana-Aranda, 2013) and *Plectostoma retrovens* (Diplommatinidae) (Berry, 1962). exhibit increased growth rates in full darkness, so the opaque containers might have had a greater effect than just making the snails feel more protected during their shell growth phase (Chapter 2).

Unlike in *Nucella*, where there was too much variation in shell growth, the rigid growth patterning of *Ceratostoma* showed that growth in the laboratory had some effect, as some control snails grew unusually, both in the laboratory and in the ocean (Chapter 2). I don't know what might be causing malformation, which is almost never seen in the wild without shell damage. Whatever might have caused this disruption of *Ceratostoma* might also have affected the growth of *Nucella*, but there is no way to know what, if anything that might have been.